Metabolism of androstane derivatives with focus on hydroxylation reactions

Inaugural-Dissertation

to obtain the academic degree

Doctor rerum naturalium (Dr. rer. nat.)

submitted to the Department of Biology, Chemistry and Pharmacy

of Freie Universität Berlin

by

Jan Felix Joseph

from Bremen

2016

Research of the present study was conducted from 2012 till 2016 under supervision of Prof. Dr. Maria Kristina Parr at the Institute of Pharmacy of the Freie Universität Berlin.

1. Gutachter: Prof. Dr. Maria Kristina Parr

2. Gutachter: Prof. Dr. Francesco Botrè

Disputation am 16.12.2016

What is a poison?

All substances are poison;

There is none that is not a poison.

The right dose differentiates a poison from a drug.

(Paracelsus 1493-1541)

Acknowlegements

First of all, I would like to sincerely thank my supervisor Prof. Dr. Maria Kristina Parr for her patient guidance, enthusiastic encouragement and useful critiques of my work. I am very grateful for all the opportunities she gave me.

Further, I would like to thank Prof. Dr. Francesco Botrè for the possibility to work in his laboratory. I thank him, Dr. Xavier de la Torre and all members of the Anti-Doping Laboratory Rome for their help and kindness.

I thank all group members of the Pharmaceutical Analytics and Metabolism group for creating a friendly, creative and most of all supportive atmosphere, especially Dr. Peter Witte and Jaber Assaf.

My grateful thanks are also directed to Dr. Ursula Brümmer. Thanks to her teaching has always been a positive experience for me.

I would like to thank my friends and family for their support.
My parents, Margarete and Wolfgang Joseph, for their love and unconditional support.

Finally, I wish to thank you, Judith, for everything and for August.

Table of content

I. Abbreviations

1-AED	5α-Androst-1-ene-3,17-dione
$[M]^{\bullet+}$	Radical cation of the molecular ion
5α-AD	5α-Androstanedione
5α-DHT	5α-Dihydrotestosterone or 17β-Hydroxy-5α-androstan-3-one
AAS	Anabolic androgenic steroids
ADD	Boldione
AED	Androst-4-ene-3,17-dione
AKR	Aldo-keto reductase
ALLO	Allopregnanolone
APCI	Atmospheric pressure chemical ionization
APPI	Atmospheric pressure photo ionization
AR	Androgen receptor
BCP	Base peak chromatogram
BOLD	Boldenone
COMT	Catechol-O-methyl transferase
CYP	Cytochrome P450
CYP19A1	Cytochrome P450 isoenzyme 19A1, aromatase
CYP3A4	Cytochrome P450 isoenzyme 3A4
DAD	Diode array detector
DHEA	Dehydroepiandrosterone
DHP	Dihydroprogesterone
DSMO	Dimethyl sulfoxide
E1	Estrone
E2	Estradiol
EI	Electron ionization
EIC	Extracted ion chromatogram

ER	Estrogen receptor
ESI	Electrospray ionization
Etio	Etiocholanolone
GC	Gas chromatography
GLUT	Glucuronosyl transferase
HML	Human Liver Microsomes
HPG	Hypothalamic pituitary gonadal
HPLC	High performance liquid chromatography
HRMS	High resolution mass spectrometry
IRMS	Isotope ratio mass spectrometry
LC	Liquid chromatography
MS	Mass spectrometry
MSTFA	N-Methyl-N-(trimethylsilyl)trifluoracetamide
NADPH	Nicotinamide adenine dinucleotide phosphate
PED	Performance enhancing drug
PREG	Pregnenolone
PROG	Progesterone
QTOF	Quadrupole Time-of-Flight
RT	Retention time
SULT	Sulfotransferase
TBDMSCl	tertiary Butyldimethylsilyl chloride
TBME	tert-Butyl methyl ether
THF	Tetrahydrofurane
TIC	Total ion chromatogram
TMIS	Trimethyliodsilane
TMS	Trimethylsilyl
USADA	US Antidoping Agency
WADA	World Antidoping Agency

1 Introduction

In the present work, the metabolic conversion of some androstane derivatives will be discussed with regard to enzymatic hydroxylation reactions. Androstane derivatives are for instance the endogenous prohormone androstenedione (AED) or the prominent male sex hormone testosterone, aside from numerous further synthetic examples. They are supposed to convey androgenic and anabolic physiological effects. Their administration, even of non-approved substances, usually aims for the anabolic rather than the androgenic effects with the purpose of performance enhancement.

1.1 Performance enhancing drugs

Performance enhancing drugs (PED) are substances used, or misused, to enhance certain body traits such as strength or body appearance. The 'Endocrine Society' published a scientific statement on this topic in 2014 and defined PED's to include performance enhancing drugs and body-image enhancing drugs [1]. In this way the term PED combines drugs mostly misused by athletes for strength and recovery purposes, as well as drugs used in so-called recreational sports, by non-athletes, who seek to enhance their body appearance. The wide range of substances that could be defined as PED's includes anabolic androgenic steroids (AAS), peptide hormones and growth factors, beta-2 agonists, diuretics, stimulants, narcotics, cannabinoids, glucocorticoids, beta-blockers and blood doping [2] . If one includes cognition enhancing in the term performance, even so-called smart drugs (nootropics) would be PED's. With regard to professional sports the World Anti-Doping Agency (WADA) defines substances which are prohibited in and out of competition in its annual prohibited list [2]. The most commonly used PED's are AAS. In 2014, almost one out of two (48 %) reported findings by Anti-Doping laboratories were anabolic agents [3]. The abuse of AAS regarding the general population was estimated for the US alone with up to 3 % [4]. Recently, a study suggested a global life-time prevalence by a similar magnitude (3.3 %) [5]. In the following part of the introduction, the focus will be on steroid hormones, their metabolism and involved enzymes and analytical methods to detect their administration.

1.2 Steroid hormones

Steroids consist of four fused rings (A, B, C, and D) which form a rigid, almost planar molecular structure. 5α-cholestane (Figure 1(I)) exemplifies the numbering system of steroids. Substituents either direct towards the β-space (above) or α-space (below the surface). Figure 1(II) demonstrates the two possible configurations at carbon 5 for 5α- (a) and 5β-cholestane (b) illustrating the large effect on the spatial arrangement.

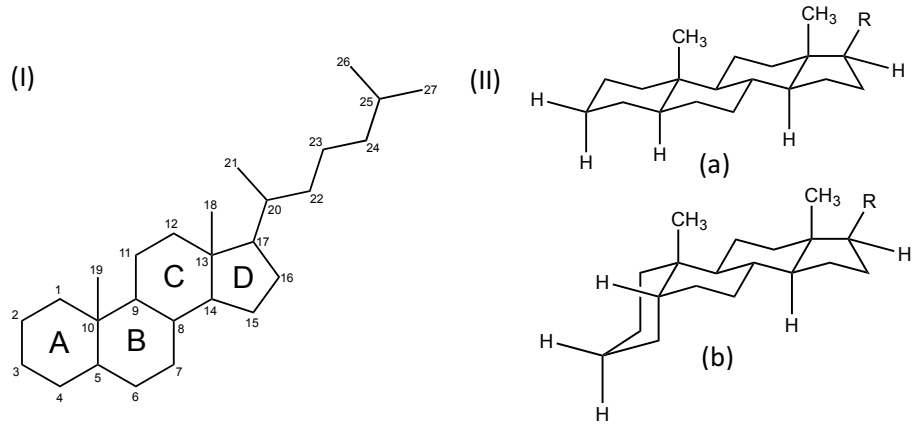

Figure 1 Chemical structure of cholestane representing the numbering system of steroids (I) and its spatial arrangement (II) of the 5α- (a) and 5β-configuration (b), R=C_8H_{17}

Cholesterol is a C27 steroid derived from 5α-cholestane. It is ubiquitous in animals and humans and serves as component of cell membranes as a precursor for steroid hormones. Cholesterol can be enzymatically transformed in two ways. First, it can be oxidatively cleaved inside the mitochondria by cytochrome P450 enzyme 11A1 (CYPscc, CYP side chain cleavage) resulting in pregnenolone. This basic C21 pregnane is the precursor of all endogenous steroid hormones. Alternatively, cholesterol can be transformed into bile acids. Beside cholestanes and pregnanes further groups of steroid structures are androstanes and estranes (Figure 2). The biosynthesis of corticosteroids (glucocorticoids, mineralocorticoids) and sex hormones (gestagens, androgens, estrogens) is partially displayed in Figure 3.

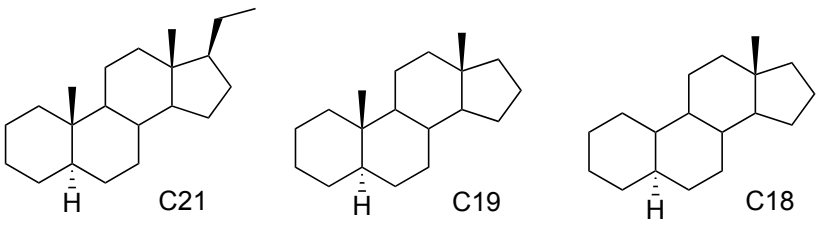

Figure 2 Chemical structures of 5α-pregnane (C21), 5α-androstane (C19) and 5α-estrane (C18)

Important enzymes in the biosynthetic pathway of steroids are, among others, oxidoreductases targeting oxygens at C3 and C17 (hydroxysteroid dehydrogenases, HSD) and 5α-reductases. Further steroidogenic CYP enzymes are mitochondrial CYP11B1 (11β-hydroxylase) and CYP11B2 (aldosterone synthase) along with microsomal CYP17A1 (17α-hydroxylase, 17,20-lyase), CYP19A1 (aromatase), and CYP21 (21-hydroxylase).

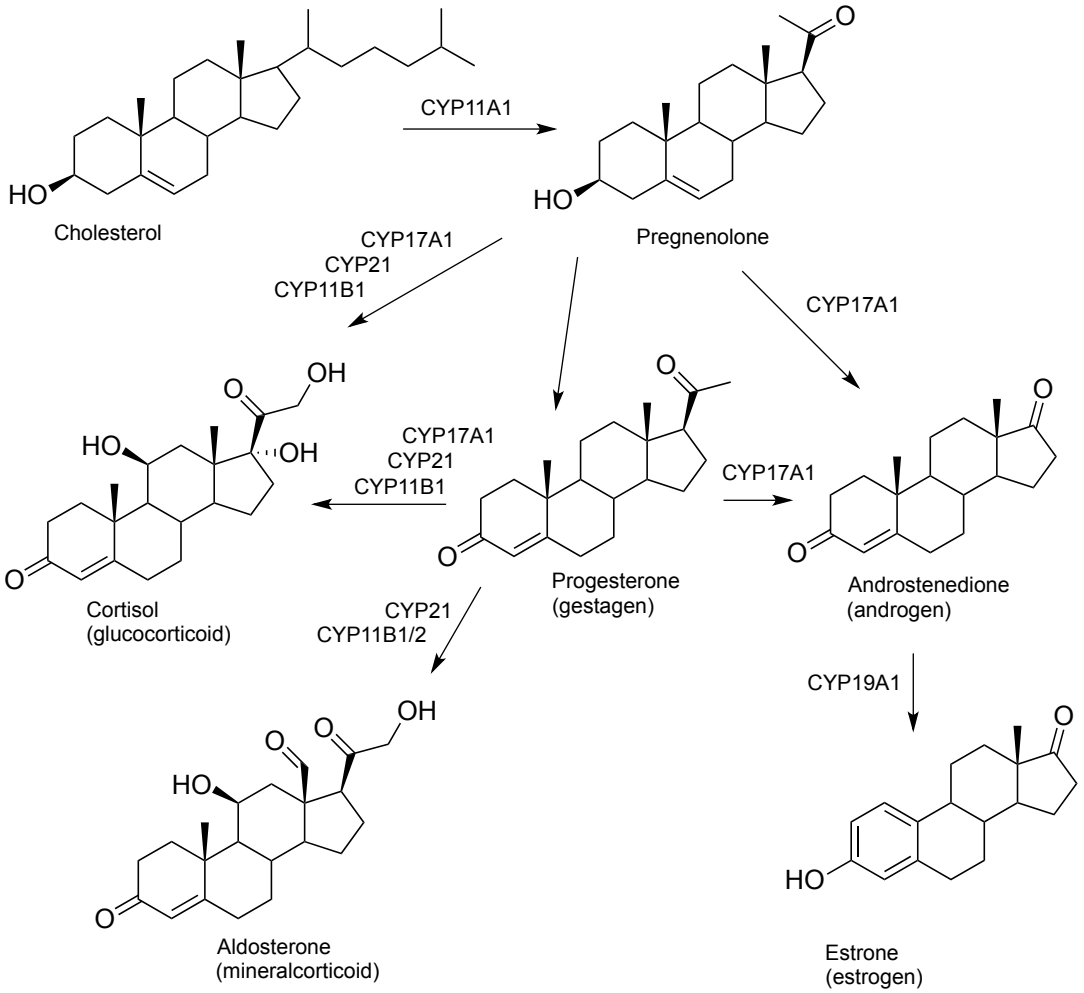

Figure 3 General biosynthetic pathway of steroid hormones starting from cholesterol via pregnenolone resulting in corticosteroids (glucocorticoids, mineralocorticoids) and sex hormones (gestagens, androgens, estrogens) with involved CYP enzymes, other involved enzymes are not displayed

1.2.1 Endogenous steroids

The male sex hormones (androgens) are all based on the structure of 5α-androstane and promote anabolic (increase of skeletal muscle mass and strength) and androgenic (reproduction, sexual maturation) effects. Testosterone, the most popular androgen, it's active metabolite dihydrotestosterone and weaker endogenous androgens such as

androstenedione (AED), dehydroepiandrosterone (DHEA), and androstenediol play important roles in the human endocrine system. Androgen biosynthesis in the testis and ovaries is regulated by the hypothalamic-pituitary-gonadal (HPG) axis whereas the weaker androgens are synthesized in both sexes in the adrenal cortex, regulated by adrenocorticotropic hormone (ACTH). Testosterone mediates its action by binding to the nuclear androgen receptor (AR). Alternatively, it is reduced by 5α-reductase to 5α-DHT or is aromatized by aromatase to estradiol. ARs are expressed in androgen target tissues like prostate, skeletal muscle, liver, and central nervous system. Testosterone mainly binds to ARs located in muscles, brain, and bone marrow. 5α-DHT in contrast has a higher affinity to ARs located in prostate, skin and hair follicles [6].

Figure 4 illustrates different pathways of androgen biosynthesis starting from cholesterol via pregnenolone (PREG) resulting in dihydrotestosterone (5α-DHT). The so-called conventional 'front door pathway' proceeds via testosterone either through DHEA (Δ5 route) or through progesterone and androstenedione (4-ene-3-oxo or Δ4 route). In the 'backdoor pathway' 5α-DHT is generated via allopregnanolone, androsterone and

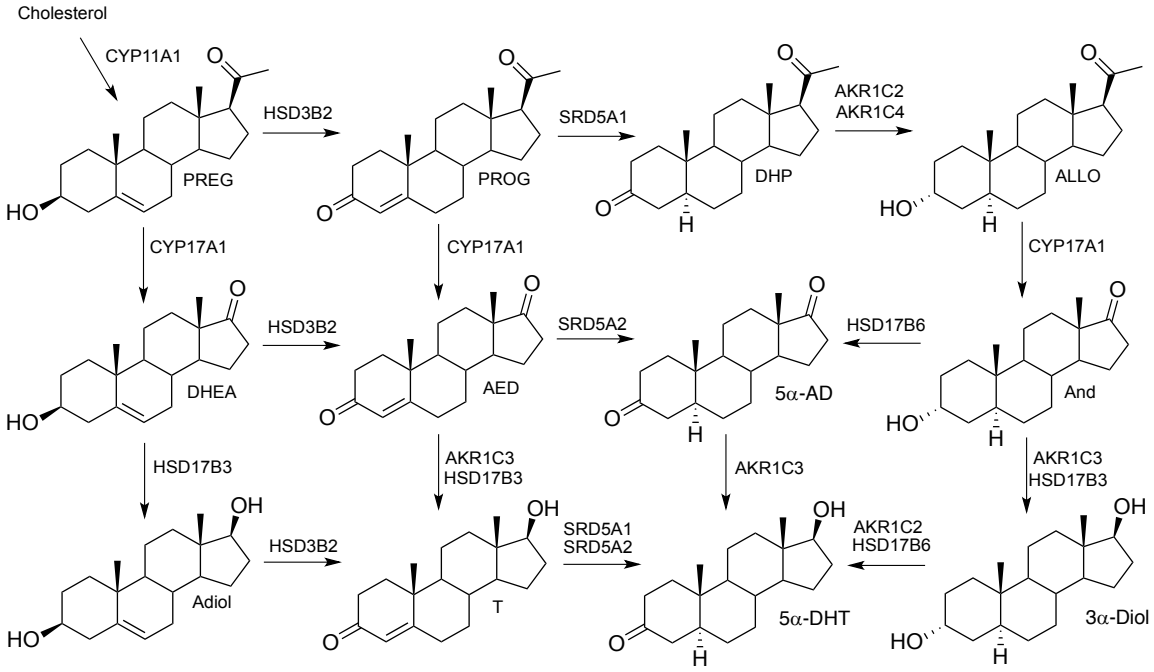

Figure 4 Biosynthetic pathways resulting in dihydrotestosterone and involved enzymes: pregnenolone (PREG), progesterone (PROG), dihydroprogesterone (DHP), allopregnanolone (ALLO), dehydroepiandrosterone (DHEA), androstenedione (AED), 5α-androstanedione (5α-AD), androsterone (And), androstenediol (Adiol), testosterone (T), 5α-dihydrotestosterone (5α-DHT), androstanediol (3α-Diol), hydroxysteroid dehydrogenase (HSD), aldo-keto reductase (AKR), SRD5A (5α-reductase), adapted from [7, 8]

androstanediol. Additionally, an 'alternative pathway' to 5α-DHT via 5α-androstanedione (5α-AD) is also possible [7, 9]. The androgens testosterone, androstenedione and 16α-hydroxyandrostenedione can be irreversibly aromatized by CYP19A1 (aromatase) and thereby transformed into the estrogens estradiol, estrone (as illustrated in Figure 2) and estriol respectively. Aromatase is expressed in granulosa cells, placenta, fat tissue, growing bones and in the brain. Estrogens are fundamental in the development of female sex charateristics, the regulation of the menstrual cycle, maintainance of pregnancy and also for spermatogenesis and sperm maturation [10]. Other sex steroids or corticosteroids are not further addressed here.

1.2.2 Exogenous steroids

Exogenous steroids are specified as anabolic androgenic steroids (AAS), prohormones, aromatase inhibitors, designer steroids and selective androgen receptor modulators (SARMs). AAS are chemically modified variations of testosterone and its active metabolite 5α-DHT. Their goal is to achieve a selectivity for anabolic rather than androgenic (side-)effects and to reduce metabolic conversion to ineffective metabolites and side effects causing estrogens. Some common chemical modifications are depicted in Figure 5.

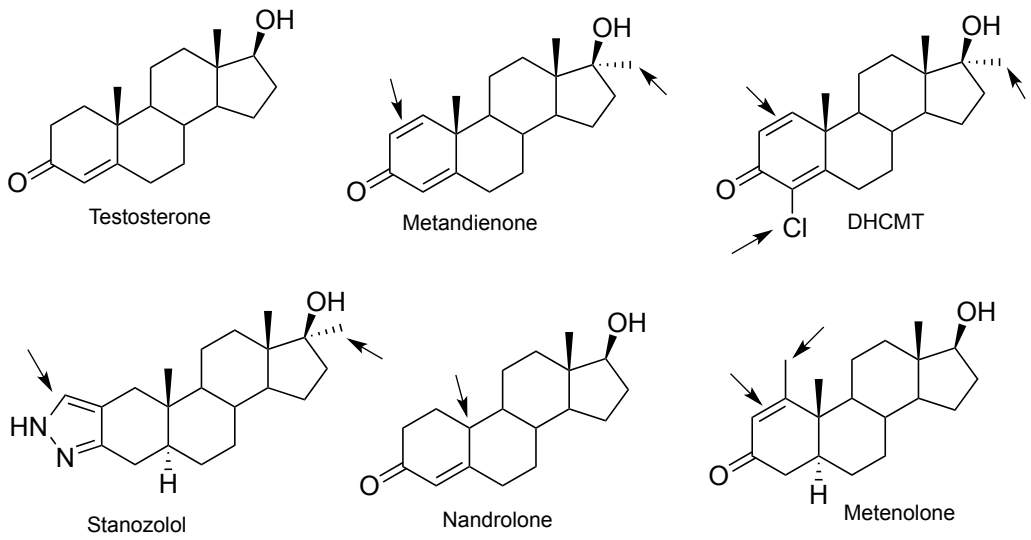

Figure 5 Chemical structures of testosterone and exemplary anabolic androgenic steroids, chemical modifications of the testosterone molecule are indicated with black arrows, DHCMT (dehydrochlormethyltestosterone)

17α-Methylation for example enables oral administration. Elimination of the C19 methyl group, C2-methylation or introduction of a 1,2-double bond hamper aromatization by aromatase and reduce estrogen related side effects [11]. Another possibility to avoid these side effects is to inhibit the responsible enzyme. Aromatase inhibitors are subgrouped in steroidal and non-steroidal inhibitors. Selective androgen receptor modulators (SARMs) are designed to primarily mediate anabolic effects, although no full separation has been achieved yet. Designer steroids comprise of synthetic anabolic androgenic steroids that have never been approved by any governmental agency and try to circumvent existing laws by further modifications of the molecule [12]. Prohormones are precursors of active hormones with only little intrinsic effects. Usually testosterone or nortestosterone are the desired active metabolic products, whereas most recently also prohormones of synthetic anabolic androgenic steroids became available.

These substances are most commonly illicitly distributed as nutritional supplements, mainly via the internet. Even cross contaminations of non-hormonal nutritional supplements with steroids have been reported in literature [13]. Unapproved substances, marketed in a poorly regulated way, together with the willingness of users to take supplements for anything bears an immense health risk [14, 15].

1.3 Metabolism

Most endogenous as well as nonessential exogenous compounds or so called xenobiotics undergo enzymatic biotransformation followed by excretion of their hydrophilic metabolites. Overall, metabolic reactions are divided in Phase I and Phase II reactions. Phase I metabolic reactions (biotransformation) include oxidation, hydroxylation, reduction, and hydrolysis. New functional groups are formed that aim towards more hydrophilic molecules and faster elimination. Phase II metabolism mostly consists of conjugation reactions. Glucuronosyltransferases (GLUT) are responsible for the process of glucuronidation, a major part of Phase II metabolism. It probably represents the most important pathway of the human body's elimination of the top 200 drugs [6]. Sulfation is performed by sulfotransferases (SULT). These enzymes catalyze the sulfate conjugation of primary and secondary alcohols including many hormones, neurotransmitters, and drugs.

1.3.1 Steroid hormones

Phase I metabolism of steroids is performed by different enzyme families: Monooxygenases from the cytochrome P450 enzyme (CYP) superfamily, oxidoreductases from the short-chain dehydrogenase reductase (SDR) superfamily and aldo-keto reductases (AKR). 5α-reductases are the only members of the polyprenol reductase family (isoenzymes SRD5A1-3). Phase II steroid metabolizing enzymes are sulfotransferases (SULT), glucuronosyl transferases (GLUT) and catechol-O-methyl transferases (COMT) [8]. The general metabolic pathway of endogenous androgens is displayed in Figure 4. Testosterone is metabolized in its target tissues or in the liver. In androgen target tissues testosterone is converted by 5α-reductase (SRD5A1) into its active metabolite 5α-DHT. A much smaller part is converted into estradiol by aromatase. These two steps are irreversible. In the liver metabolic oxidation/reduction to etiocholanolone and androsterone represents the main route of androgen Phase I metabolism, followed by glucuronidation and renal excretion [16]. Besides the illustrated metabolic steps (Figure 6) further reactions, also minor pathways resulting in hydroxylated metabolites, are possible.

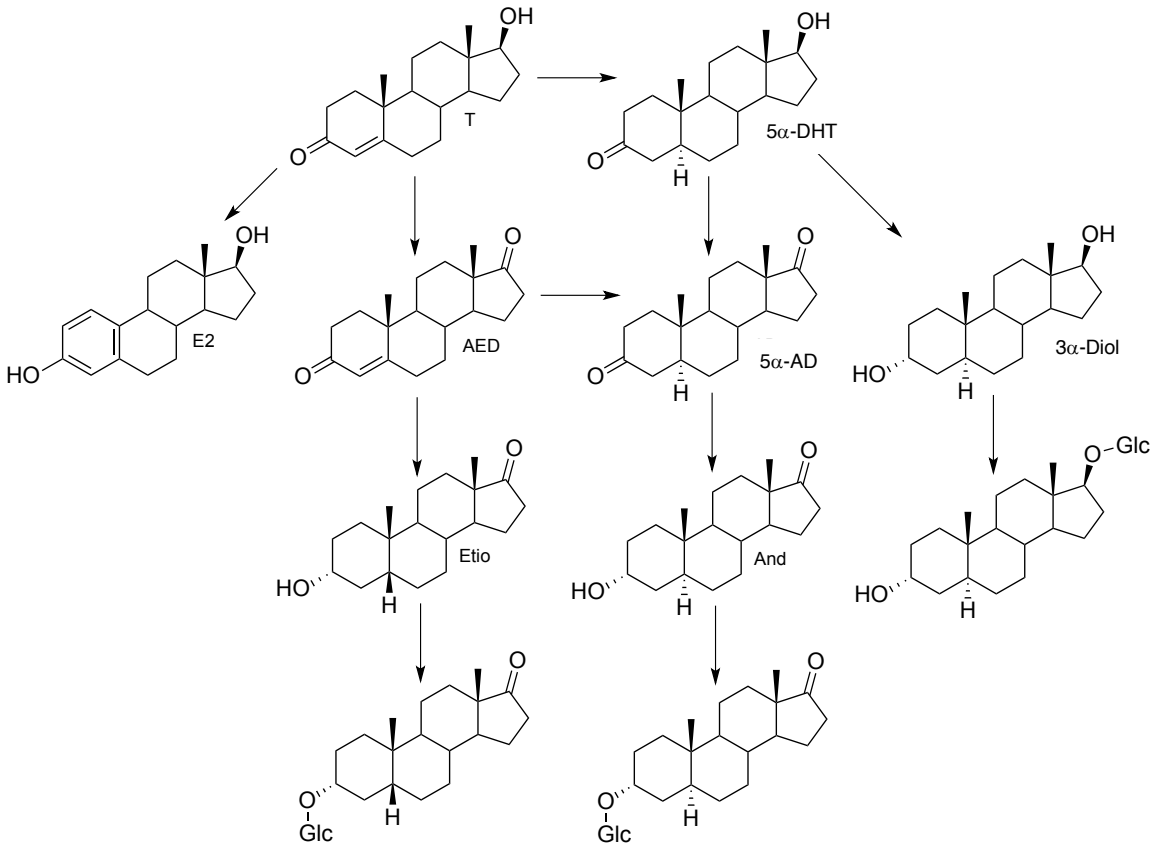

Figure 6 Androgen metabolism: testosterone (T), 5α-dihydrotestosterone (5α-DHT), estradiol (E2), androstenedione (AED), 5α-androstanedione (5α-AD), androstanediol (3α-Diol), etiocholanolone (Etio), androsterone (And), glucuronic acid (Glc), adapted from [6]

1.3.2 Anabolic androgenic steroids

Phase I and Phase II metabolism proceeds analogously for androstane derivatives and similar steroid hormones [12]. The metabolism of exogenous steroids has been intensively investigated. Besides drug metabolizing cytochrome P450 enzymes [17], and oxidoreductases [8], steroidogenic CYP enzymes [18] also play a role in the metabolic pathway of exogenously administered steroids. These could be AAS, designer steroids or endogenous relevant prohormones. Thus, Phase I metabolism mainly includes hydroxlations at different positions of the molecule as well as reductions or oxidations. Nevertheless, several hydroxylated metabolites are currently not monitored in standard steroidomic screenings because their value is underestimated.

1.4 Cytochrome P450 Enzyme System

The cytochrome P450 (CYP) enzyme system is responsible for the greater part of oxidation reactions in xenobiotic Phase I metabolism. These monooxygenases are located in the smooth endoplasmic reticulum of the liver and other extrahepatic tissues and consist of at least two proteins, a heme protein, and a flavoprotein called NADPH-CYP reductase. Their purpose is the insertion of a hydroxy group (mono-oxygenation) into an inactive substrate. This reaction involves NADPH and molecular oxygen:

$$R\text{-}H + NADPH + O_2 + H^+ \rightarrow R\text{-}OH + NADP^+ + H_2O$$

The oxygen is activated by the heme group and inserted into various substrates as illustrated in Table 1. The second oxygen atom is reduced to water which requires electrons provided by the CYP reductase. The current opinion is that the actual reactive species in the catalytic cycle of CYP enzymes is Compound I (Cpd I), an iron(IV)-oxo porphyrin radical cation as depicted in Figure 7 (a) [19].

Table 1 Reactions catalyzed by cytochrome P450 enzymes, facilitated by hydroxylation (adapted from [6])

Aromatic hydroxylation	$R\text{-}C_6H_5 \rightarrow R\text{-}C_6H_4\text{-}OH$
Aliphatic hydroxylation	$R\text{-}CH_3 \rightarrow R\text{-}CH_2\text{-}OH$
Deamination	$R\text{-}CH(NH_2)\text{-}R' \rightarrow R\text{-}CO\text{-}R' + NH_3$
O-Dealkylation	$R\text{-}O\text{-}CH_3 \rightarrow R\text{-}OH + CH_2O$
N-Dealkylation	$R\text{-}NH\text{-}CH_3 \rightarrow R\text{-}NH_2 + CH_2O$
N-Oxidation	$R_3\text{-}N \rightarrow R_3\text{-}NO + H^+$
Sulfoxidation	$R\text{-}S\text{-}R' \rightarrow R\text{-}SO\text{-}R' + H^+$

This reactive species is able to activate a CH bond by hydrogen abstraction and formation of an alkyl radical (Figure 7(b)). The following reorientation of the hydroxy group (Figure 7(c)) enables the formation of a CO bond, the oxygen rebound (Figure 7(d). The resulting oxygen-free complex accepts an electron and molecular oxygen yielding the oxy-ferrous complex in Figure 7(e). After reduction via another electron (Figure 7(f)) the protonation results in Compound 0 (Figure 7(g)) which ends up in the reactive Cpd I after elimination of water.

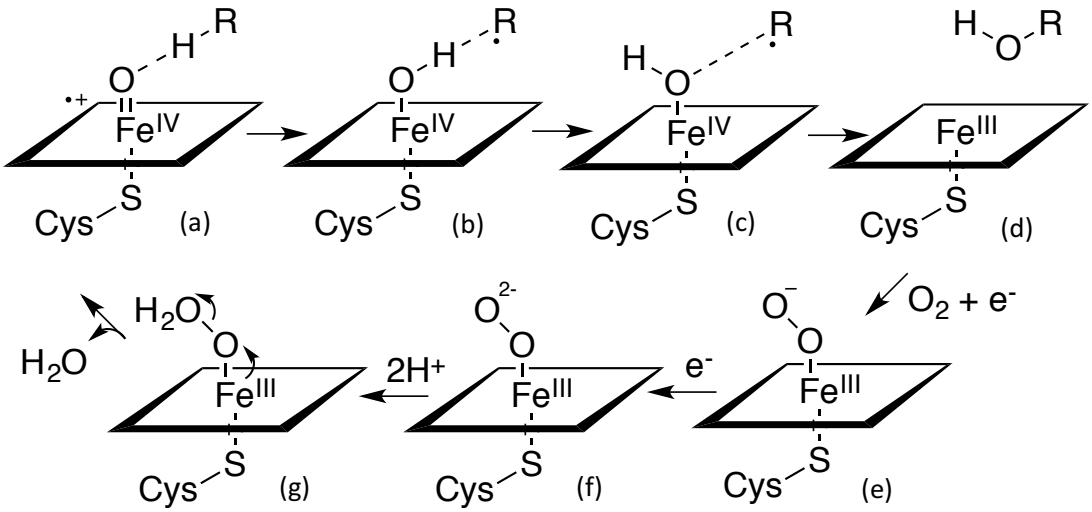

Figure 7 Catalytic cycle of Cytochrome P450, adapted from [20]

Besides the general xenobiotic metabolizing CYP enzymes, tissue specific steroidogenic CYP isoforms play an important role in the biosynthesis and metabolism of steroids. Two CYP enzymes are further discussed here: the steroidogenic CYP19A1 (aromatase), with a high substrate specificity and the capability of C19 hydroxylation. Additionally, CYP3A4 will be mentioned because of its enormous significance in xenobiotic metabolism in general.

1.4.1 CYP19A1

Aromatase (CYP19A1) is responsible for the biosynthesis of estrogens. This enzyme catalyzes the aromatization of the A ring of testosterone into estradiol and androstenedione into estrone respectively. The multi-step reaction probably includes the insertion of two hydroxy groups into carbon 19 and elimination of the whole group as formic acid concurrently as depicted in Figure 8. The first two steps in the aromatization reaction

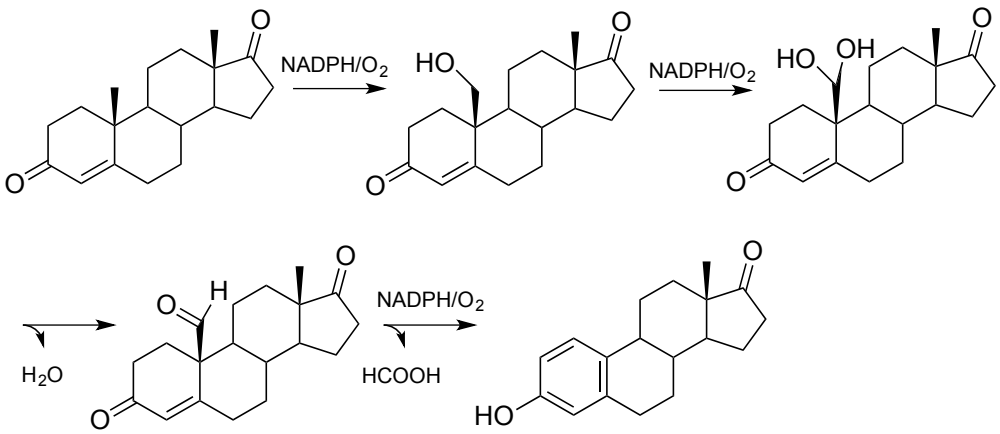

Figure 8 Aromatization of androstenedione to estrone by aromatase, each oxidative step consumes molecular oxygen (O_2) and NADPH, the C19 methyl group is eliminated as formic acid

involving 19-hydroxy and 19-aldehyde intermediates are probably proceeding via the usual hydrogen abstraction/oxygen rebound mechanism of CYP enzymes (see Figure 7) [21]. It is known that the two hydrogens at C1 and C2 are eliminated in the process [22]. The first hydroxylation step is possibly rate limiting [23]. The third step, however, is still under debate. Like in the first two steps it might also involve Compound I [24, 25] (Figure 9(II)), whereas the involvement of ferric peroxide (FeO_2^-) demonstrates another generally accepted mechanism (Figure 9(I)) [26].

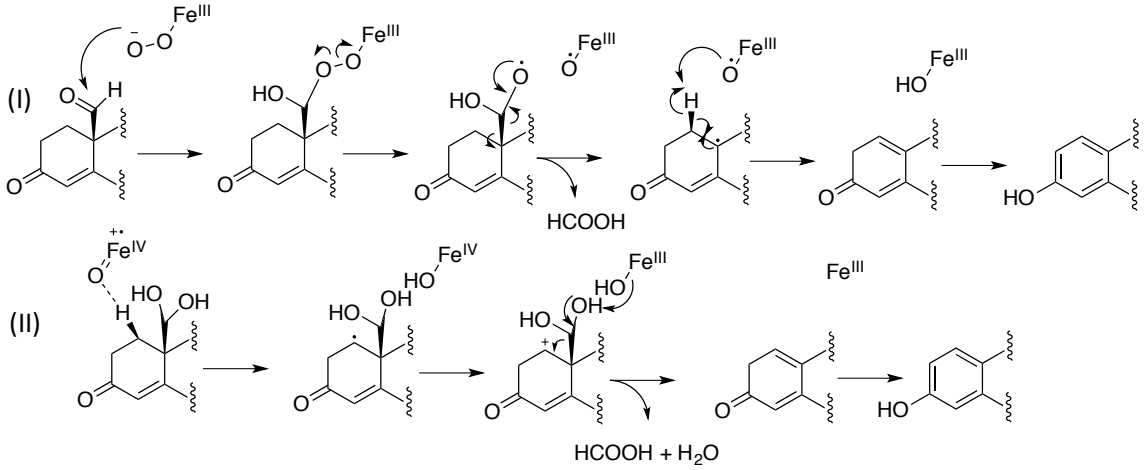

Figure 9 Proposed third step of the aromatization process showing the abstraction of 1βH by ferric peroxide (I) and alternatively by Compound I (II), adapted from [27]

In both cases the 1β-hydrogen atom is abstracted from the molecule and formic acid is released resulting in aromatization after enolization. The C19 methyl group and a β-directed C1-hydrogen seem to be crucial for the aromatization. CYP19A1 has a strict substrate specificity due to its tight active site which only accepts planar structures [28]. The angular C19 methyl group of its substrates androstenedione or testosterone is directed to the iron atom in the heme group [29].

1.4.2 CYP3A4

The most abundant xenobiotic metabolizing enzyme family CYP3A metabolizes the major part of exogenous substances. CYP3A4 represents the main isoenzyme with a low substrate specificity due to a large active site and therefore a loose binding of many substrates [28]. CYP3A4 is known to hydroxylate all different kinds of steroid hormones and in particular testosterone at positions 1β, 2α/β, 6α/β, 11α/β, 15α/β, 16β [28, 30] utilizing the above mentioned catalytic mechanism of CYP enzymes (Figure 7).

1.5 Steroid analysis

Today, steroid profiling is primarily performed utilizing GC-MS(/MS) or LC MS(/MS) based methods, both having their own advantages and disadvantages.

Steroid analysis using GC-MS is usually the method of choice [12, 31]. Effective separation of complex mixtures and high sensitivity is achieved at comparably low costs. For structure identification, especially in doping-related analyses trimethylsilylation (TMS) of steroids is usually performed prior to GC-MS measurements (see 3.2.2). The additional derivatization step enables a better chromatographic behavior and therefore an improved detection. Fragmentation of TMS derivatives after electron ionization shows characteristic fragmentation patterns which facilitate structure elucidation [32]. Tandem mass spectrometry (MS/MS) allows further fragmentation of obtained fragments and is mainly used for quantification of very low amounts of target analytes since the background noise is reduced. LC-MS(/MS) analysis is more and more applied in steroid profiling. Compared to GC-MS(/MS) often shorter run times are possible and the additional derivatization step is not necessarily needed. Additionally, it is possible to detect intact Phase II metabolites and formation of derivatization isomers can be excluded. However, it still can be useful for improving the sensitivity. Separation efficiency compared to GC on the other side is reduced significantly. High resolution accurate mass spectrometry (HRMS) is mainly utilized for an untargeted approach and represents a valuable tool for structure elucidation, especially in combination with tandem mass spectrometry. Nevertheless, targeted analysis is possible depending on the instrument.

2 Aim and objectives

1-Androstenedione (5α-androst-1-ene-3,17-dione, 1-AED, Figure 10), a prohormone of the designer steroid 1-testosterone (17β-hydroxy-5α-androst-1-en-3-one), is known to be a potent androgenic anabolic steroid [33]. Both steroids are listed on the World Anti-Doping Agency's list of prohibited substances [2]. The '1-ene' structure is a prominent structural attribute in various synthetic anabolic androgenic steroids (AAS), some of which have been marketed as dietary supplements (Table 2).

Table 2 Recent findings of designer steroids with an '1-ene' structure in nutritional supplements

Trivial name	Chemical name (IUPAC)	References
1-AD, 1-AED	5α-Androst-1-ene-3,17-dione	[34]
1-DHEA, 1-Androsterone	3β-Hydroxy-5α-androst-1-en-17-one	[35-37]
-	5α-Androst-1-ene-3β,17β-diol	[37]
-	5β-Androst-1-ene-3β,17β-diol	[38]
-	5β-Androst-1-ene-3α,17β-diol	[38]
Methylstenbolone	17β-Hydroxy-2,17α-dimethyl-5α-androst-1-en-3-one	[39-41]
-	17β-Hydroxy-17α-methyl-5α-androst-1-en-3-one	[42]

Analogously to the endogenous androgens testosterone and androstenedione (AED, Figure 6), 1-androstenedione is metabolized to 1-testosterone and vice versa. Further urinary metabolites following 1-AED administration are mainly reduced species (3α-hydroxy-5α-androst-1-en-17-one, as the main metabolite detectable up to eight days, 3β-hydroxy-5α-androst-1-en-17-one, 5α-androst-1-ene-3α,17β-diol, and 5α-androst-1-ene-3β,17β-diol) [43]. Doping control samples positively tested for 1-AED administration describe an increasing trend in last the years as depicted in Figure 7. Only recently, on 29th august 2016, Russian athlete Tatyana Firova was found guilty for committing an anti-doping rule violation. She was tested positive for 3α-hydroxy-5α-androst-1-en-17-one, a metabolite of 1-testosterone, 1-androstenedione, and 1-androstenediol [44].

Various hydroxylated metabolites of endogenous and exogenous steroids are described in literature. Earlier studies on 1-AED metabolism proposed the additional formation of hydroxylated metabolites. Based on mass spectrometric data hydroxylation of the angular methyl groups (C18 and C19) was suggested [36, 43].

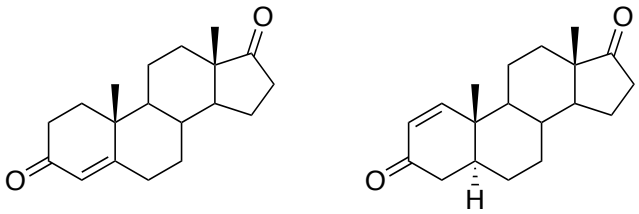

Figure 10 Chemical structures of endogenous prohormone androst-4-ene-3,17-dione (AED, left) and exogenous designer steroid 5α-androst-1-ene-3,17-dione (1-AED, right)

Besides synthetic AAS, endogenous prohormones such as AED are misused as performance enhancing drugs (PED's) and as well prohibited by WADA rules. Although the administration of AED results in an altered steroid profile [45], IRMS (isotope-ratio mass spectrometry) analysis is often required to distinguish between endogenous formation and exogenous administration. Moreover, several hydroxylated metabolites are reported after AED administration [46, 47]. Knowledge of these minor metabolic pathways contributes to a better discrimination [48]. Very recently, it has been reported that 2α-hydroxyandrost-4-ene-3,17-dione is a specific metabolite of AED that permits to extend the detection window for AED administration [49]. The possibility of 2α- and 2β-hydroxylation of closely related testosterone by different CYP enzymes [50, 51] raises the question if 2β-hydroxyandrost-4-ene-3,17-dione would be a valuable minor metabolite, too. The involvement of steroidogenic CYP enzymes (CYP11A1) in the *in vitro* formation of 2β-hydroxyandrost-4-ene-3,17-dione has been reported recently [52].

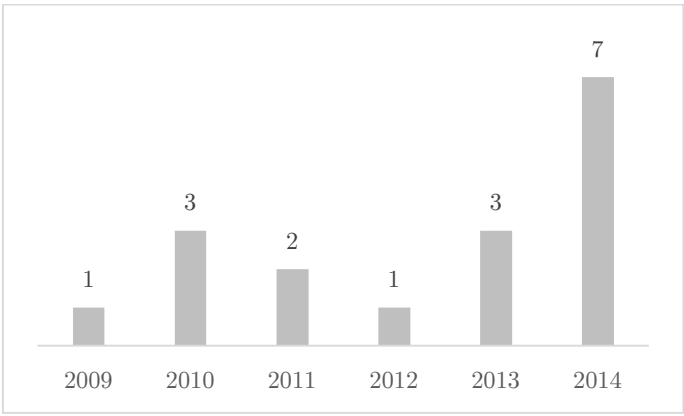

Figure 11 Number of adverse analytical findings of 1-AED reported by WADA laboratories from 2009-2014

Detailed investigation of these metabolites may reveal promising insights in uncommon metabolic pathways of exogenously administered steroids with respect to doping control purposes as well as understanding of steroid metabolism in general. Overall, the aim of this thesis was to identify hydroxylated Phase I metabolites of anabolic androgenic steroids with special regard to metabolic hydroxylation at the angular methyl groups of 1-AED (chapter 4.1) and closely related androstane derivatives (chapter 4.3). Additionally, the endogenous prohormone AED was investigated concerning the possibility of 2β-hydroxylation (chapter 4.2). Therefore, chemical synthesis of reference substances, *in vitro* biotransformation with CYP enzymes of interest, and investigation of *in vivo* formation after administration of the precursors were conducted.

3 Material and Methods

3.1 Material

3.1.1 Instruments

Table 3 Analytical instruments

NMR Bruker Advance DRX 500	Bruker
Agilent 7890A gas chromatograph	Agilent Technologies (Santa Clara)
Agilent 7890B gas chromatograph	Agilent Technologies (Santa Clara)
Agilent 5975C mass spectrometer	Agilent Technologies (Santa Clara)
Agilent 7200 accurate mass Q-TOF	Agilent Technologies (Santa Clara)
Agilent 1290 Infinity II	Agilent Technologies (Santa Clara)
Agilent 6550 iFunnel Q-TOF	Agilent Technologies (Santa Clara)
Agilent 1100 HPLC with Agilent 1100 fraction collector	Agilent Technologies (Santa Clara)
HPLC 1090 Series II	Hewlett Packard

Table 4 GC and LC columns

HP-Ultra 1 (17 m, 0.200 mm, 0.11 µm)	Agilent Technologies (Santa Clara)
Zorbax Eclipse plus Phenyl-Hexyl (5 cm, 2.1 mm, 1.8 µm)	Agilent Technologies (Santa Clara)
Discovery C18 column Supelco (25 cm, 4.6 mm, 5 µm)	Sigma-Aldrich (Milan)
VP 250/10 Nucleosil 100-7 C18 (25 cm, 10 mm, 7 µm)	Macherey Nagel (Düren)

Table 5 Miscellaneous instruments

Sample concentrator	Techne (Staffordshire)
LaboStar 2-DI/-UV ultrapure water system	SG Wasseraufbereitung und Regenerierstation GmbH (Barsbüttel).

Additionally, the usual laboratory glass ware has been utilized together with further laboratory equipment (e.g. centrifuge, drying oven).

3.1.2 Chemicals

Table 6 Steroid reference substances

19-Hydroxyandrost-4-ene-3,17-dione (19OH-AED)	Sigma Aldrich (Taufkirchen)
5α-Androst-1-ene-3,17-dione (1-AED)	Steraloids (Newport)
Androst-4-ene-3,17-dione (AED)	Sigma Aldrich (Taufkirchen), Molekula (Garching)
2α-Hydroxyandrost-4-ene-3-17-dione 2αOH-AED)	Sigma (Milan), Steraloids (Newport)
4-Hydroxyandrost-4-ene-3,17-dione (4OH-AED)	Sigma (Milan), Steraloids (Newport)
6α-Hydroxyandroist-4-ene-3,17-dione (6αOH-AED)	Sigma (Milan), Steraloids (Newport)
6β-Hydroxyandrost-4-ene-3,17-dione (6βOH-AED)	Sigma (Milan), Steraloids (Newport)
16α-Hydroxyandrost-4-ene-3,17-dione (16αOH-AED)	Sigma (Milan), Steraloids (Newport)
3,17-Dioxoandrost-4-ene-19-al (19oxo-AED)	Sigma (Milan), Steraloids (Newport)
Androsta-1,4-diene-3,17-dione (ADD)	Sigma (Milan), Steraloids (Newport)

17β-Hydroxyandrosta-1,4-diene-3,17-dione (BOLD)	Sigma (Milan), Steraloids (Newport)
17β-Hydroxy-5α-androst-1-en-3,17-one (1-T)	Sigma (Milan), Steraloids (Newport)
17α-Methyl-17β-hydroxyandrost-4-en-3-one (MT)	Sigma (Milan), Steraloids (Newport)
17α-Methyl-6β,17β-dihydroxyandrost-4-ene-3,17-dione (6βOH-MT)	Sigma (Milan), Steraloids (Newport)
17β-Hydroxy-5β-androstan-3-one	Sigma (Milan), Steraloids (Newport)
17β-Hydroxyandrosta-4,6-dien-3-one	Sigma (Milan), Steraloids (Newport)
3Hydroxyestra-1,3,5(10),6-tetraene-17-one	Sigma (Milan), Steraloids (Newport)
Estradiol	Sigma (Milan), Steraloids (Newport)
Estrone	Sigma (Milan), Steraloids (Newport)
Estrendione	Sigma (Milan), Steraloids (Newport)
17β-Hydroxy-5α-androstan-3-one (DHT)	Sigma (Milan), Steraloids (Newport)
5α-Androstane-3,17-dioen (5α-AD)	Sigma (Milan), Steraloids (Newport)

Table 7 Reagents, solvents and materials

Acetone	VWR (Dresden)
Acetonitrile	Fisher (Schwerte), VWR (Dresden)
Ammonium iodide	Sigma Aldrich (Taufkirchen)
Argon	Air liquide (Düsseldorf)
β-Glucuronidase from Escherichia coli (>140 U/mL)	Roche Diagnostics (Mannheim)
Cyclohexene	Sigma Aldrich (Taufkirchen)
CYP3A4	BD Bioscience (Milan)
Dimethyl formamide	Merck (Darmstadt)
DMSO	Merck (Darmstadt)
Ethanethiole	Sigma Aldrich (Taufkirchen)
Ethanol	VWR (Dresden)

Ethyl acetate	VWR (Dresden)
Formic acid, LC-MS grade	Sigma-Aldrich (Taufkirchen)
Glacial acetic acid	Merck (Darmstadt)
Helium	Air liquide (Düsseldorf)
HLM pooled from 50 donors	BD Bioscience (Milan)
Human CYP19 (aromatase) + oxidoreductase	Corning Supersomes (New York)
Hydrogen gas	Air liquide (Düsseldorf)
Hydrogen peroxide 30 %	Sigma Aldrich (Taufkirchen)
Imidazole	Sigma Aldrich (Taufkirchen)
Iodic acid	Sigma Aldrich (Taufkirchen)
Methanol	Fisher (Schwerte), VWR (Dresden)
Methylene chloride	VWR (Dresden)
MSTFA	Chemische Fabrik Karl Bucher, (Waldstetten)
NADPH regenerating system solution A	Corning Gentest (New York)
NADPH regenerating system solution B	Corning Gentest (New York)
Nitrogen	Air liquide (Düsseldorf)
Palladium charcoal 10 %	Sigma Aldrich (Taufkirchen)
Phosphate-buffer-system 0.5 M	BD Bioscience (Milan)
Potassium carbonate	Sigma Aldrich (Taufkirchen)
Potassium hydrogencarbonate	Sigma Aldrich (Taufkirchen)
Potassium iodide	Sigma Aldrich (Taufkirchen)
Sodium hydroxide	Sigma Aldrich (Taufkirchen)
Sulfuric acid 96 %	Merck (Darmstadt)
TBDMSCl	Sigma Aldrich (Taufkirchen)
TBME	Applichem (Darmstadt)
Tetrabutylammonium fluoride	Sigma Aldrich (Taufkirchen)
Tetrahydrofuran	Sigma Aldrich (Taufkirchen)

3.2 Methods

3.2.1 GC-MS and GC-MS/MS

In this study the greater part of the performed analyses was carried out using gas chromatographic separation and mass spectrometric detection after electron ionization of either derivatized or underivatized analytes.

3.2.1.1 Derivatization for gas chromatography

Derivatization of steroids for GC analysis was performed using two different derivatization methods. On the one hand per-TMS (trimethylsilyl) formation was achieved using N-methyl-N-(trimethylsilyl)trifluoracetamide (MSTFA) together with ammonium iodide and ethanethiol, MSTFA/NH_4I/ethanethiol (1000:2:3, v/w/v), as introduced by Donike and Geyer [53, 54]. In this derivatization procedure hydroxy groups of a molecule are transformed into the corresponding trimethylsily ethers and oxo groups are converted into TMS enol ethers after enolization. The actual derivatization proceeds via the reactive TMIS (trimethyliodosilane) that is formed *in-situ* from MSTFA and ammonium iodide as displayed in Figure 8. Ethanethiol reacts with the formed iodine and converts it into hydrogen iodide to prevent possible reactions of iodine with the molecule. MSTFA additionally acts as the solvent in this reaction.

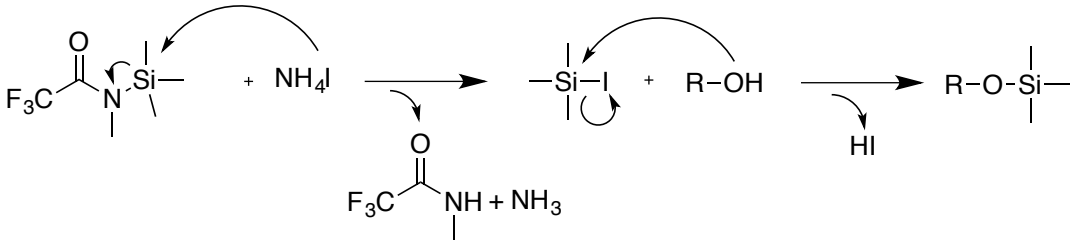

Figure 14 Generation of TMIS in-situ from MSTFA and ammonium iodide and successive trimethylsilylation of a primary alcohol to the corresponding TMS ether, R=alkyl

Derivatization using MSTFA alone on the other hand (without any catalysts) results in TMS ethers of hydroxy groups only. Oxo groups or sterically hindered hydroxy groups are not derivatized with MSTFA. 6β-Hydroxyandrost-4-ene-3,17-dione exemplarily illustrates the different possible TMS derivatives resulting from both derivatization methods. The obtained tris-TMS and mono-TMS derivatives are depicted in Figure 14 and Figure 15 respectively.

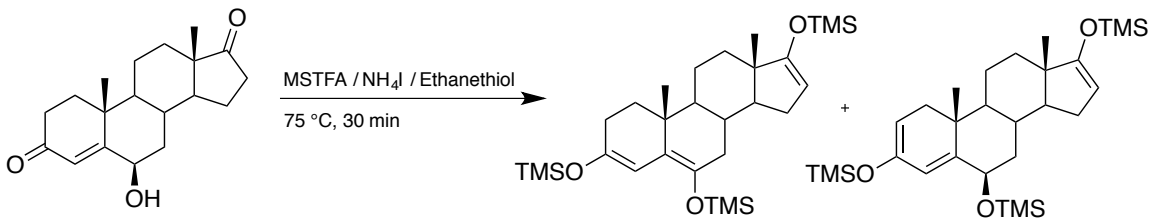

Figure 15 Derivatization of 6β-hydroxyandrost-4-ene-3,17-dione with TMIS resulting in the two derivatization isomers 3,5,16-triene-3,6,17-triol tris-TMS (>99 %) and 2,4,16-triene-3,6β,17-triol tris-TMS (<1 %)

Utilizing TMIS the formation of derivatization isomers is possible. In case of 3-oxo-4-ene steroids the main derivatization isomer is the 3,5-diene derivative (usually >99 %). Moreover, due to enolization it is possible to loose stereochemical information. The 3,5,16-triene-3,6,17-triol tris-TMS derivative of 6β-hydroxyandrost-4-ene-3,17-dione could alternatively result from the corresponding α-isomer. Thus, a differentiation of the isomers after derivatization is not possible. Derivatization of mono-hydroxylated AED yields the mono-TMS derivative using MSTFA. Accordingly, mono-hydroxylated testosterone would result in the corresponding bis-TMS.

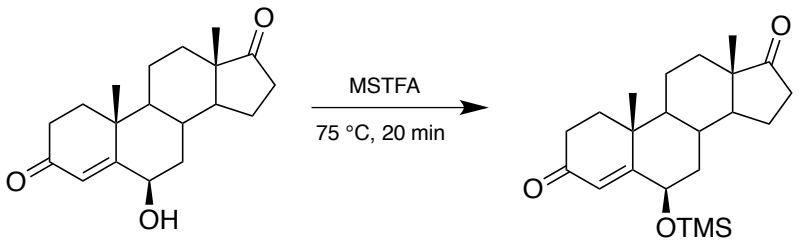

Figure 16 Derivatization of 6β-hydroxyandrost-4-ene-3,17-dione with MSTFA resulting in the mono-TMS derivative

Before derivatization the samples were dried under nitrogen at 75 °C. Then, either 50 µL TMIS reagent (MSTFA/NH_4I/ethanethiol, 1000:2:3, v/w/v) or 50 µL MSTFA were added and incubated at 75 °C for 30 min or 20 min.

3.2.1.2 GC-MS(/MS) conditions

A GC-MS instrument equipped with single quadrupole mass selective detector (Agilent 6975C MSD) and, for high resolution accurate mass spectrometry and GC-MS/MS experiments, a GC-QTOF-MS instrument (Agilent 7720 accurate mass QTOF) have been utilized. Both mass spectrometric devices were equipped with an electron ionization (EI) source. The different gas chromatographic methods were both operating with the same type of column but an adjusted oven temperature program. Detailed information on various fundamental parameters of the different applied methods are listed below (Table 8, Table 9, Table 10).

Table 8 GC-MS parameters, method a)

Device	Agilent 7890A gas chromatograph, Agilent 5975C mass selective detector (MSD)
Column	Agilent HP1-Ultra (17 m, 200 µm, 0,11 µm)
Injection volume	2 µL
Carrier gas	Helium
Flow rate	1 mL/min, constant flow
Inlet parameters	Split injection 1:16, inlet temperature 300 °C
Oven temperature program	183 °C, 3 °C/min to 232 °C, 40 °C/min to 310 °C (2 min hold)
Ionization	Electron ionization, 70 eV at 250 °C
Data acquisition	Full scan mode 40-1000 m/z

Table 9 GC-QTOF-MS parameters, method b)

Device	Agilent 7890B gas chromatograph, Agilent 7720 accurate mass QTOF
Column	Agilent HP1 (17 m, 200 µm, 0,11 µm)
Injection volume	2 µL
Carrier gas	Helium
Flow rate	1 mL/min, constant flow
Inlet parameters	Split injection 1:20, inlet temperature 280 °C
Oven temperature program	150 °C, 50 °C/min to 240 °C, 3 °C/min to 266 °C, 50 °C/min to 320 °C (2 min hold)
Ionization	Electron ionization, 70 eV at 250 °C
MS	Full scan mode m/z 50-750, scan speed 200ms/spectrum

Table 10 GC-QTOF-MS/MS parameters, method c)

Device	Agilent 7890B gas chromatograph, Agilent 7720 accurate mass QTOF
Column	Agilent HP1 (17 m, 200 µm, 0,11 µm)
Injection volume	2 µL
Carrier gas	Helium
Flow rate	1 mL/min, constant flow
Inlet parameters	Split injection 1:20, inlet temperature 280 °C
Oven temperature program	150 °C, 50 °C/min to 240 °C, 3 °C/min to 266 °C, 50 °C/min to 320 °C (2 min hold)
Ionization	Electron ionization 70 eV at 250 °C
MS	Full scan mode m/z 50-750, scan speed 200ms/spectrum, Collision energy 25 eV

3.2.2 LC-MS(/MS) and LC-UV

The LC-QTOF system was used for accurate mass measurements and MS/MS experiments of underivatized steroids. The MS/MS method e) used the same chromatographic conditions of method d).

3.2.2.1 LC-MS(/MS) conditions

Table 11 HPLC-QTOF-MS parameters, method d)

Device	Agilent 1290 Infinity II HPLC, Agilent 6550 iFunnel accurate mass QTOF
Column	Zorbax Eclipse plus Phenyl-Hexyl (5 cm x 2.1 mm, 1.8 µm)
Injection volume	1 µL
Solvent A	0.1 % formic acid in water
Solvent B	acetonitrile
Gradient	5 % B for 0.5 min, 45 % B 7 min, 95 % B at 11 min, 1 min hold
Flow rate	0.400 mL/min
MS parameters	VCap 3000 V Nozzle Voltage (V) 500 Fragmentor 365 V Gas Temp 200°C Gas Flow 13 L/min Nebulizer 30 psig SheathGasTemp 375 °C SheathGasFlow 11 L/min Mass range 50-1000

Table 12 HPLC-QTOF-MS/MS parameters, method e)

MS/MS parameters	precursor m/z 303 Collision energy 20 eV

3.2.2.2 LC-UV conditions

HPLC UV and fraction collection

Two different HPLC instruments were used for separation of synthesized steroids with subsequent fraction collection. For separation on an analytical scale method g) and on a semipreparative scale method f) have been utilized.

Table 13 HPLC fractionation, method f)

Device	HP 1090 HPLC
Column	VP 250/10 Nucleosil 100-7 C18
Injection volume	10 µL
Solvent A	water
Solvent B	acetonitrile
Gradient	50 % B for 25 min
Flow rate	4 mL/min
Fractions	peak based, collected manually
UV-DAD	192 nm

Table 14 HPLC fractionation, method g)

Device	Agilent 1100 HPLC, Agilent 1100 Fraction collector, Dioden array detector
Column	Supelco Discovery C18 (25 cm, 4.6 mm, 5 µm)
Injection volume	5 µL
Solvent A	water
Solvent B	acetonitrile
Gradient	10 % B to 55 % B in 55 min at 38 °C
Flow rate	1 mL/min
Fractions	time dependent, 36.80 min – 37.15 min, 37.59 min – 37.93 min
UV-DAD	192 nm

3.2.3 Synthesis of reference substances

3.2.3.1 19-Hydroxy-5α-androst-1-ene-3,17-dione

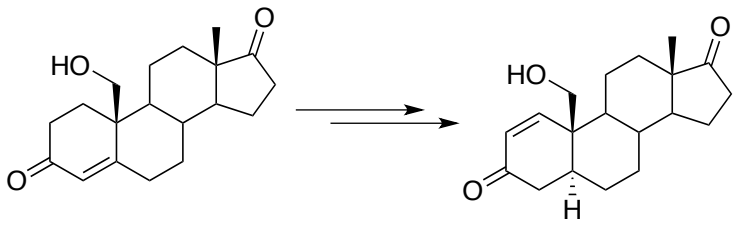

Figure 17 Chemical structures of desired product 19-hydroxy-5α-androst-1-ene-3,17-dione (right) and starting material 19-hydroxyandrost-4-ene-3,17-dione (left)

19-Hydroxy-5α-androst-1-ene-3,17-dione was synthesized in four steps starting from 19-hydroxyandrost-4-ene-3,17-dione. 153 mg (0.51 mmol) 19-Hydroxy-androst-4-ene-3,17-dione were dissolved in 1.5 mL dry DMF under inert gas (argon) atmosphere. 78 mg (0.52 mmol) tertiary butyldimethylsilyl chloride (TBDMSCl) and 68 mg (1.0 mmol) imidazole were added in one portion and stirred at room temperature for 1.5 h. 10 mL water were added and extracted three times with 2 mL TBME. The organic layers were combined and evaporated under reduced pressure.

The resulting white solid was dissolved in 5 mL ethyl acetate and 15.8 mg 10 % palladium on charcoal was suspended in the solvent. The system was flushed with hydrogen gas and stirred under normal pressure for 18 h. The suspension was filtered and the solvent was evaporated under reduced pressure.

Iodic acid (127 mg) was dissolved in 0.75 mL dimethyl sulfoxide and heated for 60 min at 80 °C. 0.25 mL of this mixture together with 65 µL cyclohexene and 50 mg product were added to the mixture and stirred for 5 h at 80 °C.

The protection group was cleaved using 75 mg tetrabutylammonium fluoride in 2 mL THF by stirring at room temperature for 1 h. The mixture was poured into 2 mL water and extracted 3 times with 3 mL methylene chloride. The combined organic layers were evaporated under reduced pressure to yield 8 mg after HPLC separation (total yield 5.2 %).

3.2.3.2 2β-Hydroxyandrost-4-ene-3,17-dione

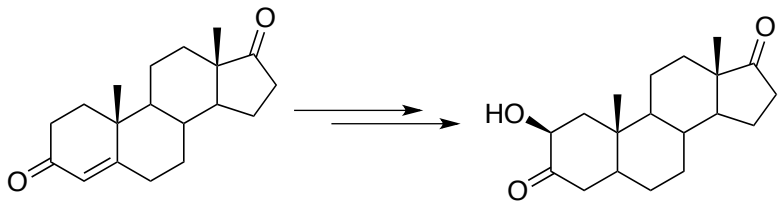

Figure 18 Chemical structures of desired product 2β-hydroxyandrost-4ene-3,17-dione (right) and starting material androst-4-ene-3,17-dione (left)

2β-Hydroxyandrost-4-ene-3,17-dione was synthesized starting from androst-4-ene-3,17-dione [55]. 1,450 g (5.4 mmol) androst-4-ene-3,17-dione were dissolved in 100 mL methanol at 0 °C. Solutions of 2,2 mL sodium hydroxide (6 N) and 1,7 mL hydrogen peroxide 30 % were slowly added dropwise. The reaction was stopped after 4 h. After dilution with 35 mL water the solution was extracted with TBME (3 x 100 mL). The organic phases were combined, washed with 50 mL water and 50 mL potassium iodide solution 5 %. The organic layer was separated and evaporated under reduced pressure yielding 1,2855 g (89 %) white product.

The white residue was dissolved in 50 mL acetone and 3 mL of sulfuric acid 25 % were added dropwise. The reaction was stopped after 65 h. After adding 60 mL of water the solution was extracted three times with 150 mL TBME. The combined ether phases were washed with 120 mL water and evaporated under reduced pressure.

Column chromatography (silica gel, column height 40 cm, diameter 3 cm) was used to separate 4-hydroxyandrost-ene-3,17-dione and other byproducts from the desired 2ξ-hydroxy derivatives using n-hexane : ethyl acetate (40:60) yielding 538 mg (37 %).

Further separation was performed by HPLC fractionation using method g).

3.2.4 Structure confirmation

Structure identification of the synthesized reference substances 19-hydroxy-5α-androst-1-ene-3,17-dione and 2β-hydroxyandrost-4-ene-3,17-dione was performed using nuclear magnetic resonance spectroscopy (NMR) and/or high resolution accurate mass spectrometry (HRMS).

3.2.4.1 NMR

For NMR structure elucidation a Bruker Avance II 600 instrument equipped with a 5 mm inverse probehead with actively shieled z-gradient coil was used. The spectra were recorded at 600 MHz (^{1}H) and 125 MHz (^{13}C) at 298 K using deuterated chloroform as solvent. For confirmation of the structure ^{1}H-, DEPT- (Distortionless Enhancement by Polarization Transfer), H,H-COSY- (Homonuclear Correlation Spectroscopy) spectra were measured together with H,C-HMQC (Heteronuclear Multiple Quantum Coherence), H,C-HMBC (Hetero Multiple Bond Correlation) and NOESY (Nuclear Overhauser Enhancement Spectroscopy) experiments.

3.2.4.2 HRMS

Analysis of the target compounds by high resolution accurate mass spectrometry was achieved utilizing quadrupole-time-of-flight (QTOF) mass spectrometric instruments (Agilent 7720 accurate mass QTOF and Agilent 6550 iFunnel accurate mass QTOF).

High mass accuracy can be achieved by a high mass resolution (to ensure that interfering ions are not overlapping) together with frequent mass calibration [56]. Due to the TOF analyzer a high resolution is achieved (>10.000). Mass axis calibration was performed permanently (LC-QTOF) or after each run (GC-QTOF). Mass accuracy was determined and is given for each accurate mass spectrum as ppm value in the subtitles for the corresponding molecular ion $[M]^{\bullet+}$ if not stated otherwise.

3.2.5 Incubation experiments

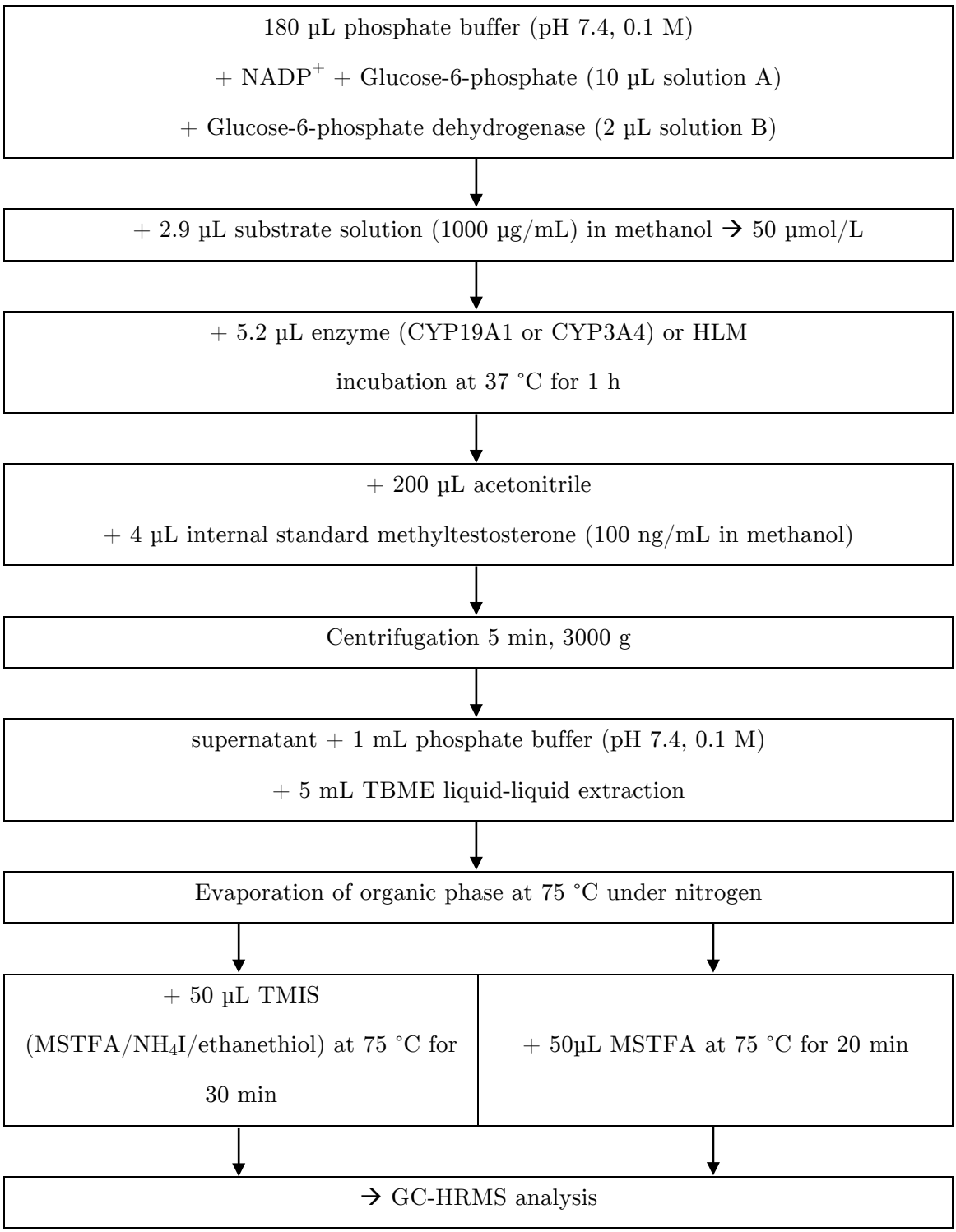

Figure 19 Incubation protocol, adapted from Kuuranne et al [57]

In an alternative incubation experiment with a final substrate concentration of 10 µmol/L all volumes were multiplied by 3 and the amount substrate solution was adjusted to 1.7 µL.

With every incubation experiment a control sample without any enzyme was prepared as well. Chromatograms of the reference substances were investigated carefully considering trace amounts of byproducts already present in the standard solutions. Contaminations of reference substances were reported before [58].

3.2.6 Urine analysis

The sample preparation protocol for the urine samples followed the usual steps used in routine doping control analysis. Potentially glucuronated phase II metabolites were cleaved with β-glucuronidase and analyzed together with the free fraction.

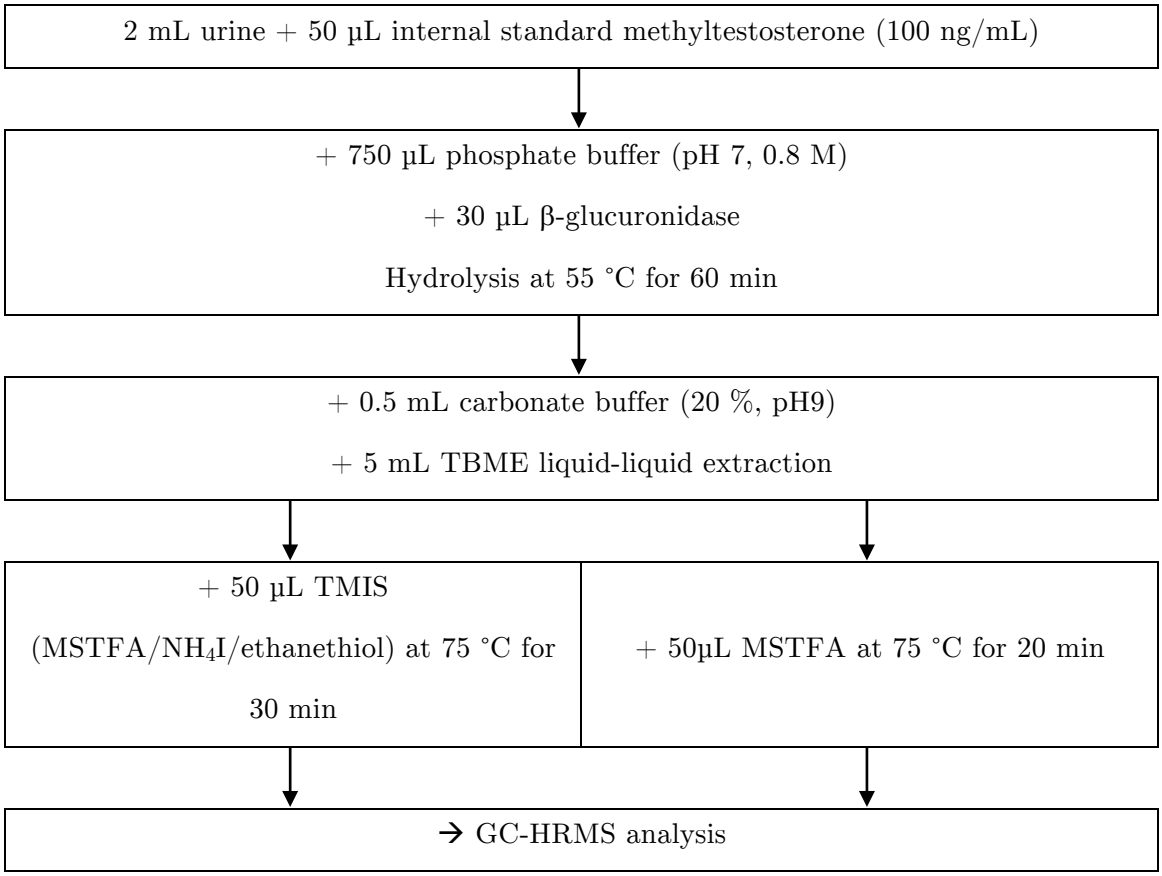

Figure 20 Sample preparation protocol for urine analysis

3.2.7 Data analysis

The obtained data files, acquired using methods a)-e) described in section 3.2.1, were analyzed with Agilent MassHunter Qualitative Analysis (Version B.07.00).

Chromatographic data illustrated in this work are either displayed as total ion chromatograms (TIC), as base peak chromatograms (BCP) or extracted ion chromatograms (EIC). In case of EICs, the corresponding extracted accurate m/z value is specified in the subtitles to clarify on which ion(s) a certain chromatogram is based on. Most of the EIC's discussed in this study represent mono-hydroxylated metabolites of androstane derivatives after trimethylsilylation. After electron ionization (EI) the mass spectra of hydroxylated androstane derivatives often lack characteristic abundant fragments beside the molecular ion $[M]^{\bullet+}$. However, in some cases the loss of a methyl group, $[M\text{-}CH_3]^+$, yields abundant base peaks.

In case of mono-hydroxylated metabolites the molecular ions $[M]^{\bullet+}$ ranged from m/z 516-524 and for $[M\text{-}CH_3]^+$ from m/z 501-509 respectively. Therefore, the exact masses of possible mono-hydroxylated metabolites as tri-TMS derivatives were calculated. The term 'extracted ion chromatogram of mono-hydroxylated metabolites' is defined here as the combined EIC of the following mass/z values: 446.3031, 501.2671, 503.2828, 505.2984 507.3141, 509.3297, 516.2906, 518.3062, 520.3219, 522.3375, 524.3532. The m/z value 446.3031 is the molecular ion of the internal standard methyltestosterone as bis-TMS. In case of 'di-hydroxylated metabolites' following m/z values have been selected: 446.3031, 589.3015, 591.3172, 593.3328, 595.3485, 597.3641, 604.3250, 606.3407, 608.3563, 610.3720, 612.3876.

4 Results and discussion

4.1 19-Hydroxylation of 5α-androst-1-ene-3,17-dione

4.1.1 Synthesis of reference material

19-Hydroxy-5α-androst-1-ene-3,17-dione (5) was synthesized starting from commercially available 19-hydroxyandrost-4-ene-3,17-dione (1) as displayed in Figure 19. In the following chapter the different intermediate products are characterized particularly with regard to their mass spectra obtained by GC-EI-MS since full structural identification was exclusively carried out for the desired end product, 19-hydroxylated 5α-androst-1-ene-3,17-dione. Derivatization utilizing TMIS yields two isomers of which the 3,5-diene derivative represents the most abundant one (ratio 0.1:99.9); the corresponding accurate mass spectrum is displayed in Figure 20. GC-EI-MS measurement of underivatized starting material 19-hydroxyandrost-4-ene-3,17-dione gave a peak with a molecular ion of m/z 272 (mass spectrum in Figure 68). Probably because of instability towards the heat in the GC inlet, the molecule may lose the C19 hydroxymethylene group. The most likely structure would be norandrostenedione (estr-4-ene-3,17-dione) which could be confirmed by comparison with authentical reference material. Thus, mainly derivatized steroids are used in this study.

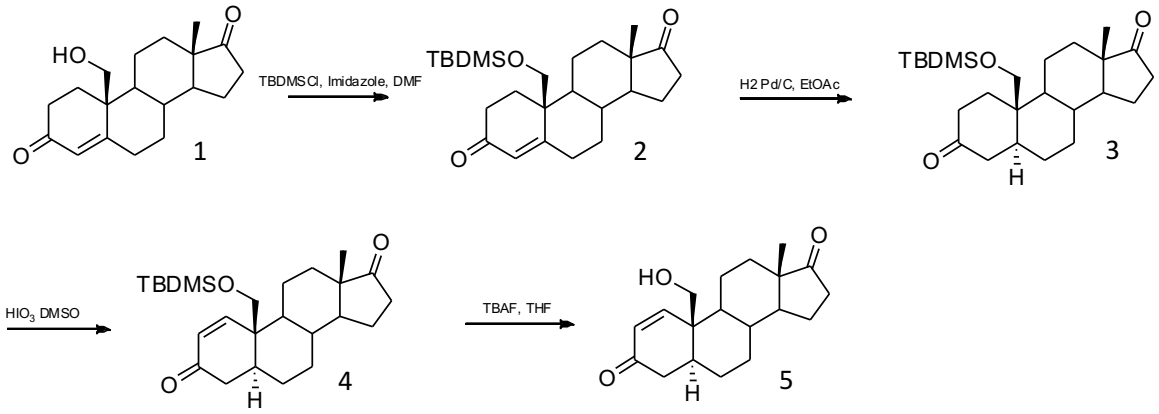

Figure 19 Overall chemical synthesis of 19-hydroxy-5α-androst-1-ene-3,17-dione (5) in four steps starting from 19-hydroxyandrost-4-ene-3,17-dione (1)

Beside the molecular ion $[M]^{\bullet+}$=518.3046 only a few abundant fragments are observed. The loss of 103.0579 Da is characteristic for trimethylsilylated primary alcohols and can most likely be explained with the fragment $[CH_2OTMS]^{\bullet}$ (theoretical mass 103,0574 Da) resulting in m/z 415.2451 $[M\text{-}103.0579]^{+}$ (assignment of further fragments in Table 15).

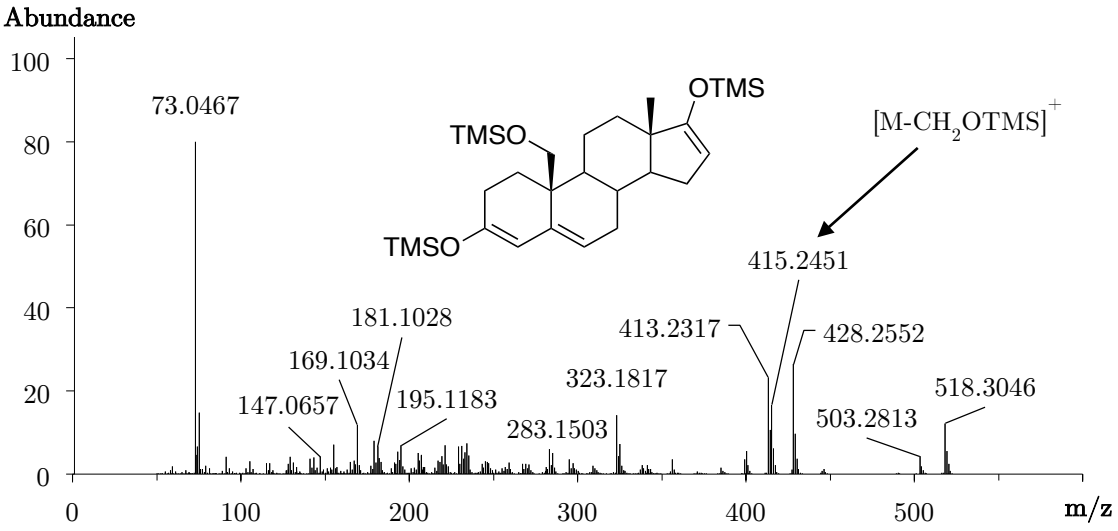

Figure 20 Accurate mass spectrum (EI) of 19-hydroxyandrost-4-ene-3,17-dione (1), 3,5,16-triene-3,17,19-triol tris-TMS, indicated is the mass loss of 103.0579 Da, $[M]^{\bullet+}$=518.3046, mass error 1.78 ppm

Another example for this characteristic mass loss is given in Figure 69 showing trimethylsilylated 19-hydroxytestosterone (17β,19-dihydroxyandrost-4-en-3-one) with the molecular ion $[M]^{\bullet+}$=520.3222 and its fragment at m/z 417.2622 due to the same mass loss. In the corresponding mono-TMS derivative of 19-hydroxyandrost-4-ene-3,17-dione (1), obtained after derivatization with MSTFA, on the other hand, the corresponding ionic fragment is clearly visible as an abundant peak at m/z 103.0578 (mass spectrum in Figure 70).

Table 15 Postulated, exemplary fragments of pertrimethylsilylated 19-hydroxyandrost-4-ene-3,17-dione (1) with their exact masses and mass errors, [1)] mass not labelled in Figure 16

Postulated fragment	Exact mass	Theoretical mass	mass error [ppm]
$[M]^{+\bullet}$	518.3046	518.3062	-3.09
$[M\text{-}CH_3]^+$	503.2813	503.2833	-3.97
$[M\text{-}TMSOH]^{+\bullet}$	428.2552	428.2567	-3.50
$[M\text{-}CH_2OTMS]^+$	415.2451	415.2483	-7.71
$[M\text{-}TMSOH\text{-}CH_3]^+$	413.2317	413.2327	-2.42
$[M\text{-}CH_2OTMS\text{-}CH_3]^{+\bullet}$	400.2226[1)]	400.2254	-7.00
$[M\text{-}2TMSOH\text{-}CH_3]^+$	323.1817	323.1826	-2.78
$[C_{18}H_{23}OSi]^+$	283.1503	283.1513	-3.53
$[TMSOSi(CH_3)_2]^+$	147.0657	147.0656	0.68

19-hydroxy-5α-androst-1-ene-3,17-dione (5) was already postulated by NMR analysis as a metabolite of 3β-acetoxycholest-5-en-19-ol after incubation with isolated soil bacterium Moraxella [59]. Nevertheless, chemical synthesis of the compound was not described in this study. Later, it was characterized as an intermediate in the chemical synthesis of potential aromatase inhibitors (information on NMR analysis see Table 17) [60]. The steps of the synthesis starting from 19-hydroxyandrost-4-ene-3,17-dione (1) described therein were adopted and partially adjusted as described before (chapter 3.2.3.1).

As first step of the synthesis, hydrogenation of the 4,5-double bond of 19-hydroxyandrost-4-ene-3,17-dione (1), was initially tested with lithium in ethylene diamine. This resulted in a mixture of three isomers after derivatization. Probably the 5α and 5β isomers and an additional derivatization isomer, since 5β-androstanes tend to form the 2-enol TMS to a greater extend. Using hydrogen gas and palladium charcoal instead, the assumed 5β isomers were still present in the reaction mixture as a byproducts (Figure 71). Therefore, the introduction of the TBDMS ether at the primary alcohol in position 19 was done prior to the hydrogenation. The bulky residue directed the hydrogenation towards the desired 5α isomer. Knox et al showed that introducing protection groups into the primary alcohol in 19 position, the ratio of beta to alpha isomers favored the 5α-formation [61]. This first reaction step yielded 19-TBDMSO-androst-4-ene-3,17-dione (2). The introduction of the silyl ether was achieved

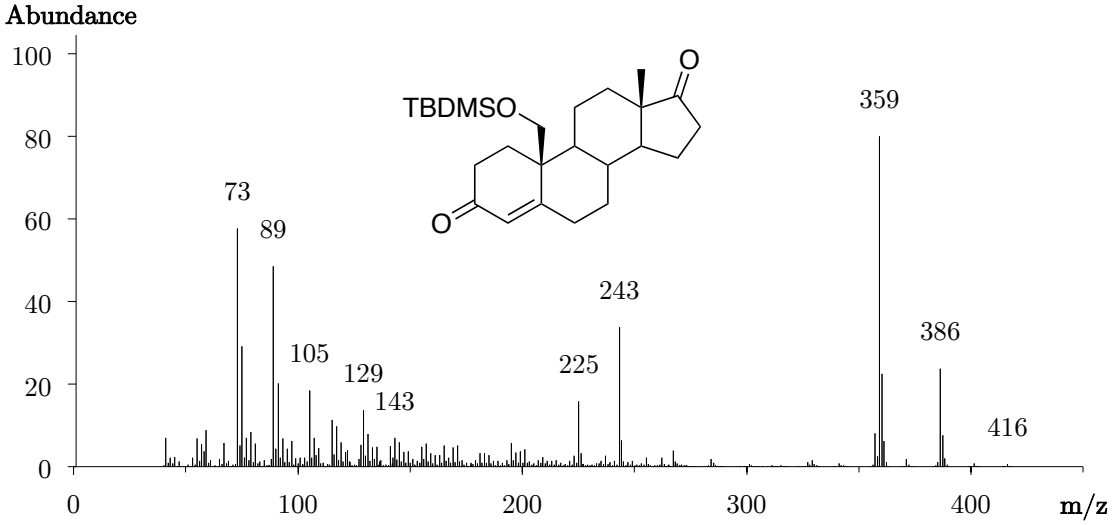

Figure 21 Mass spectrum (EI) of 19-TBDMSO-androst-4-ene-3,17-dione (2), $[M]^{\bullet+}$=416, base peak $[M-C_4H_9]^+$=359

using an excess of tertiary butyldimethylsilyl chloride in dry DMF. The molecular ion ($[M]^{\bullet+}$=416) of the underivatized product (2) is almost not abundant in the mass spectrum (Figure 21). Due to a mass loss of 57 Da, typical for the loss of a tertiary butyl

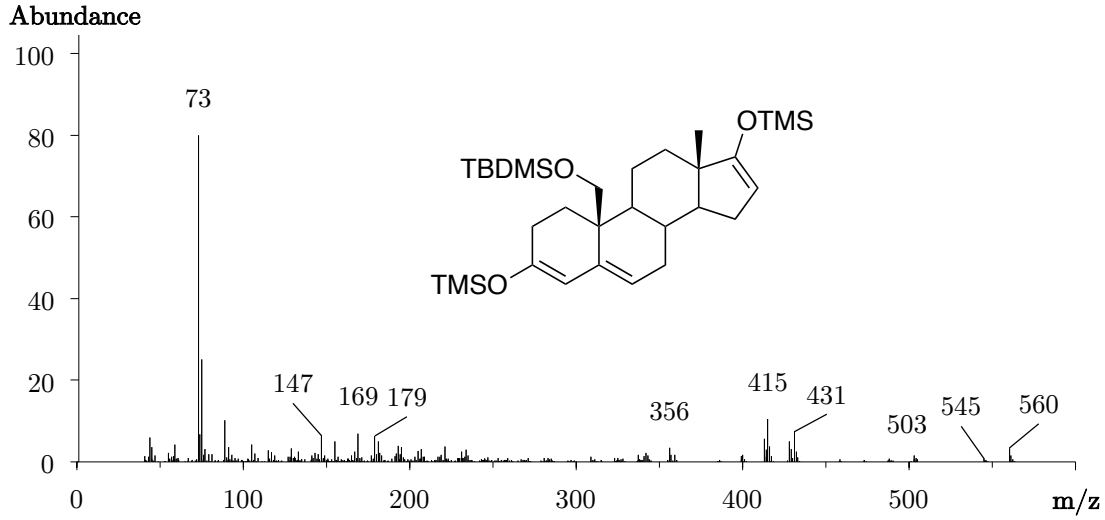

Figure 22 Mass spectrum (EI) of 19-TBDMSO-androst-4-ene-3,17-dione (2), 3,5,16-triene-3,17-diol bis-TMS, $[M]^{\bullet+}$=560

moiety, the base peak of 19-TBDMSO-androst-4-ene-3,17-dione (2) results in m/z 359 $[M\text{-}C_4H_9]^+$. The bis-TMS derivative of (2) is displayed in Figure 22 with the molecular ion $[M]^{\bullet+}$=560. The corresponding chromatogram showed the two derivatization isomers (Figure 72). Clearly visible fragments are m/z 415, probably $[M\text{-}CH_2OTBDMS]^+$, and m/z 147, which may be explained by the fragment $[(CH_3)_3OSi(CH_3)_2]^+$ resulting from the migration of one TMS group. Less abundant fragments are at m/z 545, $[M\text{-}CH_3]^+$, or m/z 503, $[M\text{-}C_4H_9]^+$.

Hydrogenation under the previously mentioned conditions (chapter 3.2.3.1) resulted almost exclusively in the 5α-isomer, 19-TBDMSO-5α-androstane-3,17-dione (3), with a molecular ion $[M]^{\bullet+}$=562 as bis-TMS derivative (chromatogram of reaction products see Figure 73). Its mass spectrum is shown in Figure 23 with a base peak at m/z 505, again showing the loss of 57 Da from the molecular ion $[M\text{-}C_4H_9]^+$. The loss of a methyl group (resulting fragment $[M\text{-}CH_3]^+$ at m/z 547) and the successive losses of $[C_4H_9]^{\bullet}$ and [TMSOH] resulting in m/z 415 are two more examples of fragment generation.

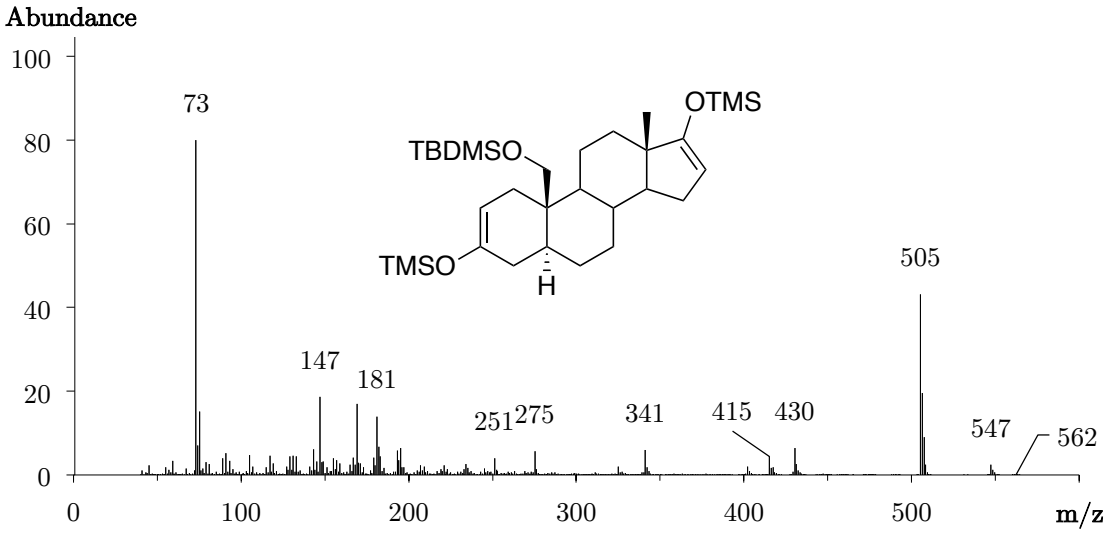

Figure 23 Mass spectrum (EI) of 19-TBDMSO-5α-androstane-3,17-dione (3), 2,16-diene-3,17-diol bis-TMS, $[M]^{\bullet+}$=562

The underivatized hydrogenation product (3) ($[M]^{\bullet+}$=418, mass spectrum in Figure 24) also shows a base peak after loss of the tertiary butyl moiety $[M\text{-}C_4H_9]^+$ at m/z 361. The fragment at m/z 145 may indicate the CH_2OTBDMS group ($[C_7H_{17}OSi]^+$).

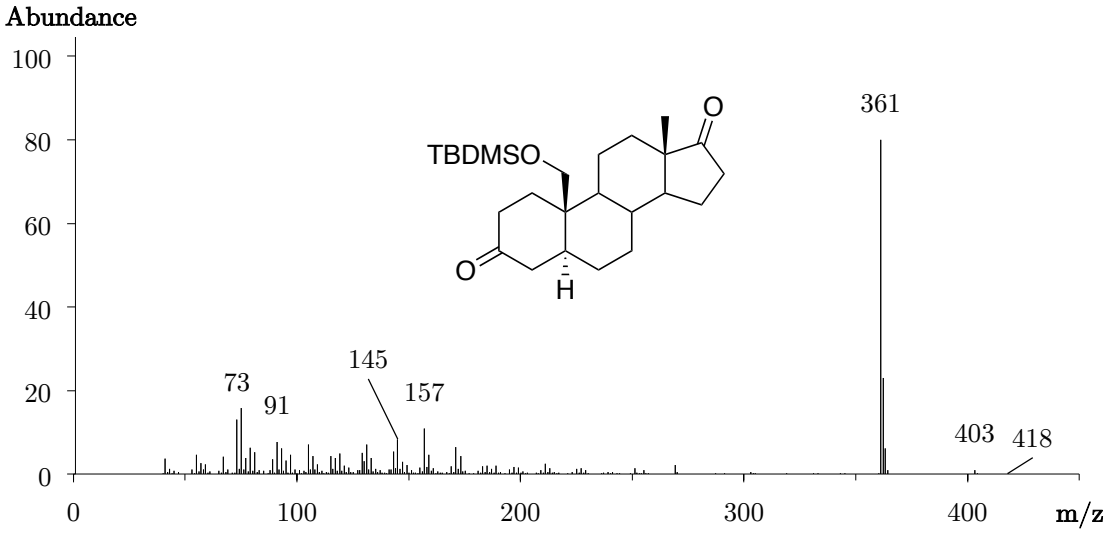

Figure 24 Mass spectrum (EI) of 19-TBDMSO-5α-androstane-3,17-dione (3), $[M]^{\bullet+}$=418, base peak $[M\text{-}C_4H_9]^+$=361

For the introduction of the 1,2-double bond HIO_3·DMSO (a complex formed *in situ*) was preferably used as an oxidation reagent as described by Nicolaou et al. [62]. They showed that iodic acid was a sufficient alternative for IBX (2-iodoxybenzoic acid) in the α,β-dehydrogenation of ketones and demonstrated this with the introduction of a 1,2-double bond into 5α-androstane-3,17-dione and dihydrotestosterone resulting in

1-androstenedione and 1-testosterone respectively obtaining comparably high yields as using IBX [63]. The proposed mechanism is displayed in Figure 25. Both described methods are reported to favor the six membered A ring of the steroid molecule rather than the five membered D ring.

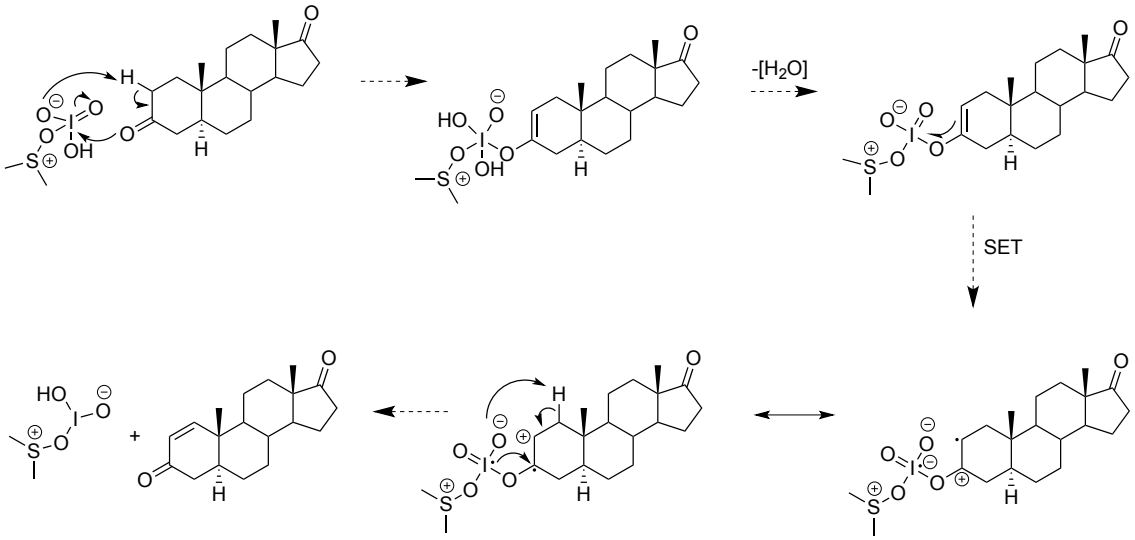

Figure 25 Postulated mechanism of action of dehydrogenation using HIO_3·DMSO, exemplified by 5α-androstane-3,17-dione, adapted from [62], SET (single electrone transfer)

The chromatogram showing the different products of the oxidation step without any derivatization (Figure 74) gave three peaks with the same molecular ions $[M]^{\bullet+}$=416. They were assigned to 19-TBDMSO-5α-androst-1-ene-3,17-dione (4, RT=17.60 min) and the two derivatization isomers (RT=17.38 min and 17.92 min) of remaining or newly formed

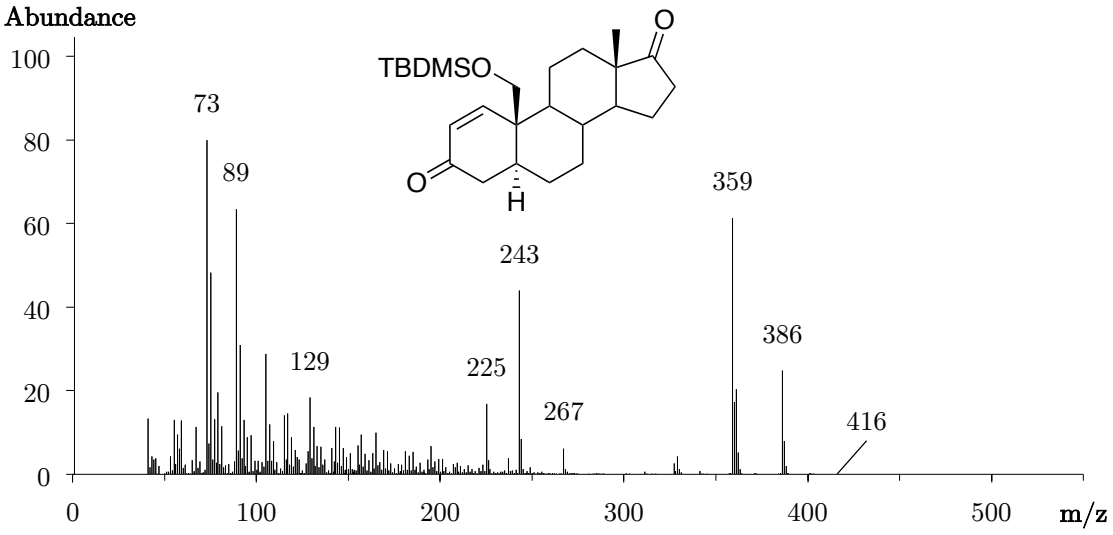

Figure 26 Mass spectrum (EI) of 19-TBDMSO-5α-androst-1-ene-3,17-dione (4), $[M]^{\bullet+}$=416

19-TBDMSO-androst-4-ene-3,17-dione (2). The mass spectra of (4) are displayed in Figure 26 (underivatized) and Figure 27 (as bis-TMS derivatives).

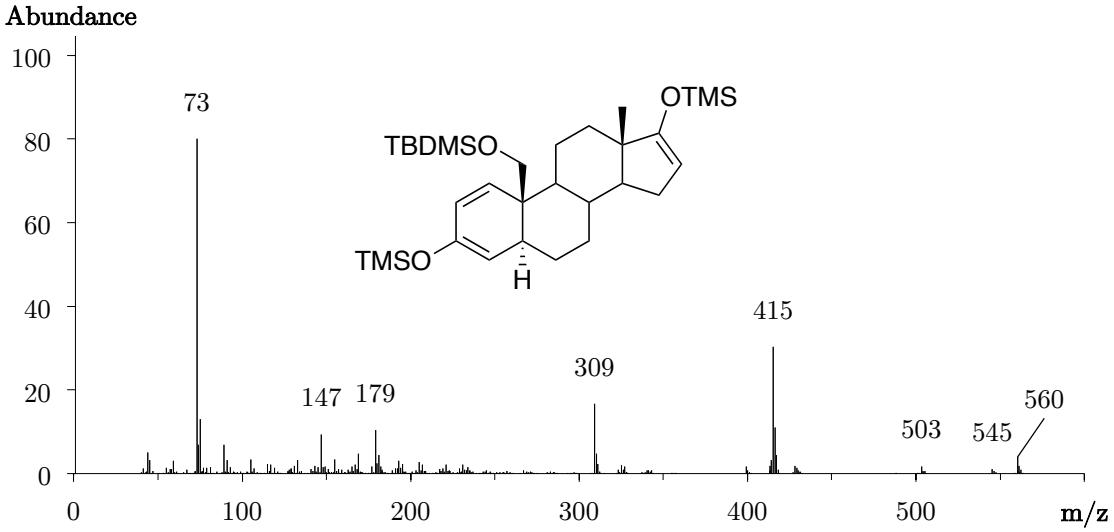

Figure 27 Mass spectrum (EI) of 19-TBDMSO-5α-androst-1-ene-3,17-dione (4), 1,3,16-triene-3,17-diol bis-TMS, $[M]^{\bullet+}$= 560

As a final reaction step the TBDMS ether was cleaved using tetrabutylammonium fluoride in THF. Monitoring the progress of the deprotection using TMIS as derivatization reagent for GC-EI-MS analysis proved to be somewhat difficult. Because the reactive TMIS seems to be able to replace the apparent TBDMS group, and underivatized sample measurement was not possible due to artifact generation the real amount of deprotected tris-TMS derivative (4) could not be stated. Hence, the reaction was stopped after a certain time and the products were separated by HPLC method f). The fractions were investigated with GC-EI-MS after derivatization (see tris-TMS derivative Figure 75) since measurement of underivatized product, 19-hydroxy-5α-androst-1-ene-3,17-dione (5), did not show the expected ion of m/z 302. As described above for 19-hydroxyandrost-4-ene-3,17-dione (1), the resulting peak indicated the m/z 272 respectively which could be analogue '1-norandrostenedione' (5α-estr-1-ene-3,17-dione, mass spectrum in Figure 76).

The structural identification of synthesized 19-hydroxy-5α-androst-1-ene-3,17-dione (5) was determined by accurate mass spectrometry using GC-EI-QTOF-MS, HPLC-ESI-QTOF-MS, and NMR experiments. Following TMIS derivatization the molecular mass was determined at $[M]^{+\bullet}$=518.3036, which is assigned to $C_{28}H_{50}O_3Si_3$ (expected m/z 518.3062, mass error 0.19 ppm). The characteristic loss of 103.0573 Da from

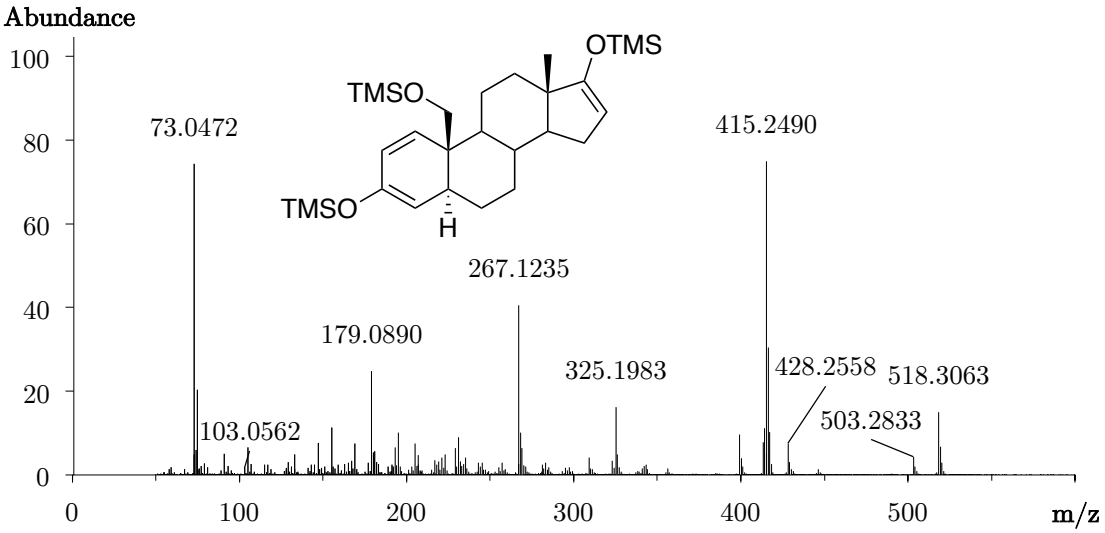

Figure 28 Accurate mass spectrum (EI) of synthesized 19-hydroxy-5α-androst-1-ene-3,17-dione (5), 1,3,16–triene 3,17,19-triol tris-TMS, $[M]^{\bullet+}$=518.3063, mass error 0.19 ppm, indicated is the mass loss of 103.0573 Da

the molecular ion m/z 518.3063 resulted in the base peak at m/z 415.2490 (mass spectrum in Figure 28). The corresponding chromatogram did not show any derivatization isomers which is likely because 2- and 3,5-enol tautomerization, as for androst-4-ene derivatives, is not possible. The obtained fragments are listed below (Table 16).

Table 16 Postulated fragments of 19-hydroxy-5a-androst-1-ene-3,17-dione and their exact masses and mass errors

Postulated fragment	Exact mass	Theoretical mass	mass error [ppm]
$[M]^{+\bullet}$	518.3063	518.3062	0.19
$[M\text{-}CH_3]^{+}$	503.2833	503.2833	0.00
$[M\text{-}TMSOH]^{+\bullet}$	428.2558	428.2567	-2.10
$[M\text{-}CH_2OTMS]^{+}$	415.2490	415.2483	1.69
$[M\text{-}CH_2OTMS\text{-}TMSOH]^{+}$	325.1983	325.1982	0.31
$[C_{13}H_{23}O_2Si_2]^{+\bullet}$	267.1235	267.1231	1.50
$[C_{10}H_{15}OSi]^{+\bullet}$	179.0890	179.0887	1.68
$[CH_2OTMS]^{+\bullet}$	103.0562	103.0574	-11.64

The corresponding mono-TMS derivative of 19-hydroxy-5α-androst-1-ene-3,17-dione (5) was obtained by derivatization with MSTFA only. The relating accurate mass spectrum (EI) shows an abundant fragment at m/z 103.0572 (theoretical mass of $[CH_2OTMS]^+$=103.0574, mass error, -1.94 ppm) and not primarily its mass loss as is the case for the tris-TMS derivative (Figure 28). The base peak at m/z 344.2176 may result from $[M\text{-}CH_2O]^{+\bullet}$ due to a migration from the TMS group of the 19-alcohol to the 3-oxo group as described by Smith et al [64]. A subsequent loss of $[CH_3]^\bullet$ may explain m/z 329.1935 $[M\text{-}CH_2O\text{-}CH_3]^+$. Following the before mentioned migration and loss of $[CH_2O]$ the observed fragment m/z 180.0973 may result from $[C_{10}H_{16}OSi]^{+\bullet}$ (theoretical m/z 180.0970, mass error 1.67 ppm) which consists of the A,B ring fragment including carbon 6 (as indicated in Figure 29).

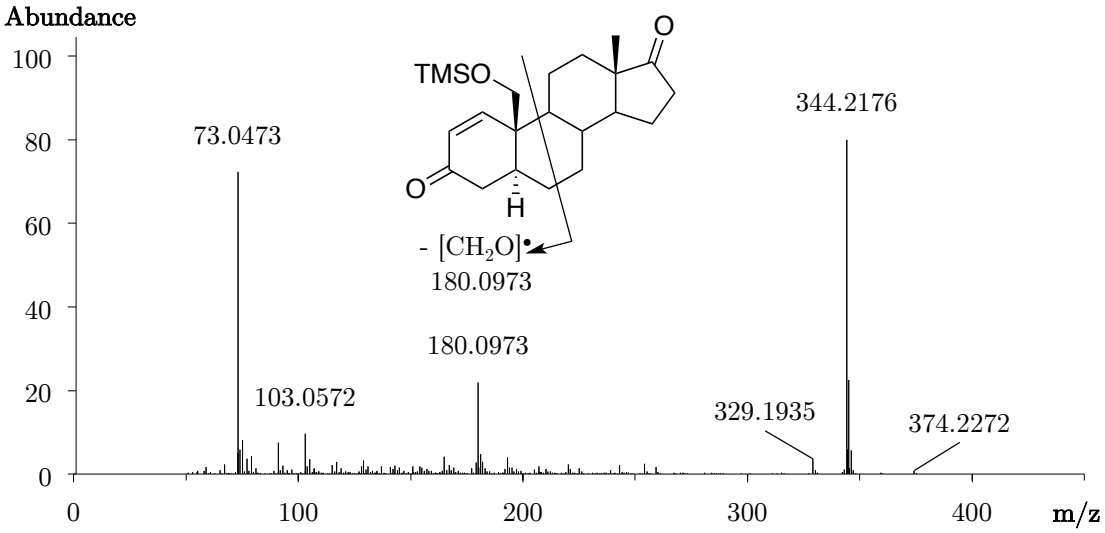

Figure 29 Accurate mass spectrum (EI) of synthesized 19-hydroxy-5α-androst-1-ene-3,17-dione (5), mono-TMS, $[M]^{\bullet+}$=374.2272, mass error 1.39 ppm

Analysis of the target compound by MS/MS using electron ionization (EI) after either mono- or tris-TMS derivatization or electrospray ionization (ESI) without derivatization revealed several fragments as specified below:

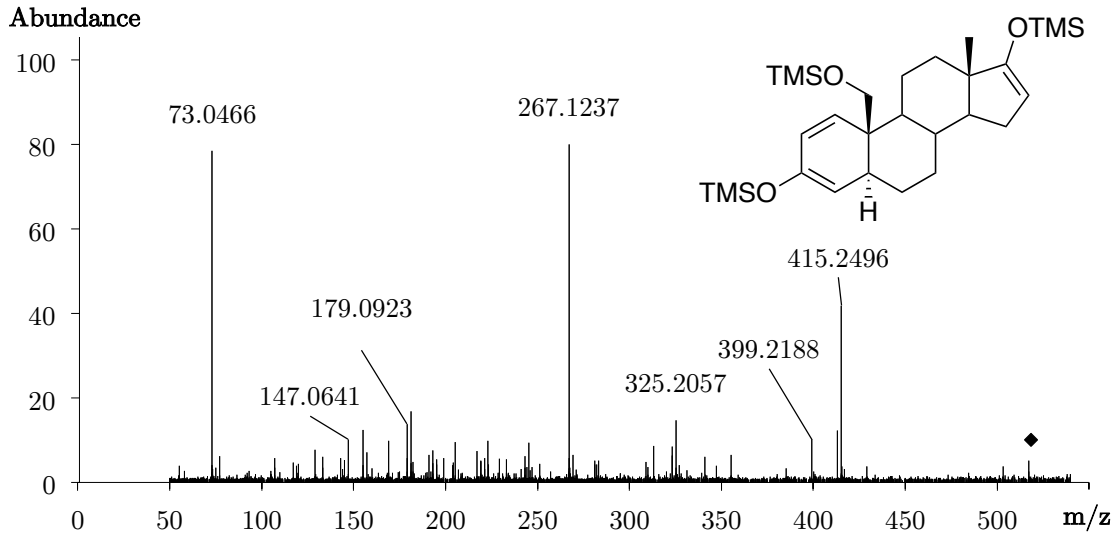

Figure 30 Accurate MS/MS spectrum (EI) of 19-hydroxy-5α-androst-1-ene-3,17-dione (5), 1,3,16-triene-3,17,19-triol tris-TMS, precursor 518.3 indicated with black rhombus, collision induced energy 25 eV

The product ion spectrum of the precursor m/z 518.3 obtained after GC-EI-MS/MS experiments confirmed the assignments described in the GC-EI accurate mass measurements (Figure 30). The EI-MS/MS spectrum of 19-hydroxy-5α-androst-1-ene-3,17-dione (5) as tris-TMS derivative with the precursor m/z 415 (base peak) shows similar fragments (Figure 77). The MS/MS spectrum of the mono-TMS derivative of the base peak m/z 344 is displayed in Figure 31. Here again, the abundant fragments show the same exact masses as in the TOF scan experiment.

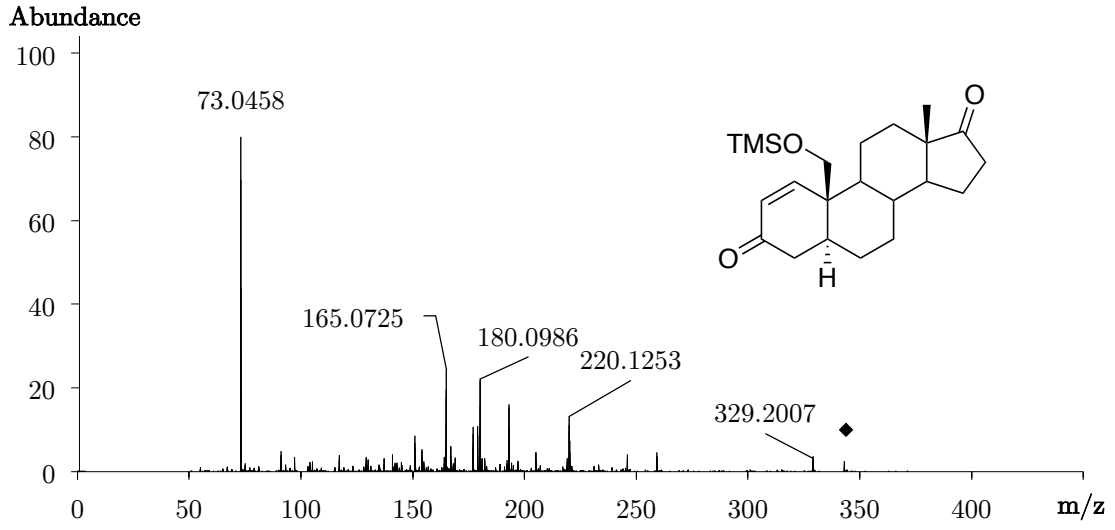

Figure 31 Accurate MS/MS spectrum (EI) of 19-hydroxy-5α-androst-1-ene-3,17-dione (5), mono-TMS, precursor 344 indicated with black rhombus, collision induced energy 25 eV

The measurement of 19-hydroxy-5α-androst-1-ene-3,17-dione (5) with liquid chromatography coupled to tandem accurate mass spectrometry was performed in positive mode (ESI+). The most abundant adduct following a short LC run was $[M+H]^+$. The corresponding MS/MS spectrum is displayed in Figure 32. For comparison, the product ion spectrum of the isomer 19-hydroxyandrost-4-ene-3,17-dione is shown in Figure 78.

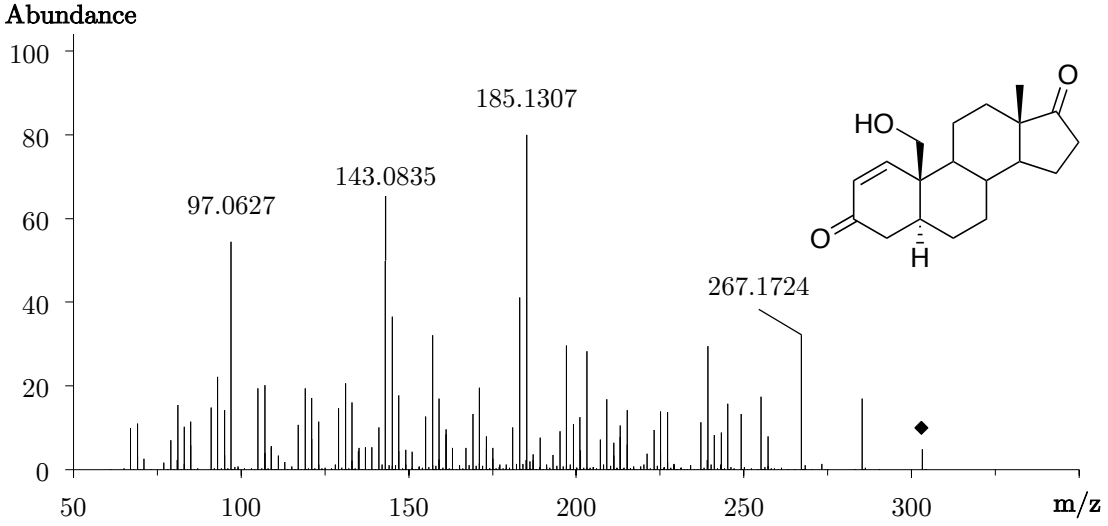

Figure 32 Accurate MS/MS spectrum (ESI+) of 19-hydroxy-5α-androst-1-ene-3,17-dione (5), precursor m/z 303 indicated with black rhombus, collision induced energy 20 eV

Nuclear magnetic resonance spectra of purified 19-hydroxy-5α-androst-1-ene-3,17-dione (5) were recorded at 600 MHz (^{1}H) and 150 MHz (^{13}C) at 298 K using a solution of about 8 mg in deuterated chloroform. For confirmation ^{1}H and ^{13}C spectra were complemented together with 2D gradient-selected H,H-COSY (spectrum Figure 80), NOESY, HSQC and HMBC experiments.

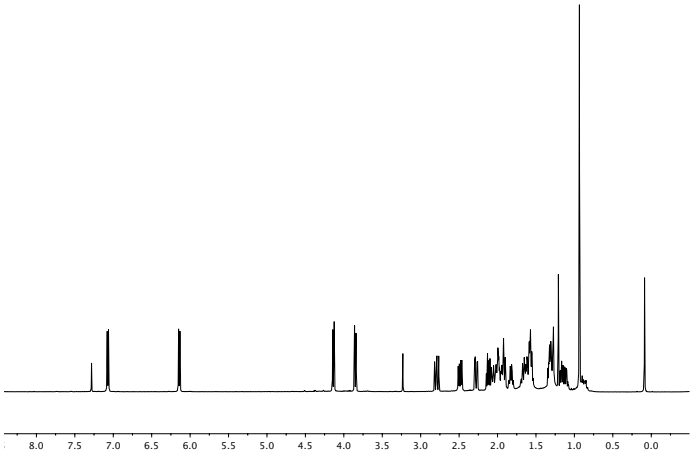

Figure 33 ^{1}H-NMR spectrum of 19-hydroxy-5α-androst-1-ene-3,17-dione (5), chemical shifts in ppm

The ^{1}H-NMR spectrum (Figure 33) shows the chemical shifts of protons in the molecule. The shifts at around 6.14 and 7.07 ppm are typical for a double bond and are assigned to the protons at C1 and C2 respectively. Figure 34 shows the ^{13}CNMR acquired in DEPT mode. The negative peak at 61.42 ppm can be assigned to the methylene group of carbon 19, where the shift results from the neighboring hydroxyl group. Two downfield shifted positive peaks at around 152.52 and 131.24 ppm correspond to the carbons 1 and 2, where the double bond is located. Full NMR assignments are given in Table 17.

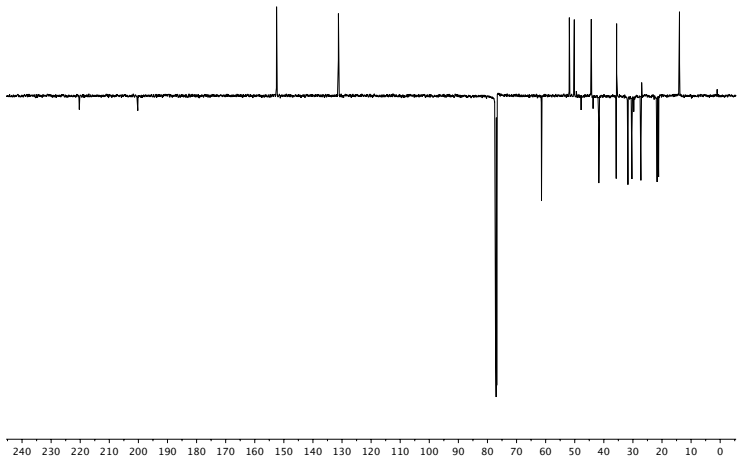

Figure 34 ^{13}C DEPT spectrum of 19-hydroxy-5α-androst-1-ene-3,17-dione (5)

The following 2D-NMR experiments confirmed the structure of the synthesized 19-hydroxy-5α-androst-1-ene-3,17-dione. For the H,C-HMQC results (spectrum in Figure 35) the coupling of the two protons (4.1 and 3.9 ppm) with the C19 (61.42 ppm) is

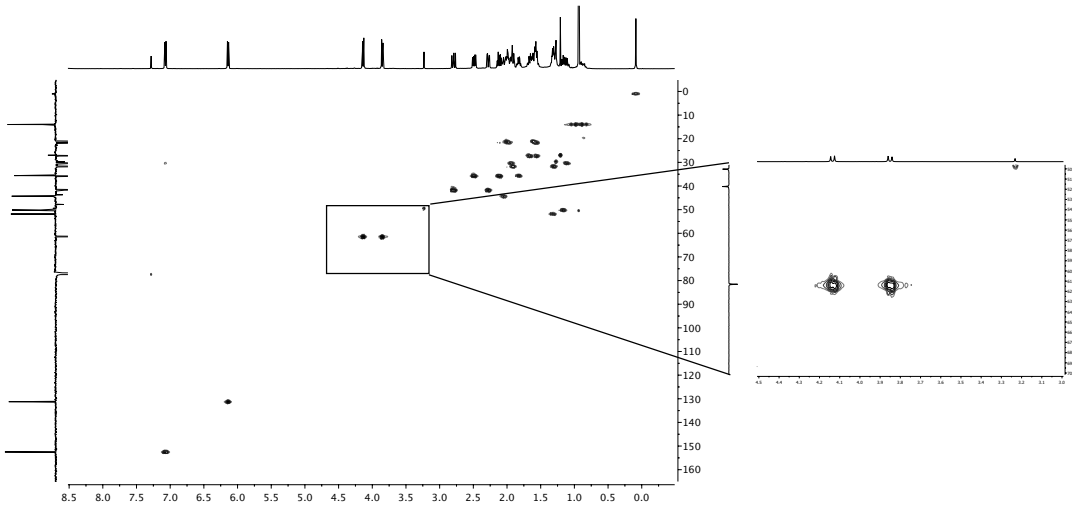

Figure 35 H,C-HMQC spectrum of 19-hydroxy-5α-androst-1-ene-3,17-dione (5), zoomed area of 3.0 – 4.5 ppm (^{1}H) and 50 – 70 ppm (^{13}C)

exemplarily zoomed in. The long range couplings depicted in the H,C-HMBC spectrum (Figure 36) confirm the double bond between carbons one and two. δ 61.42 ppm of C19 with δ 7.07 ppm of the proton on C1 or δ 41.60 ppm of carbon 4 with δ 6.14 ppm of proton on C2 are examples for this double bond confirmation.

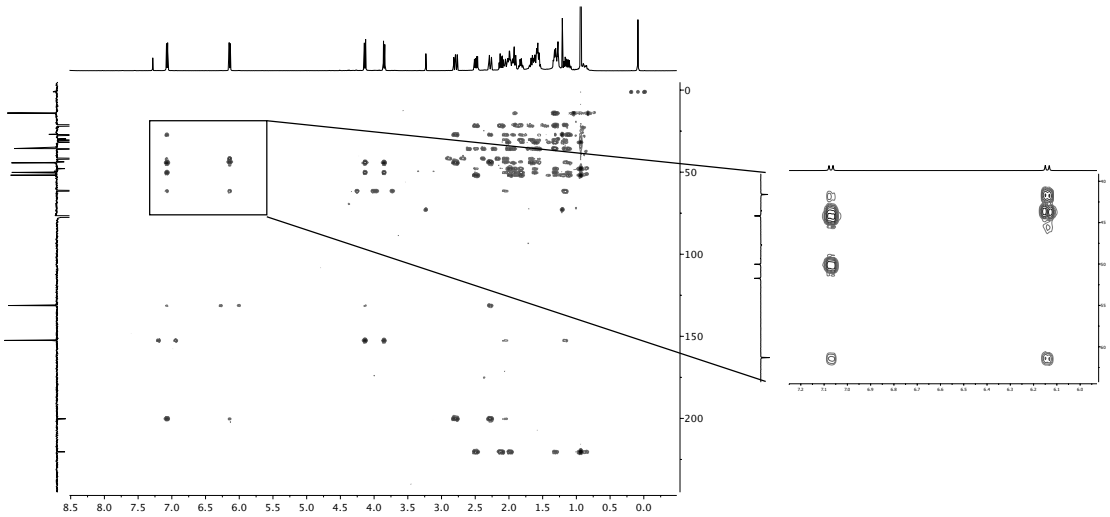

Figure 36 H,C-HMBC spectrum of 19-hydroxy-5α-androst-1-ene-3,17-dione (5), zoomed area of 3.0 – 4.5 ppm (^{1}H) and 50 – 70 ppm (^{13}C)

The A/B-ring fusion were determined by NOESY (spectrum Figure 81). 5α-Androstanes show a proton coupling of the 4β proton with the protons at C19, exemplified for the final product (Figure 37).

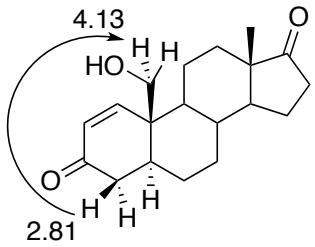

Figure 37 NOE experiment of 19-hydroxy-5α-androst-1-ene-3,17-dione (5), arrow showing the coupling of 4βH and 19H

To strengthen the argumentation of the NMR results, a comparison with data from literature and predicted ^{1}H-NMR and ^{13}C-NMR values using ChemDraw Professional Version 15.0 are integrated in Table 17.

Table 17 ^{1}H and ^{13}C NMR spectral data of 19-hydroxy-5α-androst-1-ene-3,17-dione (5) compared with published and predicted data

	synthesis		literature [60]		predicted (ChemDraw)	
	δ_C	δ_H	δ_C	δ_H	δ_C	δ_H
1	152.52	7.07	131.13	7.01 d	156.2	6.66
2	131.24	6.14	152.54	6.11 d	128.0	5.98
3	200.24	----------	200.16	----------	200.0	----------
4	41.61	α 2.30 β 2.81	41.70	2.51	41.4	2.73 2.98
5	44.31	2.05	44.31	n.a.	36.9	1.59
6	27.25	1.55 1.66	27.25	n.a.	27.2	1.38 1.62
7	30.34	1.12 1.93	30.34	n.a.	30.6	1.38 1.63
8	35.60	1.82	35.60	n.a.	38.0	1.14
9	51.85	1.31	51.85	n.a.	50.54	1.17
10	43.69	----------	43.68	----------	49.73	----------
11	21.17	1.60 1.99	21.16	n.a.	21.43	1.38 1.62
12	31.71	1.30 1.91	31.71	n.a.	31.76	1.66 1.91
13	47.69	----------	47.79	----------	47.94	----------
14	50.15	1.16	50.16	n.a.	51.41	1.36
15	21.69	1.57 1.97	21.67	n.a.	21.83	1.59 1.84
16	35.74	2.12 2.48	35.72	n.a.	35.76	2.20 2.30
17	220.32	----------	220.22	----------	220.56	----------
18	13.99	0.93	13.98	0.92 s	14.13	0.86
19	61.42	3.85 4.13	61.39	3.97 d	63.12	3.58 3.83

4.1.2 Biotransformation of 5α-androst-1-ene-3,17-dione *in-vitro* and *in-vivo*

To investigate the formation of 19-hydroxy-5α-androst-1-ene-3,17-dione (5) as a potential metabolite after 1-androstenedione (5α-androst-1-ene-3,17-dione, 1-AED) administration, *in vitro* experiments with selected CYP enzymes as well as human liver microsomes (HLM) were conducted. The enzyme most likely capable of 19-hydroxylation was the aromatase (CYP19A1). In addition, CYP3A4, as the most prominent xenobiotic metabolizing enzyme, and HLM were tested. As proof of concept of efficient aromatase, incubation was performed using androst-4-ene-3,17-dione (AED, accurate mass spectrum in Figure 82) as natural substrate of aromatase. The expected formation of estrone (accurate mass spectrum in Figure 83) was achieved. In contrast, incubation of AED with CYP3A4 or human liver microsomes did not result in the formation of estrone (chromatogram of CYP3A4 incubation in Figure 87). The chromatogram obtained after 18 h is displayed in Figure 38. The formation of intermediates of the aromatization process of AED, 2α-hydroxyandrost-4-ene-3,17-dione (Figure 84), 19-hydroxyandrost-4-ene-3,17-dione (Figure 20), and 3,17-dioxoandrost-4-en-19-al (Figure 85), was verified by time dependent incubation experiments of AED with aromatase and the EI mass spectrometric derived fragmentation of their TMS derivatives (chromatogram showing intermediates Figure 86).

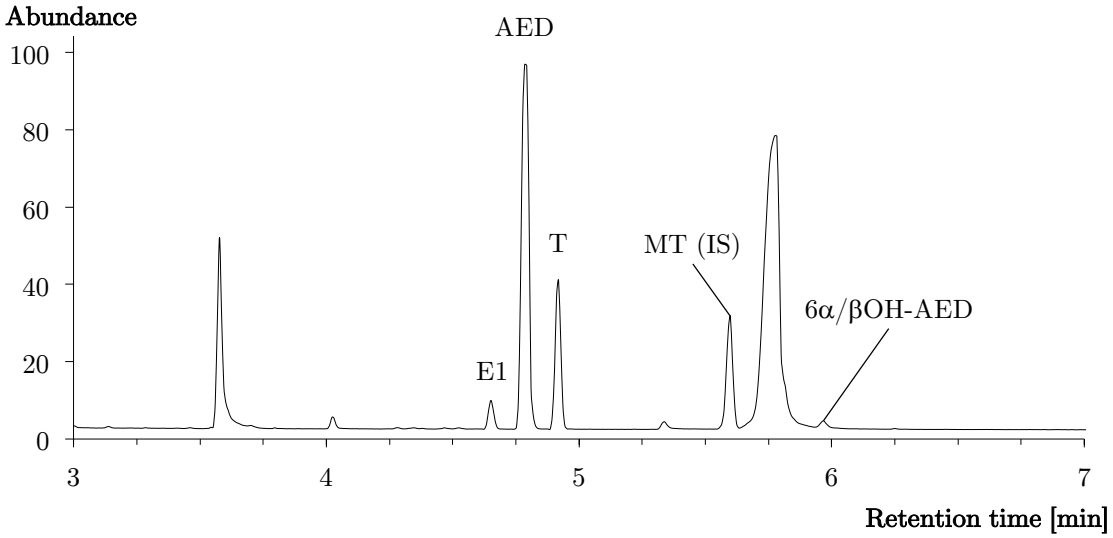

Figure 38 Base peak chromatogram showing the formation of estrone (E1) after incubation of AED with CYP19A1, byproducts testosterone (T) and 6ξ-hydroxyandrost-4-ene-3,17-dione (6α/βOH-AED), internal standard methyltestosterone (MT, 8 µg/mL),

Initial incubations with 1-AED started with 50 µM substrate solutions where no 19-hydroxylated product was detectable. Nevertheless, several other metabolites were generated. Structures were proposed based on their accurate masses and characteristic fragments. Hydroxylated and reduced-hydroxylated metabolites were postulated, whereby the true number of hydroxylated metabolites remained unclear using this method since formation of derivatization isomers is possible (chromatograms of incubation with aromatase Figure 95, CYP3A4 Figure 96, and HLM Figure 97).

To minimize a potential saturation of the enzyme at 50 µM substrate concentration in these incubation experiments, the concentration and total amount of starting volume were adjusted. By incubation of a 10 µM solution of 1-AED with CYP19A1 and CYP3A4 at a larger scale (600 µL total volume) the 19-hydroxylated metabolite was detectable in a very low amount in case of aromatase. This was shown utilizing high resolution mass spectrometry (GC-QTOF) after tris-TMS (formation in Figure 39, mass spectrum of 19-hydroxy-5α-androst-1-ene-3,17-dione in Figure 90) as well as mono-TMS (formation in Figure 40, mass spectrum in Figure 91) derivatization and comparison with the chemically synthesized reference. CYP3A4 incubation and control samples did not show any formation of the 19-hydroxylated metabolite (chromatograms in Figure 88 and Figure 89).

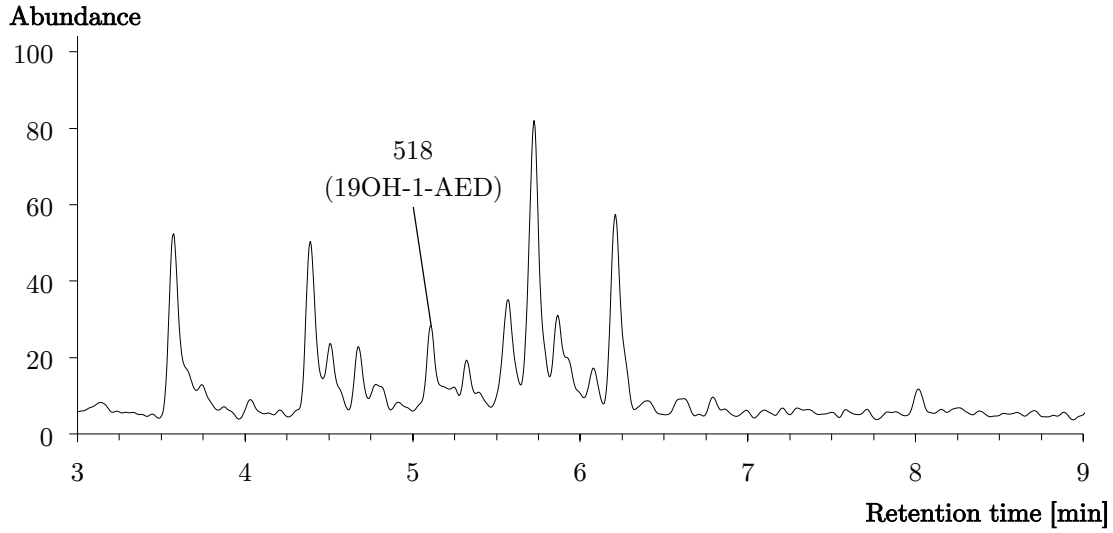

Figure 39 Extracted ion chromatogram (m/z 518.3062) after incubation of a 10 µM solution of 1-AED with CYP19A1 as per-TMS derivatives, '19OH-1-AED' indicating the formation of 19-hydroxy-5α-androst-1-ene-3,17-dione

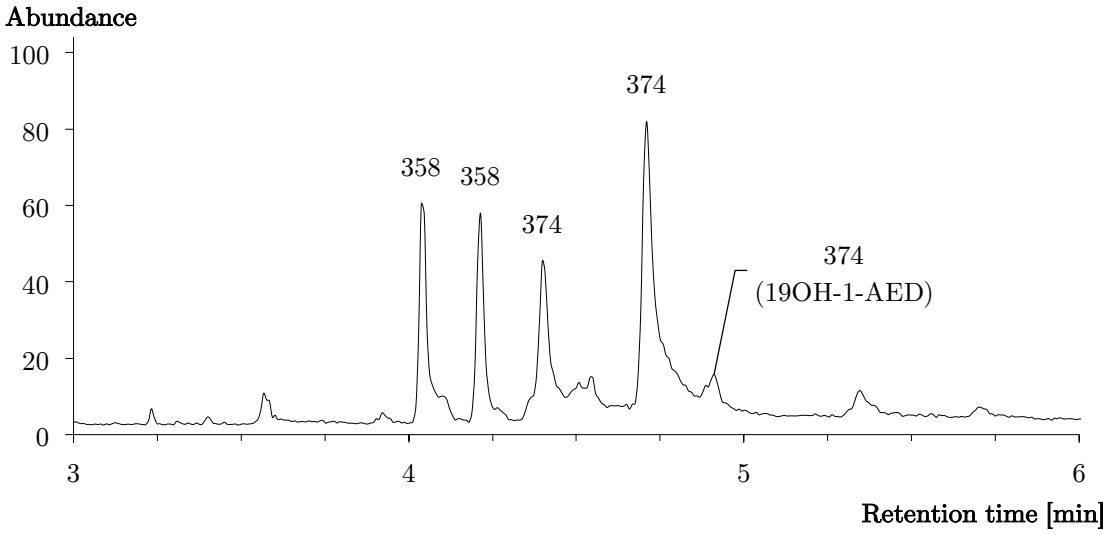

Figure 40 Extracted ion chromatogram (m/z 344.2 and 374.2) showing the nominal masses after incubation of a 10 µM solution of 1-AED with CYP19A1 after derivatization with MSTFA, '19OH-1-AED' indicating the formation of 19-hydroxy-5α-androst-1-ene-3,17-dione as mono-TMS derivative

However, aromatization of the A ring occurred in both enzyme incubation experiments with 1-AED as a substrate in trace amounts. As expected, the formation through aromatase did to a slightly higher extent. On the other hand, formation of small quantities estrone bis-TMS were observed after trimethylsilylation of 19-hydroxy-5α-androst-1-ene-3,17-dione alone as artifact. Thus, the trace amounts observed after incubation may indicate enzymatic 19-hydroxylation and aromatization as a derivatization artifact. This may be seen as indirect evidence of 19-hydroxylation through CYP19A1 and CYP3A4.

The incubation with CYP3A4 and human liver microsomes (as described in 3.2.5, 200 µL total volume) resulted in several hydroxylated metabolites as mentioned before, whereby the 19-hydroxylation was not detectable. The formation of 18-hydroxy-5α-androst-1-ene-3,17-dione ($M1_{1\text{-AED}}$) by CYP3A4 and HLM (RT=5.47 min, chromatograms in Figure 96 and Figure 97) on the other hand seems likely due to mass spectral data showing the characteristic loss of $[CH_2OTMS]^{\bullet}$ (m/z 103.0572) from the molecular ion $[M]^{+\bullet}$=518.3050 resulting in an abundant base peak at m/z 415.2472 (mass spectrum Figure 41). The m/z value of 179.0881 Da may also confirm this argumentation as a possible fragment typical for 3-oxo-1-ene steroids.

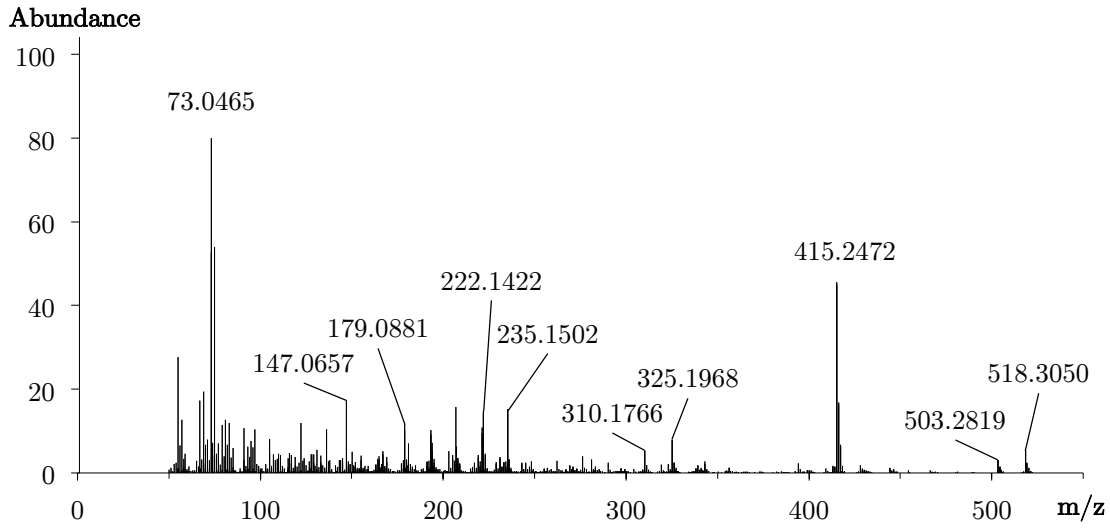

Figure 41 Accurate mass spectrum (EI) of potentially 18-hydroxylated 1-AED ($M1_{1\text{-}AED}$) after incubation with CYP3A4 as tris-TMS derivative, retention time 5.47 min, $[M]^{\bullet+}$=518.3050, mass error 2.55 ppm

This metabolite was already reported based on mass spectral data by Parr et al [36]. In that study, the fragments obtained by GC-EI-MS experiments assigned to 18-hydroxy-5α-androst-1-ene-3,17-dione ($M1_{1\text{-}AED}$) showed similar relative abundancies and m/z values (compare [36]). The same metabolite is therefore postulated again in the absence of reference material, but by means of accurate mass data, which do not verify but still strongly support the earlier findings.

Concordantly, the formation of 18-hydroxylated AED may be very likely after incubation with CYP3A4 (or HLM). One obtained metabolite $M1_{AED}$ yielded a molecular ion $[M]^{\bullet+}$=518.3062 and a fragment at m/z 415.2481 possibly indicating 18-hydroxyandrost-4-ene-3,17-dione (RT=6.06 min, chromatogram in Figure 105, mass spectrum in Figure 92).

However, the second hydroxylated metabolite (supposedly 19-hydroxylated) postulated by Parr et al contradicts the GC-EI-HRMS results from the synthesized 19-hydroxy-5α-androst-1-ene-3,17-dione (5) described earlier (Figure 28). The data from literature showing a mass spectrum of putative 19-hydroxylated 1-androstenedione differ in obtained fragments and ratios of their abundancies. Nonetheless, it still can be argued that the reported metabolite showed the distinctive fragment m/z 415 (after loss of 103 Da corresponding to $[CH_2OTMS]^{\bullet}$) along with the molecular ion m/z 518 [36]. Interestingly, a seemingly similar metabolite $M2_{1\text{-}AED}$ was obtained after biotransformation of 1-AED by

CYP3A4 as the main hydroxylated metabolite (mass error -2.12 ppm, mass spectrum Figure 42). The theoretical mass of the resulting fragment after loss of the potential trimethylsilylated hydroxymethylene group (from $[M]^{\bullet+}$=518.3062) would be 415.2483 Da. The actual fragment, however, corresponds to m/z 415.2135 (mass error -83.81 ppm). Slightly smaller is the fragment m/z 413.2321 likely resulting from $[M\text{-}TMSOH\text{-}CH_3]^+$ (mass error -2.66 ppm). The m/z value 415.2135 might be assigned to an unknown fragment instead and the mass spectrum itself to an unknown hydroxylated metabolite of 1-AED.

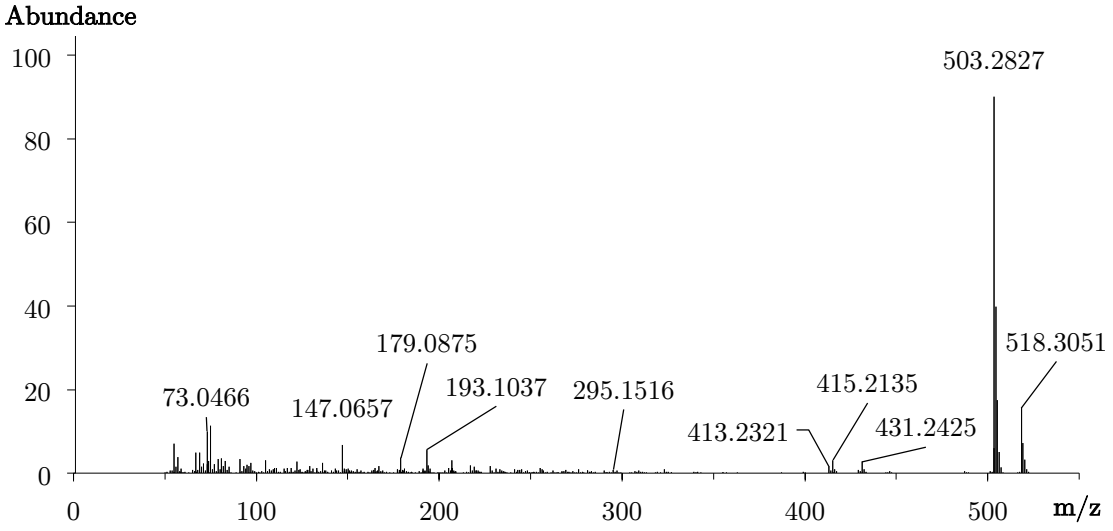

Figure 42 Accurate mass spectrum (EI) of a hydroxylated metabolite of 1-AED after incubation with CYP3A4 ($M2_{1\text{-}AED}$) as tris-TMS derivative, retention time 6.23 min, $[M]^{\bullet+}$=518.3051, mass error -2.12ppm

Following the incubation experiments, *in vivo* confirmation of the discussed 19-hydroxylated metabolite was the logical consequence. A doping control sample, positively tested for 1-AED misuse, was reinvestigated using the before mentioned protocol (chapter 3.2.6). Possible hydroxylated steroid metabolites based on their accurate masses are proposed and are depicted with their nominal masses in the chromatogram displayed in Figure 43. However, the postulated 19-hydroxylated metabolite of 1-androstenedione was not detected in this exemplary urine sample. So were neither the proposed 18-hydroxylated metabolite of 1-AED ($M1_{1\text{-}AED}$) nor the (allegedly 19-hydroxylated) metabolite $M2_{1\text{-}AED}$. The vast number of hydroxylated metabolites however elucidates their relevance.

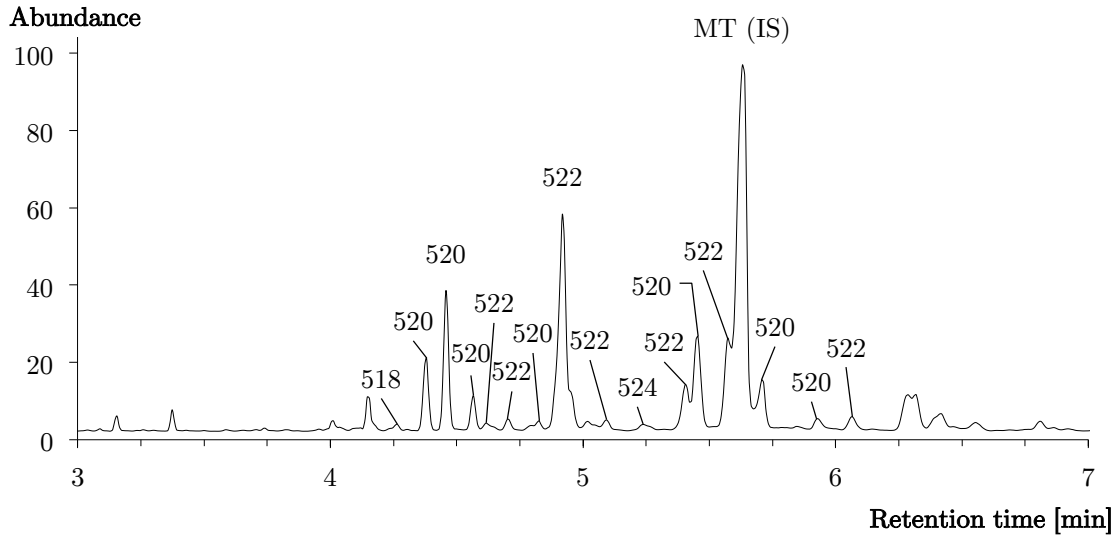

Figure 43 Extracted ion chromatogram showing mono-hydroxylated urinary steroid metabolites after 1-AED administration with nominal masses of the tris-TMS derivatives, internal standard methyltestosterone (MT, 8 µg/mL)

Nevertheless, *in-vitro* formation of 19-hydroxy-5α-androst-1-ene-3,17-dione (5) by aromatase was verified with chemically synthesized reference material, whereas metabolite generation *in-vivo* was not detectable. Aromatization of 1-AED through aromatase, however, remains questionable since the generated amount was very low and traces of estrone were detectable as artifact analyzing 19-hydroxylated 1-AED as tris-TMS alone. The 1,2-double bond of 1-AED supposedly hampers the hydrogen abstraction of C1 in the aromatization process. The possibility of alternative 5βH-abstraction, radical formation at C10 and enolization of the 3-oxo group resulting in estrone remains doubtful.

Based on accurate mass data, the formation of 18-hydroxy-5α-androst-1-ene-3,17-dione ($M1_{1\text{-AED}}$) by CYP3A4 and HLM is proposed, supporting earlier structure proposals of *in vivo* formation [36, 43]. 18-Hydroxylation occurs endogenously in the biotransformation of corticosterone to aldosterone by CYP11B2 and has been reported for various synthetic anabolic androgenic steroids as well [18, 65]. The main hydroxylated metabolite $M2_{1\text{-AED}}$ represents an unknown metabolite of 1-AED, arguably hydroxylated at C16. Further investigation is needed for detailed structure proposals.

4.2 2β-Hydroxylation of androst-4-ene-3,17-dione

4.2.1 Synthesis of reference material

The synthesis of 2β-hydroxyandrost-4-ene-3,17-dione (10) started from commercially available androst-4-ene-3,17-dione (6) (androstenedione, AED). The initial intention was to obtain (10) from AED via the epoxide 4β,5β-epoxyandrostane-3,17-dione (7) resulting in 2α-hydroxyandrost-4-ene-3,17-dione (9) [55, 66]. The alpha configuration of the hydroxy group ought to be inverted applying a Mistunobu conversion at carbon two of the androstane derivative (9) resulting in 2β-hydroxyandrost-4-ene-3,17-dione (10). Attempts to obtain the desired 2β-hydroxyandrost-4-ene-3,17-dione (10) directly by bromination of AED (6) at carbon six following rearrangement to the 2ξ-acetoxy derivatives (after refluxing with potassium acetate in glacial acetic acid) and subsequent hydrolysis of the esters as reported by Rao et al [67] have not been achieved satisfactorily in this study. It has been reported in literature that the acid catalyzed ring opening of 4α,5α-epoxyandrostane-3,17-dione (8), as described in the primarily mentioned method, has a tendency to result in 4-hydroxyandrost-ene-3,17-dione (11), while 4β,5β-epoxyandrostane-3,17-dione (7) preferably forms the intermediate 2α-hydroxyandrost-4-ene-3,17-dione (9) [66]. Thus, 4-hydroxy-androst-4-ene-3,17-dione (11) was an expected byproduct of this reaction step.

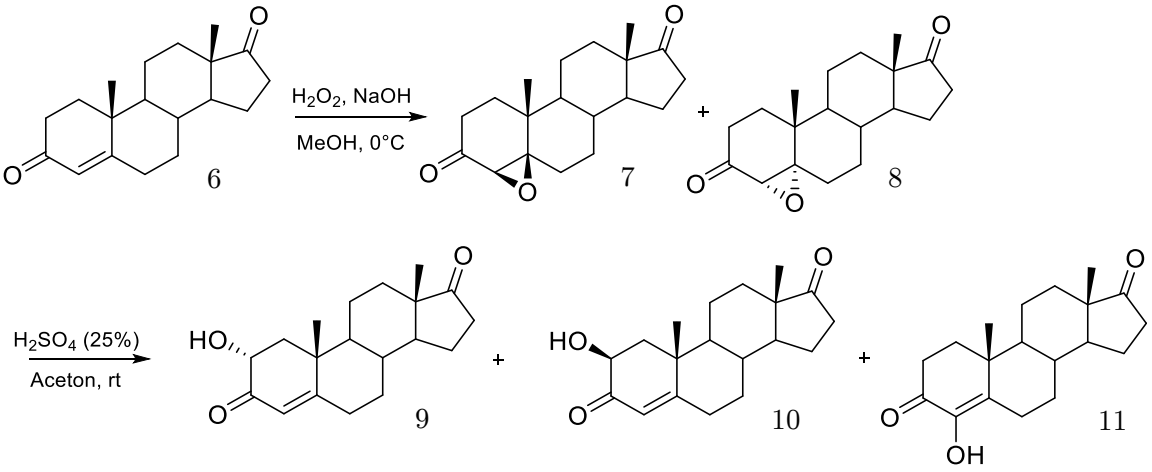

Figure 44 Overall chemical synthesis of 2β-hydroxyandrost-4-ene-3,17-dione (10) starting from androst-4-ene-3,17-dione (6), intermediates 4β,5β-epoxyandrostane-3,17-dione (7), 4α,5α-epoxyandrostane-3,17-dione (8), and byproducts 2α-hydroxyandrost-4-ene-3,17-dione (9), 4-hydroxyandrost-4-ene-3,17-dione (11)

The actually applied steps of the chemical synthesis are displayed in Figure 44. Generation of the 4ξ,5ξ-epoxyandrostane-3,17-dione derivatives (7,8) from AED (6) was achieved using hydrogen peroxide and sodium hydroxide in methanol at 0 °C. The two obtained isomeric products (7) and (8) (ratio 70:30) were identified based on GC-EI-MS analysis with EI mass spectra from literature without any derivatization (Figure 98 and Figure 99). Separation of the epoxides by column chromatography failed, and crystallization from ethyl acetate also did not fully separate the desired β- from the α-isomer. As a result, the acid catalyzed ring opening was performed on a mixture of both epoxides. Aqueous sulfuric acid (25 %) was added dropwise to a solution of the epoxides (7,8) in acetone at room temperature and stirred for 65 h. The postulated mechanism of that reaction - adapted from Tomoeda et al [55] - is displayed in Figure 45. It is suggested that the nucleophilic attack at carbon C2 resulting in the ring opening of the epoxide may proceed via the 2,3-enol following subsequent elimination of the remaining hydroxy group at carbon five. Detection of a potentially di-hydroxylated androstenedione derivative after TMIS derivatization (m/z 608, data not shown) indicates incomplete elimination and supports the mechanistic explanation.

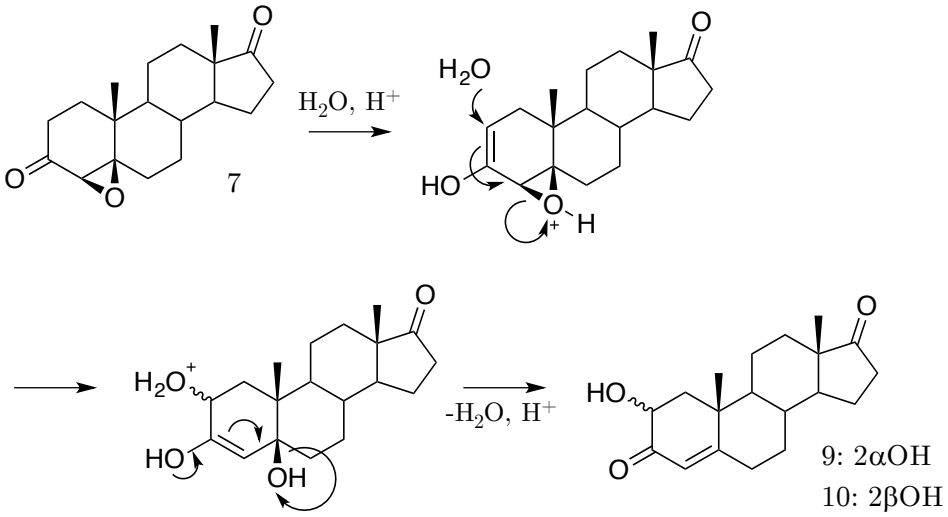

Figure 45 Postulated reaction mechanism of the acid catalyzed ring opening of 4β,5β-epoxyandrostane-3,17-dione (2) resulting in 2ξ-hydroxyandrost-4-ene-3,17-dione derivatives (4,5)

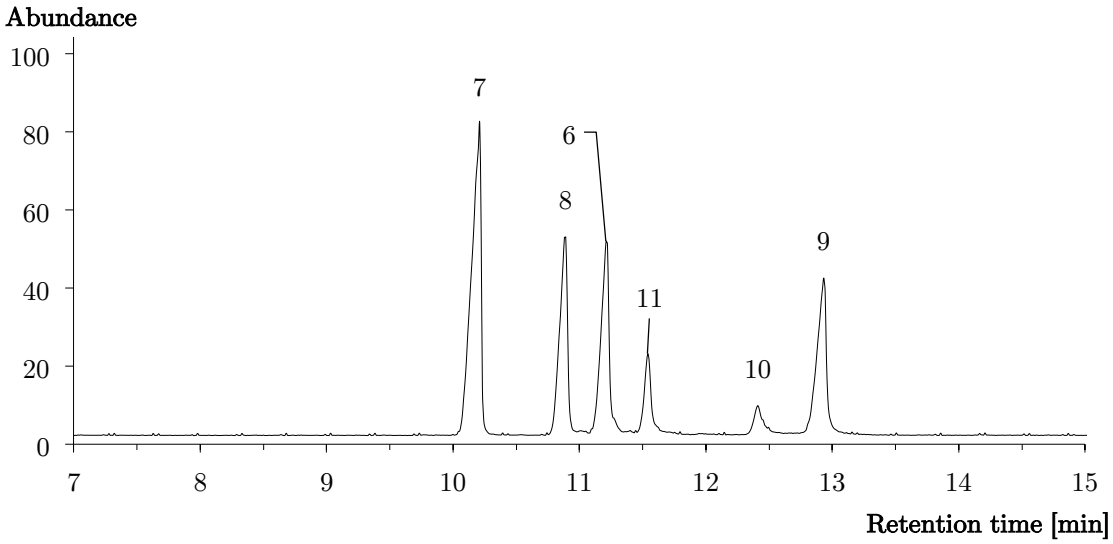

Figure 46 Total ion chromatogram of the intermediates and byproducts of the synthesis of 2ε-hydroxyandrost-4-ene-3,17-dione, 4ξ,5ξ-epoxyandrostane-3,17-diones (7,8), androst-4-ene-3,17-dione (6), 4-hydroxyandrost-4-ene-3,17-dione (11), 2β-hydroxyandrost-4-ene-3,17-dione (10), and 2α-hydroxyandrost-4-ene-3,17-dione (9), acquired using method a)

Figure 46 represents the total ion chromatogram of the second reaction step in the overall chemical synthesis, showing the underivatized starting material AED (6, mass spectrum Figure 100), intermediates (7,8), byproduct (11, mass spectrum Figure 101), the desired intermediate product 2α-hydroxyandrost-4-ene-3,17-dione (9, mass spectrum Figure 47) and an additional peak at around 12.4 min. Formation of 4-hydroxyandrost-4-ene-3,17-dione (11) and 2α-hydroxy-androst-4-ene-3,17-dione (9) was confirmed with commercially available reference material.

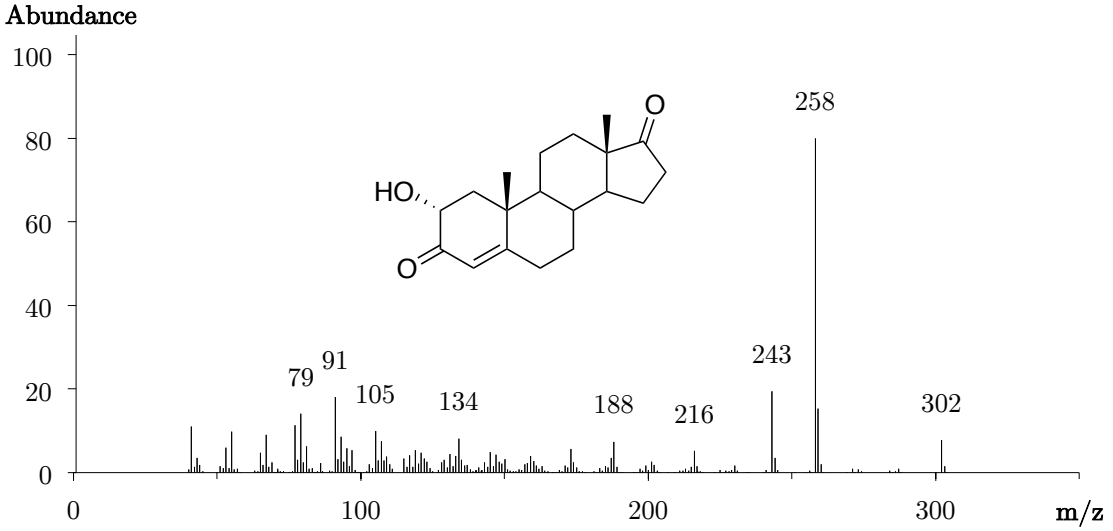

Figure 47 Mass spectrum (EI) of underivatized 2α-hydroxyandrost-4-ene-3,17-dione (9) obtained from 4ξ,5ξ-epoxyandrostane-3,17-diones (7,8), $[M]^{\bullet+}$=302

The mass spectrum of the underivatized compound (10) is shown below in Figure 48. It illustrates a very similar mass spectrum compared to that of underivatized 2α-hydroxyandrost-4-ene-3,17-dione (9). Both spectra show a molecular ion $[M]^{+\bullet}$=302 and a base peak at m/z 258 possibly resulting from the loss of CH_3CHO.

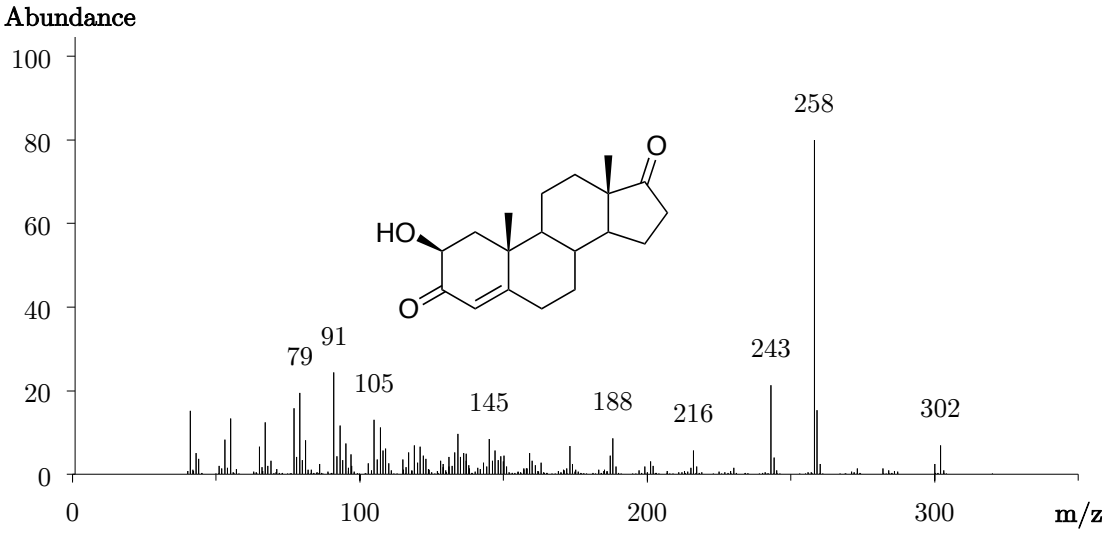

Figure 48 Mass spectrum (EI) of underivatized 2β-hydroxyandrost-ene-3,17-dione (10), obtained from 4ξ,5ξ-epoxyandrostane-3,17-diones (7,8), $[M]^{\bullet+}$=302

The m/z value of 243 Da may thus represent $[M\text{-}44\text{-}CH_3]^+$ resulting from a subsequent loss of $[CH_3]^\bullet$ from m/z 258. Compound (10) was then assumed to be the desired 2β-hydroxyandrost-4-ene-3,17-dione (10). According to Rao et al. the 2α isomer of 2ξ-hydroxyandrost-4-ene-3,17-dione seems to be more stable than the 2β form and isomerization is possible [67]. Based on the suggested reaction mechanism (as described above) it may be likely that the 2β isomer is formed as well. A study investigating potential new aromatase inhibitors demonstrated the formation of 2β,6β-difluoroandrost-4-ene-3,17-dione from the corresponding 4β,5β-epoxy-6β-fluoroandrost-4-ene-3,17-dione via the 2,3-enol in a similar way [68].

Separation of the reaction mixture by column chromatography was able to separate both 2ξ-hydroxyandrost-4-ene-3,17-diones (9,10) from the residual substances. Further investigation of the potentially formed 2β-hydroxyandrost-4-ene-3,17-dione (10) (and its isomer (9)) revealed that separation of the per-TMS derivatives using the former gas chromatographic conditions could not be achieved. A chromatogram showing both coeluting 2ξ-hydroxyandrost-4-ene-3,17-diones as tris-TMS derivatives is depicted in the

Annex (Figure 102). Derivatization with MSTFA only resulted in the formation of the equivalent mono-TMS derivatives. These derivatives could be separated using the gas chromatographic method a) as demonstrated in Figure 49.

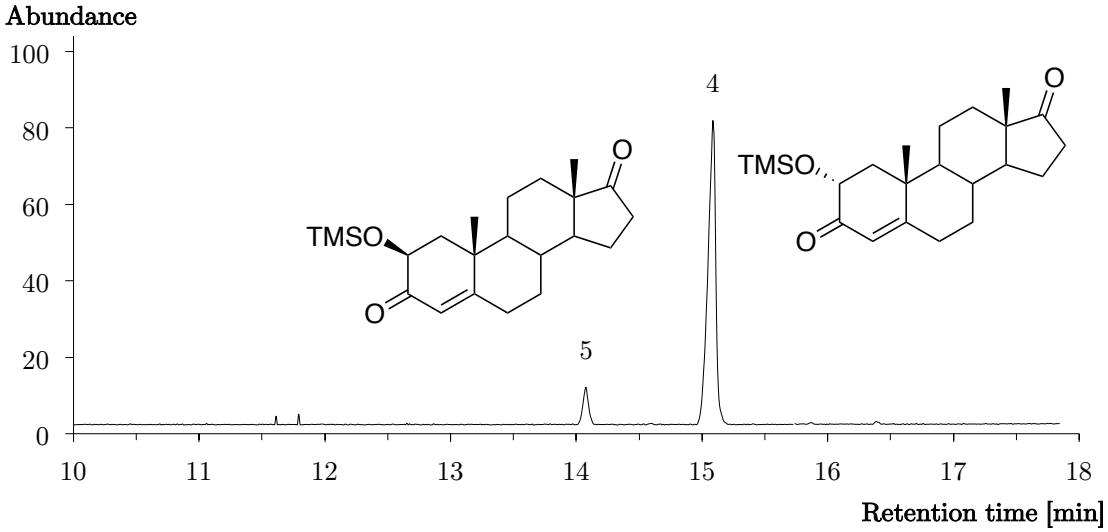

Figure 49 Base peak chromatogram of 2α- (9) and 2β-hydroxyandrost-4-ene-3,17-dione (10) after column chromatography, as mono-TMS derivatives, acquired method a)

Since separation of the 2ξ-hydroxyandrost-4-ene-3,17-diones was unsuccessful using column chromatography, isolation was achieved by HPLC on an analytical scale. This was accomplished by applying the relatively slow chromatographic conditions mentioned earlier of method g). Consequent analysis of the obtained fractions as mono-TMS derivatives with

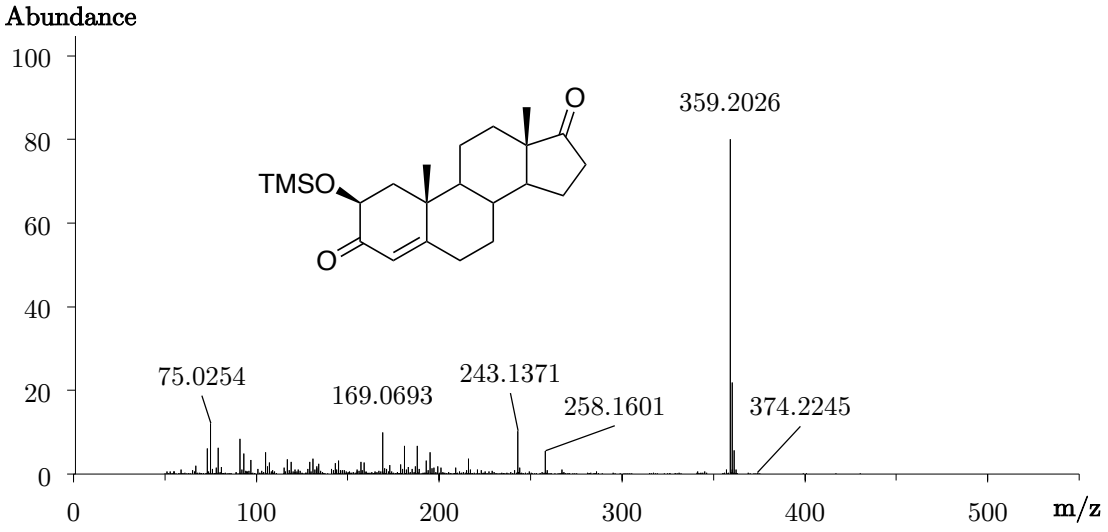

Figure 50 Accurate mass spectrum (EI) of 2β-hydroxyandrost-4-ene-3,17-dione (10), mono-TMS, $[M]^{\bullet+}$=474.2245, mass error of base peak 4.45 ppm

high resolution mass spectrometry gave a molecular ion $[M]^{+\bullet}$=374.2245 and a base peak probably resulting from $[M\text{-}CH_3]^+$ at m/z 359.2026 (theoretical mass 359.2042 Da, mass error 4.45 ppm, mass spectrum in Figure 50). Accurate mass spectra (EI) of the α-isomer (9, Figure 103) and 4-hydroxyandrost-4-ene-3,17-dione (11, Figure 104) as mono-TMS derivatives show similar fragmentations. Nonetheless, accurate mass measurements and chromatographic behavior taken into account, together with the underlying reaction mechanism, compound (10) was postulated to be the desired 2β-hydroxyandrost-4-ene-3,17-dione. Due to HPLC separation of (9) and (10) on an analytical scale, amounts were too small for NMR experiments.

4.2.2 Biotransformation of androst-4-ene-3,17-dione *in-vitro* and *in-vivo*

Hydroxylated metabolites of the endogenous prohormone AED have been extensively investigated including biotransformation *in-vitro* and *in-vivo*. In this thesis, aromatase-dependent biotransformation of AED has been investigated previously (chapter 4.1.2, chromatogram of hydroxylated products Figure 86) and incubation experiments of AED with CYP3A4 (chromatogram Figure 105) and HLM (chromatogram Figure 106) resulted in the common hydroxylated metabolites. Analysis as tris-TMS derivatives revealed the formation of 6α/β-hydroxyandrost-4-ene-3,17-dione (5.98 min), 4-hydroxyandrost-4-ene-3,17-dione (6.27 min), and 16α-hydroxyandrost-4-ene-3,17-dione (6.86 min). For detection of an AED administration in doping control analysis only recently 2α-hydroxyandrost-4-ene-3,17-dione (9) has been recommended as a new target (as discussed in chapter 2). The commonly used gas chromatographic method a) does not separate the tris-TMS derivatives of 2α-hydroxyandrost-4-ene-3,17-dione (9) and 4-hydroxyandrost-ene-3,17-dione (11) (chromatograms in Figure 107 and Figure 108) which show very similar retention times and mass spectra, respectively (Figure 84 and Figure 109) [49]. Even the adjusted gas chromatographic method b) does not fully separate these two isomers (Figure 110 and Figure 111). In fact, the additional analysis of the androstenedione metabolites 6α/β-hydroxyandrost-4-ene-3,17-dione (12,13), 16α-hydroxyandrost-4-ene-3,17-dione (14), and the

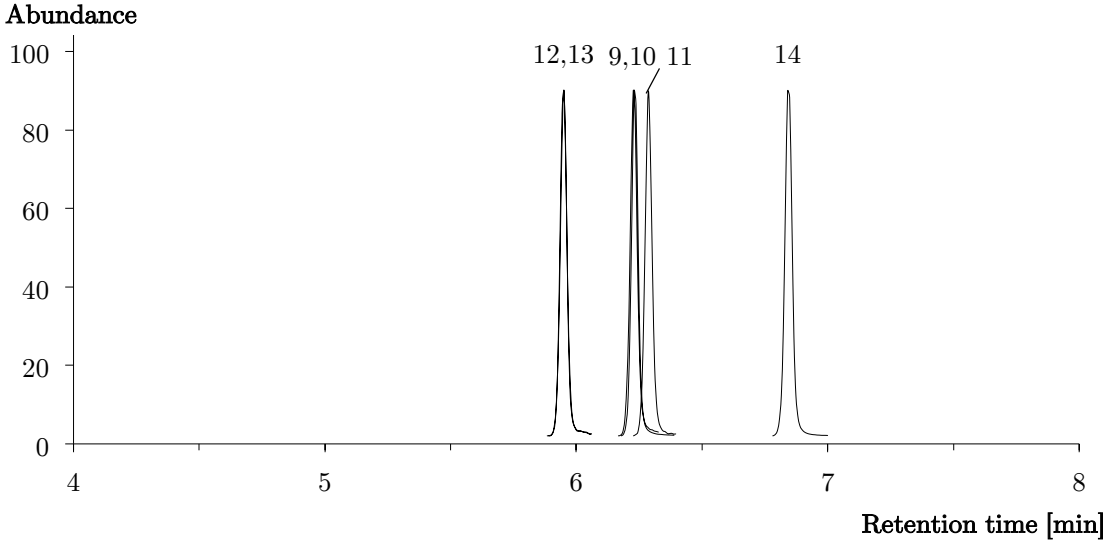

Figure 51 Overlay chromatogram of reference substances as tris-TMS derivatives, 6α/β-hydroxyandrost-4-ene-3,17-dione (12,13), coeluting 2α/β-hydroxyandrost-4-ene-3,17-dione (9,10), 4-hydroxyandrost-4-ene-3,17-dione (11), 16α-hydroxyandrost-ene-3,17-dione (14), acquired using method b)

synthesized 2β-hydroxyandrost-4-ene-3,17-dione (10) after TMIS derivatization resulted in the overlay chromatogram displayed in Figure 51. It demonstrates the coeluting tris-TMS derivatives of 6α/β-hydroxyandrost-4-ene-3,17-dione (12,13) (which form the same derivatization isomer after enolization, 3,5,16-triene-3,6,17-triol tris-TMS), 2α/β-hydroxyandrost-4-ene-3,17-diones (9,10) (either as 3,5,16-triene-2α/β,3,17-triol tris-TMS derivatives or as 2,4,16-triene-2,3,17-triol tris-TMS), and the virtually coeluting 4-hydroxyandrost-ene-3-17-dione (11).

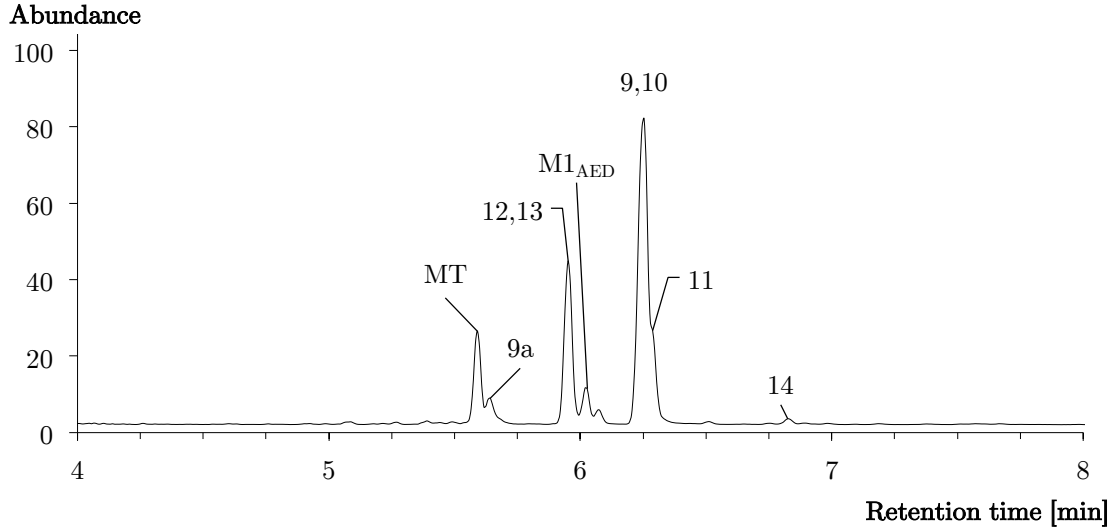

Figure 52 Extracted ion chromatogram (m/z 518.3062) of a AED post administration urine sample after derivatization with TMIS, derivatization isomer of 2α-hydroxyandrost-4-ene-3,17-dione (9a), 6α/β-hydroxyandrost-4-ene-3,17-dione (12,13), proposed 18-hydroxyandrostenedione ($M1_{AED}$), 4-hydroxyandrost-4-ene-3,17-dione (11), 16α-hydroxyandrost-4-ene-3,17-dione (14), internal standard methyltestosterone (MT, 8 µg/mL), acquired using method b)

Applied to a AED post administration urine sample and following the usual sample preparation and TMIS derivatization gas chromatographic method b) gave the extracted ion chromatogram depicted in Figure 52. The main peak represents the expected 2α-hydroxyandrost-4-ene-3,17-dione (9) and the shoulder suggests the presence of 4-hydroxyandrost-ene-3,17-dione (11). The peak at 6.02 min (7, m/z 518.3083) might represent 18-hydroxyandrost-4-ene-3,17-dione ($M1_{AED}$) based on the accurate EI mass spectrum and retention time discussed earlier (chapter 4.1.2, corresponding mass spectrum Figure 92). Additionally, minor amounts of 16α-hydroxyandrost-4-ene-3,17-dione (14) and the derivatization isomer of 2α-hydroxyandrost-4-ene-3,17-dione (9a) were detected and verified with reference material. To overcome the separation difficulties, derivatization

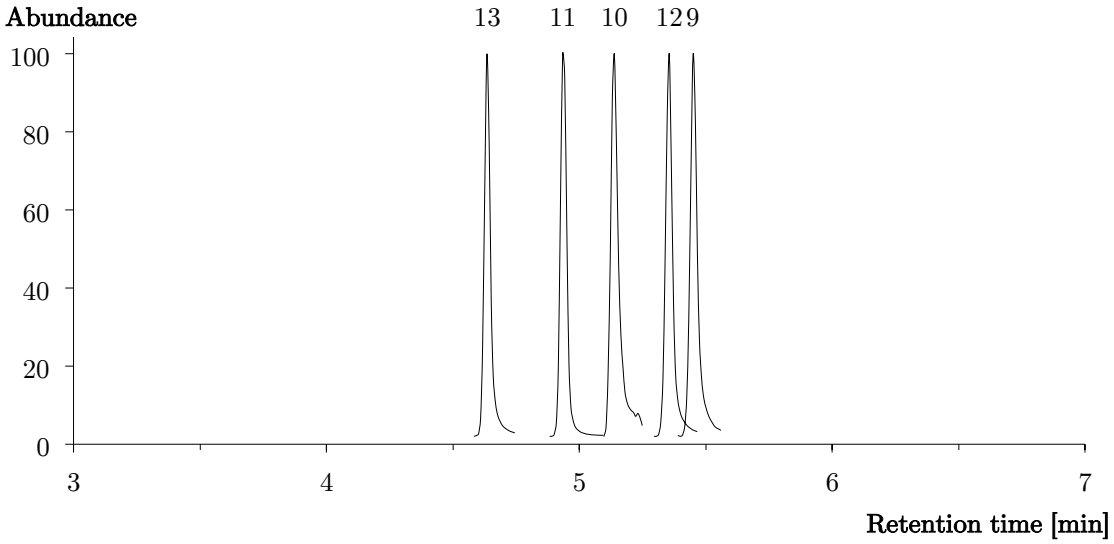

Figure 53 Overlay chromatogram of reference substances as mono-TMS derivatives, 6β-hydroxyandrost-4-ene-3,17-dione (13), 4-hydroxyandrost-4-ene-3,17-dione (11), 2β-hydroxyandrost-4-ene-3,17-dione (10), 6α-hydroxyandrost-4-ene-3,17-dione (12), 2α-hydroxyandrost-4-ene-3,17-dione (9)

utilizing MSTFA only was carried out. This yielded the mono-TMS derivatives in case of hydroxylated androstenedione metabolites which allowed for successful chromatographic separation as shown before (chapter 4.2.1, and mass spectra of 6α/β-hydroxyandrost-4-ene-3,17-dione (12,13) as mono-TMS derivatives in Figure 112 and Figure 113). The corresponding overlay chromatogram of the reference standards is depicted in Figure 53. Based on the derivatization technique, formation of derivatization

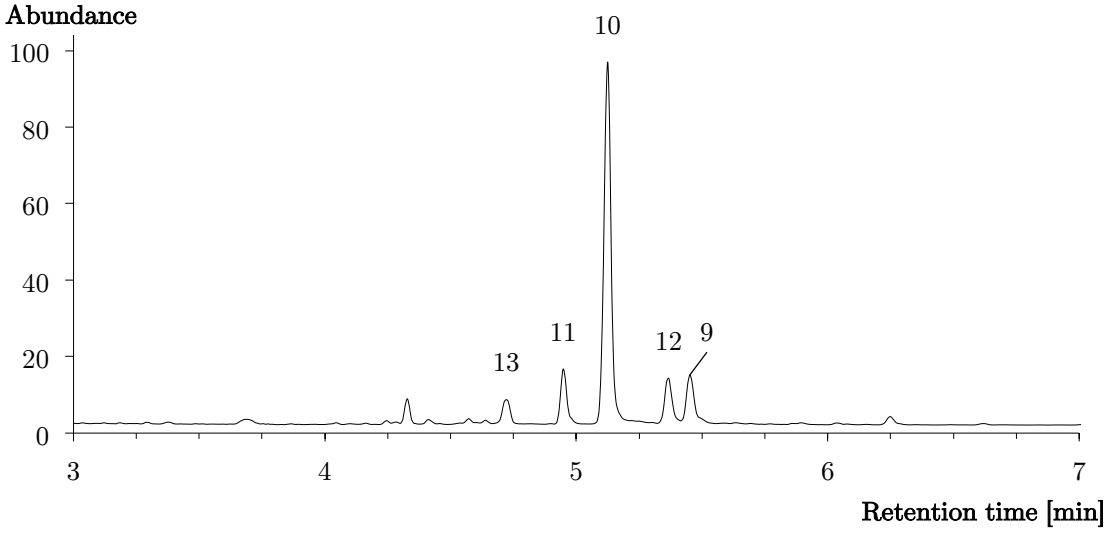

Figure 54 Extracted ion chromatogram (base peak m/z 359.2043) of a AED post administration urine sample after derivatization with MSTFA, 6β-hydroxyandrost-4-ene-3,17-dione (13), 4-hydroxyandrost-4-ene-3,17-dione (11), 2β-hydroxyandrost-4-ene-3,17-dione (10), 6α-hydroxyandrost-4-ene-3,17-dione (12), 2α-hydroxyandrost-4-ene-3,17-dione (9), acquired using method b)

isomers is excluded. 16α-hydroxyandrost-4-ene-3,17-dione (14) was neglected due to its minor formation in the urine. After trimethylsilylation of the alcohols only, the very same urine sample as analyzed above resulted in the extracted ion chromatogram as shown in Figure 54. The main peak unexpectedly lead to the conclusion that 2β-hydroxyandrost-4-ene-3,17-dione (10) is in fact, the major hydroxylated AED metabolite in this urine sample. A control urine sample after per-TMS as well as mono-TMS derivatization showed the complete absence of the discussed hydroxylated metabolites (chromatograms Figure 114 and Figure 115). Only recently, the formation of 2β-hydroxyandrost-4-ene-3,17-dione (10) has been reported from using an *E.coli*-based biocatalytic system containing bovine CYP11A1 (CYPscc) [52]. The evidence that this hydroxylated metabolite of AED is generated *in-vitro* by a steroidogenic CYP enzyme suggests its importance for *in-vivo* formation. 2β-Hydroxyandrost-4-ene-3,17-dione (10) has also been described in urine of neonates after GC-MS/MS analysis without reference material [69] and as a metabolite of AED incubation with human fetal liver microsomes (confirmed with enzymatically oxidized 2β-hydroxytestosterone) [70]. Exclusive beta-hydroxylation of steroids by some CYP enzymes (housefly CYP6A1 [71]) also marks the possibility of 2β-hydroxylation. Taken together, 2β-hydroxyandrost-4-ene-3,17-dione (10) may represent an interesting metabolite indicating AED administration in future doping analysis.

4.3 Hydroxylation of further androstane derivatives

4.3.1 Biotransformation of 1-testosterone *in-vitro* and *in-vivo*

To compare the formation of hydroxylated metabolites of the designer steroid 5α-androst-1-ene-3,17-dione (1-AED) obtained by incubation experiments, closely related 1-testosterone (1-T, 17β-hydroxy-5α-androst-1-en-3-one, mass spectrum of the bis-TMS derivative Figure 116) was investigated regarding hydroxy-metabolite formation as well. The focus was also on the hydroxylation of the angular methyl groups.

Up to ten different isomers of hydroxylated metabolites of 1-AED or its hydrogenated analogues have been detected. No further dehydrogenated metabolite was detected. The number of possible hydroxylated metabolites based on their accurate masses after 1-AED or 1-T incubation or administration are displayed below (Table 18, shown are the nominal masses). The metabolite content in the urines is obviously not necessarily related only to the 1-androgens but could originate from any other endogenous androstane derivative with the same accurate mass as well. Since no reference material was available, the structures of all potential hydroxylated metabolites are solely proposed based on their EI mass spectrometric derived fragments of their per-TMS derivatives after derivatization.

Table 18 Number of detected hydroxylated metabolites after incubation (CYP19A1, CYP3A4, HLM) or administration (urine) of 1-AED or 1-T and their nominal masses of the tris-TMS derivatives (m/z)

	CYP19A1		CYP3A4		HLM		Urine	
m/z	1-AED	1-T	1-AED	1-T	1-AED	1-T	1-AED	1-T
516	-	-	-	-	-	-	-	-
518	1	-	3	1	5	2	1	1
520	-	1	-	3	5	5	7	6
522	1	3	1	2	2	10	7	3
524	-	-	-	-	-	-	1	-

Biotransformation of 1-testosterone by means of incubation with aromatase, CYP3A4 and HLM resulted in the formation of small amounts of hydroxylated metabolites. Control samples without addition of any enzymes or microsomes already yielded the formation of

two hydroxylated metabolites (with the nominal m/z values 522 at 6.03 min, and 520 at 6.47 min, data not shown), both of which showed fragments at m/z 194 and m/z 179. This may indicate a conserved 1-ene-3-oxo structure of these metabolites and unspecific hydroxylation.

Incubation with aromatase (CYP19A1) generated these two peaks as well, together with one newly formed metabolite $M1_{1\text{-}T}$ at 6.40 min with the molecular ion $[M]^{+\bullet}$=522.3328 and the characteristic fragments at m/z 194.1095 and m/z 179.0863 (chromatogram in Figure 117, mass spectrum in Figure 118). A loss of 103.0574 Da, indicative for a primary hydroxy group at carbon 18 or, as presumed at carbon 19, was not detectable. Further research is needed to allow a structure proposal for this metabolite.

Biotransformation of 1-testosterone by CYP3A4 (chromatogram in Figure 119) yielded three more hydroxylated metabolites (with the nominal m/z values 518 at 6.22 min, m/z 520 at 6.10 min and 6.30 min, data not shown) all with the typical 1-ene-3-oxo fragments (m/z 194 and m/z 179), but still, hydroxylation of the angular methyl groups was not likely based on mass spectrometric data.

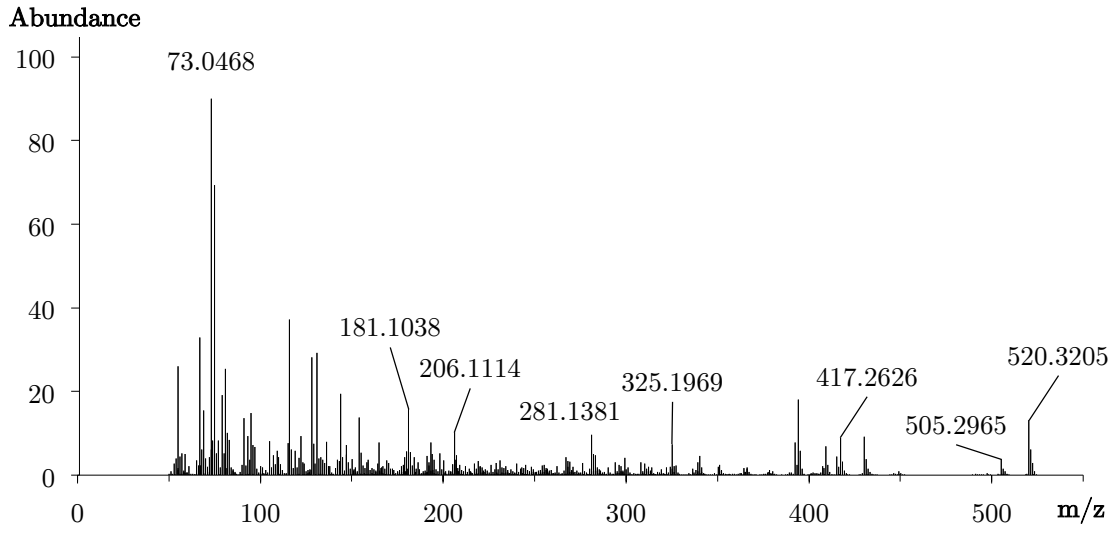

Figure 55 Accurate EI mass spectrum of potentially C18 or C19 hydroxylated 1-testosterone ($M2_{1\text{-}T}$) after incubation of 1-testosterone with HLM (tris-TMS derivative, retention time 5.67 min, $[M]^{\bullet+}$=520.3205, mass error -3.71 ppm)

The chromatogram obtained after incubation of 1-testosterone with human liver microsomes showed several peaks of potentially hydroxylated derivatives (even though to a much lesser extent than the biotransformation of 1-AED), including the three hydroxylated '1-ene-3-oxo' metabolites also detected in CYP3A4 incubation. Furthermore,

various hydroxylated metabolites presumably missing the 1,2-double bond are detected as well (chromatogram in Figure 120). Based on the loss of 103.0574 Da, one metabolite ($M2_{1\text{-}T}$, RT=5.67 min) possibly bearing a hydroxy group at one of the angular methyl groups was assigned (Figure 55). The fragment at m/z 417.2626 in direct comparison with the molecular ion $[M]^{+\bullet}$=520.3205 (mass error -3.71 ppm), may originate from the loss of 103.0578 Da corresponding to $[CH_2OTMS]^{\bullet}$ (mass error of the fragment 3.88 ppm). Microsome dependent biotransformation of 1-testosterone also resulted in metabolites with four oxygen functions based on mass spectrometric data. An example demonstrates $M3_{1\text{-}T}$ with the molecular ion $[M]^{+\bullet}$=608.3537 (theoretical mass of $C_{31}H_{60}O_4Si_4$ 608.3563 Da, mass error -4.27 ppm) detected at 7.13 min with corresponding fragments at m/z 194.1112 and m/z 179.0873 indicating a di-hydroxylated and oxidized 1-testosterone metabolite with a 1,2-double bond (mass spectrum in Figure 121).

Analysis of a doping control sample, positively tested for 1-testosterone administration, showed the extracted ion chromatogram for mono-hydroxylated species displayed in Figure 56. None of the peaks were assigned to hydroxylated 3-oxo-1-ene-androstanes. Potentially hydroxylated metabolites detected in this sample were most likely derived from endogenous or 1,2-double bond reduced, dihydrotestosterone-like metabolites since no characteristic fragments (m/z 194 or m/z 179) were observed.

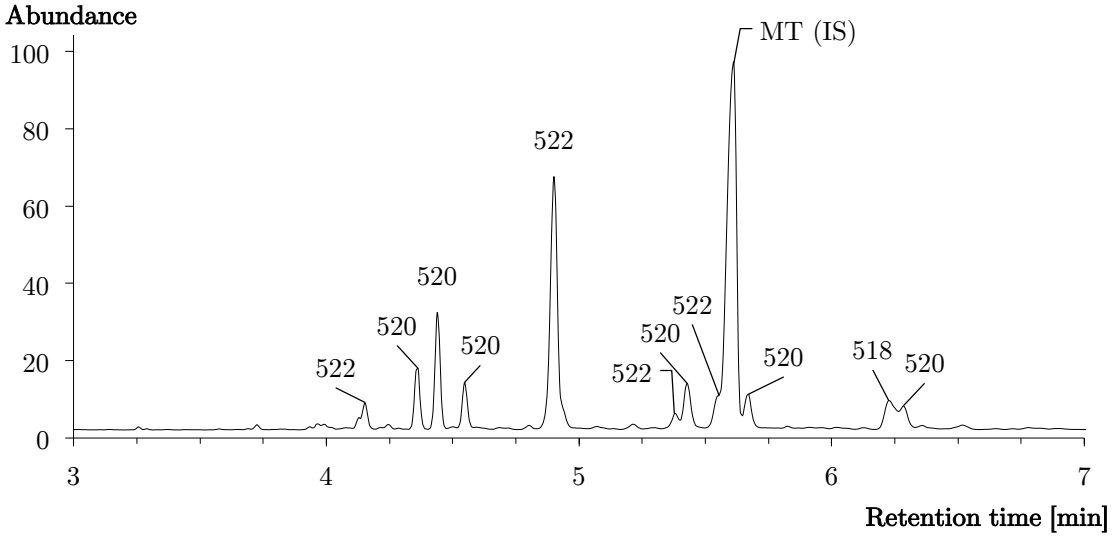

Figure 56 Extracted ion chromatogram showing mono-hydroxylated urinary metabolites after 1-testosterone administration with nominal masses of the tris-TMS derivatives, internal standard methyltestosterone (MT, 8 µg/mL), acquired using method b)

Nevertheless, non-hydroxylated metabolites as well as the parent compound were identified with the modified gas chromatographic method b) (not indicated in Figure 56).

1-Testosterone is reported to be metabolized within the human body to 1-AED [72], comparable with the oxidation of testosterone to androstenedione. Some additionally proposed metabolites of 1-testosterone featuring a 1,2-double bond are 3β-hydroxy-5α-androst-1-en-17-one, 5α-androst-1-ene-3β,17β-diol or 5α-androst-1-ene-3α,17β-diol [72-74]. Enzymatic hydroxylation was confirmed to occur *in-vitro* at carbon 16 (16ξ,17ξ-dihydroxy-5α-androst-1-en-3-one [73]).

Here, various hydroxylated metabolites of 1-testosterone were generated *in-vitro*, although to a very low extent. Based on accurate mass data, two metabolites potentially hydroxylated at C18/19 ($M2_{1\text{-}T}$ and $M3_{1\text{-}T}$) are proposed. $M1_{1\text{-}T}$ on the other hand is most likely hydroxylated at the gonane backbone. However, confirmation *in-vivo* was not achieved. The importance of hydroxylated 1-testosterone metabolites seems to play a minor role in the elimination of this steroid.

4.3.2 Biotransformation of selected androgens *in-vitro*

Other examples of closely related androstane derivatives were chosen for *in-vitro* experiments with aromatase, CYP3A4 and HLM. Two more exogenous androgenic anabolic steroids were selected: boldenone (BOLD, 17β-hydroxyandrosta-1,4-dien-3-one, mass spectrum Figure 122) and boldione (ADD, androsta-1,4-diene-3,17-dione, mass spectrum Figure 123), both prohibited substances in sports mentioned under section S1 1. a) in the WADA prohibited list [2] (from 2017 on these two steroids are assorted to section S1 1. b) [75]). In addition, the two endogenous androgens, androstanedione (5α-AD, 5α-androstane-3,17-dione, mass spectrum Figure 124) and dihydrotestosterone (5α-DHT, 17β-hydroxy-5α-androstane-3-one, mass spectrum Figure 125), were part of this study. Boldenone and boldione, both contain a 3-oxo-1,4-diene structure whereas 5α-AD and 5α-DHT both consist of a saturated A-ring and a 5α configuration between rings A and B. The latter structural attributes should prevent aromatization of the A ring by aromatase. Several mono- as well as di-hydroxylated metabolites were detected based on the EI mass spectrometric fragmentation of their per-TMS derivatives and are discussed hereafter. The m/z values of their expected molecular ions $[M]^{\bullet+}$ are listed below (Table 19). Incubations were performed with 50 µM substrate solutions as described in chapter 3.2.5.

Table 19 Exemplary androgenic anabolic steroids and their hydroxylated metabolites with their theoretical accurate masses (m/z) of the molecular ion $[M]^{+\bullet}$

	underivatized	bis-TMS	mono-hydroxylated tris-TMS	di-hydroxylated tetrakis-TMS
1-AED	286.1927	430.2718	518.3062	606.3407
1-T	288.2084	432.2874	520.3219	608.3563
BOLD	286.1927	430.2718	518.3062	606.3407
ADD	284.1771	428.2561	516.2906	604.3250
5α-AD	288.2084	432.2874	520.3219	608.3563
5α-DHT	290.2240	434.3031	522.3375	610.3720

In this study, incubation experiments yielded mainly reduced hydroxylated metabolites probably due to additional reductase activity in the assay. Mono-hydroxylation of 5α-AD and subsequent TMS derivatization results in a molecular ion $[M]_{theor.}^{+\bullet}$=520.3219. The chromatogram of the biotransformation of 5α-AD by aromatase shows small amounts of four different hydroxylated metabolites (Figure 126). One oxidized (dehydrogenated) 5α-AD derivative ($M1_{5\alpha\text{-AD}}$, RT=4.79 min, mass spectrum in Figure 57) most likely is hydroxylated either at C18 or, more likely, at C19 (assigned due to loss of 103. Da). The molecular ion $[M]^{+\bullet}$=518.3086 (theoretical mass of the bis-TMS 518.3062 Da, mass error 4.63 ppm) together with the fragment at m/z 415.2489 may correspond to the loss of $[CH_2OTMS]^{\bullet}$ and therefore to a hydroxylation of either carbon 18 or 19. The site of oxidation remains unclear, as formation of 19-hydroxyandrost-4-ene-3,17-dione (Figure 20) and 19-hydroxy-5α-androst-1-ene-3,17-dione (Figure 29) could be excluded by comparison with reference material. The accurate mass spectra of the three remaining metabolites indicate hydroxylation at the gonane backbone (data not shown). Structure proposal would need further experiments.

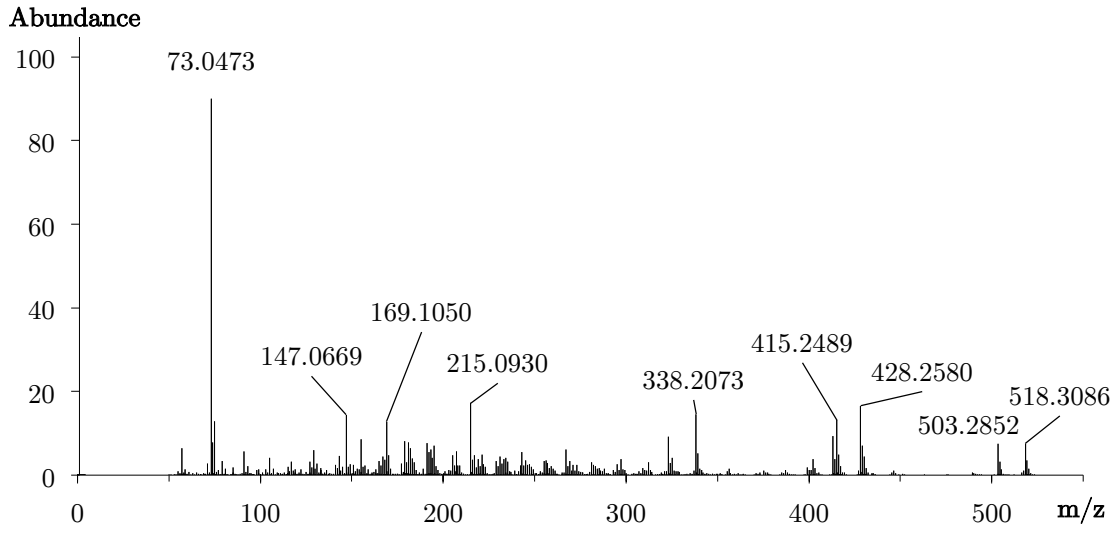

Figure 57 Accurate mass spectrum (EI) of an oxidized (dehydrogenated) and hydroxylated metabolite of 5α-androstane-3,17-dione ($M1_{5\alpha\text{-AD}}$) after incubation with CYP19A1 as tris-TMS derivative, retention time 4.79 min, $[M]^{\bullet+}$=518.3086, mass error 4.63 ppm

Biotransformation by CYP3A4 (chromatogram in Figure 127) produced greater amounts of hydroxylated metabolites. Based on the resulting mass spectra an assignment of hydroxylation sites other than the gonane backbone are not likely.

Incubation of 5α-AD with HLM resulted in the formation of seven potential hydroxylated metabolites (chromatogram of HLM incubation in Figure 128), five of which showed the same retention times and mass spectra as in the CYP3A4 experiments. Thus, the two additional hydroxylated metabolites only present after HLM incubation might not result from CYP3A4 but any other CYP enzyme also present in the microsomes. One hydroxylated metabolite $M2_{5\alpha\text{-AD}}$, generated by HLM, is most likely hydroxylated at C18 or C19 (mass spectrum in Figure 58). The corresponding molecular ion $[M]^{+\bullet}$ at m/z 522.3368 (theoretical mass 522.3375 Da, mass error -1.34 ppm) yielded several fragments, whereby the fragment at m/z 419.2778 presumably indicates $[M\text{-}CH_2OTMS]^+$ and m/z 329.2277 an additional loss of a trimethylsilanol group. Thus, a hydroxylation of one of the two angular methyl groups together with a reduction of an oxo group probably in position C17 seems very likely. Metabolite $M3_{5\alpha\text{-AD}}$ (RT=6.37 min, $[M]^{\bullet+}$=522.3381, mass error 1.15 ppm) was identified as 3β,16α-dihydroxy-5α-androstan-17-one (mass spectrum Figure 129) utilizing reference material. Small amounts of this metabolite were also detectable after CYP3A4 incubation. The structures of the remaining metabolites are not further addressed.

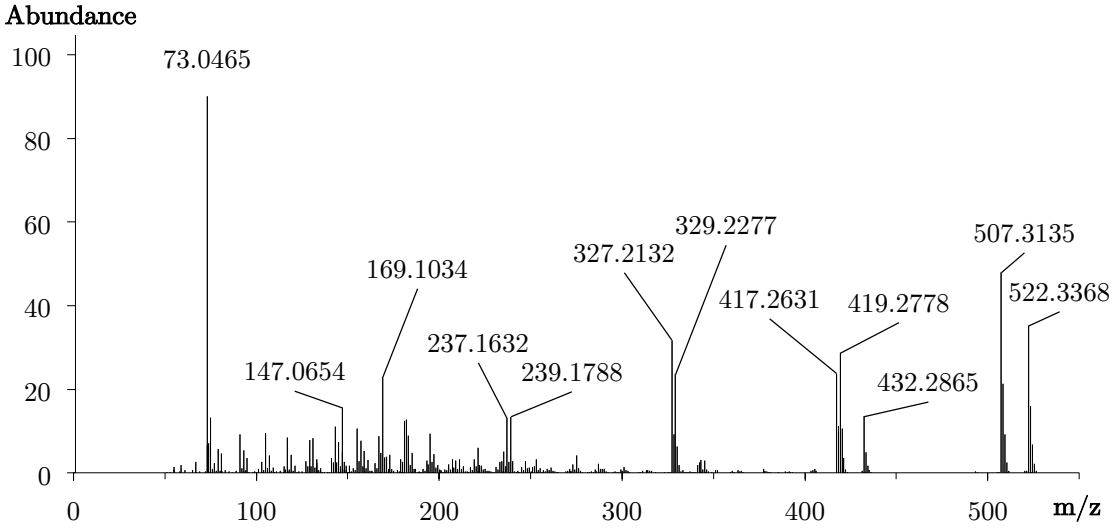

Figure 58 Accurate mass spectrum (EI) of a reduced and hydroxylated metabolite of 5α-androstane-3,17-dione ($M2_{5\alpha\text{-AD}}$) after incubation with HLM as tris-TMS derivative, retention time 4.93 min, $[M]^{\bullet+}$=522.3368, mass error -1.34 ppm

5α-AD originates from AED by reduction of the 4,5-double bond through the enzyme 5α-reductase. Generally, 5α-AD itself is metabolized within the human body by 3α-HSD into androsterone, by 3β-HSD into epiandrosterone, or by 17β-HSD into dihydrotestosterone. Nevertheless, hydroxylation of the molecule has already been reported in literature. Here, the *in vitro* generation of uncommon hydroxy-metabolites of 5α-AD is reported, whereas only in reduced and oxidized molecules.

Per-TMS derivatives of mono-hydroxylated dihydrotestosterone would show a molecular ion $[M]^{+\bullet}$=522.3375 (Table 19). Here, CYP19A1 incubation experiments with 5α-DHT gave very small amounts of three different hydroxylated metabolites (chromatogram in Figure 130). One showed a molecular ion of a potentially oxidized-hydroxylated metabolite ($M1_{5\alpha\text{-DHT}}$, $[M]^{+\bullet}$=520.3219, RT=4.91 min), similar to $M1_{5\alpha\text{-AD}}$ detected in 5α-AD incubation with aromatase. The accurate EI mass spectrum of this 5α-DHT metabolite $M1_{5\alpha\text{-DHT}}$ (Figure 59) indicates a molecular ion $[M]^{+\bullet}$=520.3219 (theoretical mass 520.3219, mass error 0 ppm), and a fragment at m/z 417.2636 which, taken together, lead to the assumption that the loss of 103.0583 Da originates from the fragment $[CH_2OTMS]^+$ (theoretical mass 103.0574) and can be assigned to C18- or C19-hydroxylation. Interstingly, oxidized-hydroxylated metabolites $M1_{5\alpha\text{-AD}}$ and $M1_{5\alpha\text{-DHT}}$ were only detectable after incubation with CYP19A1, but not CYP3A4 or HLM.

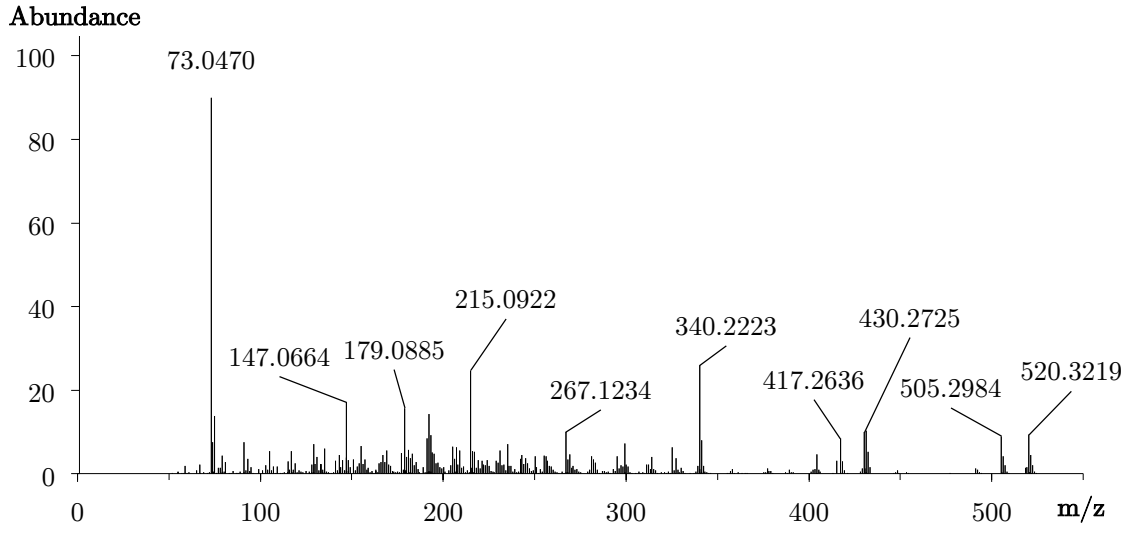

Figure 59 Accurate mass spectrum (EI) of an oxidized and hydroxylated metabolite of dihydrotestosterone after incubation with CYP19A1 ($M1_{1\text{-}T}$), as tris-TMS derivative, retention time 4.91 ion, $[M]^{+\bullet}$=520.3219, mass error -1.02 ppm

The two other obtained metabolites of aromatase incubation did not show any fragments suggesting a hydroxylation either at positions 18 or 19. Moreover, biotransformation of 5α-DHT by aromatase revealed two more potential metabolites $M2_{5\alpha\text{-DHT}}$ ($[M]^{+\bullet}$=418.2715, RT=4.55 min, mass spectrum in Figure 60) and $M3_{5\alpha\text{-DHT}}$ ($[M]^{+\bullet}$=418.2728, RT=5.87 min, mass spectrum in Figure 131). The molecular formula $C_{24}H_{42}O_2Si_2$ ($[M]^{+\bullet}$=418.2718) possibly complies with a '19-nor-DHT' derivative which has already been described by Cheng et al [76]. They introduced 17β-hydroxy-5α-estr-1(10)-en-3-one, 17β-hydroxy-5α-estr-9(10)-en-3-one and 17β- hydroxyestr-5(10)-en-3-one as potential products of the reaction of aromatase with 5α-DHT. In this study only two instead of three possible '19-nor' metabolites are postulated based on their accurate mass spectra.

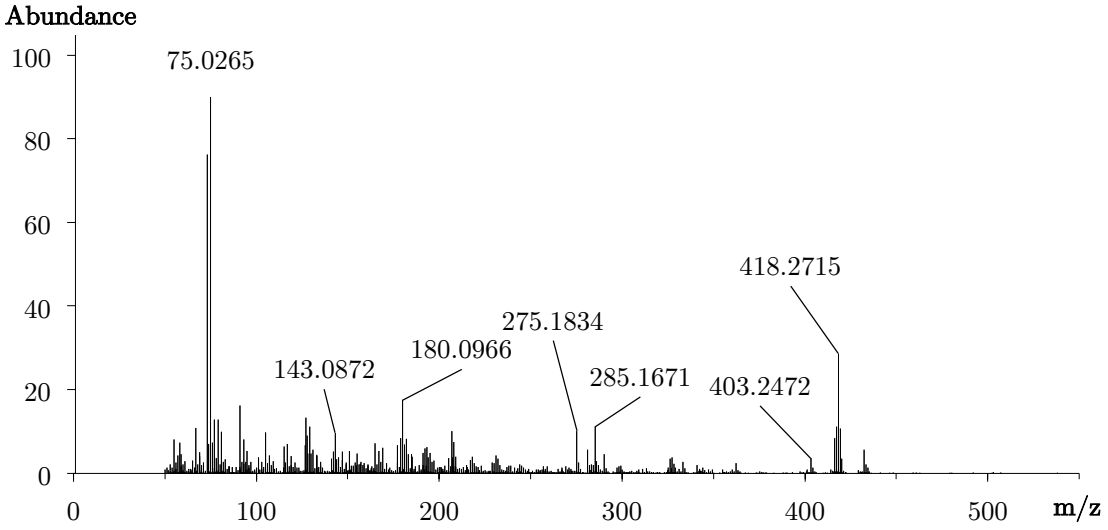

Figure 60 Accurate mass spectrum (EI) of a 19-nortestosterone isomer ($M2_{5\alpha\text{-DHT}}$) as bis-TMS, retention time 4.55 min, $[M]^{\bullet+}$=418.2715, mass error -1.98 ppm

CYP3A4 incubation on the other hand only yielded one main hydroxylated metabolite $M4_{5\alpha\text{-DHT}}$ (chromatogram in Figure 132, mass spectrum in Figure 133), which was also present after aromatase incubation but to a much lesser extent.

Biotransformation of 5α-DHT by HLM resulted in 12 different hydroxylated derivatives based on the obtained chromatogram and the corresponding accurate mass spectra (chromatogram Figure 134). Two of these metabolites may be assigned as 18- and 19-hydroxydihydrotestosterone. The hydroxylated metabolite $M5_{5\alpha\text{-DHT}}$ corresponding to the mass spectrum displayed in Figure 61 (RT=4.92 min) shows the same retention time as well as EI derived fragmentation of the molecular ion $[M]^{+\bullet}$=522.3366 (mass

error -1.72 ppm) as the metabolite $M2_{5\alpha\text{-AD}}$ of 5α-AD obtained by incubation with HLM (mass spectrum in Figure 58). This supports the argumentation of reduction at carbon 17 rather than carbon 3 of 5α-AD. Thus, metabolites $M2_{5\alpha\text{-AD}}$ and $M5_{5\alpha\text{-DHT}}$ may represent in fact the same substance.

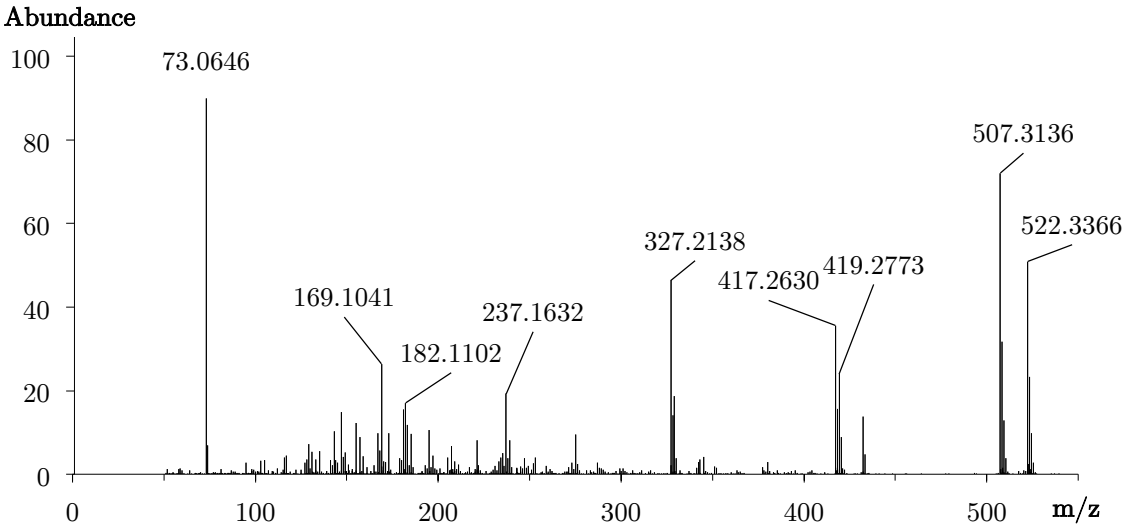

Figure 61 Accurate mass spectrum (EI) of a hydroxylated metabolite of dihydrotestosterone after incubation with HLM ($M5_{5\alpha\text{-DHT}}$) as tris-TMS derivative, retention time 4.92 min, $[M]^{\bullet+}$=522.3366, mass error -1.72 ppm

The main metabolite $M4_{5\alpha\text{-DHT}}$ of CYP3A4 incubation was also present after HLM incubation but to a slightly lesser degree. The accurate mass spectrum (EI) of $M4_{5\alpha\text{-DHT}}$ (RT=6.04 min, mass spectrum after HLM incubation in Figure 62). shows a base peak and molecular ion $[M]^{+\bullet}$=522.3398 (mass error -4.40 ppm) and a small fragment at m/z 419.2792 which may indicate the loss of 103.0606 Da. This could imply hydroxylation either at carbon 18 or at carbon 19.

5α-DHT is usually generated *in-vivo* from testosterone by 5α-reductase. An alternative pathway of 5α-DHT formation is the reduction of 5α-AD by 17β-HSD. Phase I metabolism usually includes reduction of the 3-oxo group to 5α-androstanediol by 3α-HSD or oxidation by 17β-HSD back to 5α-AD following reduction to androsterone by 3α-HSD. Subsequent glucuronidation to the corresponding 3- or 17-glucuronates represent the main routes in phase II metabolism. Nonetheless, as is the case for 5α-AD, metabolic hydroxylation reactions have also been reported for 5α-DHT including but not limited to 2β-, 6β-, 7α-, 16α-, 18-, and 19-hydroxylations [76-78]. Nonetheless, two metabolites of dihydrotestosterone hydroxylated by HLM or CYP3A4 potentially at carbon 18 or 19

($M5_{5\alpha\text{-DHT}}$ in Figure 61 and $M4_{5\alpha\text{-DHT}}$ in Figure 62) and an oxidized metabolite hypothetically hydroxylated at carbon 19 by aromatase ($M1_{5\alpha\text{-DHT}}$ in Figure 59) are postulated, partly confirming earlier findings of 18- and 19-hydroxylation of 5α-DHT by aromatase and CYP3A4 (HLM) [76]. 3-oxo-17β-hydroxy-5α-androstan-19-al (19oxo-DHT) and a '19-nor' derivative (such as $M2_{5\alpha\text{-DHT}}$ and $M3_{5\alpha\text{-DHT}}$) hydroxylated at C2, as proposed in a study by Cheng et al [76] could not be confirmed here. The various number of hydroxylated metabolites communicated here strengthen earlier *in-vitro* findings by Gustafsson et al [77, 78].

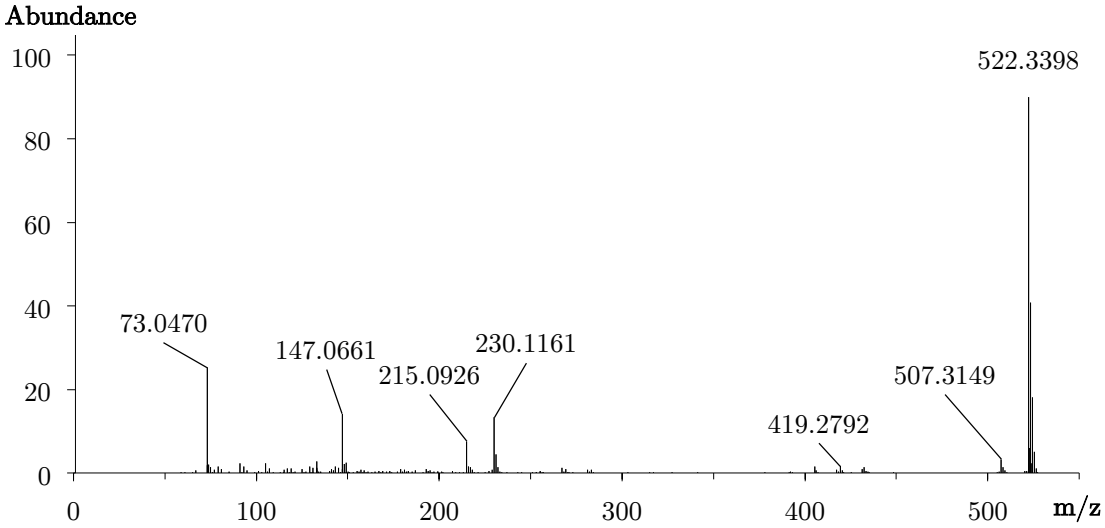

Figure 62 Accurate mass spectrum (EI) of a hydroxylated metabolite of dihydrotesotsterone after incubation with HLM ($M4_{5\alpha\text{-DHT}}$) as tris-TMS derivative, retention time 6.04 min, $[M]^{\bullet+}$=522.3398, mass error -4.40 ppm

Boldenone (BOLD) and boldione (ADD) are synthetic androgenic anabolic steroid with a 3-oxo-1,4-diene structure (as in the prominent synthetic steroids metandienone or dehydrochlormethyltestosterone, oral turinabol), whereas endogenous formation has been reported recently [79]. The 1,2-double bond hampers reduction of the A-ring by 5α-reductase. Therefore, main metabolites of BOLD and ADD are reported as 5β-reduced derivatives e.g. 17β-hydroxy-5β-androst-1-en-3-one. This particular metabolite also occurred in this study after incubation of BOLD with human liver microsomes and was confirmed with reference material (mass spectrum in Figure 135). Hydroxylation at position six resulting in 6β,17β-dihydroxyandrosta-1,4-dien-3-one, 6β-hydroxyandrosta-1,4-dien-3,17-dione or 6β-hydroxy-5β-androst-1-ene-3,17-dione, are metabolic hydroxylation reactions reported in literature [17, 80, 81], but insignificant *e.g.* for doping analysis due to low excreted amounts and detection windows [82]. Investigation of boldenone metabolism in horses revealed a variety of metabolites based on mass spectral analysis including hydroxylated derivatives *e.g.* 16ξ-hydroxy-5α-androst-1-ene-3,17-dione, 16ξ,17ξ-dihydroxyandrosta-1,4-dien-3-one, or 6ξ,16ξ,17ξ-trihydroxy-androsta-1,4-dien-3-one [83]. 6β,17β-dihydroxyandrosta-1,4-dien-3-one and 16α,17β-dihydroxyandrosta-1,4-dien-3-one were also confirmed after incubation of boldenone with subcellular fractions of cattle liver and kidney with the use of reference material by LC-MS/MS [84]. Further metabolites of ADD are 6β-hydroxylated boldenone/boldione [85]. Another hydroxylated ADD like metabolite is for example 4-hydroxyandrosta-1,4-diene-3,17-dione (or dehydroformestane), although this metabolite was reported after 4-hydroxytestosterone administration [86] and did not originate from ADD itself.

However, compared for instance to 1-T and 1-AED, the quantity of hydroxylated metabolites generated in this study was notably larger in case of BOLD and ADD, even though incubation experiments yielded far less different mono-hydroxylated metabolites. Biotransformation of BOLD by aromatase gave two potentially hydroxylated metabolites (chromatogram in Figure 136) that were also present in control experiments almost to the same amount, which indicates unspecific oxidation/hydroxylation. Nonetheless, a potentially di-hydroxylated and reduced metabolite $M1_{BOLD}$ after biotransformation by

aromatase was detected ($[M]^{+\bullet}$=608.3505, retention time 7.11 min, mass spectrum Figure 63). The corresponding mass spectrum indicates the loss of a $[CH_2OTMS]^{\bullet}$ due to the mass loss of 103.0569 Da (resulting in m/z 505.2955). Thus, hydroxylation at carbon 19 may be suggested.

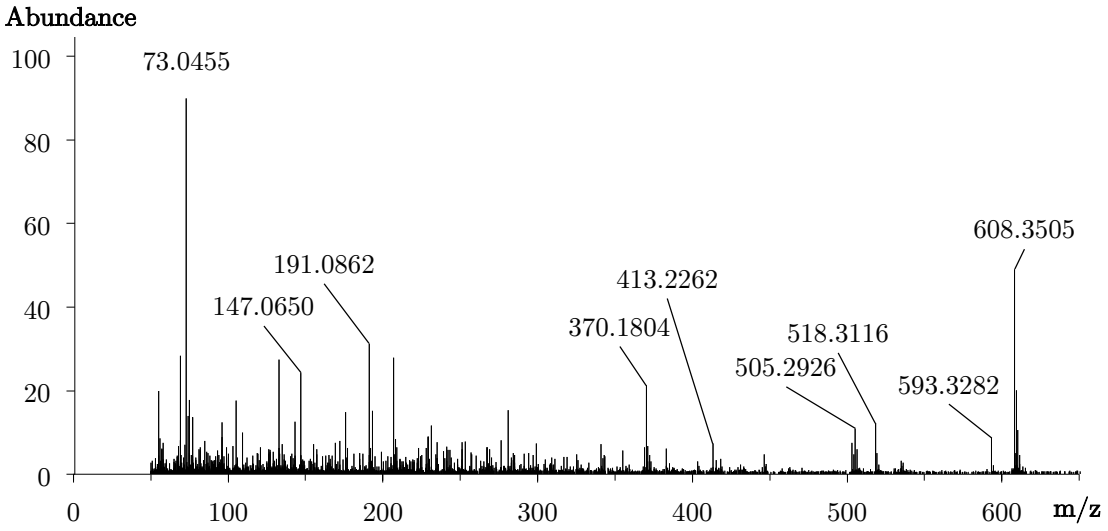

Figure 63 Accurate mass spectrum (EI) of a reduced and di-hydroxylated metabolite of boldenone after incubation with CYP19A1 ($M1_{BOLD}$) as tetrakis-TMS derivative, retention tim 7.11 min, $[M]^{\bullet+}$=608.3505, mass error -9.53 ppm

The incubation of ADD with aromatase (CYP19A1) resulted in the formation of BOLD as anticipated due to reductase activity in the assay. Hydroxylated metabolites (chromatogram Figure 144) occurred only to that amount generated in control experiments, analogously to the biotransformation of BOLD by unspecific hydroxylation/oxidation. Moreover, a di-hydroxylated and reduced metabolite $M1_{ADD}$ is postulated again here with a molecular ion $[M]^{\bullet+}$=606.3383 (RT=6.94 min, mass error -3.96 ppm) showing a mass loss of 103.0622 Da resulting in the fragment m/z 503.2761 (mass spectrum in Figure 145). Thus, the formation of a primary hydroxylated metabolite is proposed, arguably at C19.

Computational docking experiments showed that ADD fits into the active site of aromatase comparably well, just like androstenedione [87]. Furthermore, aromatization of ADD to estrone by aromatase has been described in literature [88], whereby ADD itself counts as a suicide substrate for aromatase and is responsible for aromatase inactivation. The involved mechanism still remains unsolved. Postulated are a non-enzymatic, chemical aromatization after enzymatic C19 hydroxylation resulting in estrone and formaldehyde or

a formation of an enzyme-bound product and formic acid [89]. However, 19-hydroxylated BOLD or ADD might not be stable because of a chemically induced aromatization [89] or not detectable due to aromatase inactivation. Since formation of estradiol/estrone was not observed, 19-hydroxylation alone seems less likely and may therefore be undetectable. The reported di-hydroxylated metabolites $M1_{BOLD}$ and $M1_{ADD}$ however may somehow represent stable primary hydroxylated structures.

Biotransformation of BOLD by CYP3A4 (chromatogram Figure 137) revealed metabolite $M2_{BOLD}$ ($[M]^{+\bullet}$=518.3053, RT=5.96 min, mass spectrum Figure 138) as the main metabolite with a base peak at m/z 503.2827 which might be assigned to 6β,17β-dihydroxyandrosta-1,4-dien-3-one (6β-hydroxyboldenone = $M2_{BOLD}$) in comparison with EI derived fragmentation patterns reviewed from literature [81, 90]. This peak was also detectable in control samples, indicating unspecific hydroxylation. Some control samples showed small amounts of a hydroxylated metabolite, probably in position six. This was verified exemplarily for AED with standards of 6α/β-hydroxyandrost-4-ene-3,17-dione. The 3-oxo-4-ene structure is most likely supporting the 6-hydroxylation since the internal standard methyltestosterone was also hydroxylated in position 6 (verified with reference substance 6β,17β-dihydroxy-17α-methylandrost-4-en-3-one, mass spectrum in Figure 139) in all samples, even though it was added to the incubation experiments after stopping the enzymatic reaction with acetonitrile and worked up shortly after. Thus, 6-hydroxylation probably occurs non-enzymatically as well – at least to a small extent.

CYP3A4 incubation of ADD (chromatogram Figure 146) revealed the formation of boldenone (approx. 15 % of the parent compound). Additionally, concerning hydroxylated metabolites, the main peak was assigned to $M2_{ADD}$ with the molecular ion $[M]^{\bullet+}$=516.2917 (RT=5.78 min, mass error 2.13 ppm, mass spectrum in Figure 147), probably being 6β-hydroxyandrosta-1,4-dien-3,17-dione by comparison with data from literature [81]. $M2_{BOLD}$ (6β,17β-dihydroxyandrosta-1,4-dien-3-one, $[M]^{\bullet+}$=518.3041, RT=5.94 min) is also proposed as a reduced hydroxylated metabolite respectively. Compared to the BOLD incubations, mass spectra and retention time were similar and furthermore, the amount generated (approx. 18 %) complies with the ratio of formed BOLD (approx. 15 %).

A further hydroxylated metabolite $M3_{BOLD}$ ($[M]^{\bullet+}$=520.3207, mass error -2.69 ppm, mass spectrum in Figure 140) was detected after CYP3A4 incubation of BOLD (RT=6.11 min) presumably representing a reduced form of the postulated 6β,17β-dihydroxyandrosta-1,4-dien-3-one. Accordingly, yet another peak was detectable in the ADD experiment and assigned to $M3_{ADD}$ (RT=6.65 min). The corresponding mass spectrum shows a base peak at m/z 501.2677 (and a molecular ion $[M]^{\bullet+}$=516.2922, mass error 3.10 ppm mass spectrum in Figure 64) and characteristic fragments at m/z 206.1117 and m/z 191.0873, indicating hydroxylation most likely at the D-ring. The fragment at m/z 413.2215 primary implying the loss of a trimethylsilylated hydroxy methylene group does not show the required exact mass and was therefore neglected.

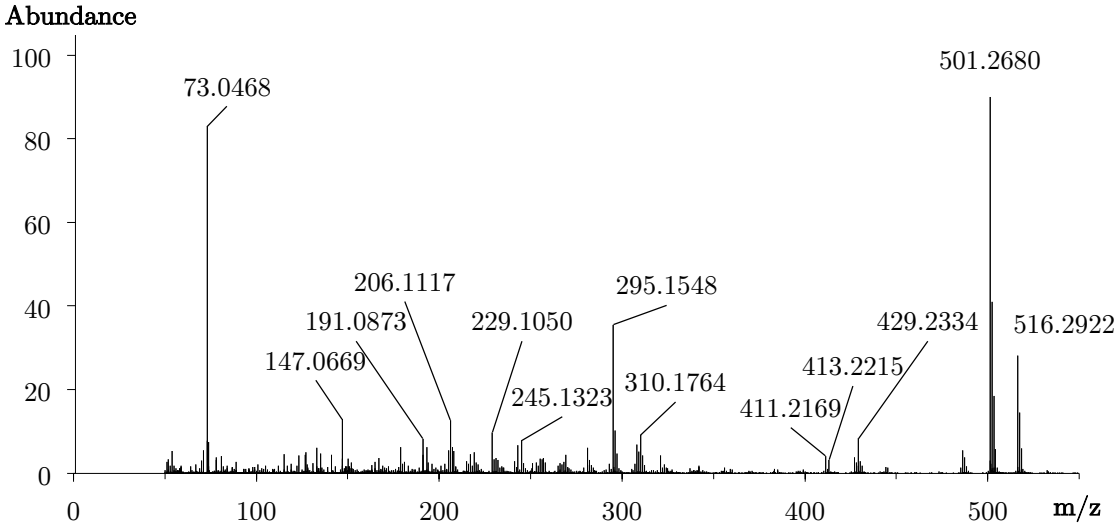

Figure 64 Accurate mass spectrum (EI) of a minor hydroxylated metabolite of boldione after incubation with CYP3A4 ($M3_{ADD}$) as tris-TMS derivative, retention time 6.65 min, $[M]^{\bullet+}$=516.2922, mass error 3.10 ppm

The chromatogram of the incubation of BOLD with HLM (Figure 141) revealed four peaks. Besides the main metabolite $M2_{BOLD}$ (RT=5.97 min), that also occurred after CYP19A1 and CYP3A4 incubations, and the metabolite $M3_{BOLD}$ ($[M]^{\bullet+}$=520.3202, RT=6.11 min, compare Figure 140), two more hydroxylated BOLD metabolites are postulated. An oxidized form, supposedly corresponding to a hydroxylated derivative of ADD (therefore assigned to $M2_{ADD}$, m/z 516.2891, mass error -2.91 ppm, mass spectrum in Figure 142), showed a peak at 5.79 min. Additionally, small amounts of a hydroxylated BOLD derivative $M4_{BOLD}$ were detected (RT=6.61 min, mass error -3.47 ppm, mass spectrum in

Figure 65). The molecular ion $[M]^{+\bullet}$=518.3044, together with the A/B-ring fragments m/z 206.1114 and m/z 191.0876, would indicate hydroxylation of the BOLD molecule at rings C or D, arguably at carbon 16.

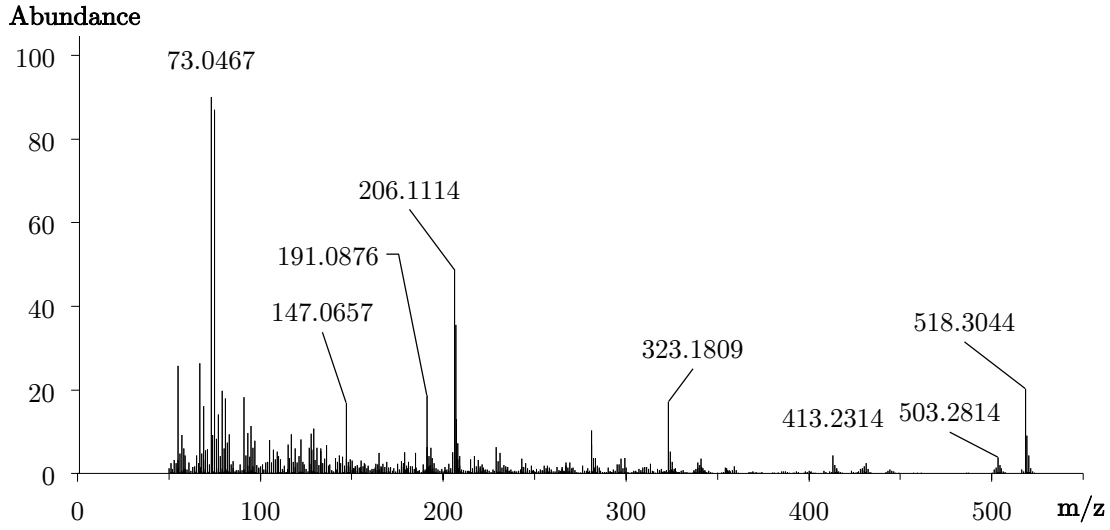

Figure 65 Accurate mass spectrum (EI) of a minor hydroxylated metabolite of boldenone after incubation with HLM ($M4_{BOLD}$) as tris-TMS derivative, retention time 6.61 min, $[M]^{\bullet+}$=518.3044, mass error -3.47 ppm

Biotransformation of ADD by human liver microsomes resulted in a few but abundant peaks of hydroxylated derivatives (chromatogram in in Figure 148). The main metabolite $M2_{ADD}$ (RT=5.79 min), the reduced hydroxylated metabolite $M2_{BOLD}$ (RT=5.96 min), and the above mentioned metabolite $M3_{ADD}$ (RT=6.65 min) already described after CYP3A4 biotransformation were detected again, but to a much greater extent.

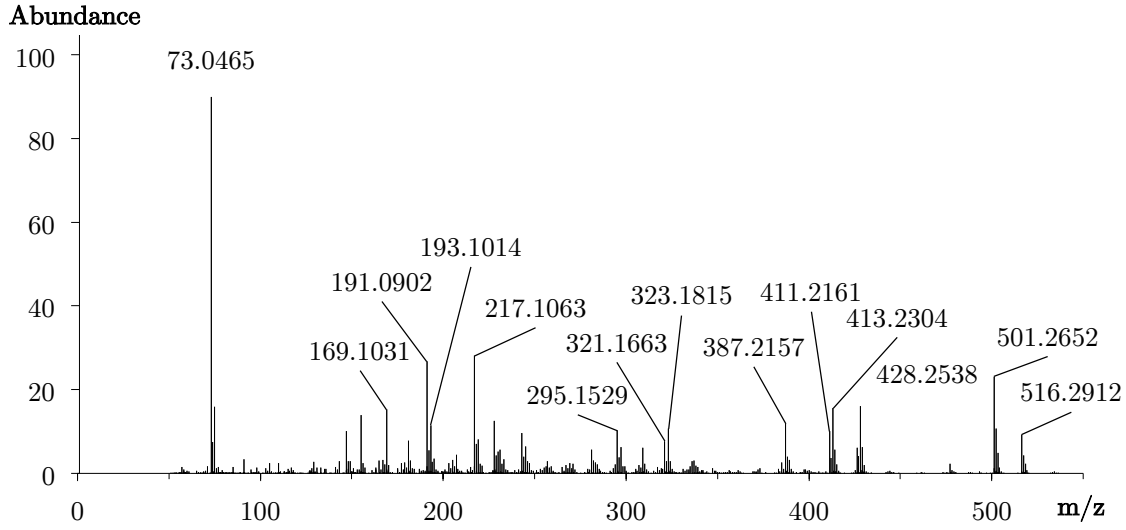

Figure 66 Accurate mass spectrum (EI) of a minor hydroxylated metabolite of boldione after incubation with HLM ($M4_{ADD}$) as tris-TMS derivative, retention time 5.11 min, $[M]^{\bullet+}$=516.2912, mass error 1.16 ppm

At 5.11 min a peak with the molecular ion $[M]^{\bullet+}$=516.2912 (mass error 1.16 ppm) and the fragment m/z 413.2304 indicate a mass loss of 103.0608 Da probably representing the loss of $[CH_2OTMS]^{\bullet}$ (mass spectrum in Figure 66). This particular metabolite $M4_{ADD}$ was not detectable after incubation of ADD with CYP3A4. In all incubation experiments with BOLD 3,17β-dihydroxyestra-1,3,5(10),6-tetraene ($[M]^{+\bullet}$=414.2405 as bis-TMS derivative) was detected, and verified by comparison with the derivatization artifact of 17β-hydroxyandrosta-1,4,6-trien-3-one (mass spectrum Figure 143) as described by Parr et al [91]. The artifact was also detected in the CYP3A4 and control incubations, albeit in a lower amount compared to the aromatase experiment. Minor amounts of a possible hydroxylated estrenedione derivative (theoretical mass of $[M]^{\bullet+}$ as tris-TMS derivative 502.2749 Da) were detected as well (m/z 502.2743, mass error -1.19 ppm, retention time 6.23 min, mass spectrum of the tris-TMS derivative in Figure 67). Therein, the m/z value 487.2504 may be explained as $[M\text{-}CH_3]^{+}$ and m/z 412.2236 may result from the loss of trimethylsilanol ($[M\text{-}TMSOH]^{+\bullet}$). This substance was also detected in control experiments indicating artifact formation from a hydroxylated boldenone derivative, likely 6β,17β-dihydroxyandrosta-1,4-dien-3-one, generated non-enzymatically and hypothetically resulting in 3,6,17β-trihydroxyestra-1,3,5(10),6-tetraene. Consequently, 3-hydroxy-estra-1,3,5(10),6-tetraene-17-one was detected in experiments containing ADD and verified

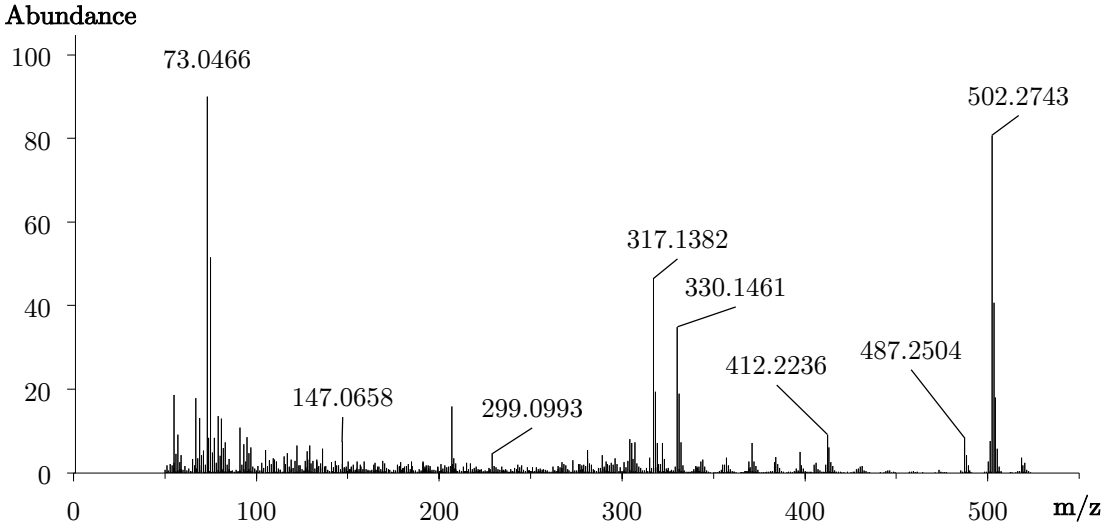

Figure 67 Accurate mass spectrum (EI) of a hydroxylated estrenedione-like derivatization artifact of hydroxylated boldenone as tris-TMS after incubation of boldenone with HLM, retention time 6.23 min, $[M]^{\bullet+}$=502.2743, mass error -1.19 ppm

after comparison with reference material (bis-TMS derivative m/z 412.2248, mass spectrum Figure 149). This could indicate the formation of a derivatization artifact comparable to boldenone as reported in literature [91]. A hydroxylated derivatization artifact comparable to boldenone incubations was not detected.

ADD biotransformation by aromatase revealed a reduced and potentially di-hydroxylated metabolite analogously to the incubation of BOLD with CYP19A1. The generated amount was very small in both cases, but absent in CYP3A4 and HLM experiments, concluding that both metabolites may be of aromatase-specific origin. Biotransformation by CYP3A4/HLM of ADD and BOLD resulted in a few but abundant hydroxylated metabolites, whereby a hydroxylation of an angular methyl group was only postulated for ADD in trace amounts, arguably C18 hydroxylation. Based on accurate mass measurements and analysis of characteristic fragments obtained by electron ionization after TMS derivatization several hydroxylated metabolites of androstane derivatives were postulated. The variety of hydroxylation products was greater for the endogenous substrates 5α-AD, 5α-DHT and the two 1-androgens than for ADD and BOLD, whereby the amount of hydroxylated metabolites based on peak area was higher in case of the 1,4-diene-3-oxo steroids.

5 Summary and Outlook

The most common type of performance enhancing drugs (PED) are anabolic androgenic steroids (AAS). These substances are derived from the male sex hormones testosterone and 5α-dihydrotestosterone and are supposed to promote mainly anabolic effects.

Cytochrome P450 (CYP) enzymes play an important role in the biosynthesis of steroid hormones. In Phase I metabolism of endogenous as well as exogenous steroids their part is also clearly relevant. Drug metabolizing CYP enzymes are seemingly as important as their steroidogenic counterpart. The most prominent reaction catalyzed by CYP enzymes is the insertion of a hydroxy group.

The designer steroid 1-androstenedione (1-AED) and the endogenous prohormone androstenedione (AED) have been investigated regarding the formation of hydroxylated Phase I metabolites. Therefore, chemical synthesis of reference substances, *in vitro* biotransformation with CYP enzymes of interest (CYP19A1, CYP3A4 and human liver microsomes) and investigation of *in vivo* formation after administration of the precursors were conducted.

The formation of 19-hydroxylted 1-AED by CYP19A1 was verified with synthesized reference material. *In vitro* generation of this metabolite could not be confirmed and remains doubtful. The 2β-hydroxylation of endogenous AED was shown *in vivo* (post administration) by comparison with a synthesized reference. Several other hydroxylated metabolites of AED and 1-AED and closely related steroids were postulated based on accurate mass spectrometric data and structure proposals are made.

Future work could focus on structure confirmation of the proposed metabolites reference material. This could be achieved by chemical synthesis supported by biocatalytic hydroxylation.

5 Zusammenfassung und Ausblick

Anabole androgene Steroide (AAS) sind die am häufigsten missbräuchlich angewendeten leistungssteigernden Substanzen (kurz: PED). Sie leiten sich von den männlichen Sexualhormonen Testosteron und 5α-Dihydrotestosteron ab und werden vor allem wegen ihrer anabolen Wirkung genutzt.

Cytochrom P450 (CYP) Enzyme spielen eine wichtige Rolle in der Biosynthese von Steroidhormonen. Im Phase-I-Metabolismus von endogenen als auch exogenen Steroiden sind sie ebenfalls relevant. Dabei sind Xenobiotika metabolisierende CYP-Enzyme scheinbar ebenso wichtig wie steroidspezifische CYP-Enzyme. Die bedeutendste Metabolisierungsreaktion dabei ist die Hydroxylierung.

Das Designersteroid 1-Androstendion (1-AED) und das endogen vorkommende Prohormon Androstendion (AED) wurden hinsichtlich der Bildung von hydroxylierten Phase-I-Metaboliten untersucht

Dazu sind Referenzsubstanzen möglicher Hydroxy-Metaboliten synthetisiert worden. Es wurden *in-vitro* Experimente mit in Frage kommenden CYP-Enzymen (CYP19A1, CYP3A4 und Mikrosomen) sowie der Nachweis *in-vivo* nach Verabreichung der Vorläufersubstanzen untersucht.

Die Bildung von 19-hydroxyliertem 1-AED durch CYP19A1 konnte mit dem zuvor synthetisierten Referenzmaterial bestätigt werden. In Postapplikationsurinen dagegen konnte kein Nachweis erbracht werden. Die Bildung von 2β-hydroxyliertem AED *in-vivo* dagegen konnte mit Referenzmaterial abgesichert werden. Neben AED und 1-AED wurden weitere strukturell eng verwandte Steroide *in-vitro* umgesetzt und zahlreiche mögliche Metaboliten aufgrund von MS Daten mit Strukturvorschlägen postuliert.

In Zukunft wäre eine Strukturbestätigung mit Referenzsubstanzen interessant. Die komplexen Synthesen könnten durch biokatalytische Systeme ergänzt werden.

6 References

[1] Pope HG, Jr., Wood RI, Rogol A, Nyberg F, Bowers L, Bhasin S. Adverse health consequences of performance-enhancing drugs: an Endocrine Society scientific statement. *Endocrine reviews* 35 (2014) 341-375

[2] WADA Prohibited List. (2016)

[3] WADA 2014 Anti-Doping Testing Figures Report. (2014)

[4] Kashkin KB, Kleber HD. Hooked on hormones?: An anabolic steroid addiction hypothesis. *JAMA* 262 (1989) 3166-3170

[5] Sagoe D, Molde H, Andreassen CS, Torsheim T, Pallesen S. The global epidemiology of anabolic-androgenic steroid use: a meta-analysis and meta-regression analysis. *Annals of epidemiology* 24 (2014) 383-398

[6] Foye. *Medicinal Chemistry*,

[7] Fukami M, Homma K, Hasegawa T, Ogata T. Backdoor pathway for dihydrotestosterone biosynthesis: implications for normal and abnormal human sex development. *Dev Dyn* 242 (2013) 320-329

[8] Rižner TL, Penning TM. Role of aldo-keto reductase family 1 (AKR1) enzymes in human steroid metabolism. *Steroids* 79 (2014) 49-63

[9] Auchus RJ. The backdoor pathway to dihydrotestosterone. *Trends in endocrinology and metabolism: TEM* 15 (2004) 432-438

[10] Carreau S, Wolczynski S, Galeraud-Denis I. Aromatase, oestrogens and human male reproduction. *Philosophical transactions of the Royal Society of London. Series B, Biological sciences* 365 (2010) 1571-1579

[11] Kicman AT. Pharmacology of anabolic steroids. *Br J Pharmacol* 154 (2008) 502-521

[12] Parr MK, Schänzer W. Detection of the misuse of steroids in doping control. *J Steroid Biochem Mol Biol* 121 (2010) 528-537

[13] Geyer H, Parr MK, Koehler K, Mareck U, Schänzer W, Thevis M. Nutritional supplements cross-contaminated and faked with doping substances. *J Mass Spectrom* 43 (2008) 892-902

[14] Joseph JF, Parr MK. Synthetic Androgens as Designer Supplements. *Current Neuropharmacology* 13 (2015) 89-100

[15] Graham MR, Ryan P, Baker JS, Davies B, Thomas NE, Cooper SM, Evans P, Easmon S, Walker CJ, Cowan D, Kicman AT. Counterfeiting in performance- and image-enhancing drugs. *Drug Test Anal* 1 (2009) 135-142

[16] Schänzer W. Metabolism of anabolic androgenic steroids. *Clinical chemistry* 42 (1996) 1001-1020

[17] Rendic S, Nolteernsting E, Schänzer W. Metabolism of anabolic steroids by recombinant human cytochrome P450 enzymes: Gas chromatographic–mass spectrometric determination of metabolites. *Journal of Chromatography B: Biomedical Sciences and Applications* 735 (1999) 73-83

[18] Parr MK, Zöllner A, Fußhöller G, Opfermann G, Schlörer N, Zorio M, Bureik M, Schänzer W. Unexpected contribution of cytochrome P450 enzymes CYP11B2 and CYP21, as well as CYP3A4 in xenobiotic androgen elimination – Insights from metandienone metabolism. *Toxicology letters* 213 (2012) 381-391

[19] Rittle J, Green MT. Cytochrome P450 compound I: capture, characterization, and C-H bond activation kinetics. *Science* 330 (2010) 933-937

[20] Sevrioukova IF, Poulos TL. Understanding the mechanism of cytochrome P450 3A4: recent advances and remaining problems. *Dalton Trans* 42 (2013) 3116-3126

[21] Groves JT. Key elements of the chemistry of cytochrome P-450: The oxygen rebound mechanism. *Journal of Chemical Education* 62 (1985) 928

[22] Brodie HJ, Pillai AK, Hay CE. Studies on the mechanism of estrogen biosynthesis. VII. 2β-Hydroxylation of estr-4-ene-3,17-dione in human placenta, in vitro. *Biochimica et Biophysica Acta (BBA) - Lipids and Lipid Metabolism* 187 (1969) 275-277

[23] Di Nardo G, Castrignanò S, Sadeghi SJ, Baravalle R, Gilardi G. Bioelectrochemistry as a tool for the study of aromatization of steroids by human aromatase. *Electrochemistry Communications* 52 (2015) 25-28

[24] Khatri Y, Luthra A, Duggal R, Sligar SG. Kinetic solvent isotope effect in steady-state turnover by CYP19A1 suggests involvement of Compound 1 for both hydroxylation and aromatization steps. *FEBS Lett* 588 (2014) 3117-3122

[25] Yoshimoto FK, Guengerich FP. Mechanism of the third oxidative step in the conversion of androgens to estrogens by cytochrome P450 19A1 steroid aromatase. *J Am Chem Soc* 136 (2014) 15016-15025

[26] Akhtar M, Wright JN, Lee-Robichaud P. A review of mechanistic studies on aromatase (CYP19) and 17alpha-hydroxylase-17,20-lyase (CYP17). *J Steroid Biochem Mol Biol* 125 (2011) 2-12

[27] Hackett JC, Brueggemeier RW, Hadad CM. The final catalytic step of cytochrome p450 aromatase: a density functional theory study. *J Am Chem Soc* 127 (2005) 5224-5237

[28] Niwa T, Murayama N, Imagawa Y, Yamazaki H. Regioselective hydroxylation of steroid hormones by human cytochromes P450. *Drug metabolism reviews* (2015) 1-22

[29] Sugimoto H, Shiro Y. Diversity and Substrate Specificity in the Structures of Steroidogenic Cytochrome P450 Enzymes. *Biological and Pharmaceutical Bulletin* 35 (2012) 818-823

[30] Krauser JA, Voehler M, Tseng LH, Schefer AB, Godejohann M, Guengerich FP. Testosterone 1 beta-hydroxylation by human cytochrome P450 3A4. *Eur J Biochem* 271 (2004) 3962-3969

[31] Thevis M, Kuuranne T, Geyer H, Schänzer W. Annual banned-substance review: analytical approaches in human sports drug testing. *Drug Test Anal* 6 (2014) 164-184

[32] Thevis M, Schänzer W. Mass spectrometry in sports drug testing: Structure characterization and analytical assays. *Mass spectrometry reviews* 26 (2007) 79-107

[33] Friedel A, Geyer H, Kamber M, Laudenbach-Leschowsky U, Schänzer W, Thevis M, Vollmer G, Zierau O, Diel P. 17beta-hydroxy-5alpha-androst-1-en-3-one (1-testosterone) is a potent androgen with anabolic properties. *Toxicology letters* 165 (2006) 149-155

[34] Reilly CA, Crouch DJ. Analysis of the Nutritional Supplement 1AD, Its Metabolites, and Related Endogenous Hormones in Biological Matrices Using Liquid Chromatography-Tandem Mass Spectrometry. *Journal of analytical toxicology* 28 (2004) 1-10

[35] Parr MK, Westphal F, Sönnichsen F, Geyer H, Schänzer W. 1-DHEA identification in seized dietary supplement. In: Schänzer W, Geyer H, Gotzmann A, Mareck U (Eds.) *Recent Advances in Doping Analysis (18)*, Sport & Buch Strauss, Cologne (2010) 241-244

[36] Parr MK, Opfermann G, Geyer H, Westphal F, Sönnichsen FD, Zapp J, Kwiatkowska D, Schänzer W. Seized designer supplement named "1-Androsterone": identification as 3beta-hydroxy-5alpha-androst-1-en-17-one and its urinary elimination. *Steroids* 76 (2011) 540-547

[37] Kazlauskas R, Hasick N. ASDTL Supplements Project 2010. In: Schänzer W, Geyer H, Gotzmann A, Mareck U (Eds.) *Recent Advances in Doping Analysis (19)*, Sport & Buch Strauss, Cologne (2011) 10-14

[38] Parr MK, Geyer H, Opfermann G, Schänzer W. Prescription drugs and new anabolic steroids in nutritional supplements. In: Schänzer W, Geyer H, Gotzmann A, Mareck U (Eds.) *Recent advances in doping analysis (12)*, Sport & Buch Strauss, Cologne (2004) 71-80

[39] Cavalcanti Gde A, Leal FD, Garrido BC, Padilha MC, De Aquino Neto FR. Detection of designer steroid methylstenbolone in "nutritional supplement" using gas chromatography and tandem mass spectrometry: elucidation of its urinary metabolites. *Steroids* 78 (2013) 228-233

[40] Krug O, Thomas A, Walpurgis K, Piper T, Sigmund G, Geyer H, Schänzer W, Thevis M. Mass spectrometric analysis of black market products by HPLC-(HR)MS, GC-(HR)MS and 1D-gel electrophoresis-UPLC-MS^n. In: Schänzer W, Thevis M, Geyer H, Mareck U (Eds.) *Recent Advances in Doping Analysis (21)*, Sport & Buch Strauss, Cologne (2013) 169-172

[41] Geldof L, Lootens L, Polet M, Eichner D, Campbell T, Nair V, Botre F, Meuleman P, Leroux-Roels G, Deventer K, Eenoo PV. Metabolism of methylstenbolone studied with human liver microsomes and the uPA(+/+) - SCID chimeric mouse model. *Biomedical chromatography : BMC* 28 (2014) 974-985

[42] Parr MK, Opfermann G, Schänzer W. Detection of new 17-alkylated anabolic steroids on WADA 2006 list. In: Schänzer W, Geyer H, Gotzmann A, Mareck U (Eds.) *Recent Advances in Doping Analysis (14)*, Sport & Buch Strauss, Cologne (2006) 249-258

[43] Müller D, Opfermann G, Rojas S, Schlörer N, Pokrywka A, Kwiatkowska D, Diel P, Schänzer W, Parr MK. 5alpha-Androst-1-ene-3,17-dione: metabolism, influence on steroid profile and biological activity. In: Schänzer W, Geyer H, Gotzmann A, Mareck U (Eds.) *Recent Advances in Doping Analysis (20)*, Sport & Buch Strauss, Cologne (2012) 197-200

[44] IOC. https://stillmed.olypmic.org/media/Document%20Library/OlympicORg/IOC/Who-We-Are/Commissions/Disciplinary-Commission/IOC-Disciplinary-

Commission-Decision-Tatyana - Firova.pdf#_ga=1.165230713.73568322.1472773598 accessed 3.9.2016

[45] Wang J, Wu M, Liu X, Xu Y. Profiling of urinary steroids by gas chromatography-mass spectrometry detection and confirmation of androstenedione administration using isotope ratio mass spectrometry. *Steroids* 76 (2011) 1560-1565

[46] Cawley AT, Trout GJ, Kazlauskas R, George AV. The detection of androstenedione abuse in sport: a mass spectrometry strategy to identify the 4-hydroxyandrostenedione metabolite. *Rapid communications in mass spectrometry : RCM* 22 (2008) 4147-4157

[47] Polet M, Van Renterghem P, Van Gansbeke W, Van Eenoo P. Studies on the minor metabolite 6a-hydroxy-androstenedione for doping control purposes and its contribution to the steroid profile. *Drug Test Anal* 6 (2014) 978-984

[48] De La Torre X, Colamonici C, Curcio D, Jardines D, Molaioni F, Parr MK, Botre F. Detection of formestane abuse by mass spectrometric techniques. *Drug Test Anal* 6 (2014) 1133-1140

[49] De La Torre X, Rosati L, Colamonici C, Parr MK, Curcio D, Jardines D, Molaioni F, Botre F. Studies on androstenedione metabolism: the never ending story? In: Schänzer W, Geyer H, Gotzmann A, Mareck U (Eds.) *Recent Advances in Doping Analysis (23)*, Sport & Buch Strauss, Cologne (2015)

[50] Parr MK, Stoll A, Botre F, De La Torre X. Structure reactivity relationship of A-ring hydroxylation of steroids by aryl hydrocarbon hydroxylases - from estrogens to androgens. in: *3rd Congress on steroid research*, Elsevier, Chicago (2015)

[51] Waxman DJ, Attisano C, Guengerich FP, Lapenson DP. Human liver microsomal steroid metabolism: Identification of the major microsomal steroid hormone 6β-hydroxylase cytochrome P-450 enzyme. *Archives of Biochemistry and Biophysics* 263 (1988) 424-436

[52] Mosa A, Neunzig J, Gerber A, Zapp J, Hannemann F, Pilak P, Bernhardt R. 2beta- and 16beta-hydroxylase activity of CYP11A1 and direct stimulatory effect of estrogens on pregnenolone formation. *J Steroid Biochem Mol Biol* 150 (2015) 1-10

[53] Donike M. N-Methyl-N-trimethylsilyl-trifluoracetamid, ein neues Silylierungsmittel aus der reihe der silylierten amide. *Journal of Chromatography A* 42 (1969) 103-104

[54] Geyer H, Schänzer W, Mareck-Engelke U, Nolteernsting E, Opfermann G. Screening procedure for anabolic steroids-control of hydrolysis with deuterated androsterone glucuronide and studies with direct hydrolysis. In: Schänzer W, Geyer H, Gotzmann A, Mareck-Engelke U (Eds.) *Recent Advances in Doping Analysis (5)*, Sport & Buch Strauss, Cologne (1998) 99-102

[55] Tomoeda M, Ishizaki M, Kobayashi H, Kanatomo S, Koga T, Inuzuka M, Furuta T. Studies on conformation and reactivity—I The polyphosphoric acid-catalyzed ring opening of 4,5-epoxy-3-oxo steroids—the synthesis of 4-ethylthiocholest-4-EN-3-one and its analogs. *Tetrahedron* 21 (1965) 733-742

[56] Chernushevich IV, Loboda AV, Thomson BA. An introduction to quadrupole-time-of-flight mass spectrometry. *J Mass Spectrom* 36 (2001) 849-865

[57] Kuuranne T, Pystynen KH, Thevis M, Leinonen A, Schänzer W, Kostiainen R. Screening of in vitro synthesised metabolites of 4,9,11-trien-3-one steroids by liquid chromatography mass spectrometry. *European journal of mass spectrometry* 14 (2008) 181-189

[58] Verheyden K, Le Bizec B, Courtheyn D, Mortier V, Vandewiele M, Gillis W, Vanthemsche P, De Brabander HF, Noppe H. Mass spectrometric detection of and similarities between 1-androgens. *Anal Chim Acta* 586 (2007) 57-72

[59] Shankar VN, Row TNG, Madyastha KM. Evidence for a new pathway in the microbial conversion of 3β-acetoxycholest-5-en-19-ol into estrone. *Journal of the Chemical Society, Perkin Transactions 1* (1993) 2233-2233

[60] Templeton JF, Lin W, Ling Y, Majgier-Baranowska H, Marat K. Synthesis of 19-hydroxy-1β,19-cyclosteroids. *Journal of the Chemical Society, Perkin Transactions 1* 19 (1997) 2037-2044

[61] Knox LH, Blossey E. Steroids. CCLXXVIII. 1 Reductions of 19-Substituted Androst-4-en-3-ones and Related Compounds. *The Journal of Organic Chemistry* 687 (1965) 2198-2205

[62] Nicolaou KC, Montagnon T, Baran PS. HIO3 and I2O5: mild and selective alternative reagents to IBX for the dehydrogenation of aldehydes and ketones. *Angew Chem Int Ed Engl* 41 (2002) 1386-1389

[63] Nicolaou KC, Montagnon T, Baran PS. Modulation of the reactivity profile of IBX by ligand complexation: ambient temperature dehydrogenation of aldehydes and ketones to alpha,beta-unsaturated carbonyl compounds. *Angew Chem Int Ed Engl* 41 (2002) 993-996

[64] Smith AG, Brooks CJW. Mass spectra of Δ4- and 5α-3-ketosteroids formed during the oxidation of some 3β-hydroxysteroids by cholesterol oxidase. *Biological Mass Spectrometry* 3 (1976) 81-87

[65] Masse R, Goudreault D. Studies on anabolic steroids -11. 18-Hydroxylated metabolites of mesterolone, methenolone and stenbolone: New steroids isolated from human urine. *Journal of steroid biochemistry* 42 (1992) 399-410

[66] Burnett RD, Kirk DN. Some observations on the preparation of 2-hydroxy-steroid 4-En-3-ones. *Journal of the Chemical Society, Perkin Transactions 1* (1973) 1830

[67] Rao PN, Gollberg HR, Axelrod LR. Synthesis of 2β-Hydroxy Steroids. II1,2. *The Journal of Organic Chemistry* 28 (1963) 270-272

[68] Mann J, Pietrzak B. The synthesis of 4-hydroxyandrost-4-ene-3,17-dione and other potential aromatase inhibitors. *Journal of the Chemical Society, Perkin Transactions 1* (1983) 2681

[69] Christakoudi S, Cowan DA, Taylor NF. Steroids excreted in urine by neonates with 21-hydroxylase deficiency. 3. Characterization, using GC-MS and GC-MS/MS, of androstanes and androstenes. *Steroids* 77 (2012) 1487-1501

[70] Lisboa BP, Plasse J-C. Studies on the Metabolism of Steroids in the Foetus. Metabolism of 4-Androstene-3,17-Dione by Human Foetal-Liver Microsomes. *European Journal of Biochemistry* 31 (1972) 378-385

[71] Jacobsen NE, Kover KE, Murataliev MB, Feyereisen R, Walker FA. Structure and stereochemistry of products of hydroxylation of human steroid hormones by a housefly cytochrome P450 (CYP6A1). *Magn Reson Chem* 44 (2006) 467-474

[72] Yiong Z, Xin L, Moutian W, Jingzhu W, Huyue Z. Analytical Data of 1-Testosterone and the Preliminary Results of Excretion Study with 1-Testosterone. In: Schänzer W, Geyer H, Gotzmann A, Mareck U (Eds.) *Recent Advances in Doping Analysis (12)*, Sport & Buch Strauss, Cologne (2004) 81-90

[73] Kwok WH, Ho EN, Leung GN, Tang FP, Wan TS, Wong HN, Yeung JH. Metabolic studies of 1-testosterone in horses. *Drug Test Anal* 5 (2013) 81-88

[74] Jain S, Beotra A, Kaur T. A case study: Detection of 1-Tesotosteron in Urine by GC-MSD. In: Schänzer W, Geyer H, Gotzmann A, Mareck U (Eds.) *Recent Advances in Doping Analysis (13)*, Sport & Buch Strauss, Cologne (2005) 407-410

[75] World Anti-Doping Agency. The World Anti-Doping Code The 2017 Prohibited List. in, (2017) 1-9

[76] Cheng Q, Sohl CD, Yoshimoto FK, Guengerich FP. Oxidation of dihydrotestosterone by human cytochromes P450 19A1 and 3A4. *The Journal of biological chemistry* 287 (2012) 29554-29567

[77] Gustafsson JA, Lisboa BP, Sjovall J. Studies on the Metabolism of C19 Steroids in Rat Liver. 2. Biosynthesis of Hydroxylated Derivatives of 17 beta-Hydroxy-5alpha-Androstan-3-One in Rat Liver Microsomes. *European Journal of Biochemistry* 5 (1968) 437-443

[78] Gustafsson JÅ, Lisboa BP. Studies on the metabolism of C19 steroids in rat liver. 5. 18-hydroxylation of 17β-hydroxy-C19 steroids in rat liver microsomes. *Steroids* 14 (1969) 659-674

[79] Piper T, Geyer H, Gougoulidis V, Flenker U, Schänzer W. Determination of (13)C/(12)C ratios of urinary excreted boldenone and its main metabolite 5beta-androst-1-en-17beta-ol-3-one. *Drug Test Anal* 2 (2010) 217-224

[80] Galletti F, Gardi R. Metabolism of 1-dehydroandrostanes in man. I. Metabolism of 17 -hydroxyandrosta-1,4-dien-3-one, 17 -cyclopent-1'-enyloxyandrosta-1,4-dien-3-one (quinbolone) and androsta-1,4-diene-3,17-dione (1). *Steroids* 18 (1971) 39-50

[81] Schänzer W, Donike M. Metabolism of boldenone in man: gas chromatographic/mass spectrometric identification of urinary excreted metabolites and determination of excretion rates. *Biol Mass Spectrom* 21 (1992) 3-16

[82] Schänzer W, Horning S, Donike M. Metabolism of anabolic steroids in humans: Synthesis of 6β-hydroxy metabolites of 4-chloro-1,2-dehydro-17α-methyltestosterone, fluoxymesterone, and metandienone. *Steroids* 60 (1995) 353-366

[83] Dumasia MC, Houghton E. Biotransformation of 1-dehydrotestosterone in the equine male castrate: Identification of the neutral unconjugated and glucuronic acid conjugated metabolites in horse urine. *Biological Mass Spectrometry* 17 (1988) 383-392

[84] Merlanti R, Gallina G, Capolongo F, Contiero L, Biancotto G, Dacasto M, Montesissa C. An in vitro study on metabolism of 17beta-boldenone and boldione using cattle liver and kidney subcellular fractions. *Anal Chim Acta* 586 (2007) 177-183

[85] De La Torre X, Curcio D, Colamonici C, Molaioni F, Botre F. Metabolism of boldione in humans by mass spectrometric techniques: detection of pseudoendogenous metabolites. *Drug Test Anal* 5 (2013) 834-842

[86] Parr M, Fußhöller G, Kohler M, Hebestreit M, Opfermann G, Schänzer W. Synthesis of Reference Compounds for the Identification of Metabolites of 4-Hydroxytestosterone. In: Schänzer W, Geyer H, Gotzmann A, Mareck U (Eds.) *Recent Advances in Doping Analysis (13)*, Sport & Buch Strauss, Cologne (2005) 65-74

[87] Hegazy ME, Gamal-Eldeen AM, El-Halawany AM, Mohamed Ael H, Pare PW. Steroidal metabolites transformed by Marchantia polymorpha cultures block breast cancer estrogen biosynthesis. *Cell Biochem Biophys* 63 (2012) 85-96

[88] Gual C, Morato T, Hayano M, Gut M, Dorfman RI. Biosynthesis of estrogens. *Endocrinology* 71 (1962) 920-925

[89] Numazawa M, Yamashita K, Kimura N, Takahashi M. Chemical aromatization of 19-hydroxyandrosta-1,4-diene-3,17-dione with acid or alkaline: elimination of the 19-hydroxymethyl group as formaldehyde. *Steroids* 74 (2009) 208-211

[90] Van Puymbroeck MK, Mariella E. M. Maas, Roel F. M., Witkamp RF, Leyssens LV, Dirk, Gelan J, Raus J. Identification of some important metabolites of boldenone in urine and feces of cattle by gas chromatography-mass spectrometry. *Analyst* 123 (1998) 2681-2686

[91] Parr MK, Fusshöller G, Schlörer N, Opfermann G, Piper T, Rodchenkov G, Schänzer W. Metabolism of androsta-1,4,6-triene-3,17-dione and detection by gas chromatography/mass spectrometry in doping control. *Rapid communications in mass spectrometry : RCM* 23 (2009) 207-218

7 Publications

Peer reviewed journals

- Parr MK, Wuest B, Naegele E, Joseph JF, Wenzel M, Schmidt AH, Stanic M, de la Torre X, Botrè F. SFC-MS/MS as Orthogonal Technique for Improved Screening for Polar Analytes in Anti-Doping Control. *Analytical and Bioanalytical Chemistry 408(24): 6789-6797*
- Joseph JF, Parr MK. Synthetic Androgens as Designer Supplements. *Current Neuropharmacology* 13 (2015) 89-100
- Empl MT, Kammeyer P, Ulrich R, Joseph JF, Parr MK, Willenberg I, Schebb NH, Baumgartner W, Rohrdanz E, Steffen C, Steinberg P. The influence of chronic L-carnitine supplementation on the formation of preneoplastic and atherosclerotic lesions in the colon and aorta of male F344 rats. *Archives of toxicology* 89 (2015) 2079-2087

Conference proceedings

- Assaf J, Joseph JF, Kollmeier A, Gomes DZ, Wuest B, Gautschi P, Parr MK Mass spectrometric characterization of ketoprofen impurities. *27th International Symposium on Pharmaceutical and Biomedical Analysis (2016)*
- Parr MK, Wuest B, Naegele E, Stanic M, Schmidt A, Joseph JF, Bredendiek F, de la Torre X, Botrè F SFC-MS/MS in Anti-Doping Control: Trace Amount Detection of Polar Analytes and Metabolites in Urine. *10th International Conference on packed column SFC (2016)*
- Parr MK, Joseph JF, Bredendiek F, Wuest B High Resolution Mass Spectrometry and Evaluation of In-Silico Assistance for Metabolite Identification – Prospects exemplified for In-Vitro and In-Vivo Metabolism of Propranolol. *The International Association of Forensic Toxicologists. 54th TIAFT meeting, Book of Abstracts (2016) 69*
- Joseph JF, Stoll A, de la Torre X, Botrè F, Parr MK Metabolic hydroxylation reactions of androstenedione and derivatives. *DPhG Landesgruppentagung Berlin-Brandenburg (2016) 1st July (oral presentation)*
- Kollmeier AS, Joseph JF, Müller C, Botrè F, Parr MK Mass spectral characterization of trimethylsilyl derivatized androgens. *DPhG Landesgruppentagung Berlin-Brandenburg (2016) 1st July*
- Joseph JF, Stoll A, de la Torre X, Botrè F, Parr MK Minor metabolic pathways of xenobiotic steroid metabolism. *3rd Congress on Steroid Research (2015) P053*
- Parr MK, Joseph JF Erlaubte Therapie oder Doping – Dos and Don'ts bei der Behandlung von Spitzensportlern. *25. Symposium Intensivmedizin und Intensivpflege Bremen (2015). Book of Abstracts 159-165*
- Joseph JF, Empl M, Röhrdanz E, Steffen C, Steinberg P, Parr MK Determination of N-nitrosodimethylamine levels in rat urine after L-carnitine intake utilizing GC-MS. *DPhG Landesgruppentagung Berlin-Brandenburg (2014), Book of Abstracts 20*

8 Curriculum vitae

9 List of Figures

10 List of Tables

11 Annex

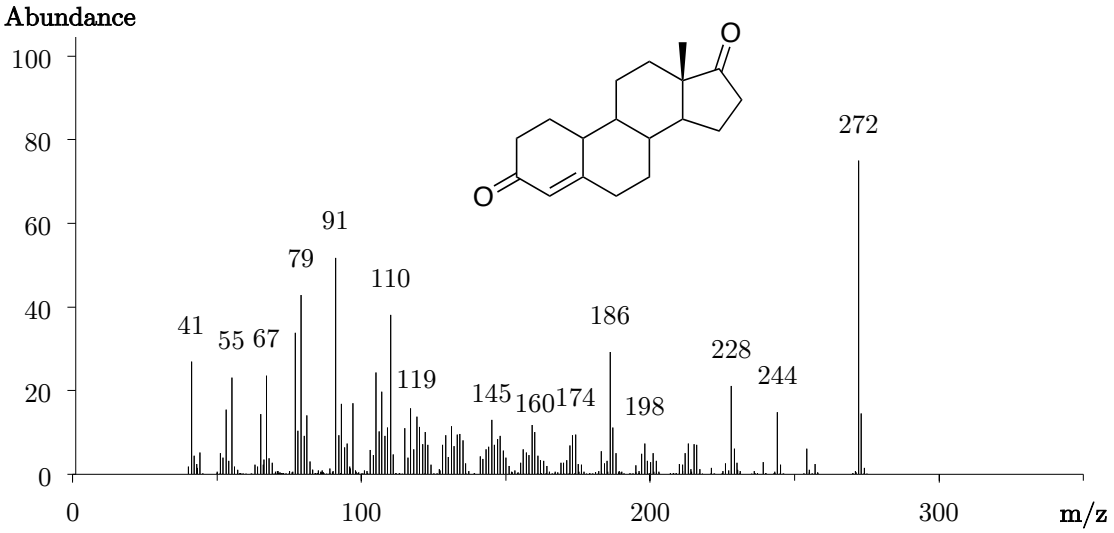

Figure 68 Mass spectrum (EI) of underivatized 19-hydroxyandrost-4-ene-3,17-dione resulting in the formation of estr-4-ene-3,17-dione, $[M]^{\bullet+}$=272

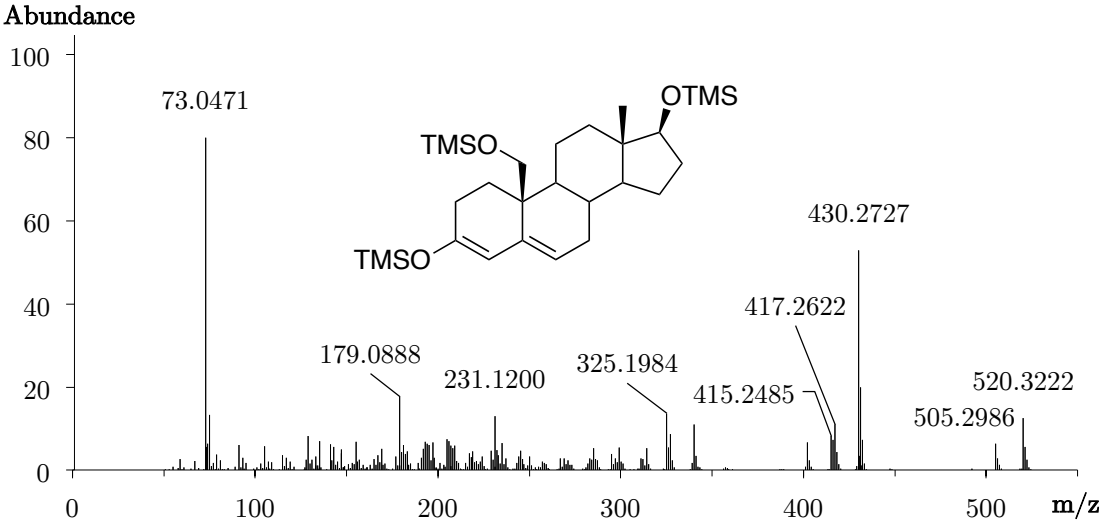

Figure 69 Accurate mass spectrum (EI) of 19-hydroxytestosterone (17β,19-dihydroxyandrost-4-en-3-one), 3,5-diene-3,17,19-triol tris-TMS, $[M]^{\bullet+}$=520.3222, mass error 0.44 ppm

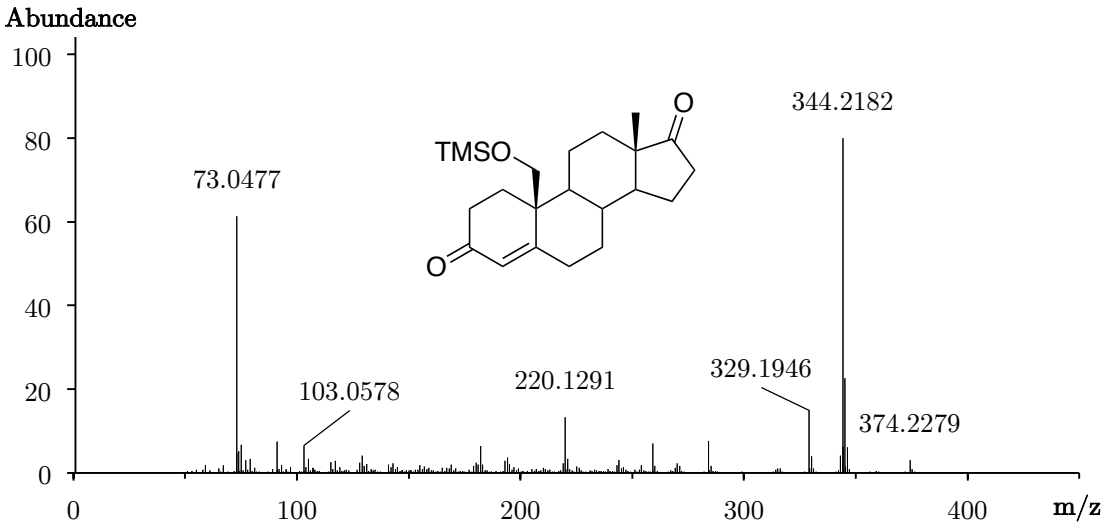

Figure 70 Accurate mass spectrum (EI) of 19-hydroxyandrost-4-ene-3,17-dione, mono-TMS derivative, $[M]^{\bullet+}$=374.2279, mass error 0.48 ppm

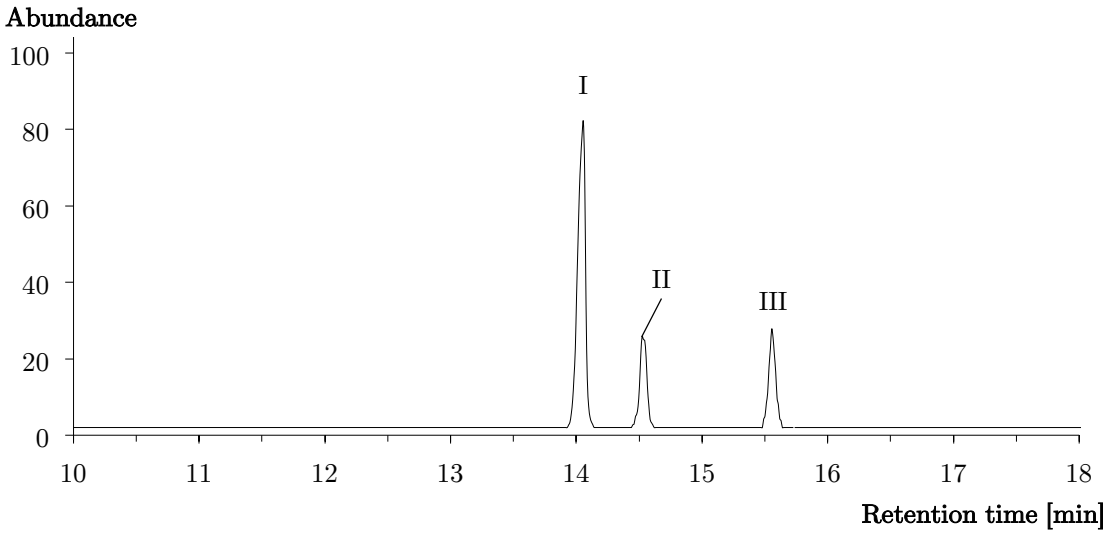

Figure 71 Extracted ion chromatogram (m/z 520) of 19-hydroxy-5ξ-androstane-3,17-dione (hydrogenation products of 19-hydroxyandrost-4-ene-3,17-dione) as tris-TMS derivative, I-III represent isomeric products, acquired using method a)

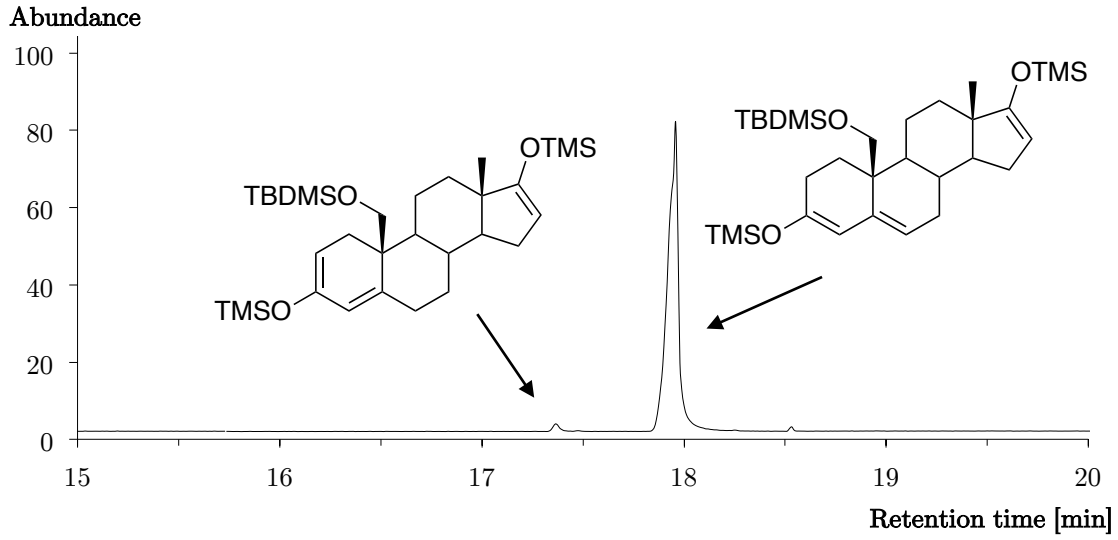

Figure 72 Base peak chromatogram of 19-TBDMSO-androst4-ene-3,17-dione (2), showing 3,5,16-triene-3,17-diol bis-TMS (right) as a main peak and the 2,4,16-triene-3,17-diol bis-TMS (left) as a derivatization isomer, acquired using method a)

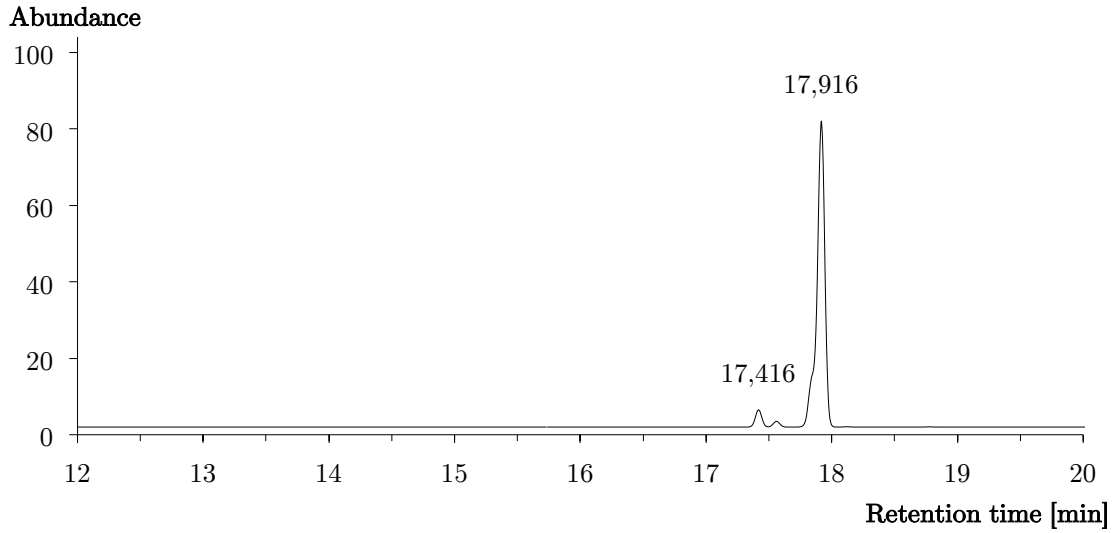

Figure 73 Extracted ion chromatogram (m/z 562eine) of 19-TBDMSO-5ξ-androstane-3,17-dione (hydrogenation products of 19-TBDMSO-androst-4-ene-3,17-dione) as bis-TMS derivative, acquired using method a)

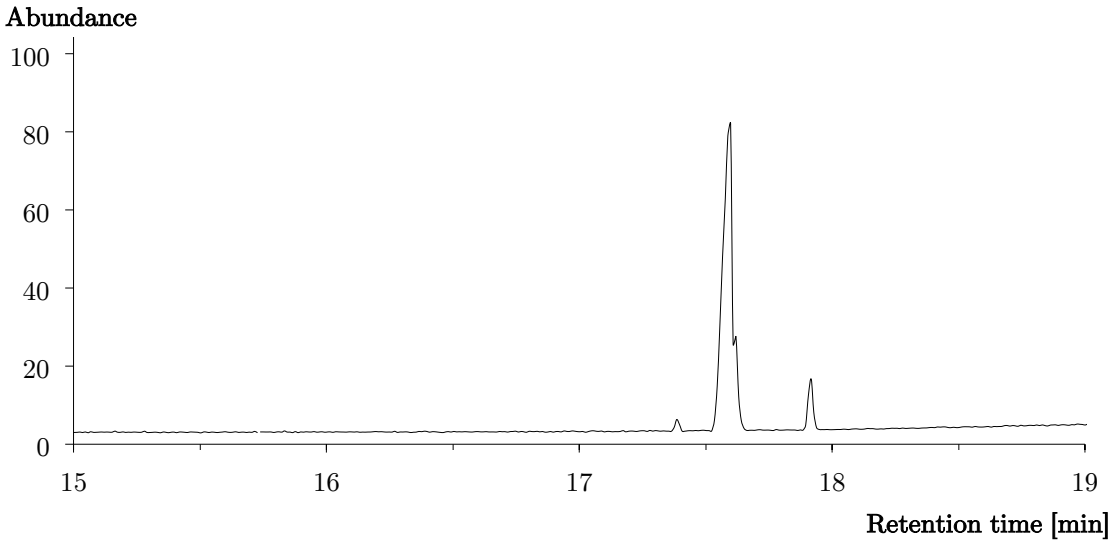

Figure 74 Base peak chromatogram showing three products of the oxidation of 19-TBDMSO-5α-androstane-3,17-dione, acquired using method a)

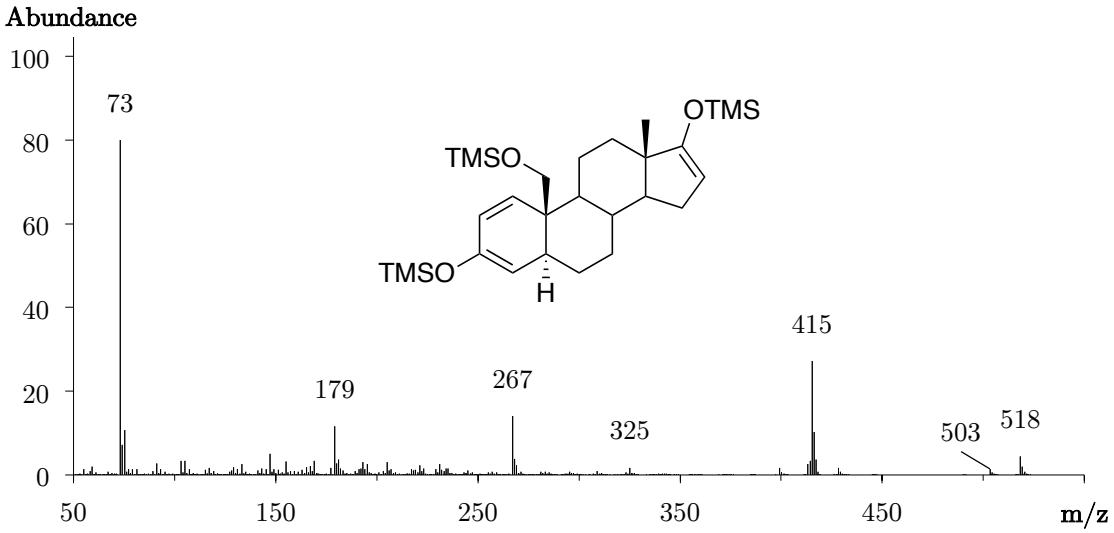

Figure 75 Mass spectrum (EI) of 19-hydroxy-5α-androst-1-ene-3,17-dione (19-TBDMSO-5α-androst-1-ene-3,17-dione after cleavage of the protection group), as tris-TMS derivative, $[M]^{\bullet+}$=518

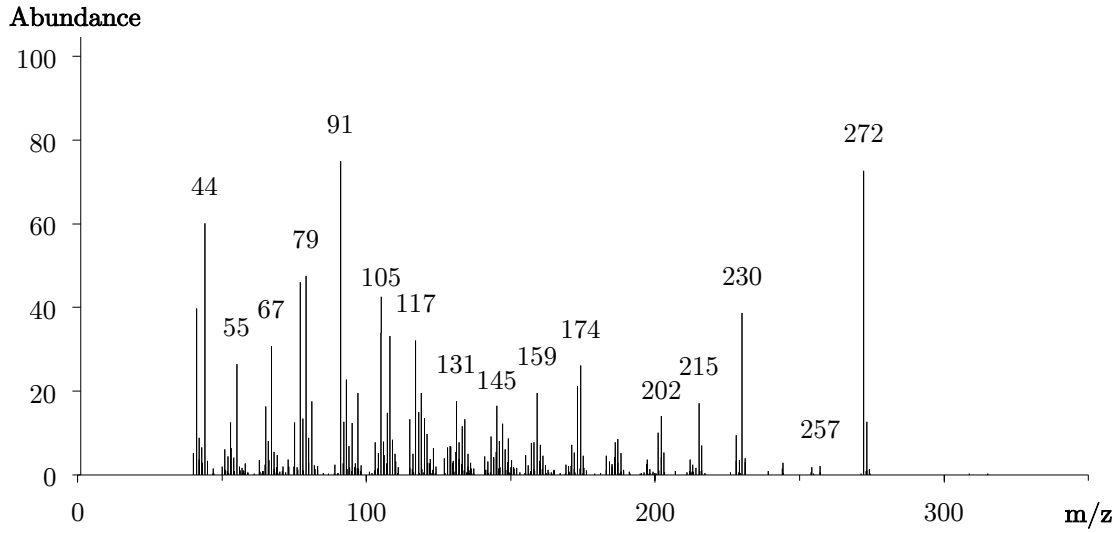

Figure 76 Mass spectrum (EI) of underivatized 19-hydroxy-5a-androst-1-ene-3,17-dione presumably resulting in a '1-norandrostenedione' derivative, $[M]^{\bullet+}$=272

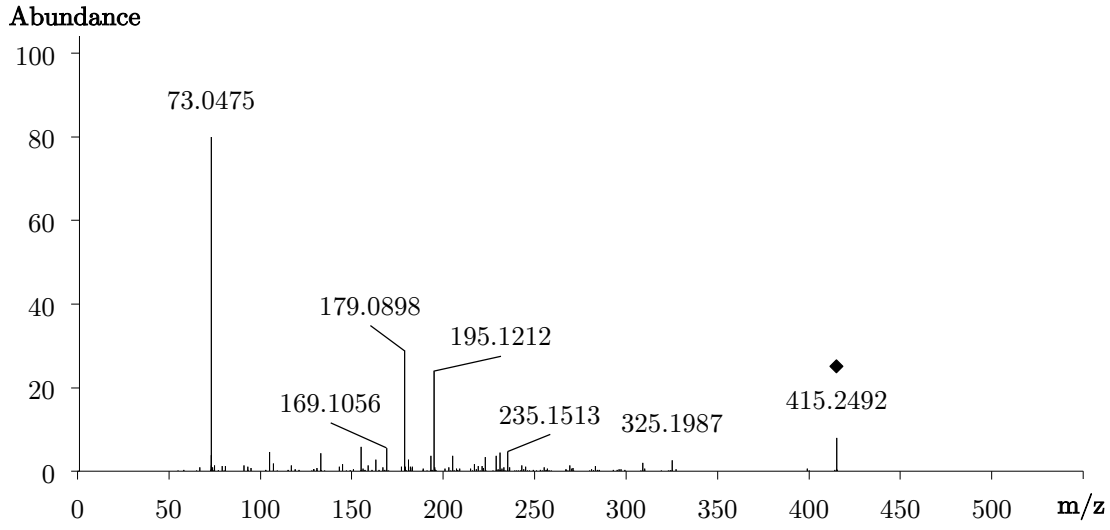

Figure 77 Accurate MS/MS spectrum (EI) of 19-hydroxy-5α-androst-1-ene-3,17-dione (5), 1,3,16-triene-3,17,19-triol tris-TMS, precursor m/z 415 indicated with black rhombus, collision energy 25 eV

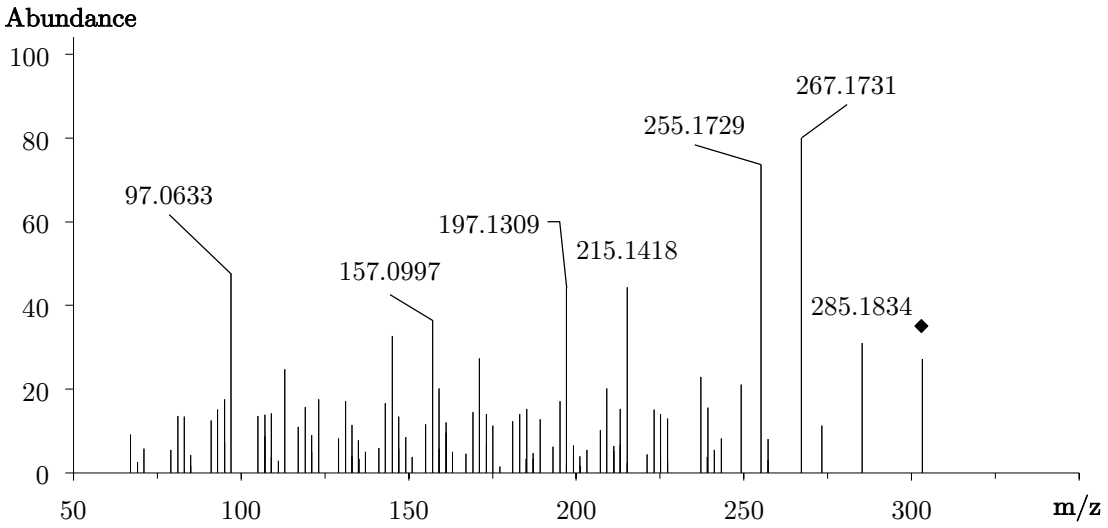

Figure 78 Accurate mass spectrum (ESI+) of 19-hydroxyandrost-4-ene-3,17-dione, precursor m/z 303 is indicated with black rhombus, collision energy 20 eV

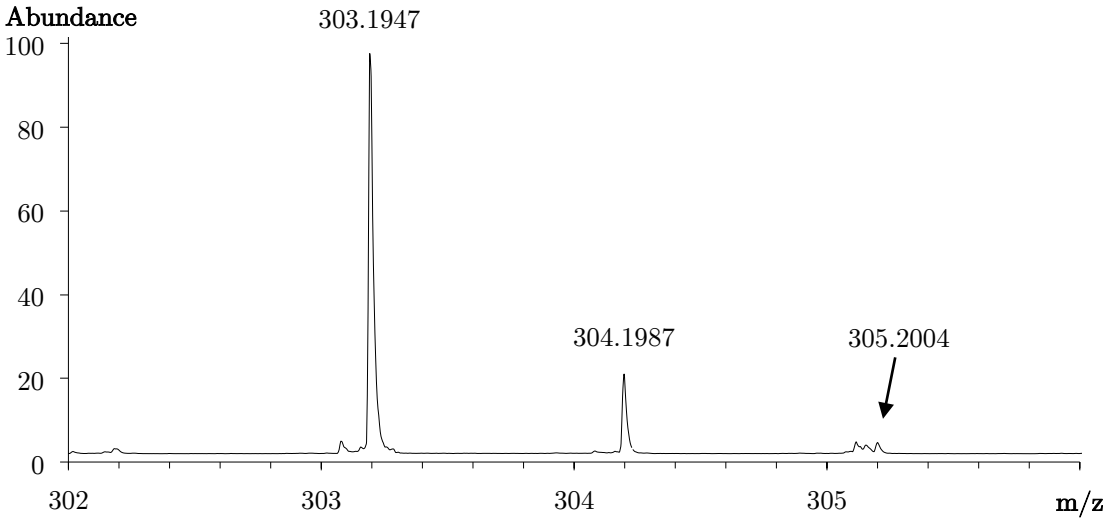

Figure 79 Accurate mass spectrum (ESI+) of 19-hydroxy-5α-androst-1-ene-3,17-dione (5), $[M+H]^+$=303.1947, mass error -2.29 ppm, acquired using method d)

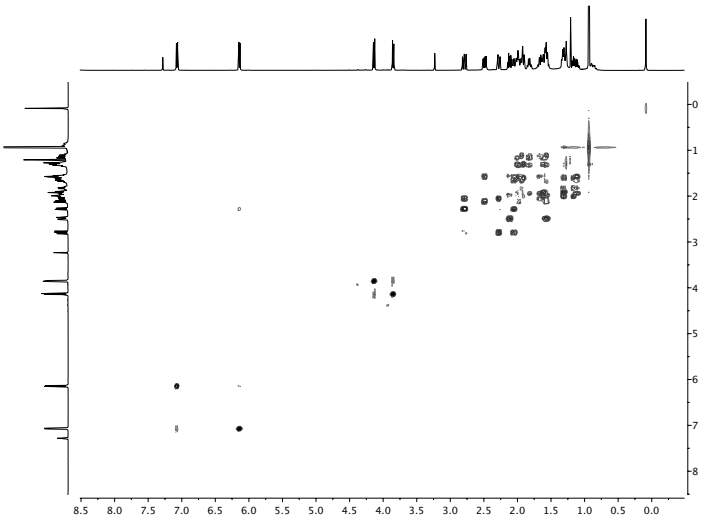

Figure 80 H,H-COSY spectrum of 19-hydroxy-5α-androst-1-ene-3,17-dione (5)

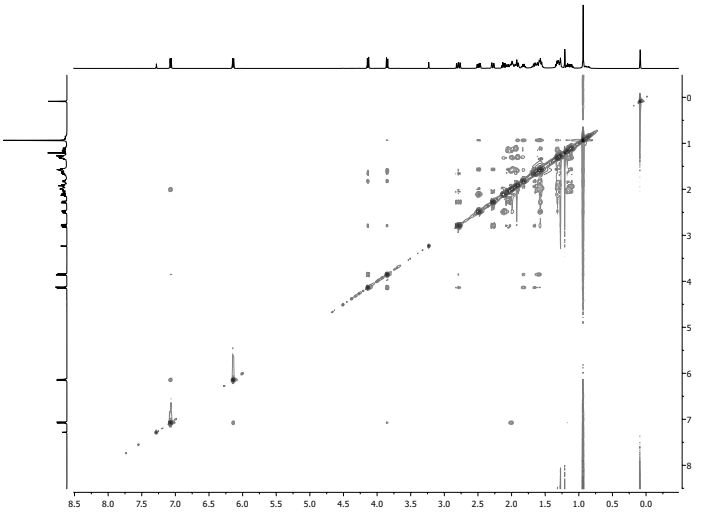

Figure 81 NOESY spectrum of 19-hydroxy-5α-androst-1-ene-3,17-dione (5)

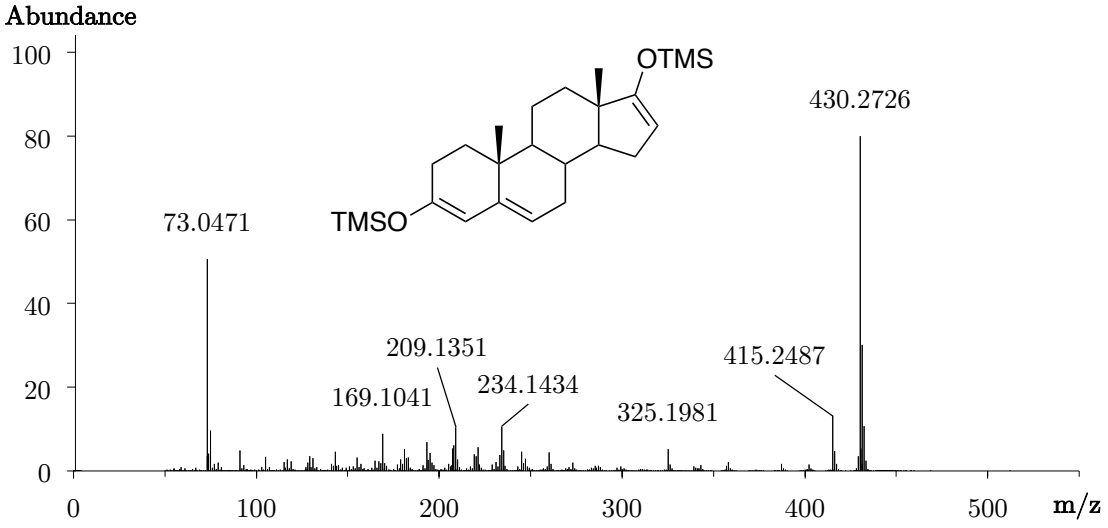

Figure 82 Accurate mass spectrum (EI) of androst-4-ene-3,17-dione, 3,5,16-triene-3,17-diol bis-TMS, $[M]^{\bullet+}$=430.2726, mass error 2.95 ppm

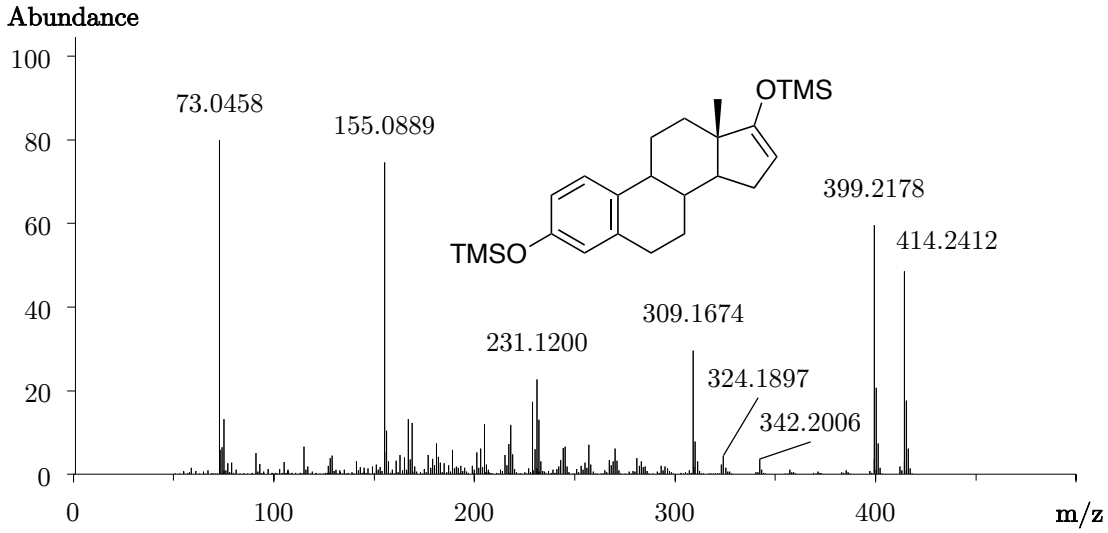

Figure 83 Accurate mass spectrum (EI) of estrone (3-hydroxyestra-1,3,5(10)-trien-17-one), 1,3,5(10),16-tetraene-3,17-diol bis-TMS, $[M]^{\bullet+}$=414.2412, mass error 0.41 ppm

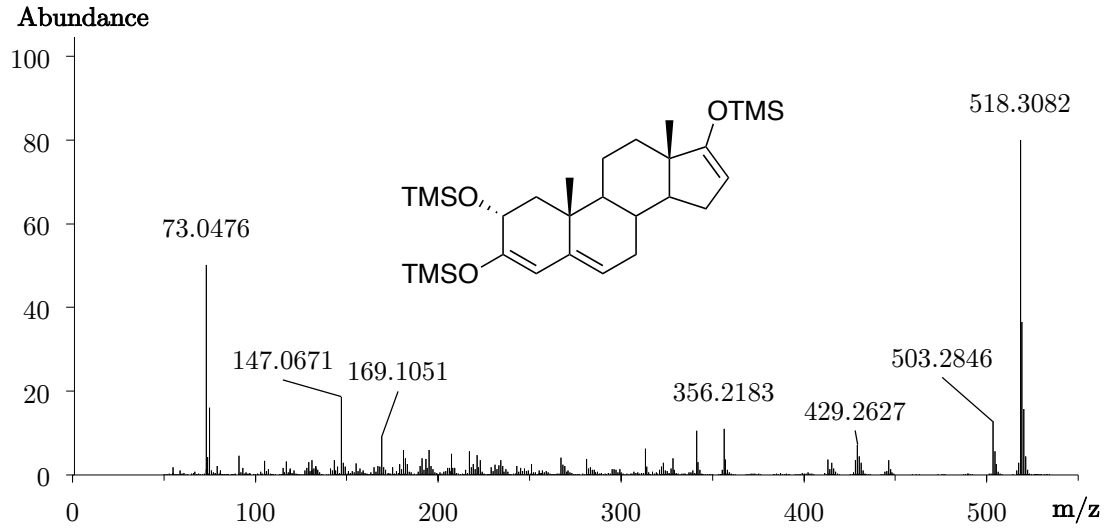

Figure 84 Accurate mass spectrum (EI) of 2α-hydroxyandrost-4-ene-3,17-dione, 3,5,16-triene-2α,3,17-triol tris-TMS, $[M]^{\bullet+}$=518.3082, mass error 3.86 ppm

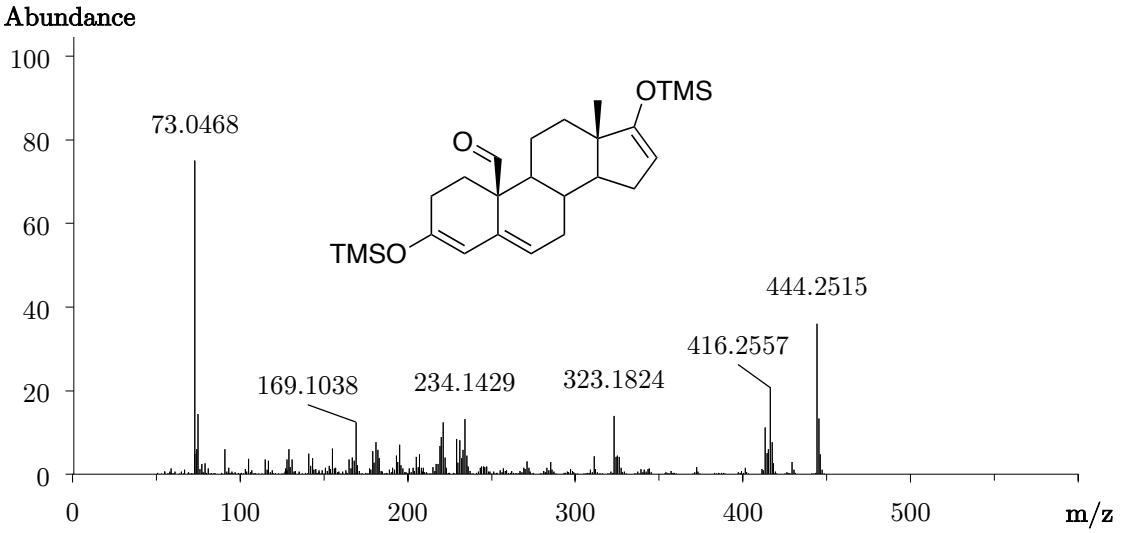

Figure 85 Accurate mass spectrum (EI) of 3,17-dioxoandrost-4-ene-19-al, 3,5,16-triene-3,17-diol bis-TMS, $[M]^{\bullet+}$=444.2515, mass error 0.23 ppm

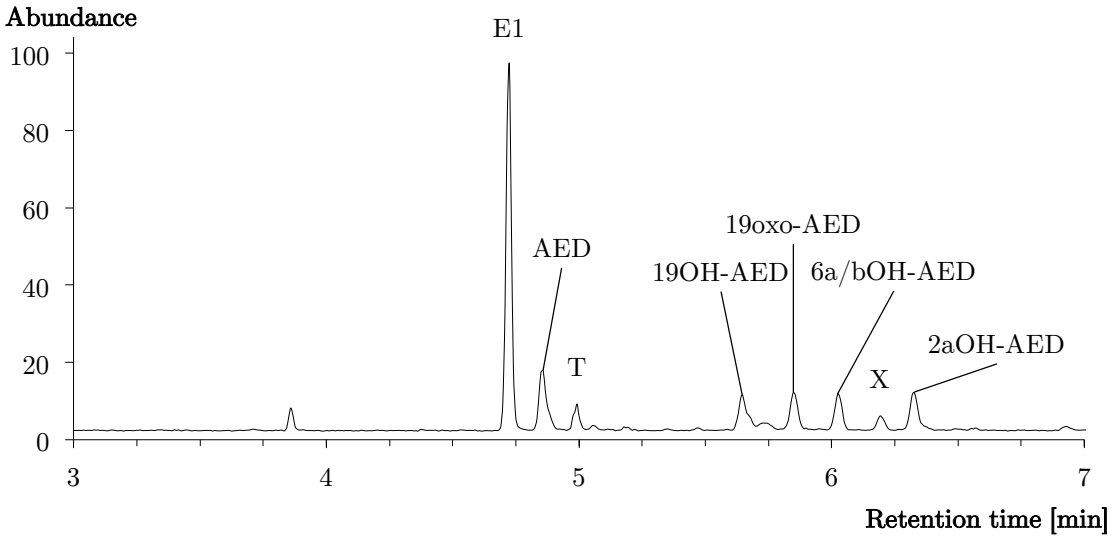

Figure 86 Extracted ion chromatogram (414.2405 ; 444.2511; 518.3062) of the incubation of AED with aromatase showing the formation of estrone (E1) and intermediates, 19-hydroxyandrost-4-ene-3,17-dione (19OH-AED), 3,17-dioxo-androst-4-en-19-al (19oxo-AED), 2α-hydroxyandrost-4-ene-3,17-dione (2aOH-AED), and byproducts testosterone (T), 6ξ-hydroxyandrost-4-ene-3,17-dione (6a/bOH-AED), m/z 520.3254 (x), as per-TMS, acquired using method b)

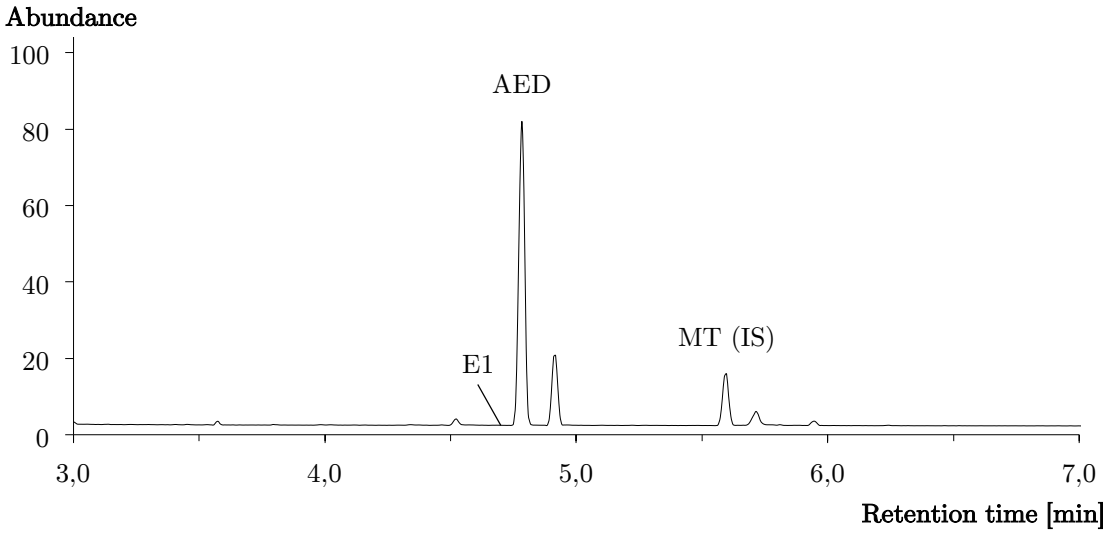

Figure 87 Base peak chromatogram of AED after incubation with CYP3A4, absence of estrone formation (E1), internal standard methyltestosterone (MT, 8 µg/mL) acquired using method b)

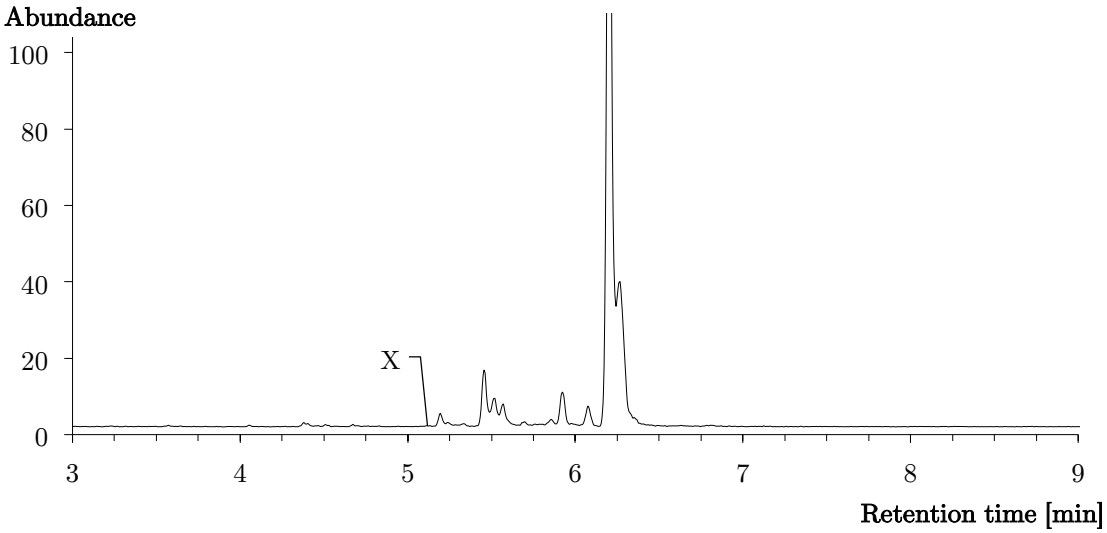

Figure 88 Extracted ion chromatogram (m/z 518.3062) of the pertrimethylsilylated derivatives after incubation of 10 µM solution of 1-AED with CYP3A4, (X) displays the absence of 19-hydroxylated metabolite formation, acquired using method b)

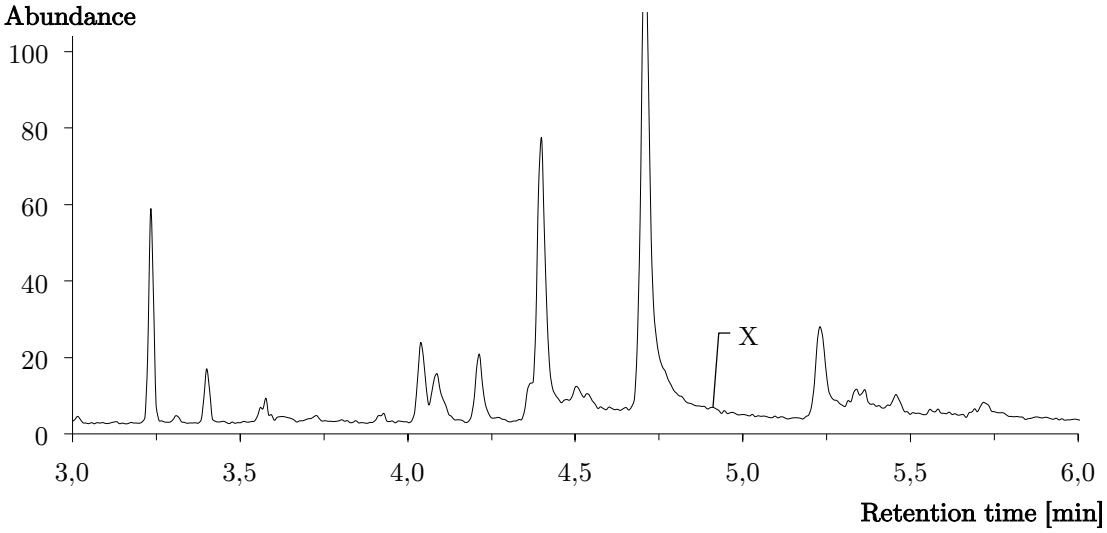

Figure 89 Extracted ion chromatogram (m/z 344.2 and 374.2) of the mono-trimethylsilylated derivatives after incubation of 10 µM solution of 1-AED with CYP3A4, (X) displays the absence of 19-hydroxylated metabolite formation, acquired using method b)

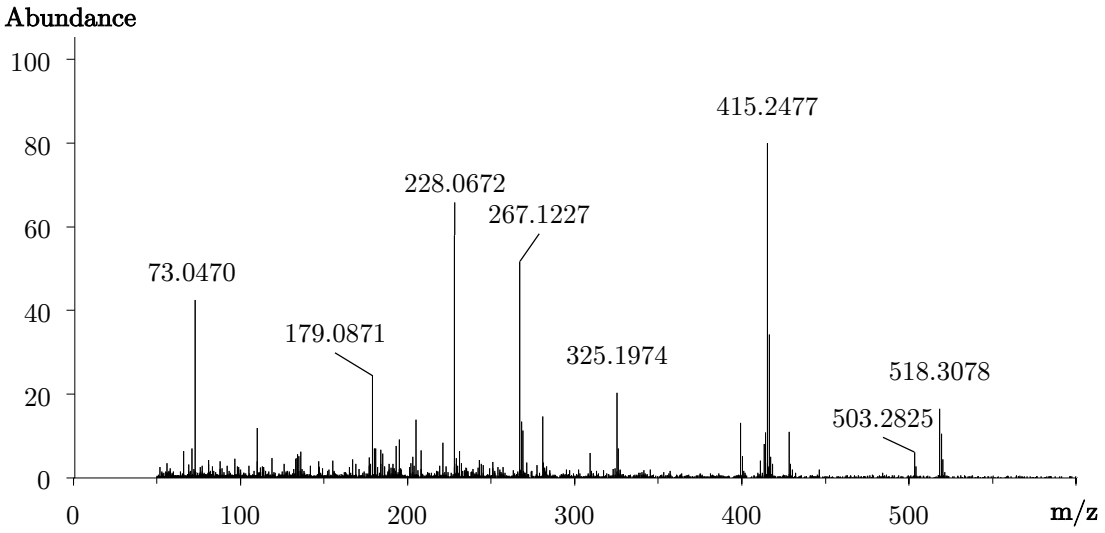

Figure 90 Accurate mass spectrum (EI) of 19-hydroxy-5α-androst-1-ene-3,17-dione as tris-TMS derivative after incubation of 1-androstenedione with CYP19A1, $[M]^{\bullet+}$=518.3078, mass error 7.95 ppm

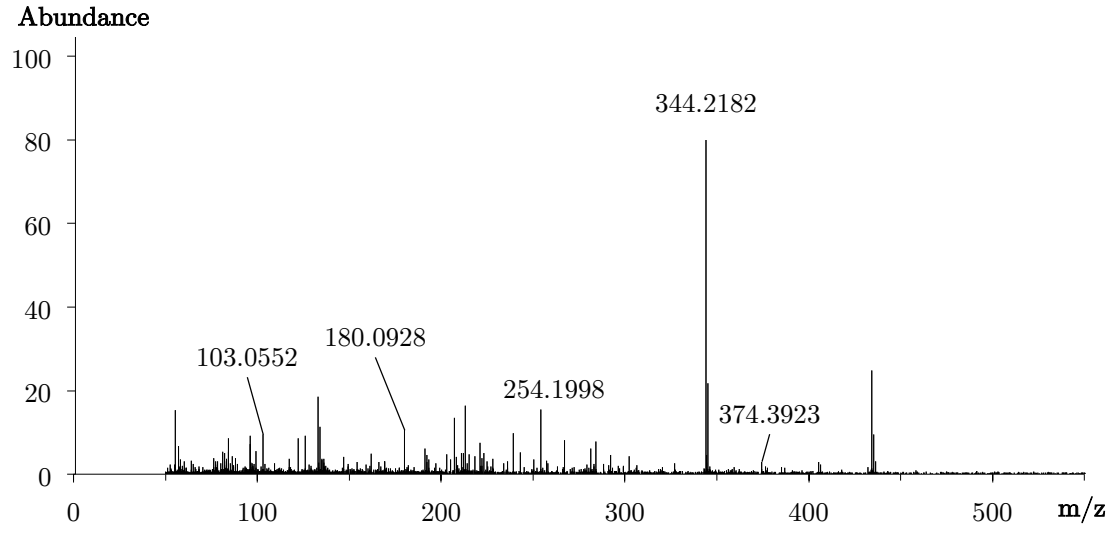

Figure 91 Accurate mass spectrum (EI) of 19-hydroxy-5α-androst-1-ene-3,17-dione as mono-TMS derivative after incubation of 1-androstenedione with CYP19A1, $[M]^{\bullet+}$=374.3923, mass error of base peak (m/z 344.2182) 2.91 ppm

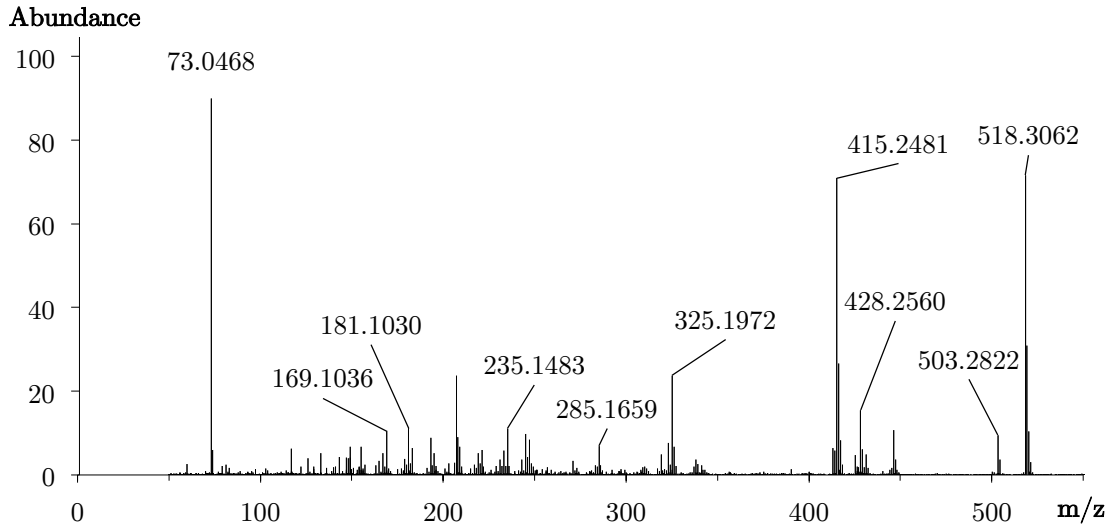

Figure 92 Accurate mass spectrum (EI) of a hydroxylated metabolite of androst-4-ene-3,17-dione ($M1_{AED}$) after incubation with HLM, potentially 18-hydroxyandrost-4-ene-3,17-dione, retention time 6.06 min, $[M]^{\bullet+}$=518.3062 mass error 0 ppm

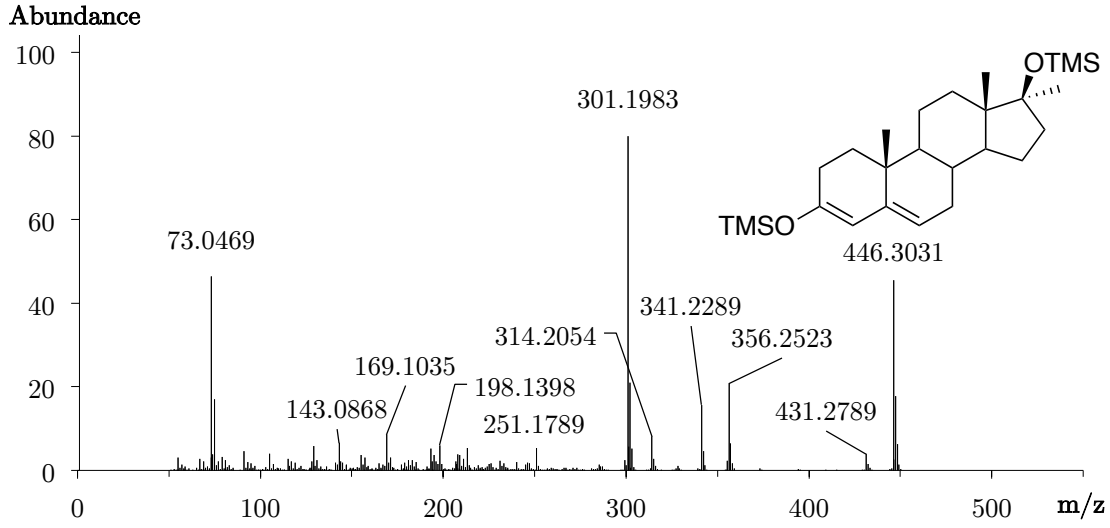

Figure 93 Accurate mass spectrum (EI) of methyltestosterone (17α-methyl-17β-hydroxyandrost-4-en-3-one), 3,5-diene-3,17-dio bis-TMS, $[M]^{\bullet+}$=446.3031, mass error -1.19 ppm

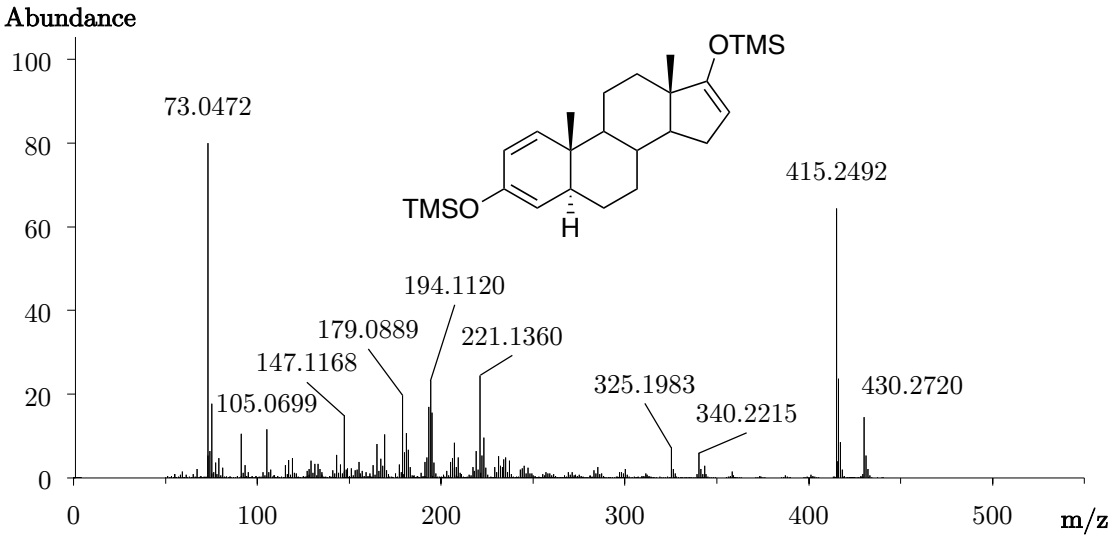

Figure 94 Accurate mass spectrum (EI) of 1-androstenedione (1-AED, 5α-androst-1-ene-3,17-dione), 1,3,16-triene-3,17-diol bis-TMS, $[M]^{\bullet+}$=430.2720, mass error 0.77 ppm

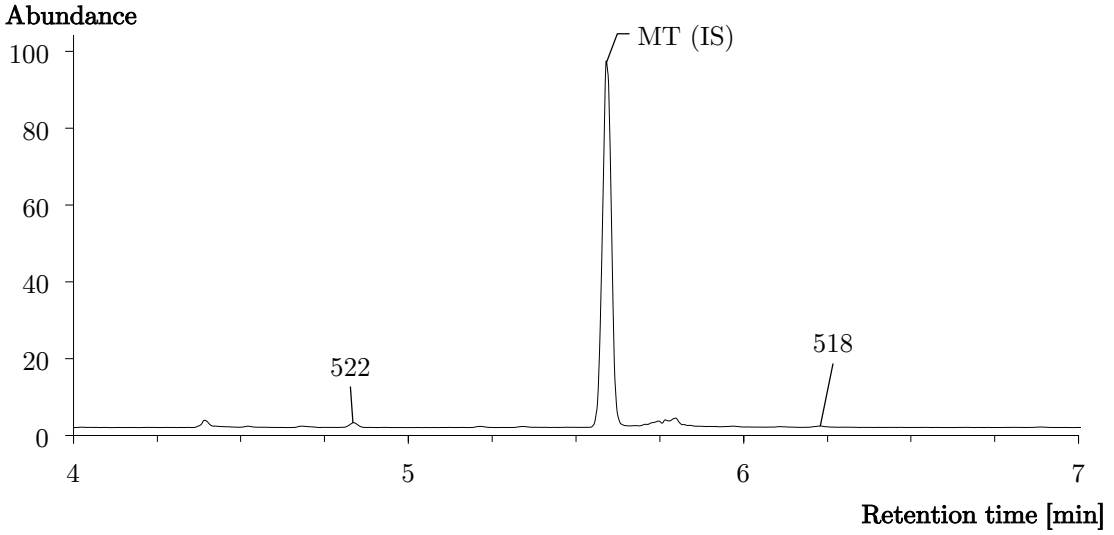

Figure 95 Extracted ion chromatogram of hydroxylated metabolites of 1-androstenedione after incubation with CYP19A1 as per-TMS derivatives, internal standard methyltestosterone (MT, 8 µg/mL), acquired using method b)

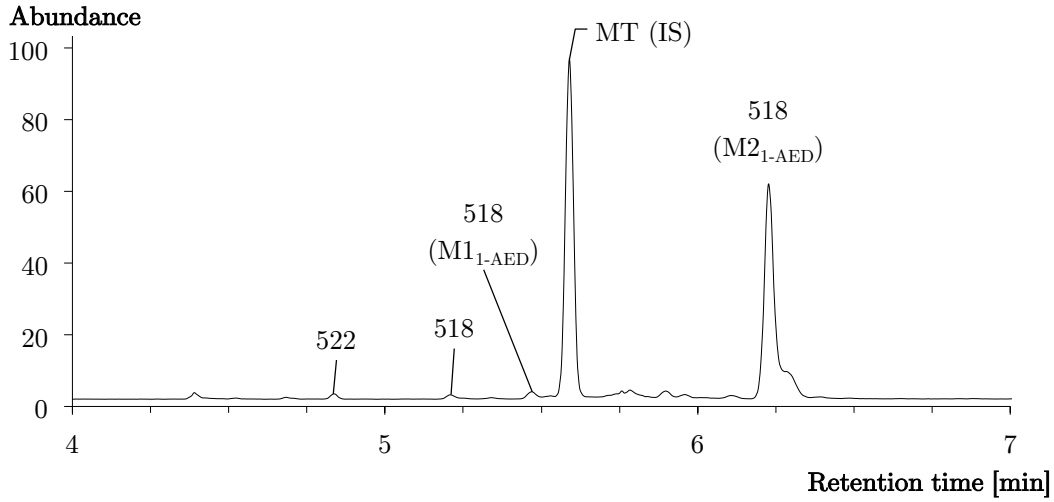

Figure 96 Extracted ion chromatogram of hydroxylated metabolites of 1-androstenedione after incubation with CYP3A4 as per-TMS derivatives, internal standard methyltestosterone (MT, 8 µg/mL), acquired using method b)

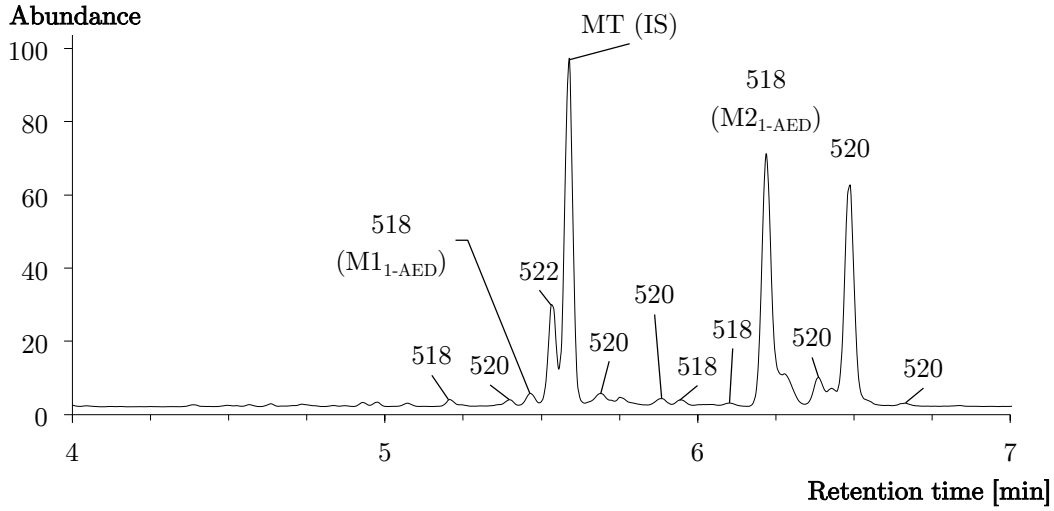

Figure 97 Extracted ion chromatogram of hydroxylated metabolites of 1-androstenedione after incubation with HLM as perTMS derivatives, internal standard methyltestosterone (MT, 8 µg/mL), acquired using method b)

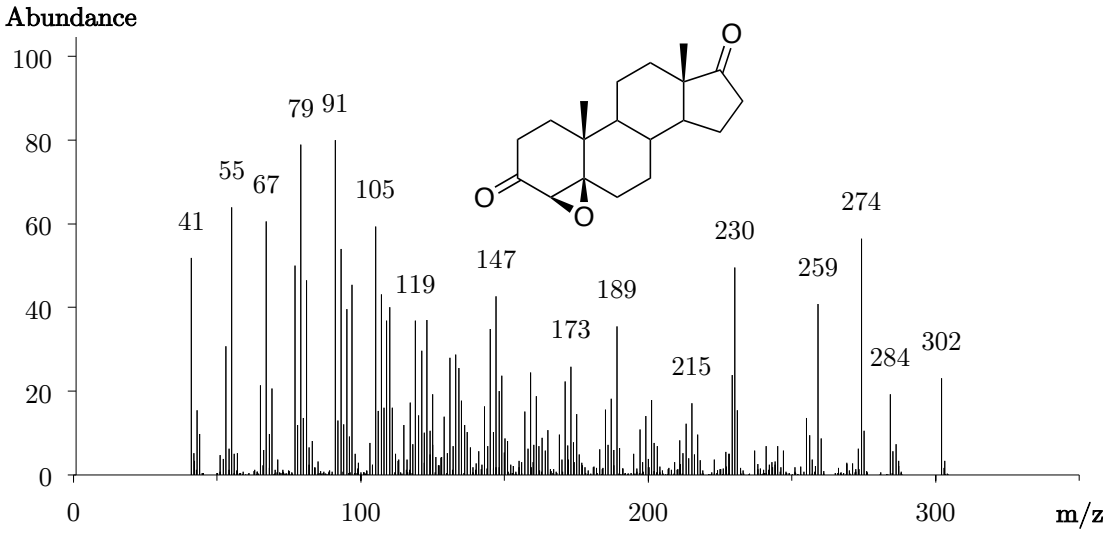

Figure 98 Mass spectrum (EI) of underivatized 4β,5β-epoxyandrostane-3,17-dione (2), $[M]^{\bullet+}$=302

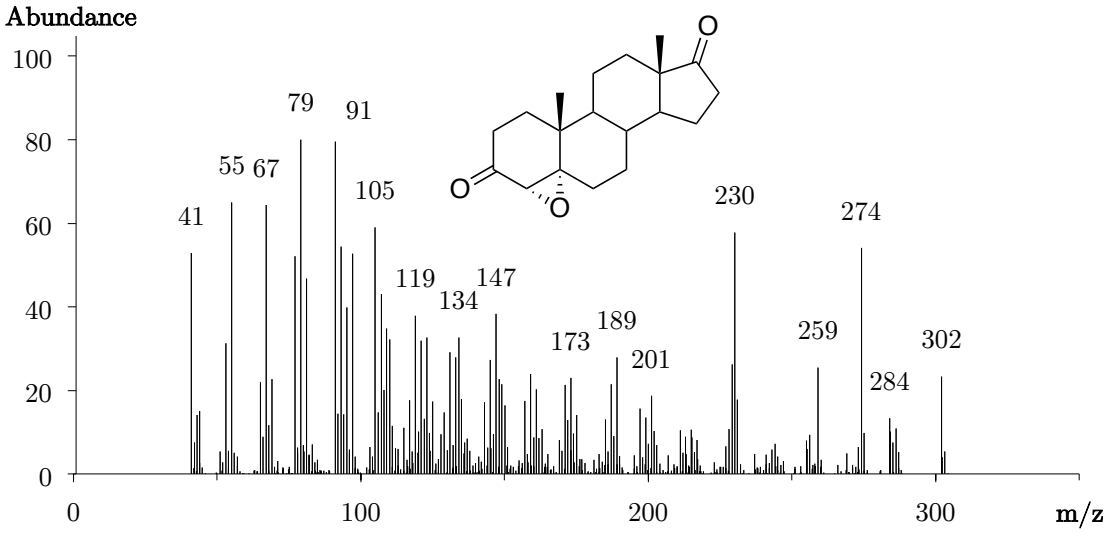

Figure 99 Mass spectrum (EI) of underivatized 4α,5α-epoxyandrostane-3,17-dione (3), $[M]^{\bullet+}$=302

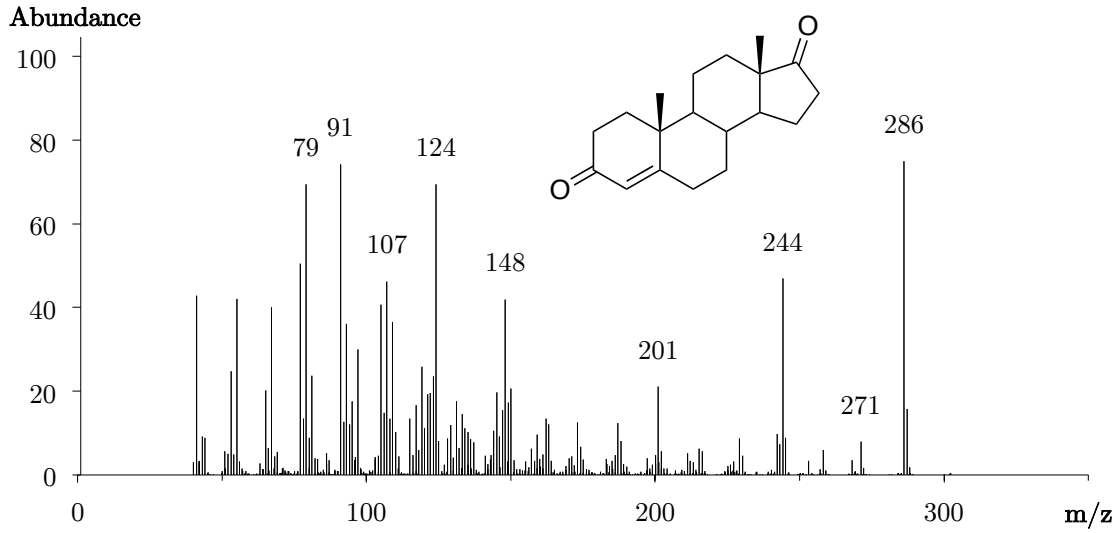

Figure 100 Mass spectrum (EI) of underivatized androst-4-ene-3,17-dione (1), $[M]^{\bullet+}$=286

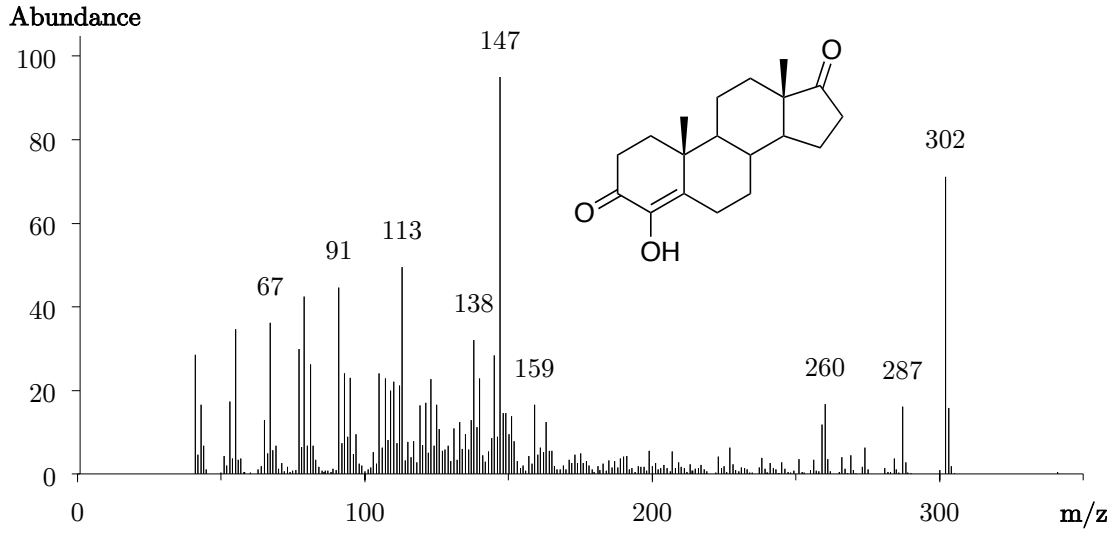

Figure 101 Mass spectrum (EI) of underivatized 4-hydroxyandrost-4-ene-3,17-dione (6), $[M]^{\bullet+}$=302

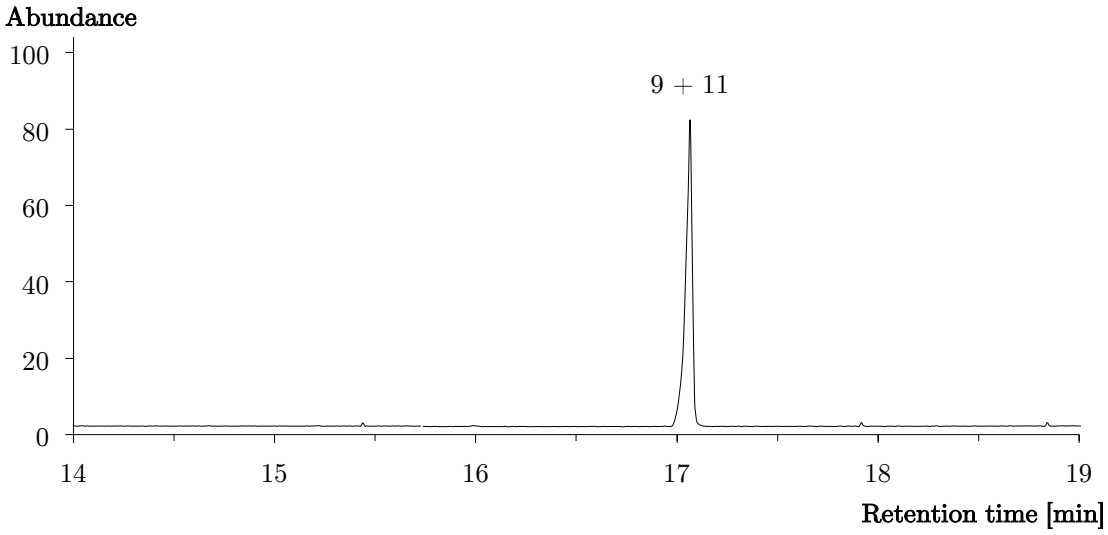

Figure 102 Base peak chromatogram of coeluting 2α- (9) and 2β-hydroxyandrost-4-ene-3,17-dione (11), as tris-TMS derivatives, acquired using method a)

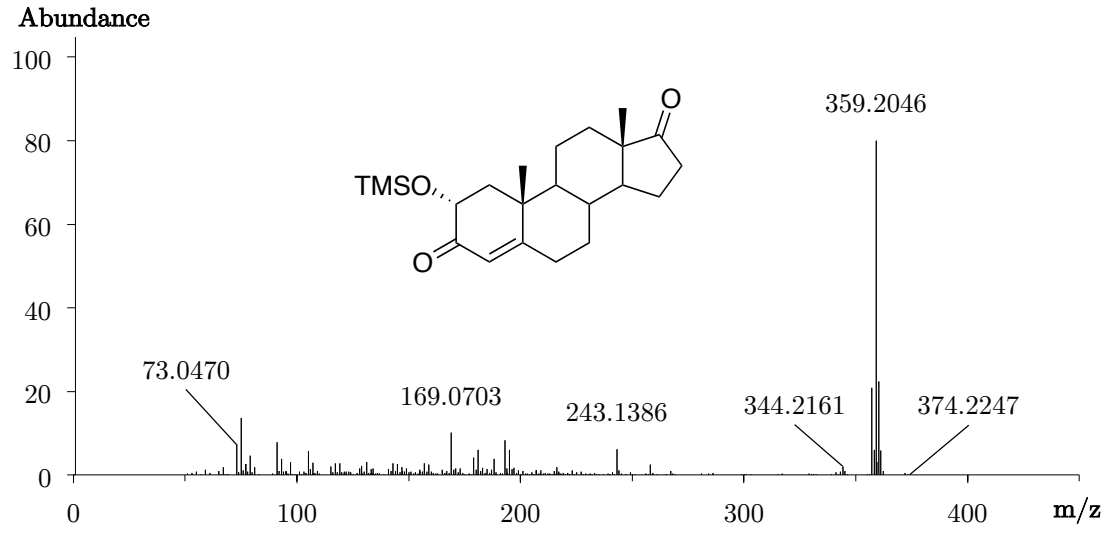

Figure 103 Accurate mass spectrum (EI) of 2α-hydroxyandrost-4-ene-3,17-dione, mono-TMS, $[M]^{\bullet+}$=374.2247, mass error 0.86 ppm

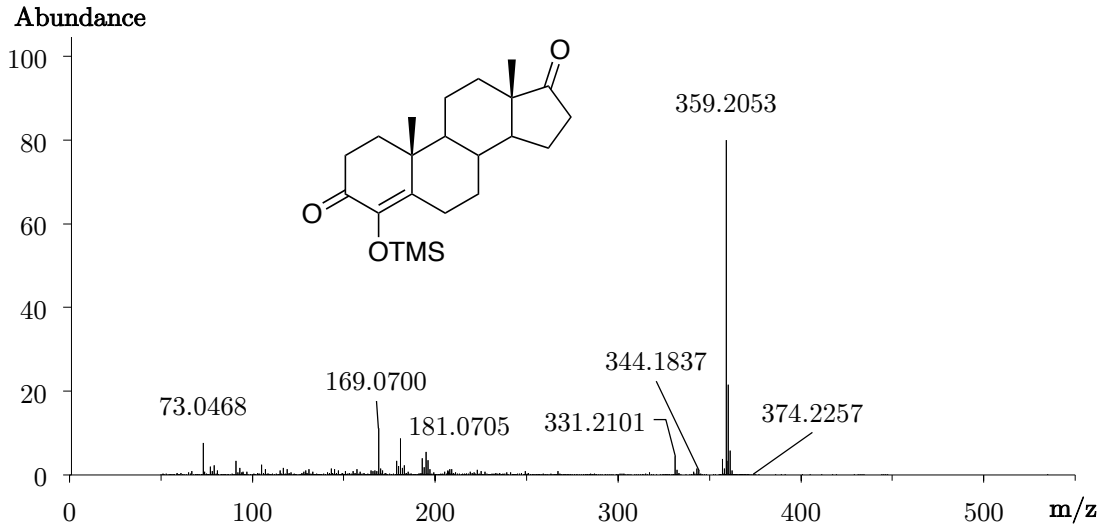

Figure 104 Accurate mass spectrum (EI) of formestane (4-hydroxyandrost-4-ene-3,17-dione), mono-TMS, $[M]^{\bullet+}$=374.2257, mass error of base peak 2.92 ppm

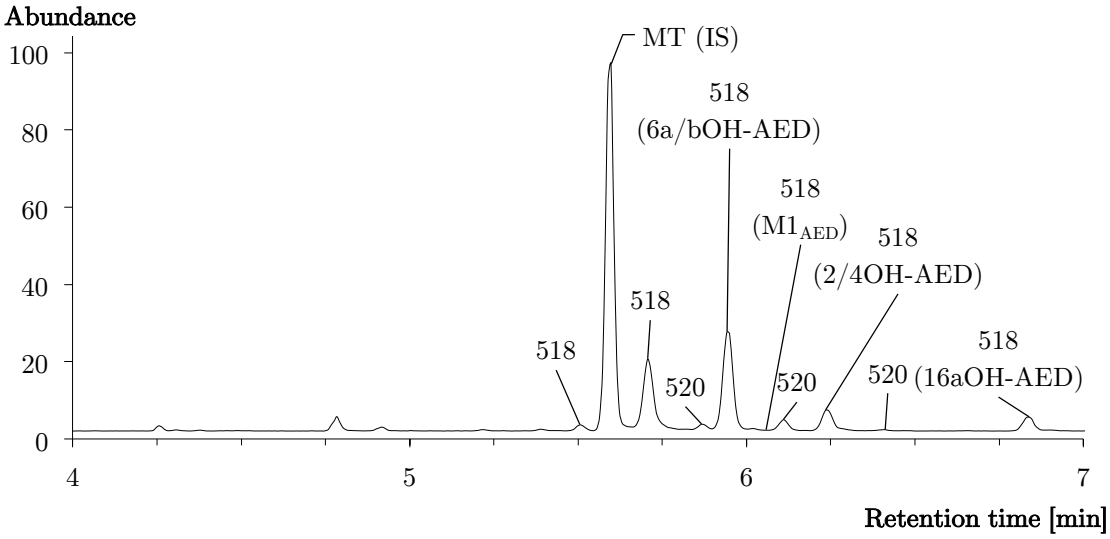

Figure 105 Extracted ion chromatogram of hydroxylated metabolites of androst-4-ene-3,17-dione after incubation with CYP3A4 as per-TMS derivatives, internal standard methyltestosterone (MT, 8 µg/mL)

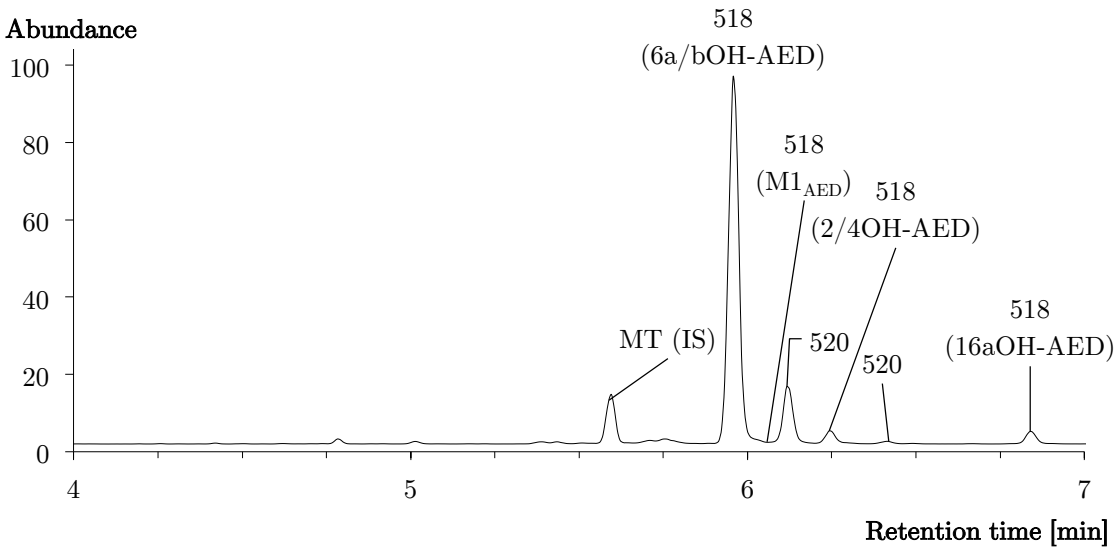

Figure 106 Extracted ion chromatogram of hydroxylated metabolites of androst-4-ene-3,17-dione after incubation with HLM as per-TMS derivatives, internal standard methyltestosterone (MT, 8 µg/mL),

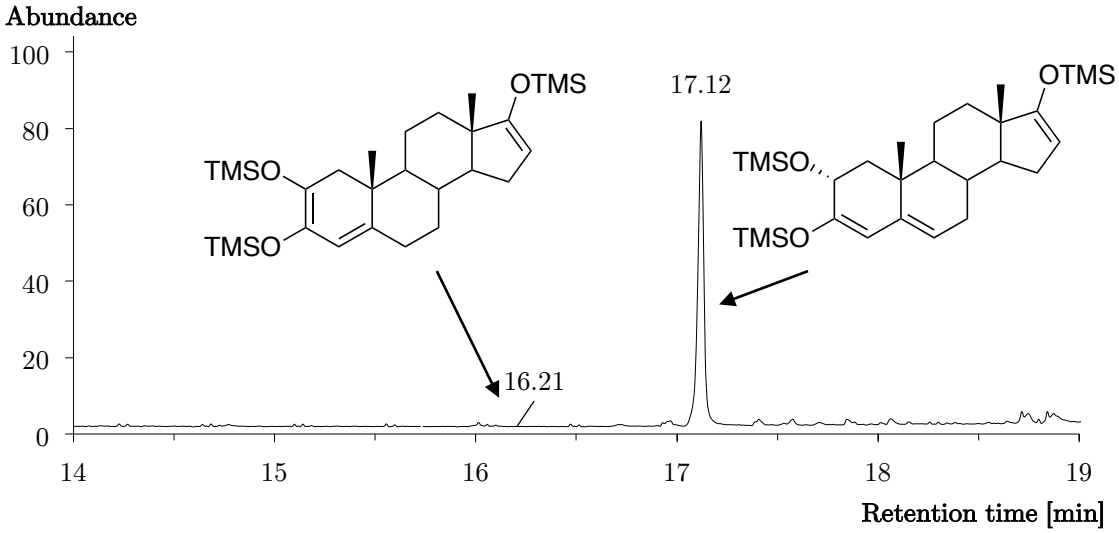

Figure 107 Base peak chromatogram of 2a-hydroxyandrost-4-ene-3,17-dione as tris-TMS derivative, displayed are both derivatization isomers, acquired using method a)

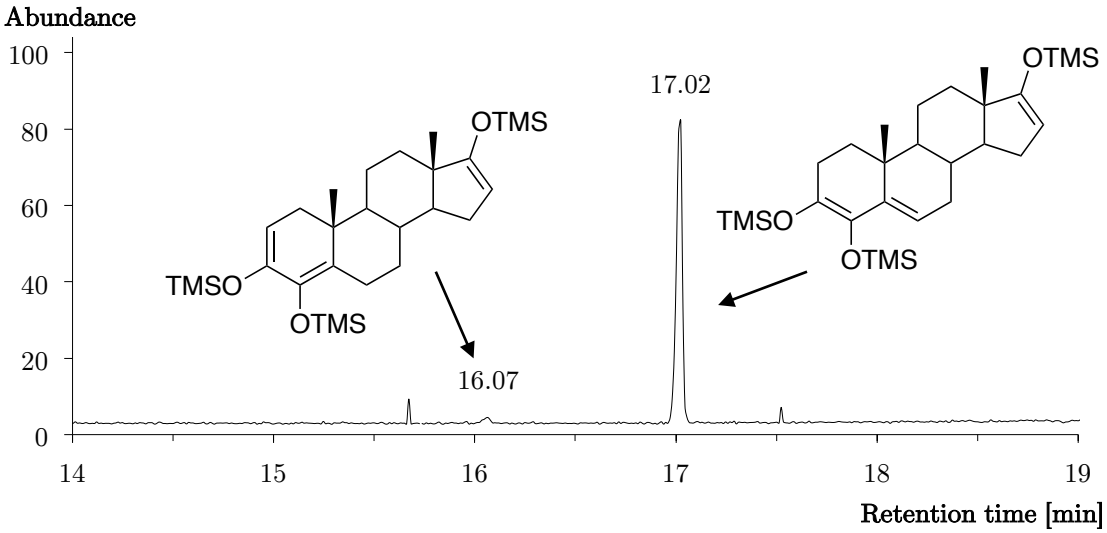

Figure 108 Base peak chromatogram of formestane (4-hydroxyandrost-4-ene-3,17-dione), tris-TMS, displayed are both derivatization isomers, acquired using method a)

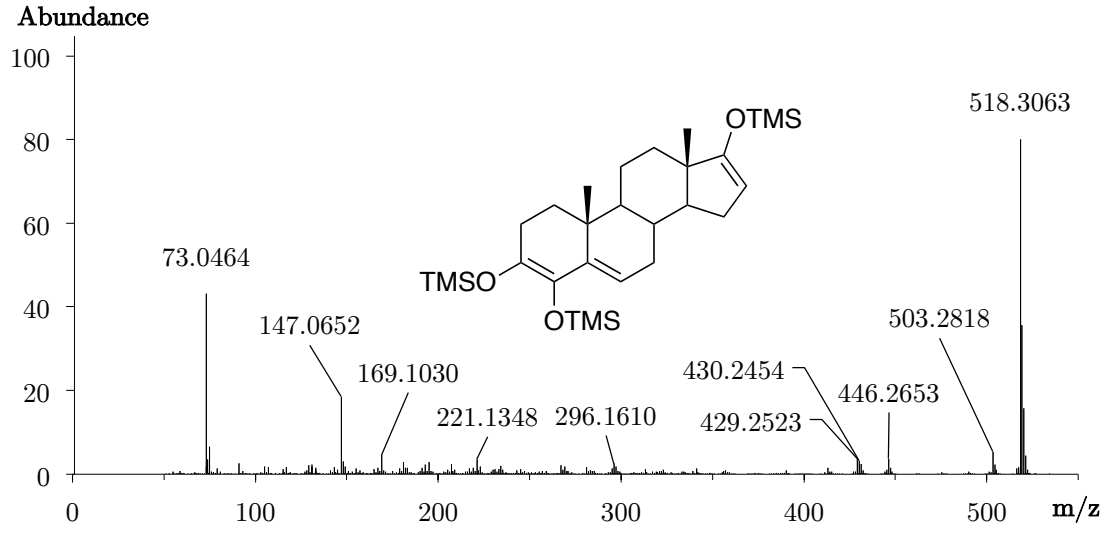

Figure 109 Accurate mass spectrum (EI) of 4-hydroxyandrost-ene-3,17-dione, 3,5,16-triene-3,4,17-triol tris-TMS, $[M]^{\bullet+}$=518.3063, mass error 0.19 ppm

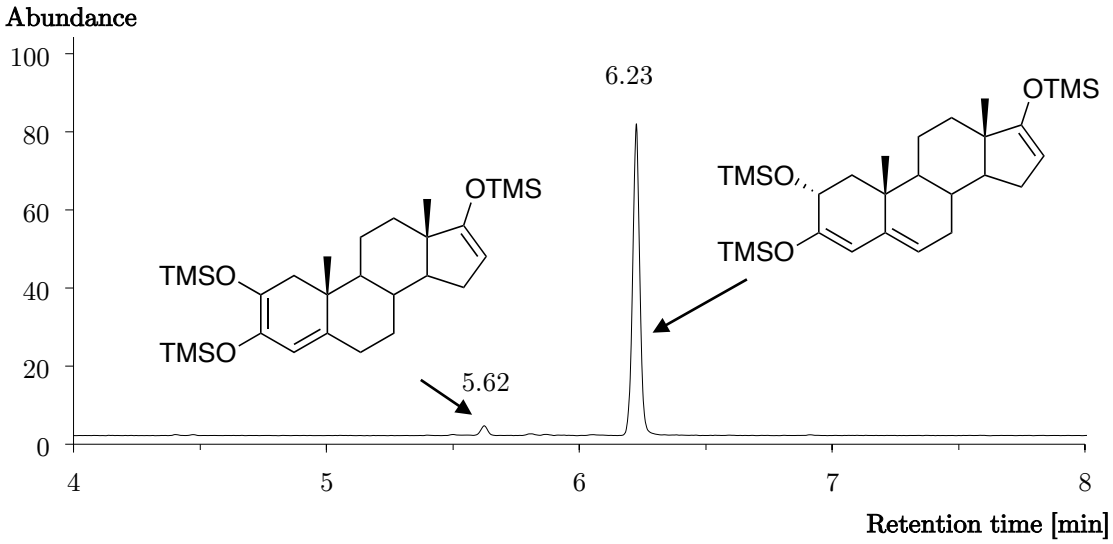

Figure 110 Extracted ion chromatogram (m/z 518.3062) of the derivatization isomers of 2a-hydroxyandrost-4-ene-3,17-dione after TMIS derivatization, acquired using method b)

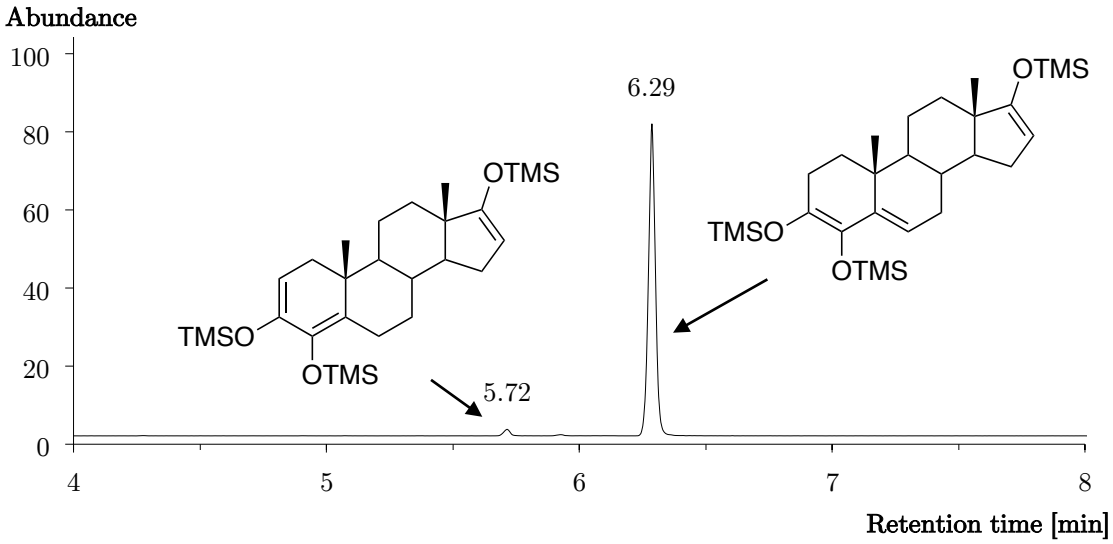

Figure 111 Extracted ion chromatogram (m/z 518.3062) of the derivatization isomers of 4-hydroxyandrost-ene-3,17-dione after TMIS derivatization, acquired using method b)

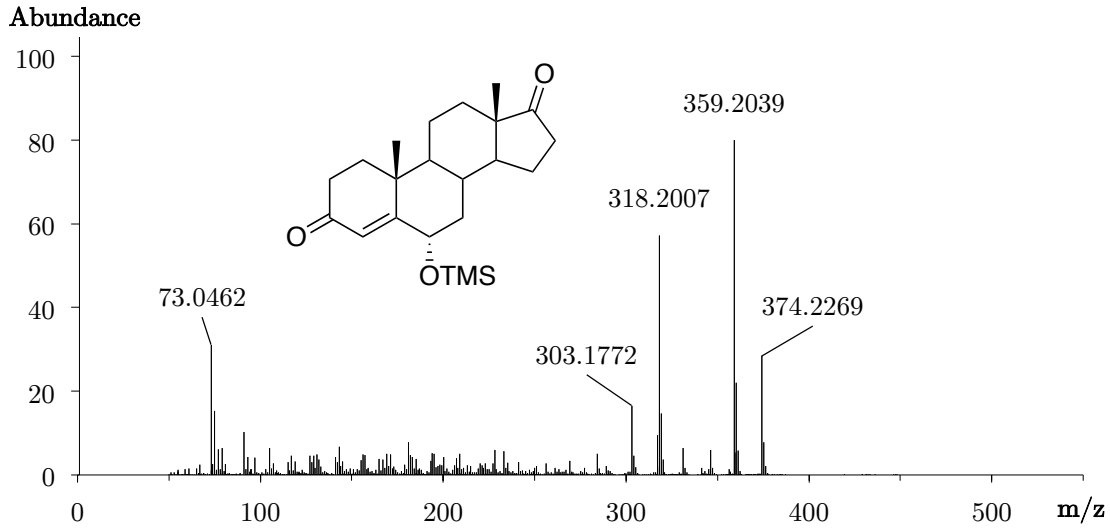

Figure 112 Accurate mass spectrum (EI) of 6α-hydroxyandrost-4-ene-3,17-dione, mono-TMS derivative, $[M]^{\bullet+}$=374.2269, mass error 2.19 ppm

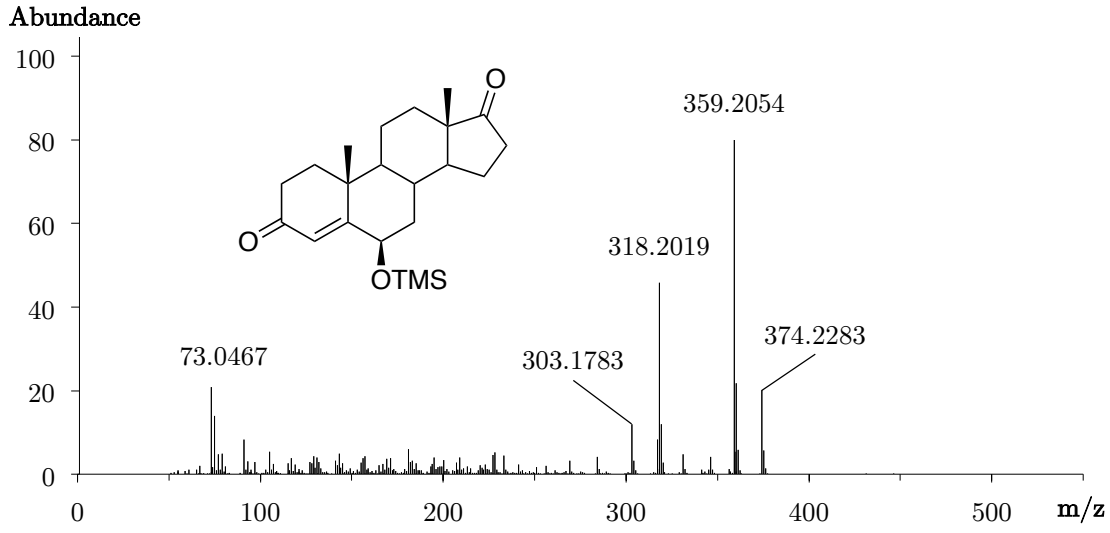

Figure 113 Accurate mass spectrum (EI) of 6β-hydroxyandrost-4-ene-3,17-dione, mono-TMS derivative, $[M]^{\bullet+}$=374.2283, mass error 1.55 ppm

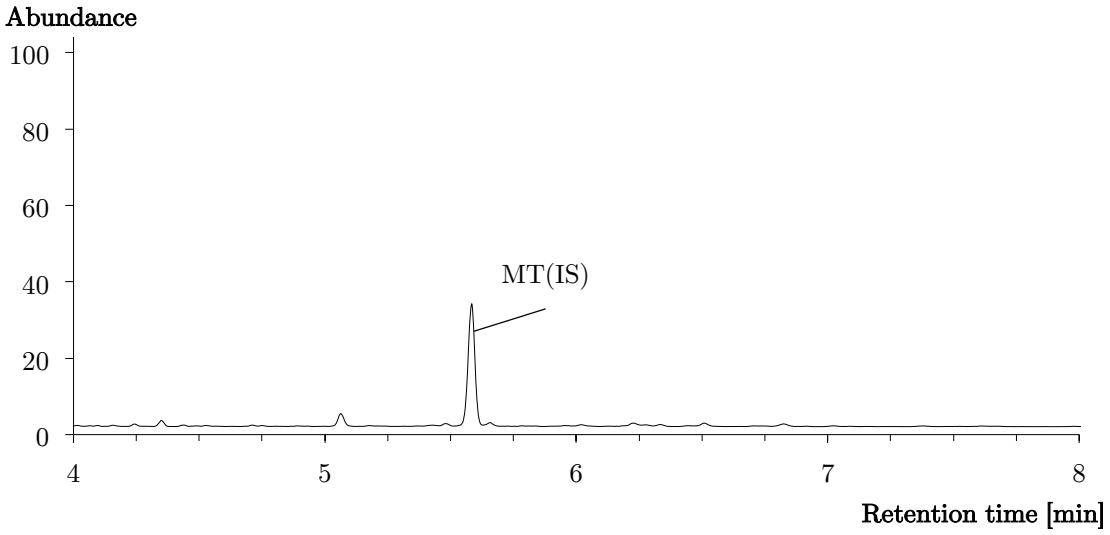

Figure 114 Extracted ion chromatogram (m/z 518.3062) of a control urine sample after TMIS derivatization, internal standard methyltestosterone (MT, 8 µg/mL)

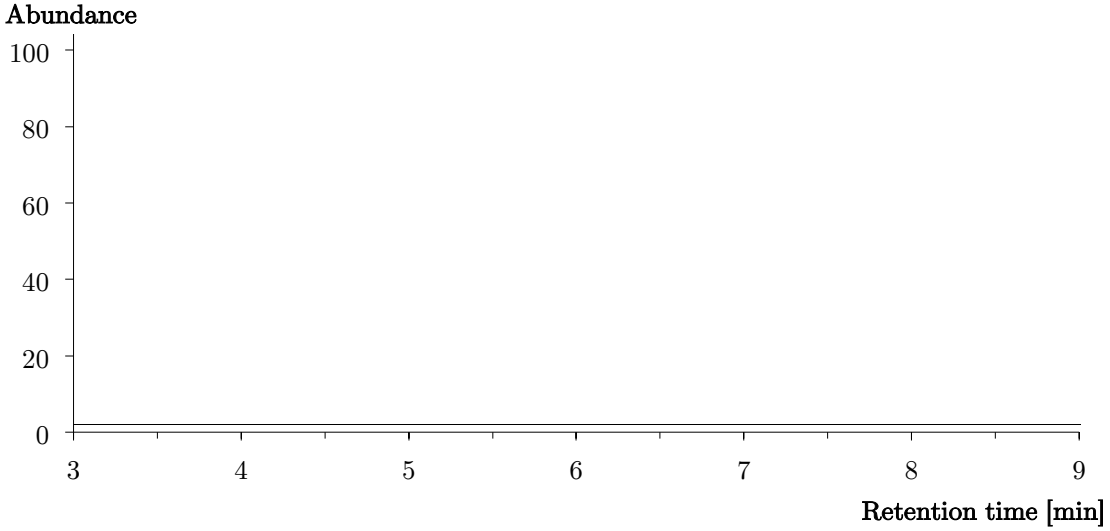

Figure 115 Extracted ion chromatogram (m/z 359.2043) of a control urine sample after MSTFA derivatization

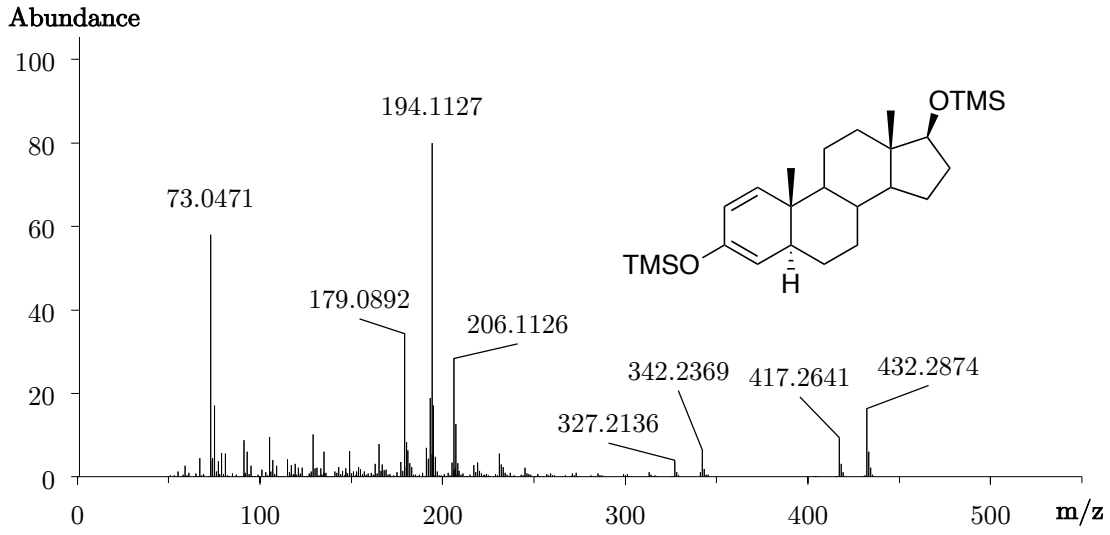

Figure 116 Accurate mass spectrum (EI) of 1-testosterone (17β-hydroxy-5α-androst-1-en-3-one), 1,3-diene-3,17-diol bis-TMS, $[M]^{\bullet+}$=432.2874, mass error -0.07 ppm

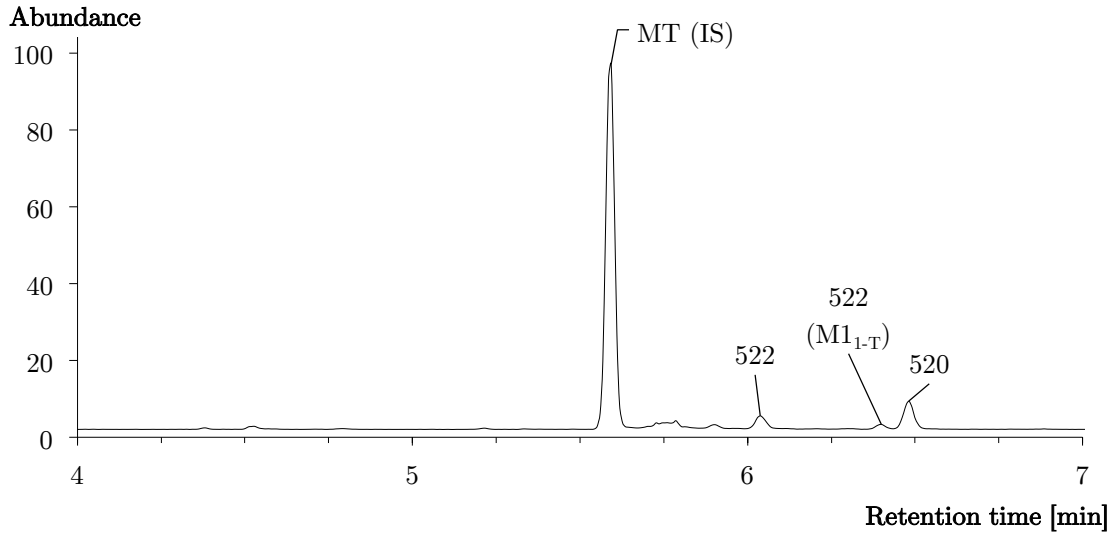

Figure 117 Extracted ion chromatogram of hydroxylated metabolites of 1-testosterone after incubation with CYP19A1 as per-TMS derivatives, internal standard methyltestosterone (MT, 8 µg/mL), acquired using method b)

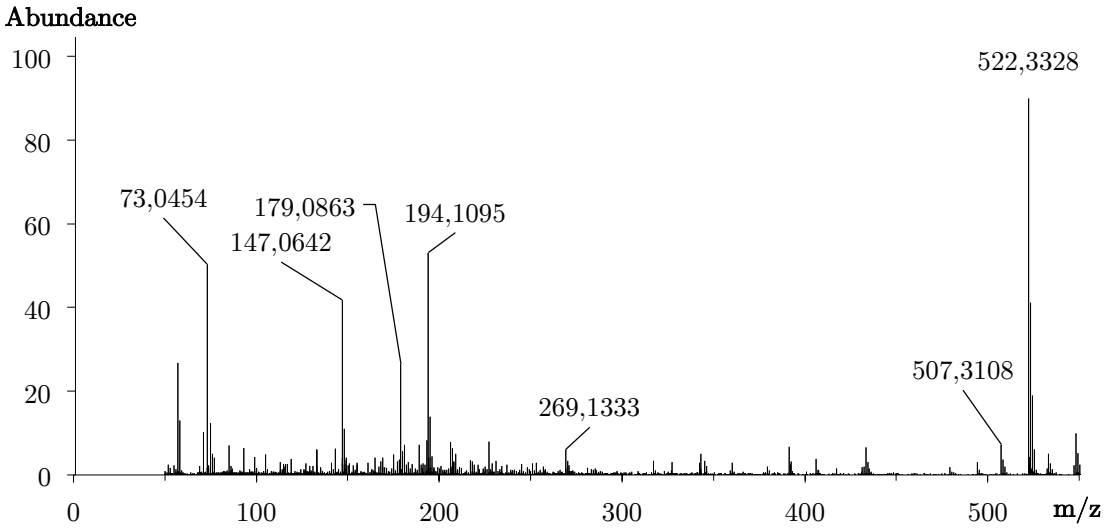

Figure 118 Accurate mass spectrum (EI) of a hydroxylated metabolite of 1-testosterone after incubation with CYP19A ($M1_{1\text{-}T}$) as tris-TMS derivative, retention time 6.40 min, $[M]^{\bullet+}$=522.3328, mass error -9.06 ppm

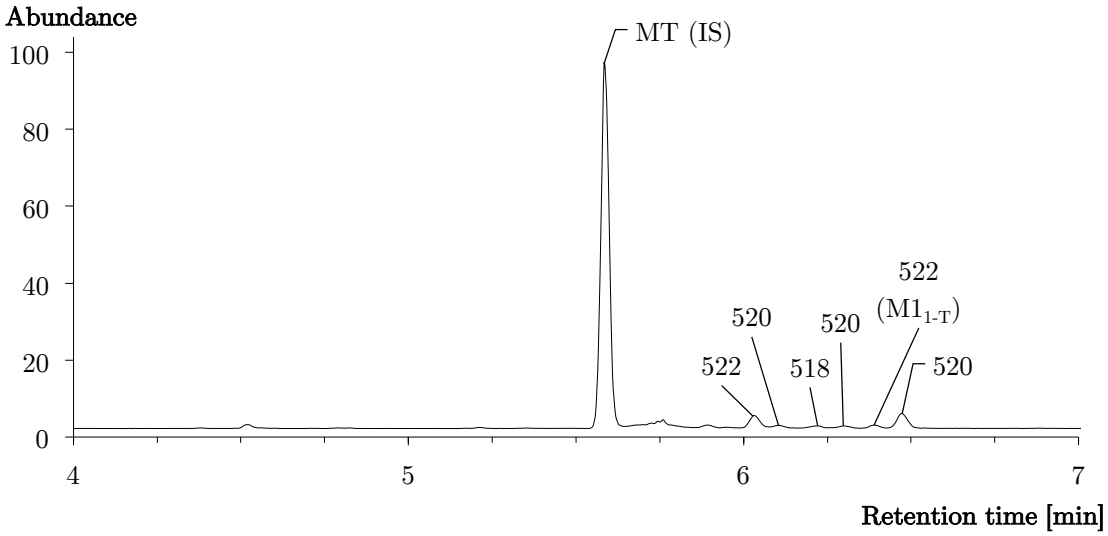

Figure 119 Extracted ion chromatogram of hydroxylated metabolites of 1-testosterone after incubation with CYP3A4 as per-TMS derivatives, internal standard methyltestosterone (MT, 8 µg/mL), acquired using method b)

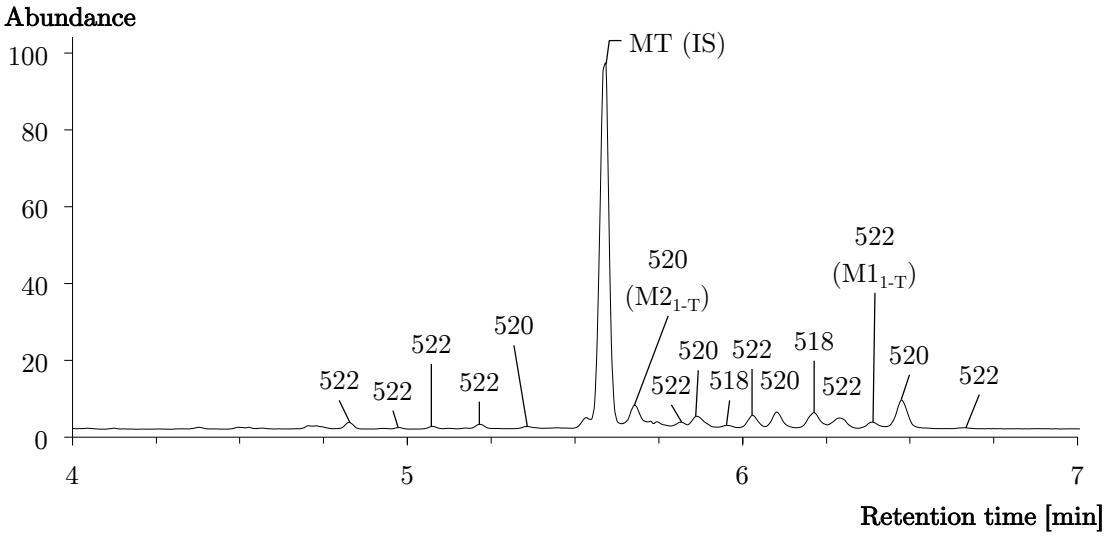

Figure 120 Extracted ion chromatogram of hydroxylated metabolites of 1-testosterone after incubation with HLM as perTMS derivatives, internal standard methyltestosterone (MT, 8 µg/mL)

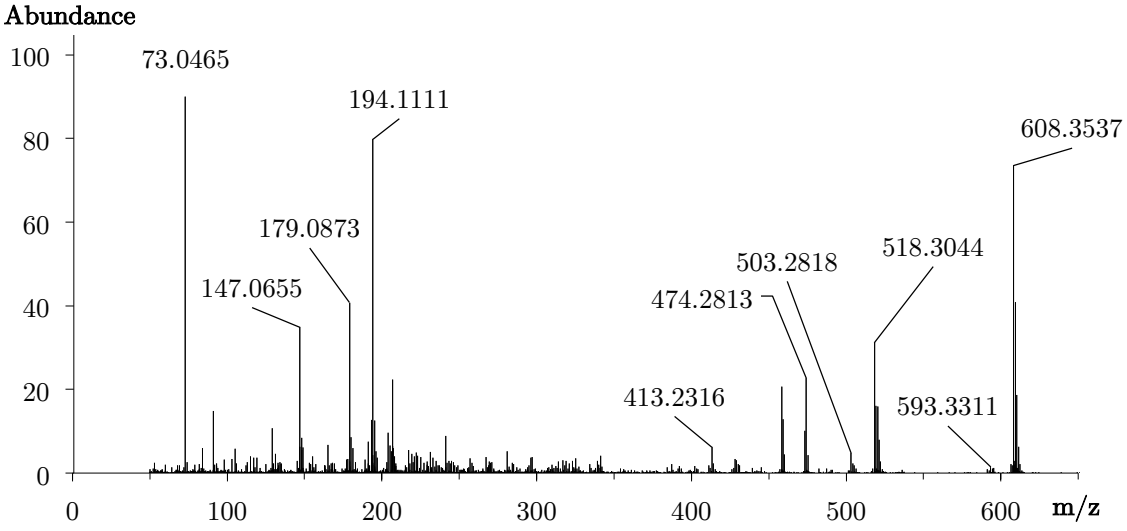

Figure 121 Accurate mass spectrum (EI) of a di-hydroxylated 1-testosterone metabolite (M3$_{1-T}$) as tetrakis-TMS derivative after incubation with HLM, retention time 7.13 min, $[M]^{\bullet+}$=608.3537, mass error -4.27 ppm

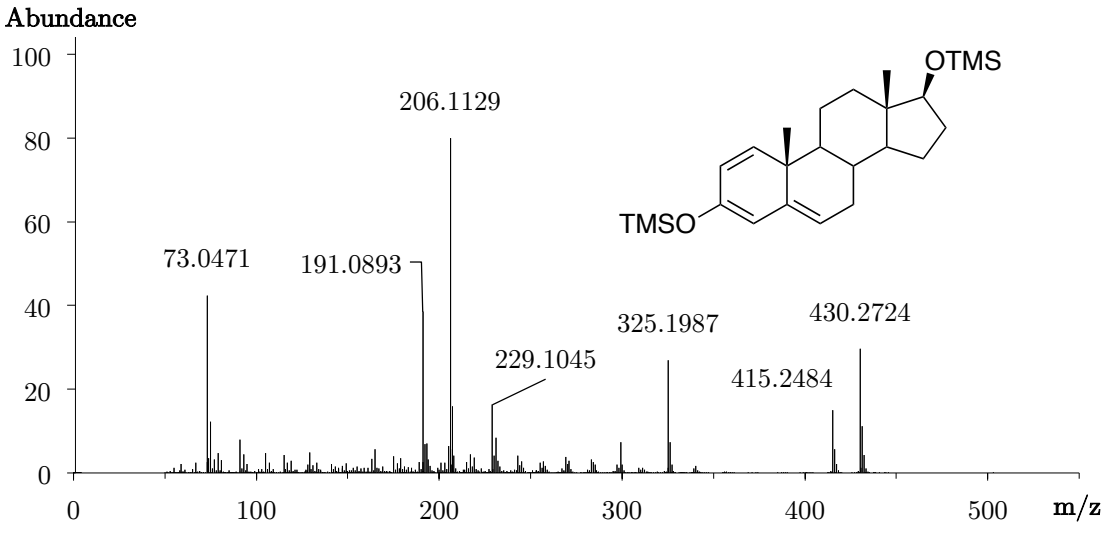

Figure 122 Accurate mass spectrum (EI) of boldenone (BOLD, 17β-hydroxyandrosta-1,4-dien-3-one), 1,3,5-triene-3,17-diol bis-TMS, $[M]^{\bullet+}$=430.2724, mass error 1.44 ppm

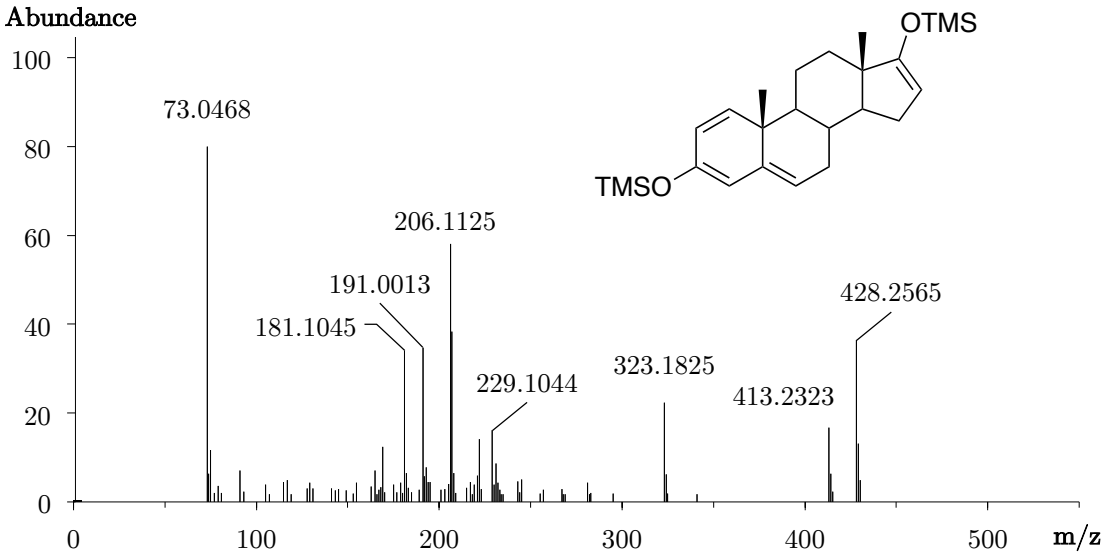

Figure 123 Accurate mass spectrum (EI) of boldione (ADD, androsta-1,4-diene-3,17-dione), 1,3,5,16-tetraene-3,17-diol bis-TMS, $[M]^{\bullet+}$=428.2565, mass error 0.86 ppm

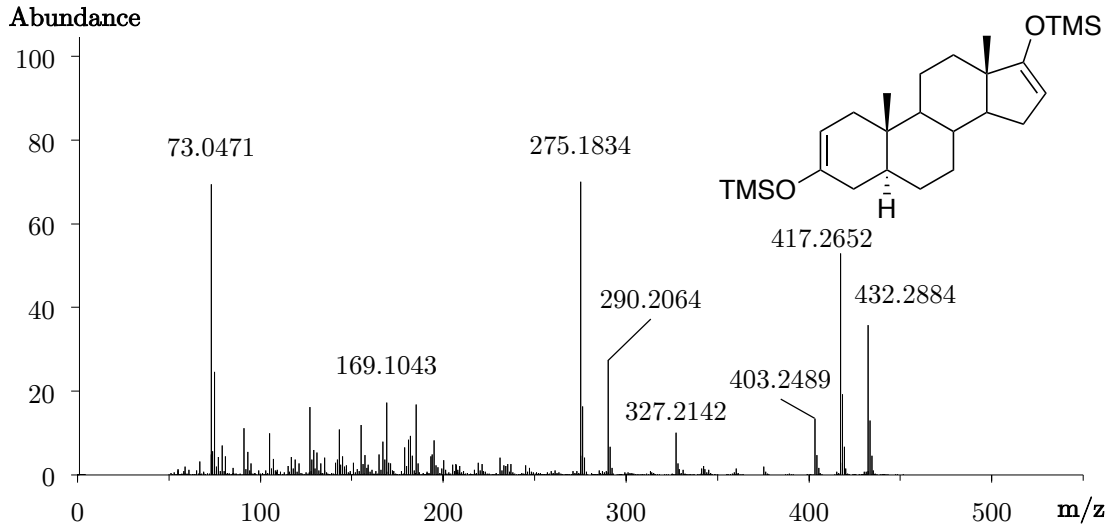

Figure 124 Accurate mass spectrum (EI) of androstenedione (5α-AD, 5α-androstane-3,17-dione), 2,16-diene-3,17-diol bis-TMS, $[M]^{\bullet+}$=432.2884, mass error 2.24 ppm

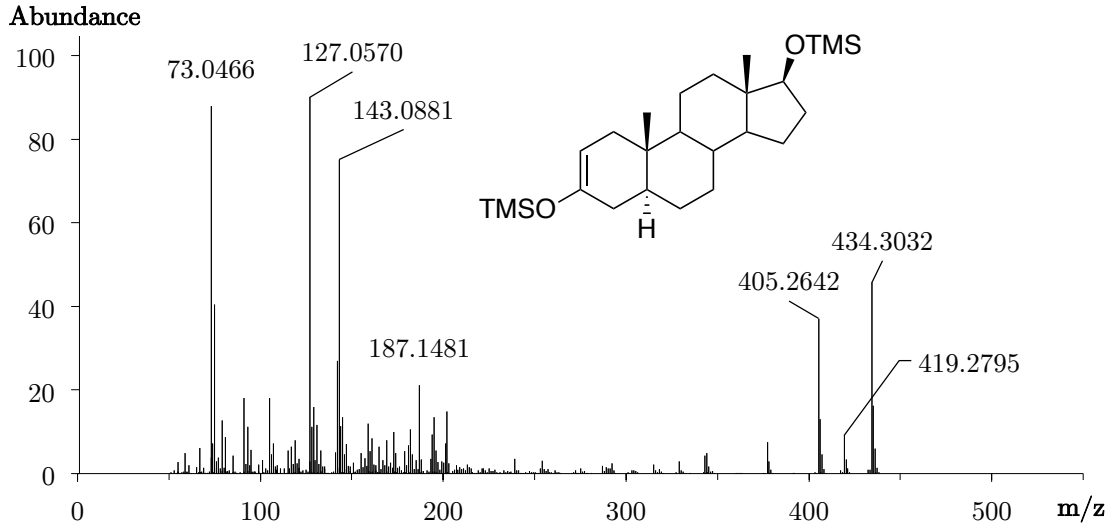

Figure 125 Accurate mass spectrum (EI) of dihydrotestosterone (5α-DHT, 17β-hydroxy-5α-androstan-3-one), 2-ene-3,17β-diol bis-TMS, $[M]^{\bullet+}$=434.3032, mass error 0.28 ppm

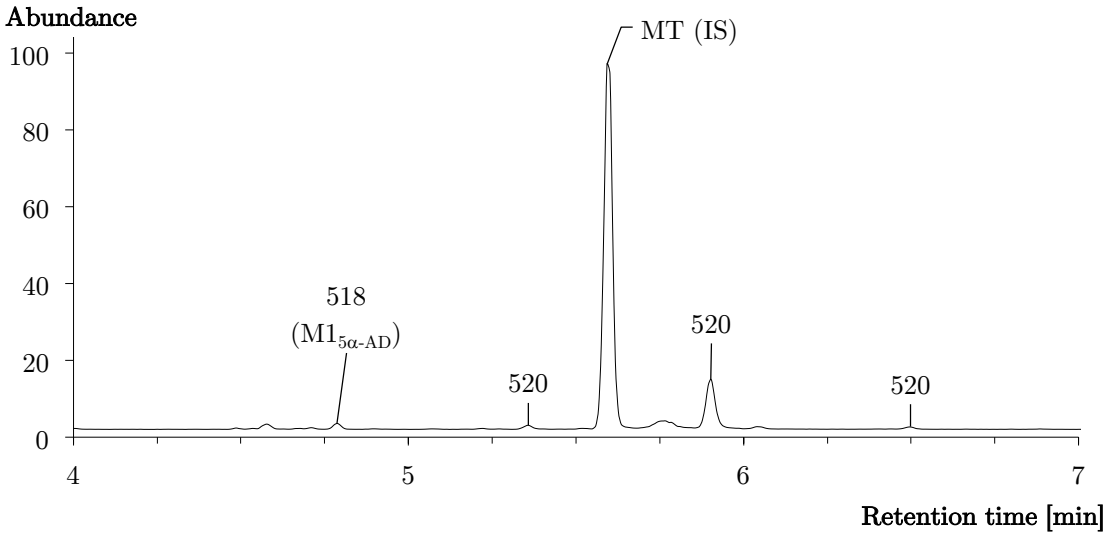

Figure 126 Extracted ion chromatogram of hydroxylated metabolites of 5α-androstane-3,17-dione after incubation with CYP19A1 as per-TMS derivatives, internal standard methyltestosterone (MT, 8 µg/mL), acquired using method b)

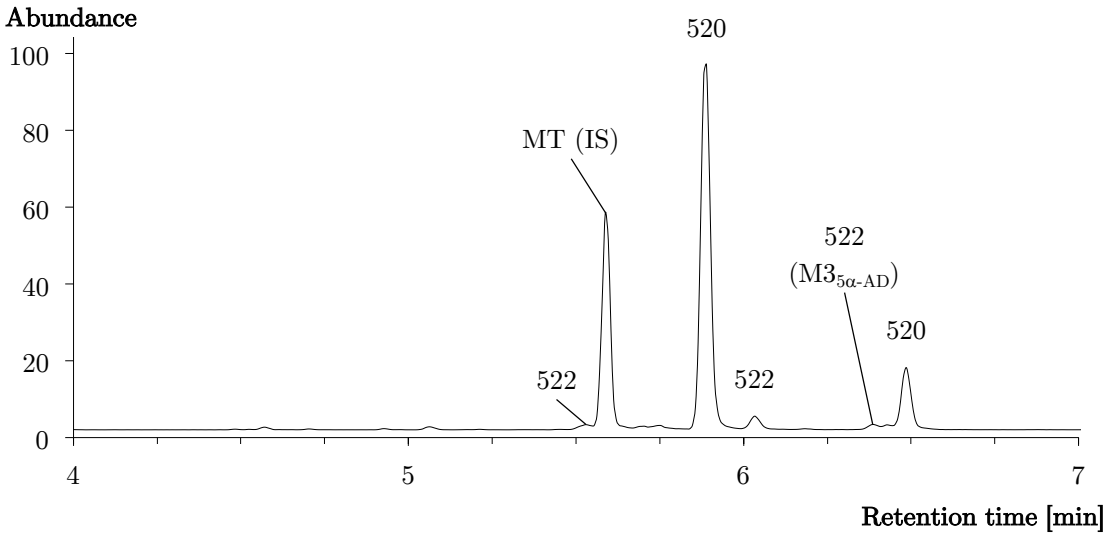

Figure 127 Extracted ion chromatogram of hydroxylated metabolites of 5α-androstane-3,17-dione after incubation with CYP3A4 as per-TMS derivatives, internal standard methyltestosterone (MT, 8 µg/mL), acquired using method b)

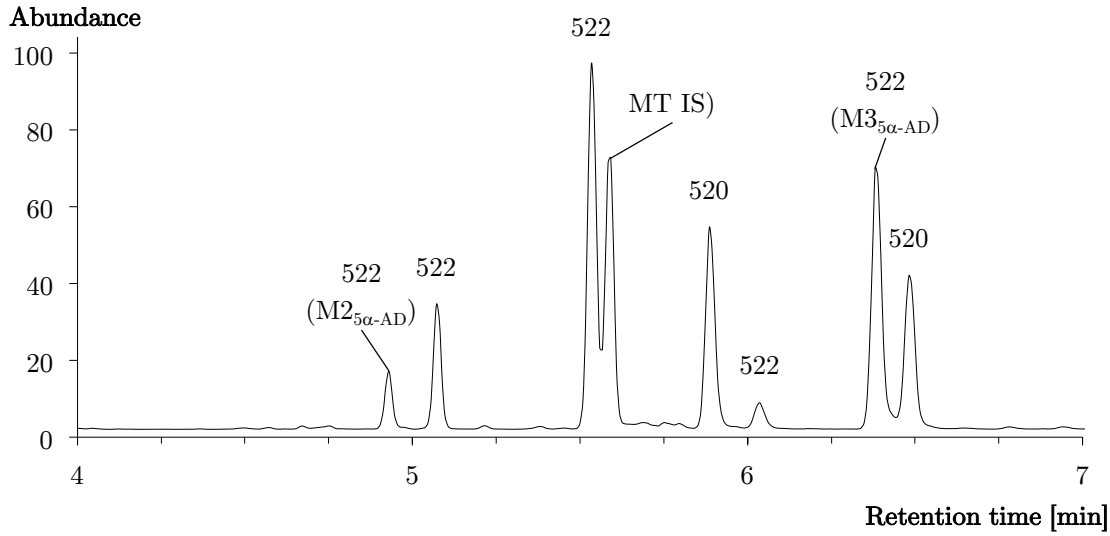

Figure 128 Extracted ion chromatogram of hydroxylated metabolites of 5α-androstane-3,17-dione after incubation with HLM as per-TMS derivatives, internal standard methyltestosterone (MT, 8 µg/mL), acquired using method b)

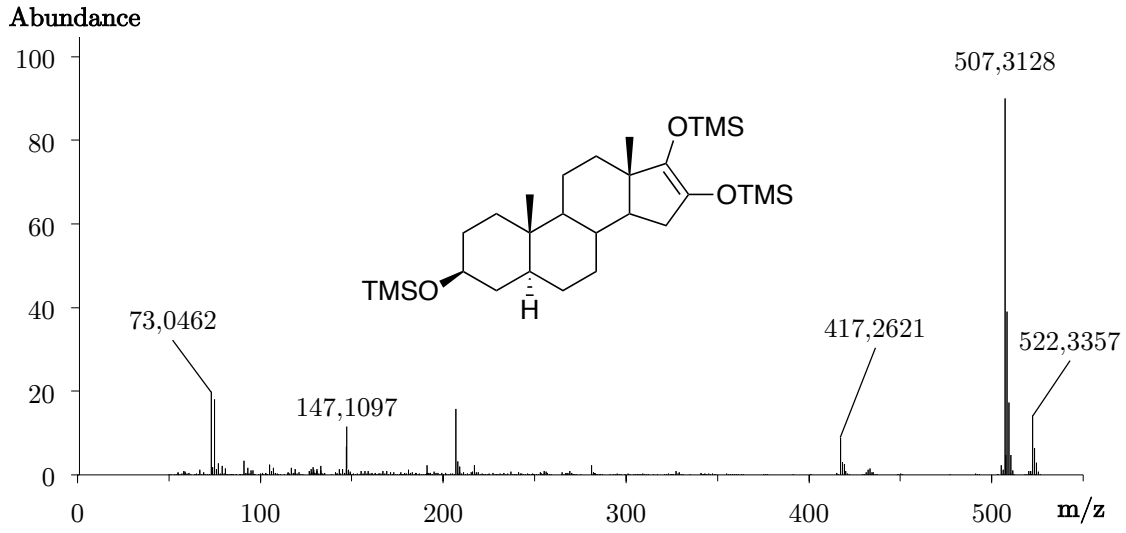

Figure 129 Accurate mass spectrum (EI) of 3β,16α-dihydroxy-5α-androstan-17-one, 16-ene-3β,16,17-triol tris-TMS, $[M]^{\bullet+}$=522.3357, mass error 1.15 ppm

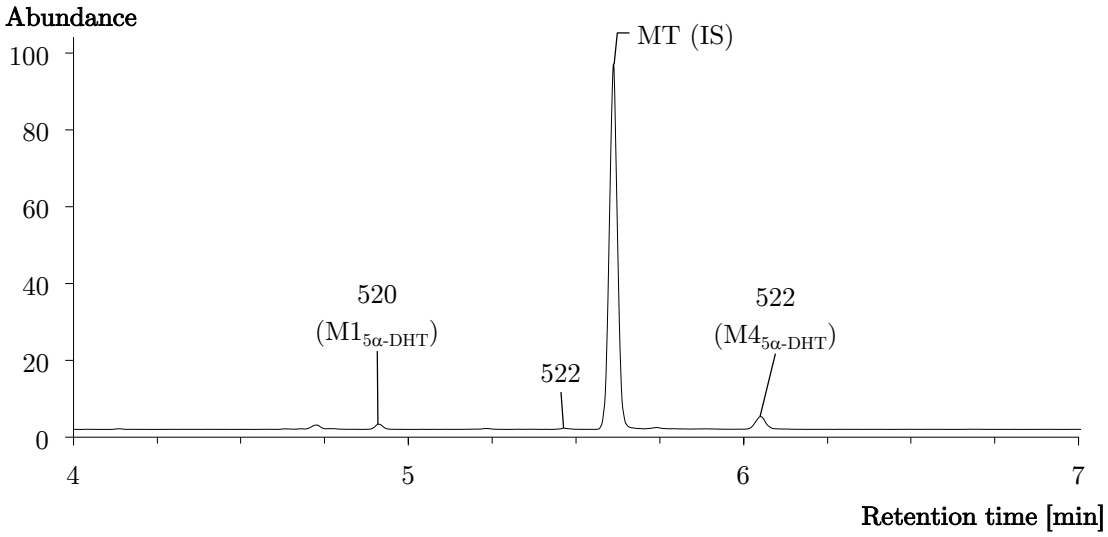

Figure 130 Extracted ion chromatogram of hydroxylated metabolites of dihydrotestosterone after incubation with CYP19A1 as per-TMS derivatives, internal standard methyltestosterone (MT, 8 µg/mL), acquired using method b)

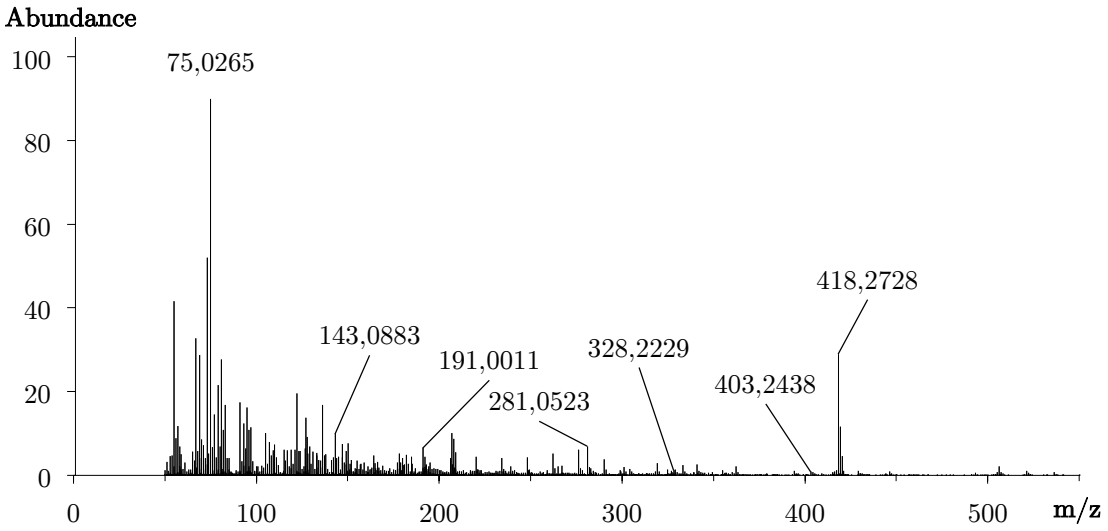

Figure 131 Accurate mass spectrum (EI) of a 19-nortestosterone isomer (M3$_{5\alpha\text{-DHT}}$) as bis-TMS, retention time 5.87 min, $[M]^{\bullet+}$=418.2728, mass error 1.12 ppm

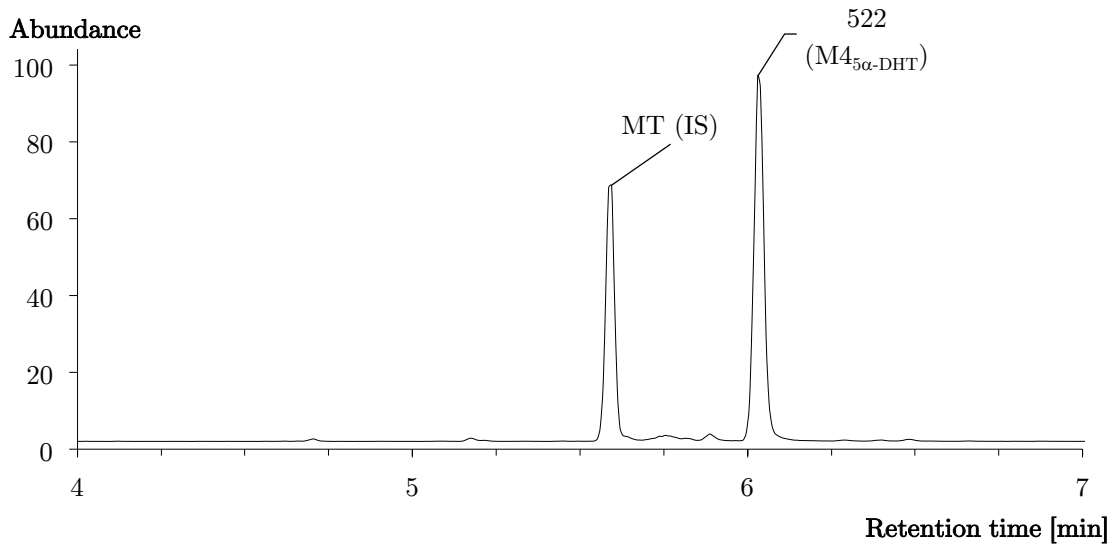

Figure 132 Extracted ion chromatogram of hydroxylated metabolites of dihydrotestosterone after incubation with CYP3A4 as per-TMS derivatives, internal standard methyltestosterone (MT, 8 µg/mL), acquired using method b)

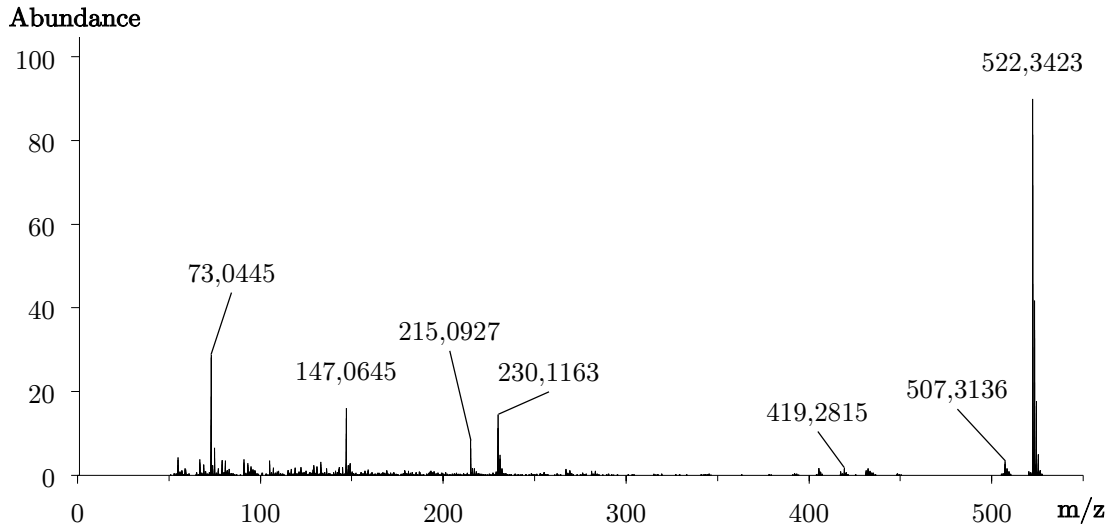

Figure 133 Accurate mass spectrum (EI) of a hydroxylated metabolite of dihydrotestosterone after incubation with CYP3A4 (M4$_{5\alpha\text{-DHT}}$) as tris-TMS derivative, retention time 6.01 min, $[M]^{\bullet+}$ = 522.3424, mass error 9.38 ppm

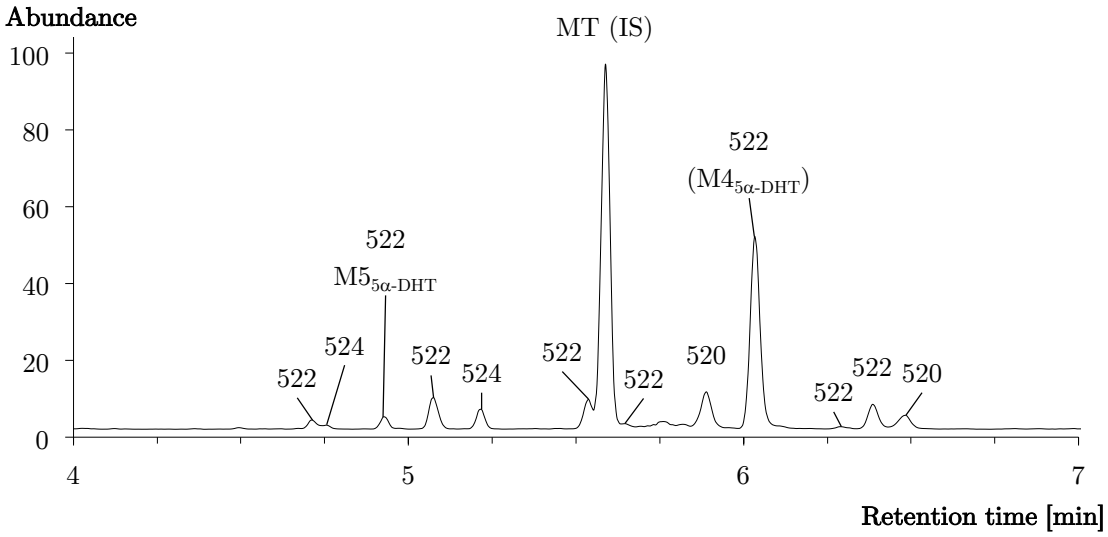

Figure 134 Extracted ion chromatogram of hydroxylated metabolites of dihydrotestosterone after incubation with HLM as per-TMS derivatives, internal standard methyltestosterone (MT, 8 µg/mL), acquired using method b)

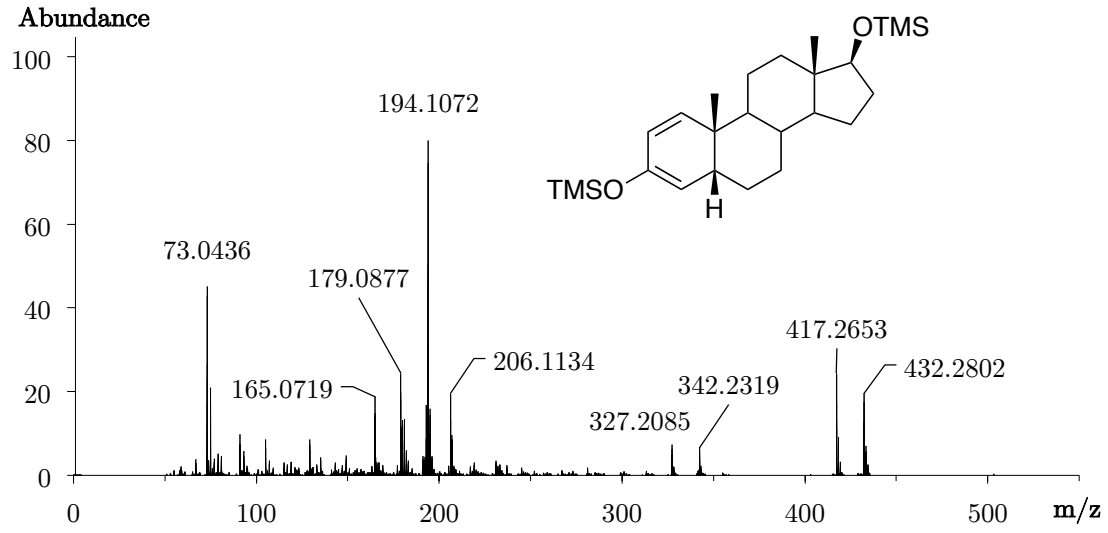

Figure 135 Accurate mass spectrum (EI) of 17β-hydroxy-5β-androst-1-en-3-one, 1,3-diene-3,17-diol bis TMS, $[M]^{\bullet+}$=432.2802, mass error -1.69 ppm

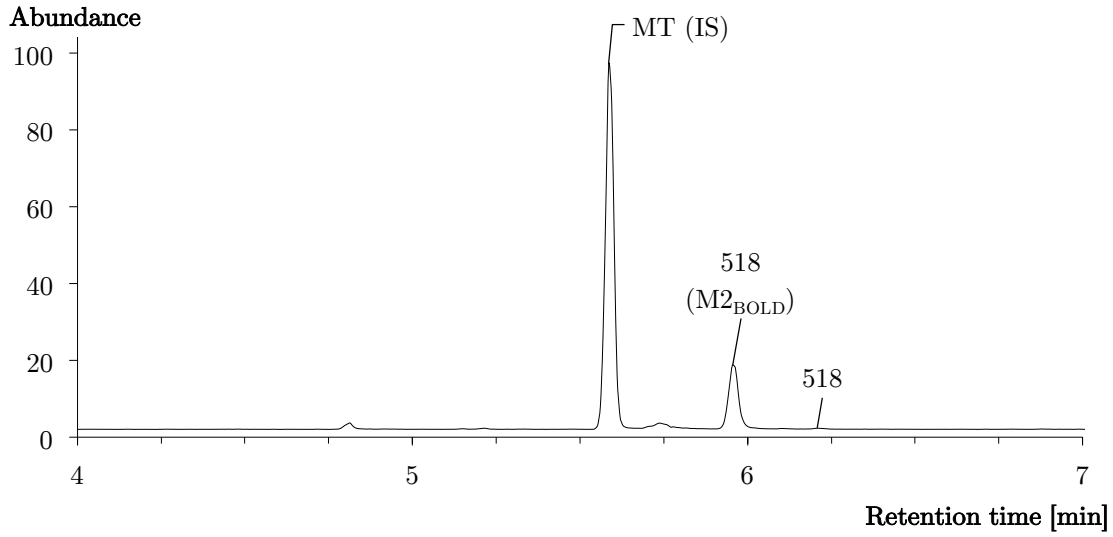

Figure 136 Extracted ion chromatogram of hydroxylated metabolites of boldenone after incubation with CYP19A1 as per-TMS derivatives, internal standard methyltestosterone (MT, 8 µg/mL), acquired using method b)

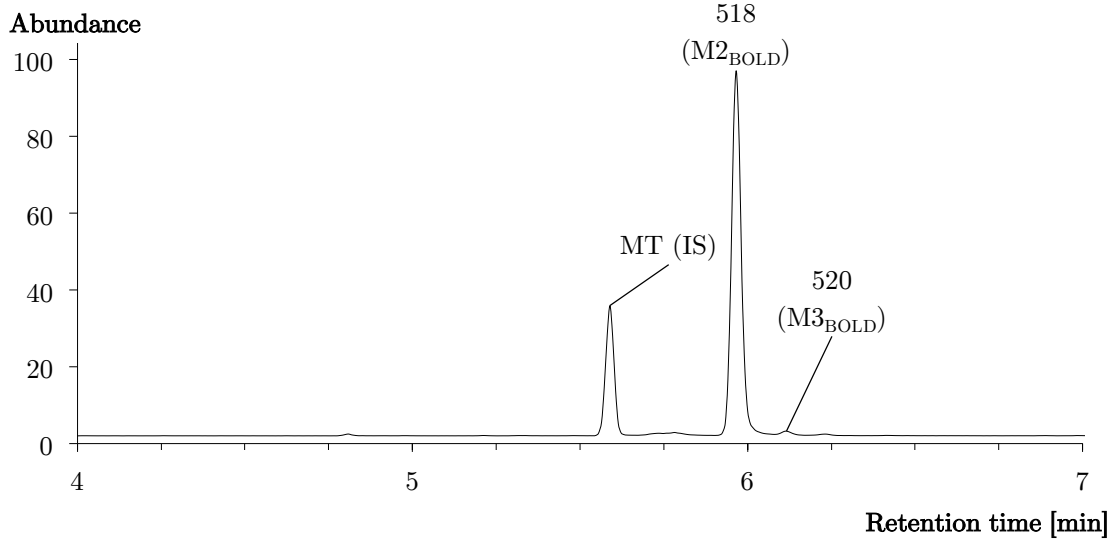

Figure 137 Extracted ion chromatogram of hydroxylated metabolites of boldenone after incubstion with CYP3A4 as per-TMS derivatives, internal standard methyltestosterone (MT, 8 µg/mL), acquired using method b)

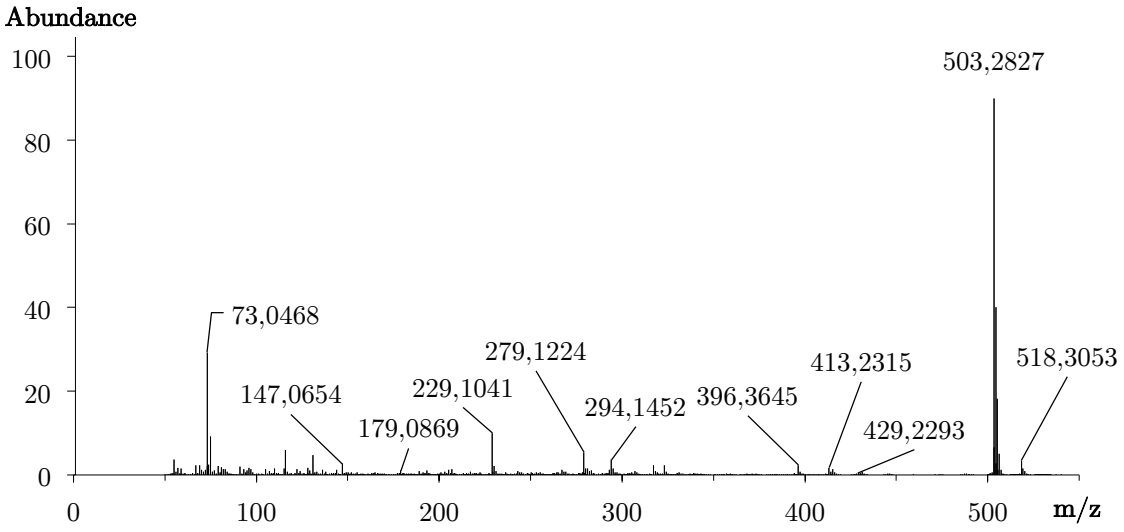

Figure 138 Accurate mass spectrum (EI) of the main hydroxylated metabolite of boldenone after incubation with CYP3A4 ($M2_{BOLD}$) as tris-TMS derivative, retention time 5.96 min, $[M]^{\bullet+}$=518.3053, mass error -1.74 ppm

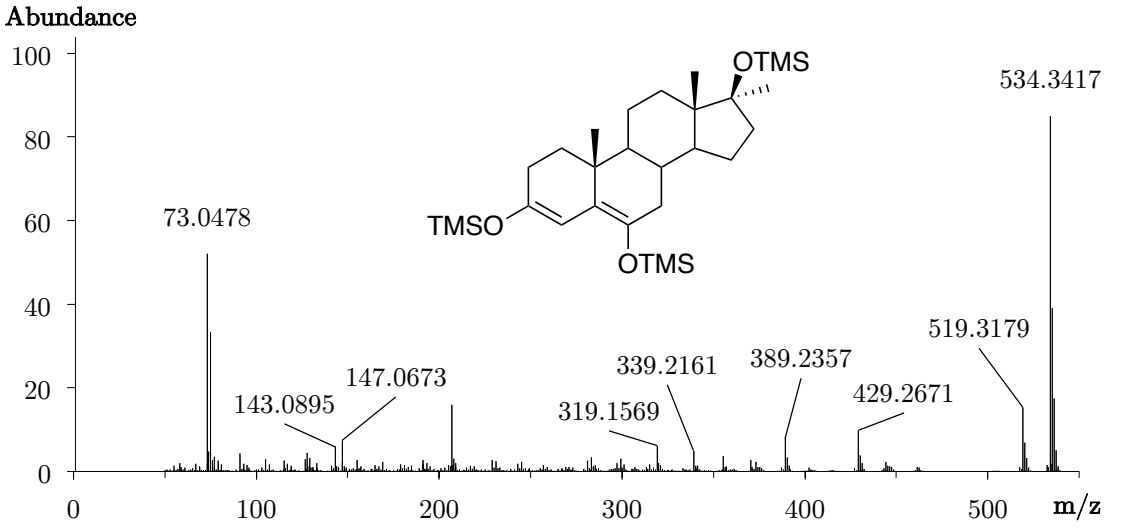

Figure 139 Accurate mass spectrum (EI) of 6β,17β-dihydroxy-17α-methylandrost-4-en-3-one, 3,5-diene-3,6,17-triol tris-TMS, $[M]^{\bullet+}$=534.3417, mass error 7.80 ppm

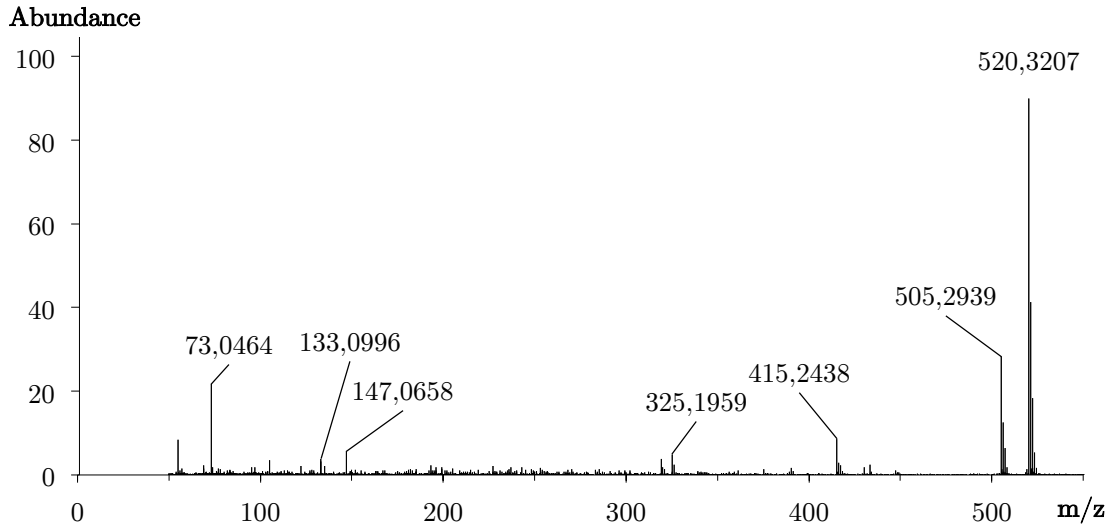

Figure 140 Accurate mass spectrum (EI) of a hydroxylated metabolite of boldenone after incubation with CYP3A4 ($M3_{BOLD}$) as tris-TMS derivative, retention time 6.11 min, $[M]^{\bullet+}$=520.3207, mass error -2.69 ppm

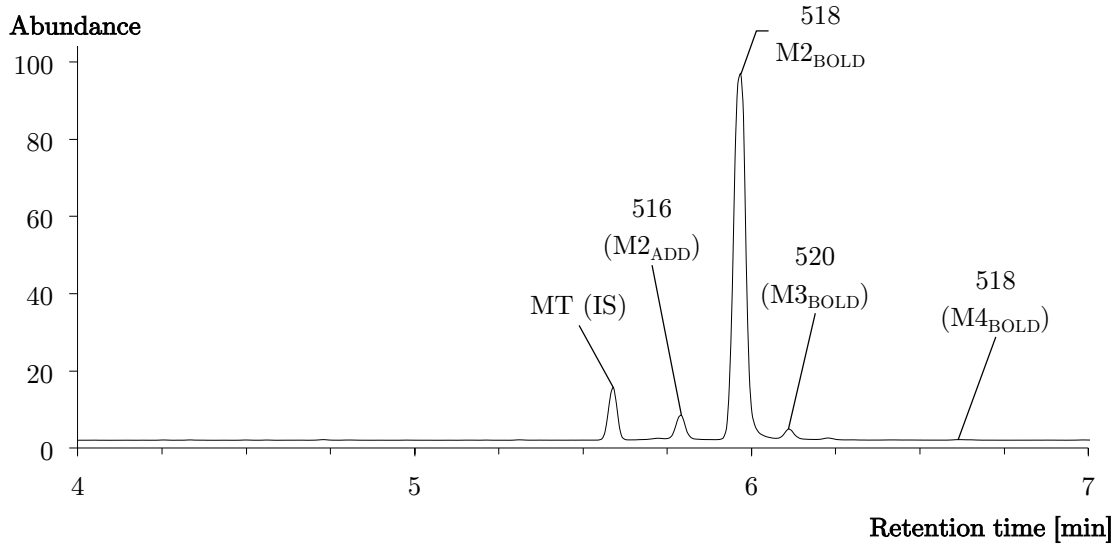

Figure 141 Extracted ion chromatogram of hydroxylated metabolites of boldenone after incubation with HLM as per-TMS derivatives, internal standard methyltestosterone (MT, 8 µg/mL), acquired using method b)

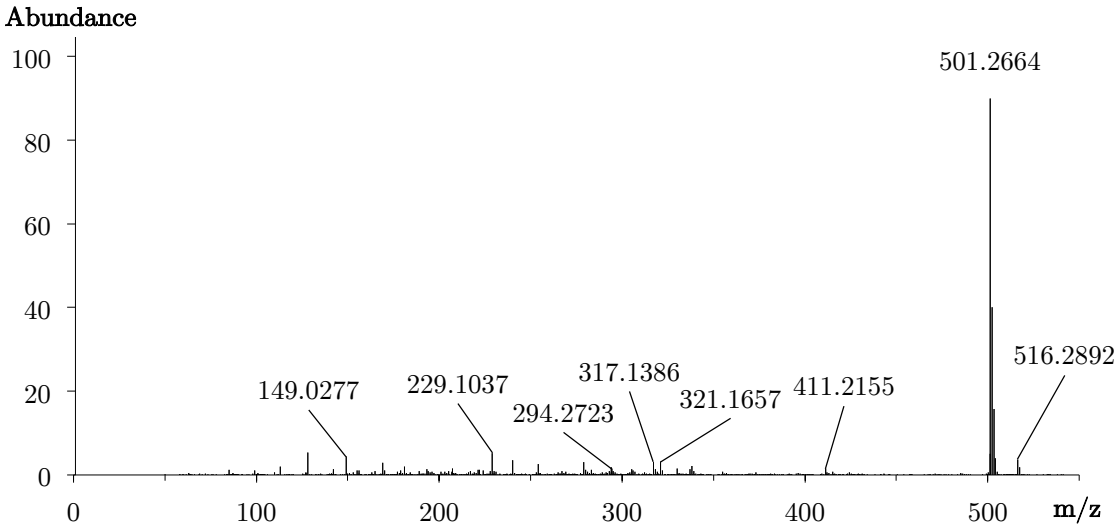

Figure 142 Accurate mass spectrum (EI) of an oxidized and hydroxylated metabolite of boldenone after incubation with HLM ($M2_{ADD}$) as tris-TMS derivative, retention time 5.79 min, $[M]^{\bullet+}$=516.2892, mass error -2.91 ppm

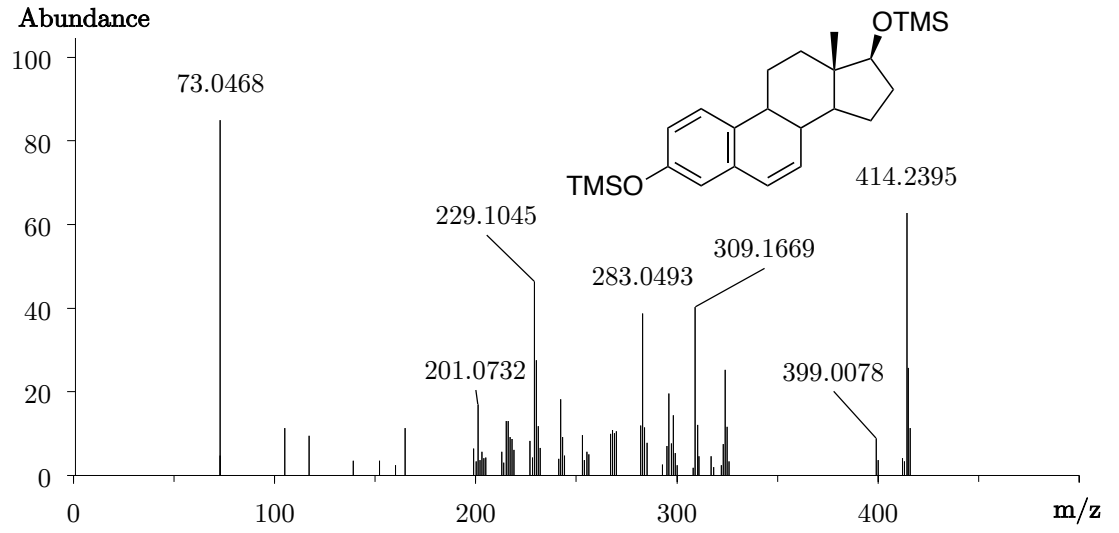

Figure 143 Accurate mass spectrum (EI) of 3,17β-dihydroxyestra-1,3,5(10),6-tetraene (as the derivatization artifact of 17β-hydroxyandrosta-4,6-dien-3-one), bis-TMS, $[M]^{\bullet+}$=414.2395, mass error -2.41 ppm

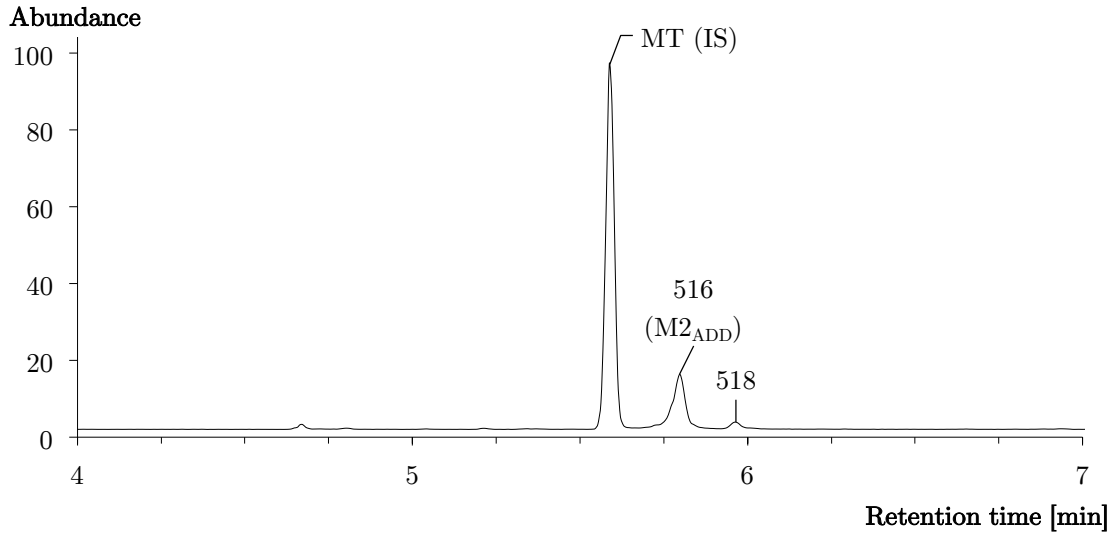

Figure 144 Extracted ion chromatogram of hydroxylated metabolites of boldione after incubation with CYP19A1 as per-TMS derivatives, internal standard methyltestosterone (MT, 8 µg/mL), acquired using method b)

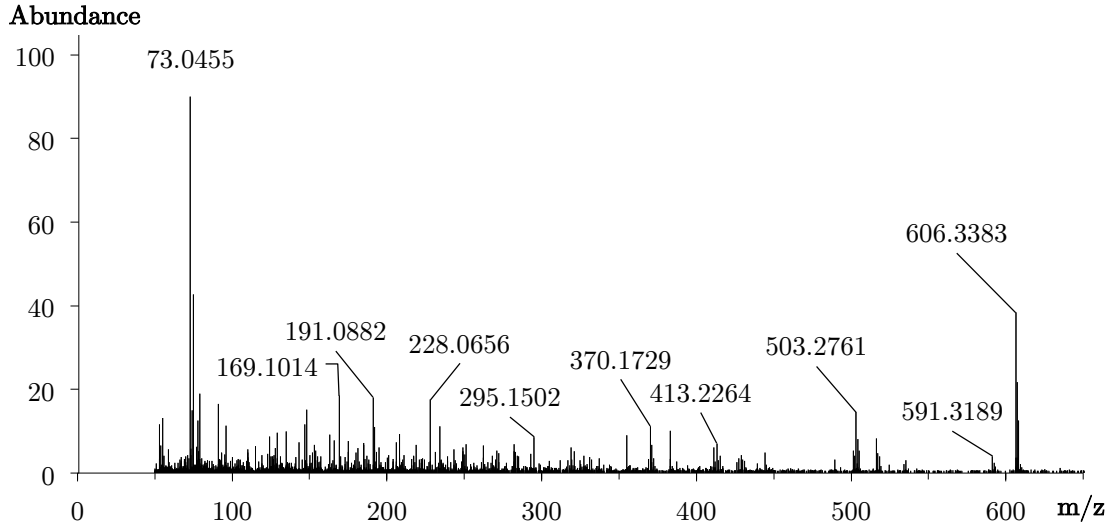

Figure 145 Accurate mass spectrum (EI) of a minor reduced and di-hydroxylated metabolite of boldione after incubation with CYP19A1 ($M1_{ADD}$) as tetrakis-TMS derivative, $[M]^{\bullet+}$=606.3383, mass error -3.96 ppm

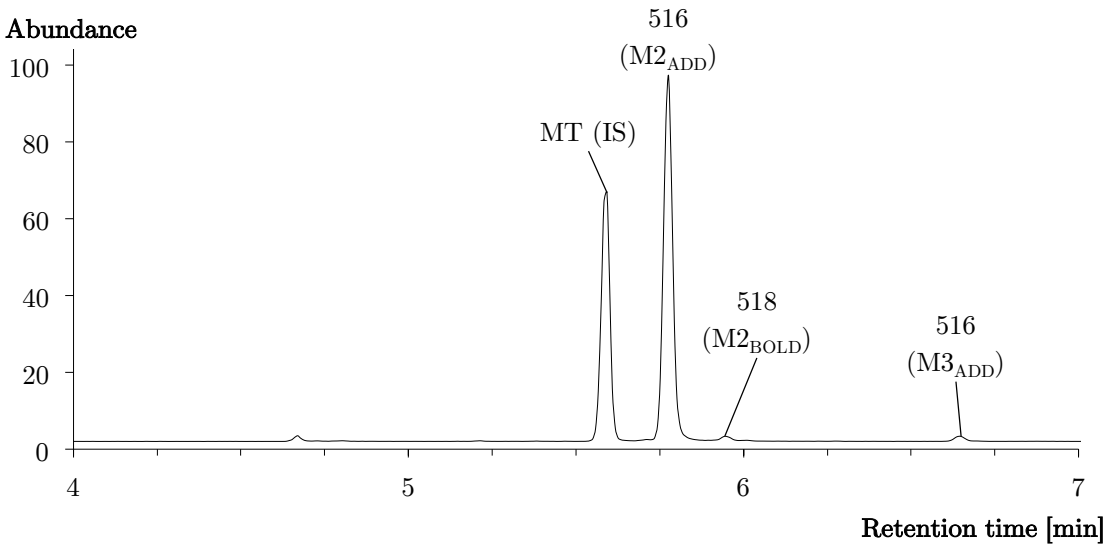

Figure 146 Extracted ion chromatogram of hydroxylated metabolites of boldione after incubation with CYP3A4 as per-TMS derivatives, internal standard methyltestosterone (MT, 8 µg/mL), acquired using method b)

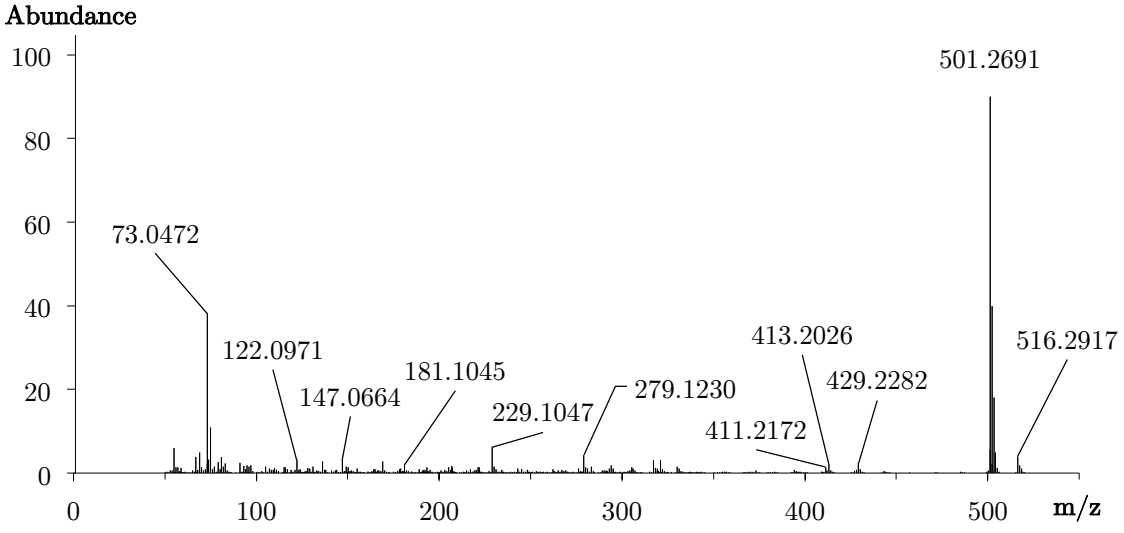

Figure 147 Accurate mass spectrum (EI) of a hydroxylated metabolite of boldione after incubation with CYP3A4 ($M2_{ADD}$) as tris-TMS derivative, retention time 5.78 min, $[M]^{\bullet+}$=516.2917, mass error 2.13 ppm

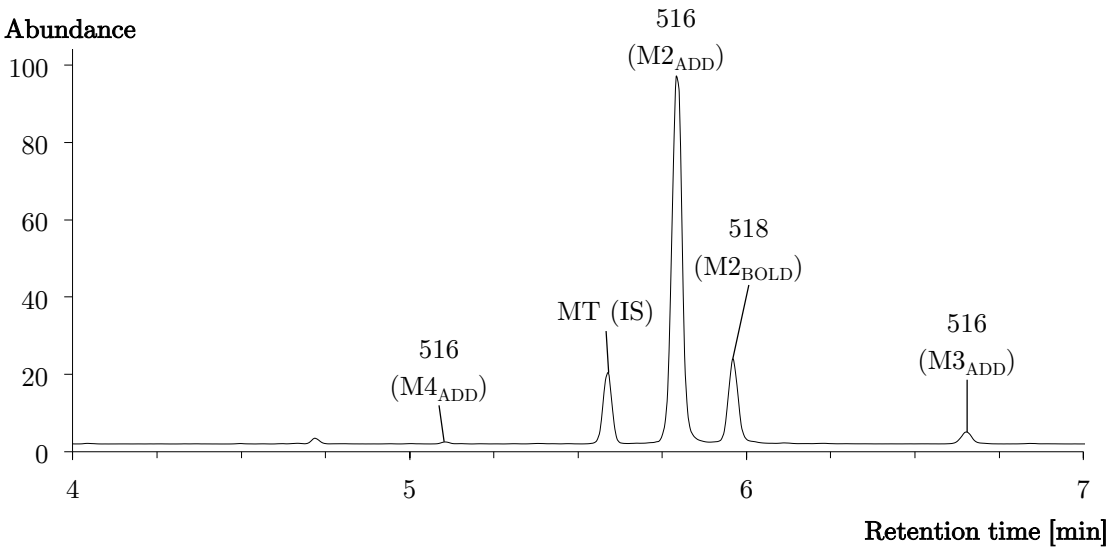

in Figure 148 Extracted ion chromatogram of hydroxylated metabolites of boldione after incubation with HLM as per-TMS derivatives, internal standard methyltestosterone (MT, 8 µg/mL), acquired using method b)

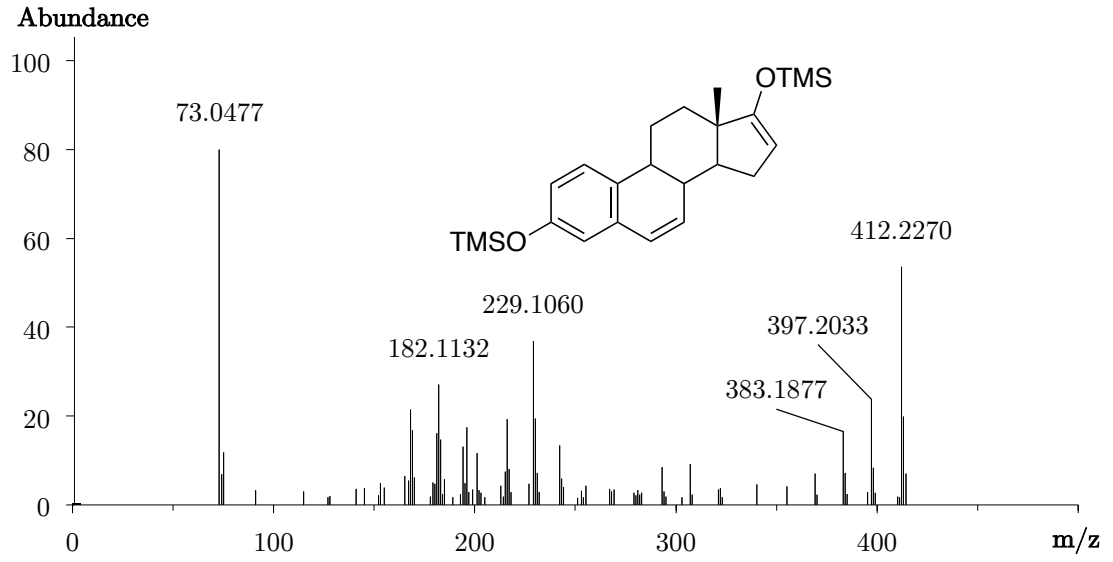

Figure 149 Accurate mass spectrum (EI) of 3-hydroxyestra-1,3,5(10),6-tetraene-17-one, bis-TMS, $[M]^{\bullet+}$=412.2270, mass error 5.34-ppm